Christina Koukelli_5115736
Theme: Facade & Products_Urban Facades
First Mentor: Alejandro Prieto Hoces_Architectural Facades & Products
Second Mentor: Serdar Asut_Design Informatics
Delft University of Technology
Master of Science Architecture, Urbanism & Building Sciences
Track: Building Technology
Research Report

S olar
hape

M orphing
emory

Kinetic Envelope

Integration of thermo-responsive Shape Memory Alloys in an autoreactive facade system to reduce the building's impact on the Urban Heat Island effect in the Mediterranean climate (case study: Athens, Greece)

Research Report for Master Thesis
in fulfilment of the requirements for the degree of
Master of Science in Building Technology,
at the Delft University of Technology,
to be defended publicly on the 21st of June 2021

Author:
Christina Koukelli
5115736
Facade & Products Graduation Studio – Theme: Urban Facades
Building Technology Track

First Mentor:
Dr. A.I. (Alejandro) Prieto Hoces MSc – Architectural Facades & Products

Second Mentor:
Dr. S. (Serdar) Asut – Design Informatics

Delegate of the Board of Examiners:
Dr.ir. R. (Roberto) Cavallo

PREFACE

Kinetic responsive facades and smart materials have attracted my interest during the last part of my studies and were topics that I wanted to explore further because of their inherent behaviour and the possibilities they can offer to enhance the building's performance with simple and passive strategies. During the graduation project, I found the chosen topic quite challenging and intriguing. This was due to its multifaceted nature, related to the UHI effect and its division into the direct and indirect impact, but also related to the constraints set in the beginning by the design guidelines and goals, which defined the overall rules and determined the design decisions in each development stage. This motivated me to examine deeper how these aspects are related to each other and to explore the potentials of autoreactive mechanisms and the extent of their contribution to the building's energy and environmental performance. In addition to that, the development of the computational workflow enabled me to explore and acquire a better knowledge and understanding of the parametric tools related to the assessment of the building's performance and to account for the various parameters involved during the design development. This process gave me the opportunity to dive more into the possibilities that can be offered by the computational tools within the Grasshopper environment through the developed workflow and to find ways to optimize the design based on the feedback from each analysis.

At this point, I would like to thank my mentors, Alejandro Prieto and Serdar Asut, for their support, valuable guidance and targeted feedback throughout the graduation project. Their inputs helped me challenge my skills and develop my critical thinking, while I appreciate the freedom and trust they gave me to explore various aspects of the research, design and computational tools. I would also like to thank Paul-Rouven Denz, for sharing his knowledge and insightful ideas, and for the encouraging support during our brainstorming sessions. His contribution was very useful to help me move forward and reflect on the design and overall project. Finally, a big thank you to my family and friends, especially my mother and brother, for their constant support and trust in me, and for always being by my side throughout the whole time, regardless of the circumstances.

ABSTRACT

Keywords: smart materials, Shape Memory Alloys, passive, autoreactive, adaptive facade technologies, kinetic, shading strategies, environmental response, Urban Heat Island effect, computational workflows, Grasshopper, performance-driven optimization, thermal, energy performance

Kinetic responsive systems are gaining attention in architectural applications, to help reduce the building's energy consumption and environmental impact, while improving the indoor comfort conditions. The thesis explores the potentials of Shape Memory Alloys (SMAs) for the design of autoreactive facade systems without using additional energy. The exploration is conducted and assessed through the design of a facade concept for the city of Athens in Greece, aiming to improve both the indoor and outdoor environment by means of a kinetic autoreactive system, with a focus on the building's direct and indirect impact on the Urban Heat Island (UHI) effect.

The methodology follows a feedback-loop logic informed by environmental and energy performance evaluation studies conducted in the Grasshopper environment to optimize the shape, geometry and movement of the proposed shading component. Throughout the facade design development, a comprehensive and systematic computational toolset is being developed, targeted on the abovementioned performance evaluation studies with the goal to compose a combined digital tool to facilitate designers and other specialists in the area. The proposed facade system, as a case study application and outcome of this iterative process, features a dynamic seasonal response, triggered by the temperature changes and exhibits a dual function. During the cooling-dominated periods, the aim is to reduce the cooling demands, by increasing the reflective surfaces directing the incoming solar radiation to the atmosphere, while also increasing the shading and self-shading effect through undulated geometries. In the contrary, during the heating-dominated periods, the system adapts a double facade function with multiple-cavity zones for heat amplification, with a higher solar absorption enabled through larger sun exposure.

The system's mechanism composed of two SMA wires, operates in coordination with a pivot axle and rotating mechanism, in combination with elastic steel threads and membranes that can accommodate the dynamic deformations. The activation of the SMAs, due to the environmental temperature changes, causes their linear deformation and initiates with a single movement the linear and rotational movement of the components involved, in a cause-effect internal system, while also controlling the cavity aperture. The design aims to minimize the need for actuators and mechanical parts with no additional energy, while the study evaluates in parallel the energy and environmental performance in the urban microclimate and the potential for passive operation. Through the development and assessment of the facade concept, the objective is to explore the potentials and limitations for the application of autoreactive envelopes in the facade design and development. At the same time, the aim is to exploit the possibilities and optimization potentials offered through the developed iterative computational workflows. This is realized through an interoperability logic of the digital tools used for the data interchange, which can be developed and used as a toolset in a broader range of applications, with the studied facade design as one demonstration example of its use in practice.

CONTENT

INTRODUCTION

1.1. PROBLEM STATEMENT

The urban built environment is one of the main attractors of population shifts from rural to urban areas, creating extreme changes in land use that result in unintended environmental, economic, and social consequences. This growth leads to the development of the so-called Urban Heat Island (UHI) phenomenon, characterized by higher temperatures in the density of built areas than the ones of the rural surroundings and is both directly and indirectly related to serious energy, environmental, health and economic problems [Santamouris, 2007]. This phenomenon is especially intense in the Mediterranean basin with a fast growth of energy consumption in the last years, due to the widespread of air conditioning systems and the increase of cooling demand. This situation is in addition highly associated with the climate change of the last decades and a significant rise of Heat Waves (HW) [Salvati et al., 2017].

Especially in Athens, Greece, UHI has been present already since the 1980s and many research studies have been focusing on the area to identify and evaluate the scale, causes and impact of the phenomenon and to propose certain mitigation strategies. Based on the outcomes of these studies, there has been an increase of the energy building demands, thermal risk and vulnerability of urban population and it has been reported that during the HWs, there is even an intensification of the average UHI magnitude by up to 3.5 °C. This is highly due to the widespread use of air conditioning in residential buildings resulting to a fast increase of electricity consumption over the last few decades. The heat that is dissipated from the buildings to the external environment increases the UHI phenomenon, and therefore, has a strong indirect impact. More specifically, in Athens an average increase of the cooling load of about 13% is estimated, with an annual global energy penalty for unit of city surface and degree of UHI intensity of 0.74 kWh m^{-2} K^{-1} [Santamouris et al., 2017].

Due to the complexity of the UHI phenomenon and the multifaceted factors that are dynamically intertwined, although certain mitigation strategies exist and have proven applications in urban environments, it concerns in general an environmental issue, which is hard to tackle and identify in a precise manner. However, what is evident is that there is a strong connection to the given climatic context, in which it emerges every time. Based on research studies, most of them agree that there is a high indirect impact of the building's energy performance on the increase of the UHI in the cooling-dominated areas, such as Athens, especially given the frequency of HWs. An improvement of the energy efficiency of the building sector might, therefore, reduce the ambient temperature and, consequently, decrease the amplitude of the UHI [Santamouris et al., 2018].

In this direction, a certain level of climatic responsiveness and adaptiveness to extreme heat changes in an energy efficient way can arise as a promising strategy, in order to reduce the building's energy consumption in the present cause-effect relation. This also gives way to the development of responsive technologies, such as passive dynamic adaptive facade systems. Thanks to their adaptive mechanisms and the ability to implement smart technologies and autoreactive materials, they are favored due to the real-time responsiveness to the also dynamic and unpredictable environmental changes, acting as the threshold between building and exterior environment. The above-mentioned framework, composed by problem and promising mitigation strategy, is the direction that is followed in the current thesis and will be further explored and developed with a focus on the incorporation of smart and shape-changing materials.

1.2. RESEARCH OBJECTIVE

In this contextual framework, the research objective aims to investigate the impact of integrated thermo-responsive SMMs in facade components on the reduction of the Urban Heat Island effect in the Mediterranean climate, taking as a case study the city of Athens, Greece.

The main sub-objectives are the following:

- To study the effect of responsive dynamic facade systems in respect to climate adaptiveness and UHI reduction and the relation to potential technologies.

- To research on the potential of thermo-responsive SMM integrated technologies to have an impact on the building's energy performance and contribute to UHI reduction in the Mediterranean climatic context.

- To explore the state-of-the art and the methods to control and pre-determine the SMM's dynamic responsiveness parameters and to identify the potentials of implementation in an adaptive facade system.

- To study the main principles and strategies of natural systems and their relevance to the SMM behavioural ones and to responsive mechanisms in controlling the building's thermal behaviour in a climatic context.

- To design a passive adaptive solar morphing envelope based on thermo-responsive SMMs in an integrated facade system combining autoreactive and bio-inspired responsive mechanisms.

- To achieve motion in an integrated facade system by using latent energy in an energy effective and autoreactive way with optimal use of sensors and actuators, where material, form, function, structure and motion are interdependent in a fit combination.

- To discuss the feasibility of SMM-based facade technologies based on a set of parameters and reflect on the challenges, restrictions and potentials for future facade applications.
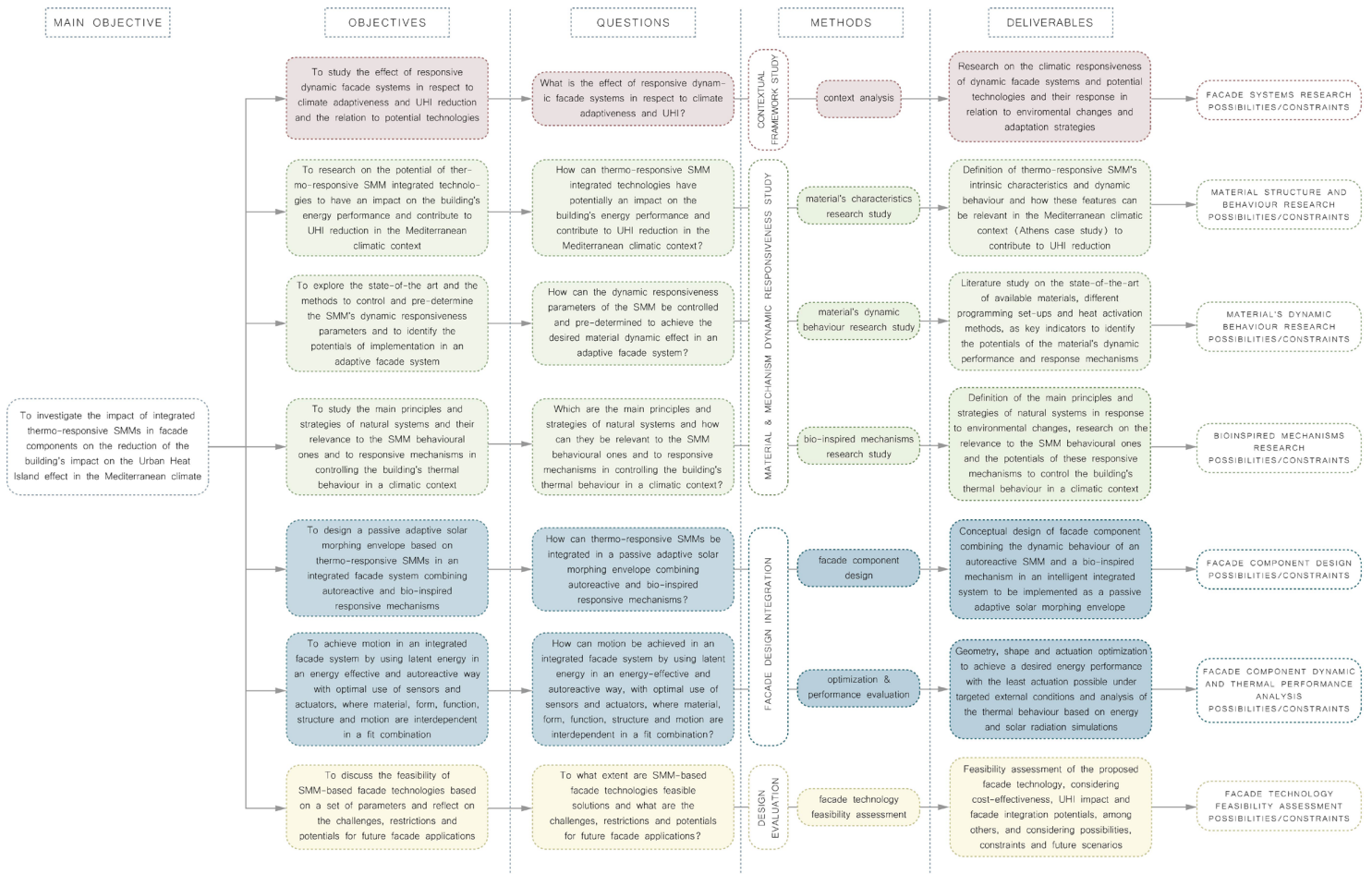
Figure 1: Research objectives and methodology scheme. [own work]

1.3. RESEARCH QUESTION

The above objectives are oriented to provide some insight to the following main research question:

*"How can **thermo-responsive Shape Memory Materials** be integrated in an **autoreactive facade system** to reduce the building's impact on the **Urban Heat Island effect** in the Mediterranean climate, with a focus on the case study of Athens, Greece?"*

1.4. RESEARCH SUB-QUESTIONS

To be able to address the main research question from different inter-linked perspectives, a few sub-questions are identified that answer various aspects which are encountered throughout the research process. These can be grouped in the following clusters, based on the process stage and focus sub-topic:

Theoretical Framework:

    Contextual Framework (Problem analysis and Facade System Strategy):

    - What is the effect of responsive dynamic facade systems in respect to climate adaptiveness and UHI?

    Material and Mechanism analysis:

    - How can thermo-responsive SMM integrated technologies have potentially an impact on the building's energy performance and contribute to UHI reduction in the Mediterranean climatic context?

    - How can the dynamic responsiveness parameters of the SMM be controlled and pre-determined to achieve the desired material dynamic effect in an adaptive facade system?

    - Which are the main principles and strategies of natural systems and how can they be relevant to the SMM behavioural ones and to responsive mechanisms in controlling the building's thermal behaviour in a climatic context?

Design Integration:

    - How can thermo-responsive SMMs be integrated in a passive adaptive solar morphing envelope combining autoreactive and bio-inspired responsive mechanisms?

    - How can motion be achieved in an integrated facade system by using latent energy in an energy-effective and autoreactive way, with optimal use of sensors and actuators, where material, form, function, structure and motion are interdependent in a fit combination?

Design Evaluation:

    - To what extent are SMM-based facade technologies feasible solutions and what are the challenges, restrictions and potentials for future facade applications?

1.5. RESEARCH METHODOLOGY

The main objective of the thesis is to develop a passive adaptive integrated facade system, based on SMM technologies and autoreactive responsive mechanisms in a solar morphing envelope. The aim is to reduce the building's impact on the UHI effect durectly by means of reflecting and dispersing the solar radiation during the heat intensive periods, and indirectly by reducing the building's energy performance and cooling demands.

At the core of the research, a theoretical framework has been formulated, to explore the main aspects of the problem statement and research question. This can be divided into two parts: First, the contextual framework with a focus on the addressing problem, the UHI in its climatic context, impact and strategies, and on the dynamic adaptive facades as the chosen mitigation strategy implementation. And secondly, the material and mechanism analysis, with a focus on the inherent material characteristics and dynamic behaviour, both in a material and a component level, to form a better understanding of the responsive mechanisms.

A contextual research has been conducted to provide a background information concerning the nature of the UHI in the studied area. A research and analysis based on literature reviews from journals and statistical data from related agencies have been realized, to collect the relevant information, which were used as a background to elaborate on the design decisions and strategies for facade implementation. These studies provide information about the causes, impact and existing mitigation strategies of the UHI effect, with a direct connection to the effect of the global climate change and the synergy to the increasing Heat Wave phenomena of the recent years. In parallel, the literature study aimed to collect data about the relevance of the UHI and HWs with the building's energy performance and inner comfort as an indirect impact with increasing influence over the years. For the purposes of the current thesis, the design strategy is also focused on the impact of a passive adaptive facade system to address the UHI. A literature study was conducted in this respect as well, to provide a classification and an overview of the available technologies and dynamic responses and types, both in terms of materiality and systems and to study the several operational systems and purposes of each type. This was used as a

guideline for the initial design decisions, to choose the most apt system based on the research's objectives and goals.

Regarding the material and mechanism research, a main objective is to provide a passive adaptive facade system that can realize the change in geometric configuration through the ingrained properties of the material it is made of, without the need for external energy or complex mechanical parts. A large part of the research was, therefore, realized in the existing smart and multifunctional materials, with a focus on the thermo-responsive ones, due to the nature of the environmental issue and climatic context, and the actuation mechanisms that would trigger the dynamic behaviour. In this direction, scientific papers, research studies and experimental lab tests have been consulted to understand the state-of-the-art knowledge and material performance. The available materials were then compared based on their intrinsic features, properties and dynamic performance, as well as availability and implementation potentials, based on existing applications, material experiments and case studies, both realized in the building industry as well as in other fields, such as biomedicine and aerospace. A further subdivision was made between the different material families, as in SMAs, SMPs and SMHs, and an evaluation and comparison were realized, based on the above research and the feedback from experts in the field, which were being consulted in parallel, to be able to opt for the most promising, suitable and feasible one to be implemented in an adaptive facade system.

As for the mechanism, the aim of the literature study was focused on dynamic mechanisms that are based on mostly hingeless movements, minimizing the use of required actuators, with minimum external energy and a real-time climatic responsiveness. Because of these features, there is a relevance between the SMMs' intrinsic characteristics and the principles found in the strategies of natural systems to adapt to environmental changes. This led to the exploration of bio-inspired mechanisms, both in realized biomimetic applications and by directly exploring natural organisms and disassembling the principles behind their response mechanisms for thermal control and heat regulation, to apply the principles in an integrated facade system.

As a mean of evaluating the proposed system, parallel to the design, parametric simulations and design optimizations were realized to fine-tune the selected shading prototype design, assisted by the feedback from performance validation and to provide design variations in conjunction with energy and environmental simulations throughout the design process. This was established by collecting data regarding weather and solar radiation, among others. Software simulation was then used as an evaluation tool to assess the performance of the SMM component under targeted conditions and to additionally perform CFD simulations to evaluate the thermal behaviour of the building envelope. The end evaluation was realized through a feasibility assessment of the proposed facade technology system, to reflect on its efficiency and applicability scenarios. This was based on the energy and environmental performance of the facade system, but also on a set of qualitative criteria, which were defined along the process, such as cost-effectiveness and facade integration potentials, and led to a reflection on the possibilities, constraints and future scenarios of SMM-based facade technologies.

Main research question:

"How can **thermo-responsive Shape Memory Materials** be integrated in an **autoreactive facade system** to reduce the building's impact on the **Urban Heat Island effect** in the **Mediterranean climate**, with a focus on the case study of Athens, Greece?"

Theoretical Framework

How can motion be achieved in an integrated facade system by using latent energy in an energy-effective and autoreactive way, with optimal use of sensors and actuators, where material, form, function, structure and motion are interdependent in a fit combination?

How can thermo-responsive SMMs be integrated in a passive adaptive solar morphing envelope combining autoreactive and bio-inspired responsive mechanisms?

Design Integration

Evaluation

To what extent are SMM-based facade technologies feasible solutions and what are the challenges, restrictions and potentials for future facade applications?
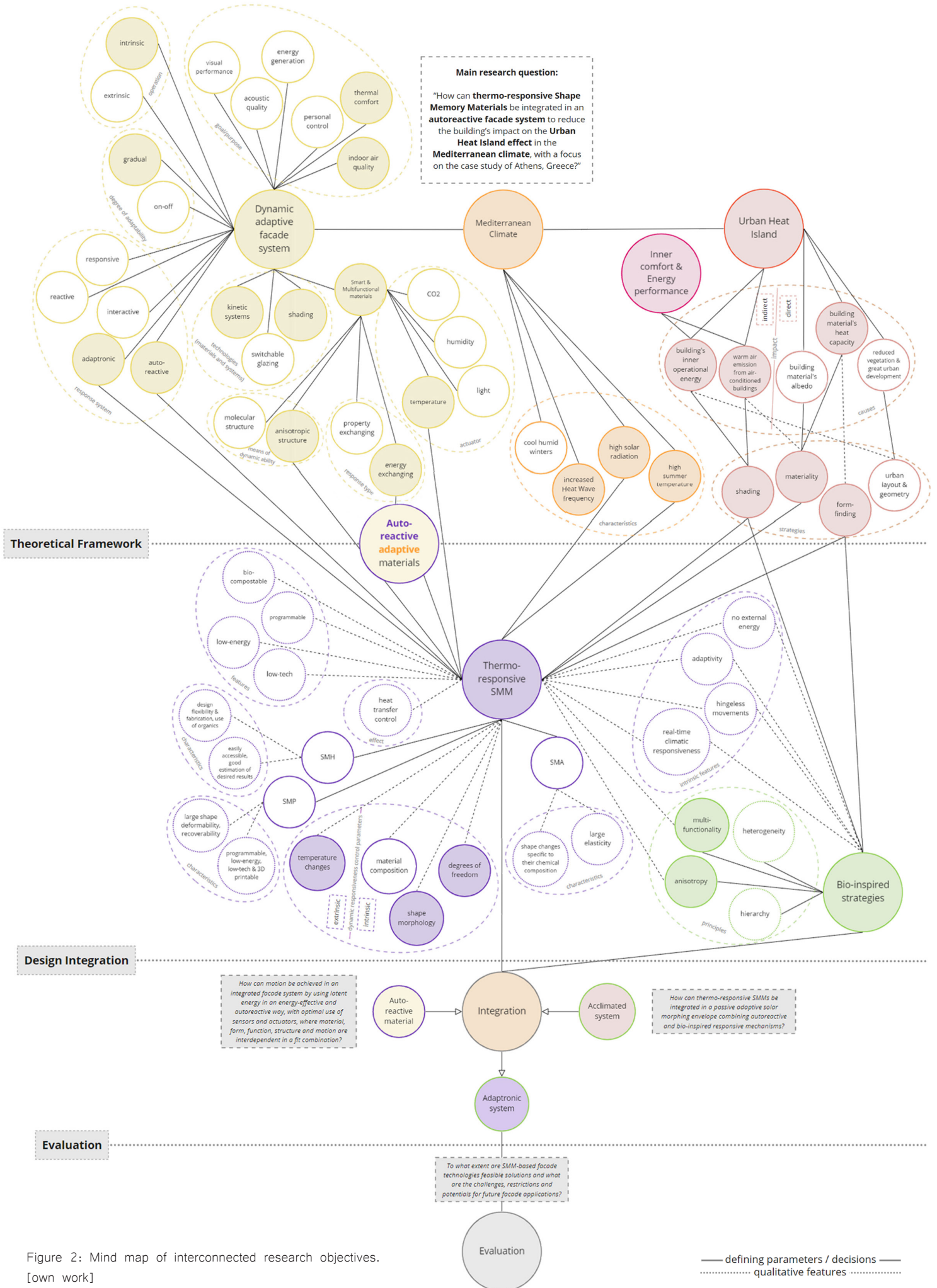
Figure 2: Mind map of interconnected research objectives. [own work]

defining parameters / decisions
qualitative features

1.6. THESIS STRUCTURE AND WORKFLOW

The structure of the thesis is comprised of three distinct sections, following the process of the research flow in a chronological order in the available timeframe. The first part includes the preliminary research, composed of the theoretical framework, which includes the environmental problem analysis, the climatic context, the facade system strategy and the material and mechanism responsiveness research study. It is followed by the design integration and facade implementation, where the information extracted from the research would aid and be applied in the facade system integration and design decisions. In the last section, the thesis presents the evaluation of the proposed system, in order to assess its environmental and energy performance. Lastly, it results to a feasibility assessment and a discussion on the level of impact of such a technology to a UHI reduction and to a reflection on the challenges, restrictions and potentials for future facade applications and further development in this direction.

Graduation Timeline

Following the framework of the methodology, the timeline of the thesis is outlined in the Figure below [Figure 3]. The approach is fairly linear with some repetition to allow for redesigning elements, feedback–optimization iterations and system adjustments.

	P1								P2												P3									P4				P5
Calendar Week	46	47	48	49	50	51	52	53	1	2	3	4	5	6	7	8	9	10	11	12	13	14	15	16	17	18	19	20	21	22	23	24	25	26
Academic Week	2.1	2.2	2.3	2.4	2.5	2.6	–	–	2.7	2.8	2.9	2.10	–	3.1	3.2	3.3	3.4	3.5	3.6	3.7	3.8	3.9	3.10	4.1	4.2	4.3	4.4	4.5	4.6	4.7	4.8	4.9	4.10	4.11

Literature Review
- Urban Heat Island
- Climatic Context
- Adaptive Dynamic Facades
- Material Research
- Thermo–responsive SMMs
- Responsive mechanisms

Façade Design
- Façade Design Guidelines
- Material Selection
- Façade Design
- Geometry Configurations

Measurement
- Performance Evaluation
- Impact on UHI

Deliverables
- Final Drawings
- Final Report
- Final Presentation

Figure 3: Thesis timeline. [own work]

BACKGROUND RESEARCH - CONTEXTUAL FRAMEWORK
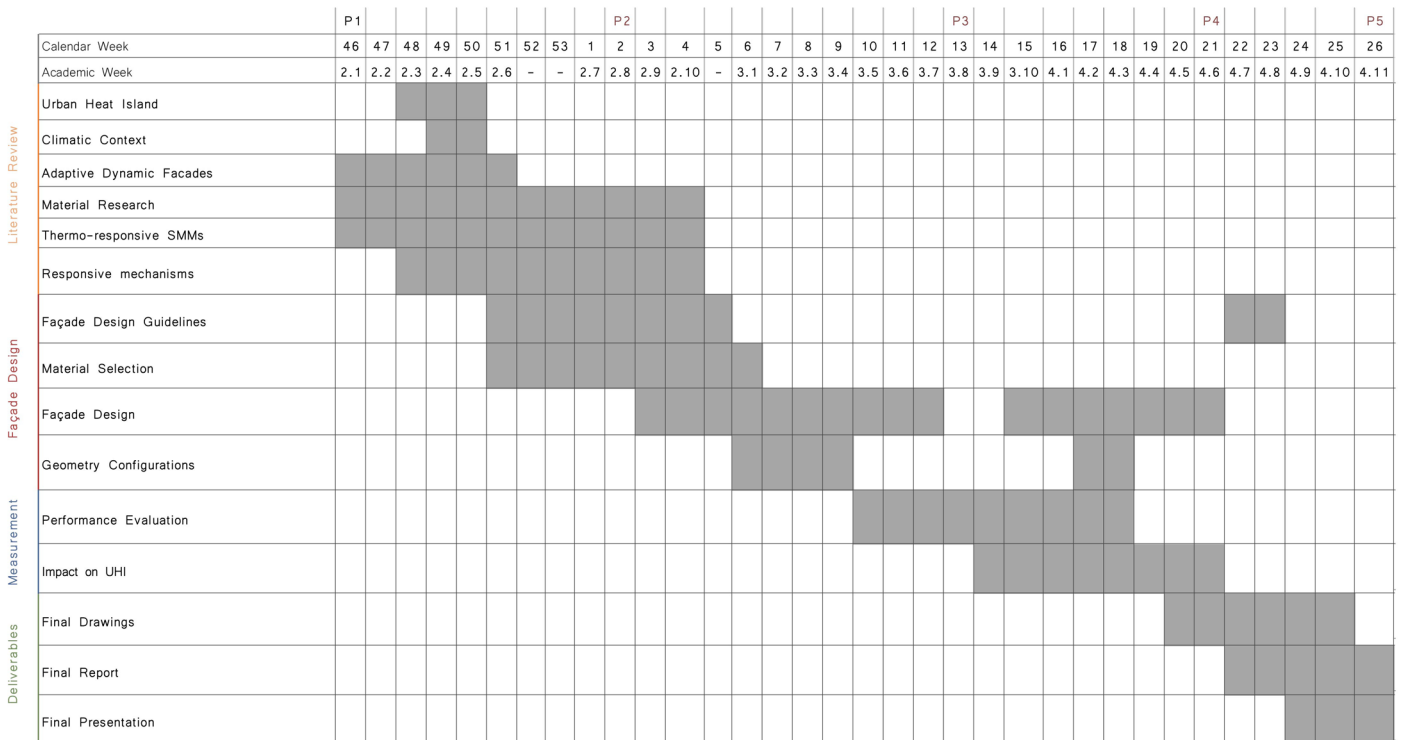
2.1. URBAN HEAT ISLAND EFFECT

The urban built environment is one of the main attractors of population shifts from rural to urban areas. As the dynamics of this population shift occur, the 21st century phenomenon of rapid urbanization is creating extreme changes in land use that result in unintended environmental, economic, and social consequences. Urban growth has impacted the energy performance of buildings and human comfort, among others, by changing the landscape, as buildings and other infrastructures substitute open land and vegetation. This growth leads to the development of the so-called Urban Heat Island (UHI) phenomenon, characterized by higher temperatures in the density of built areas than the ones of the rural surroundings ΔTu-r. According to the review by Santamouris [Santamouris, 2007], the UHI intensity varies between 2°C and 10°C [Salvati et al., 2017]. These temperature differences can range from 1°C–3°C in cities with one million or more inhabitants [Guattari, et. al., 2018]. This localized regional effect is in addition to IPCC (Intergovernmental Panel on Climate Change) estimates that put the potential of global warming to be +1.4°C to +5.0°C over the next 100 years, in addition to the 0.6°C temperature increase already observed during the 20th century. [Golden, 2004] Two types of UHI can be distinguished: (1) the canopy-layer heat island and (2) the boundary-layer heat island [Oke, 1979]. The canopy layer consists of air between the roughness elements (e.g. streets) with an upper boundary just below roof level. The boundary layer is situated above the canopy layer, with the lower boundary subject to the influence of the urban surface [Golden, 2004].
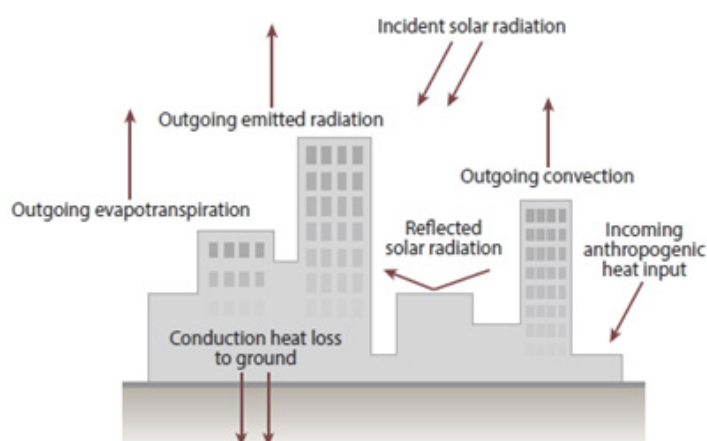

Figure 4: Relevant energy flows for the urban heat island. [Phelan et al., 2015]

2.1.1. CAUSES AND IMPACT

At its core, the UHI effect is governed by an energy balance between the input, generated, lost and stored heat in the urban environment and is a complicated phenomenon that depends on the size, density, building practices, location and season, to name a few factors of the built environment. In a similar way, the impacts are a combination of social, health, energy, economic and other issues, which are difficult to track and assess precisely [Phelan et al., 2015].

In general, urban overheating is caused by numerous reasons, including the thermal properties of the materials used in cities, the released anthropogenic heat, the canyon radiative geometry, the urban greenhouse effect, the reduction of the evaporative surfaces and the reduced turbulent transfer in the dense urban environment [Phelan et al., 2015].

Some of the main causes can be summarized as follows:

– The **urban environment**, with its paved surfaces and reduced vegetation, causes less of the incoming radiant energy from the sun to be reflected from urban areas and, likewise, less of this energy is converted to latent energy associated with evaporation or transpiration of moisture.

– The larger volume of asphalt, brick, concrete, and other materials gives urban areas a much **higher thermal storage capacity** than natural surfaces. One result is that large amounts of energy are stored in the urban canopy during the day and released after sunset – the hysteresis lag effect.

– **Anthropogenic sources** in the urban environment generate additional heat by way of air conditioning, automobiles, and machinery, which indirectly increase the UHI effect. Hence, urban temperatures tend to remain relatively high into the evening hours.

– **Albedo changes** have resulted in a forcing of $-0.4 Wm^{-2}$, about half of which is estimated to have occurred in the industrial era. These changes are mainly attributed to modifications from existing landscape to man-made infrastructure which results in decreasing surface albedo, as a result of roads and buildings.

– **Urban geometry** has changed net radiation and altered convection due to slowing winds near buildings.
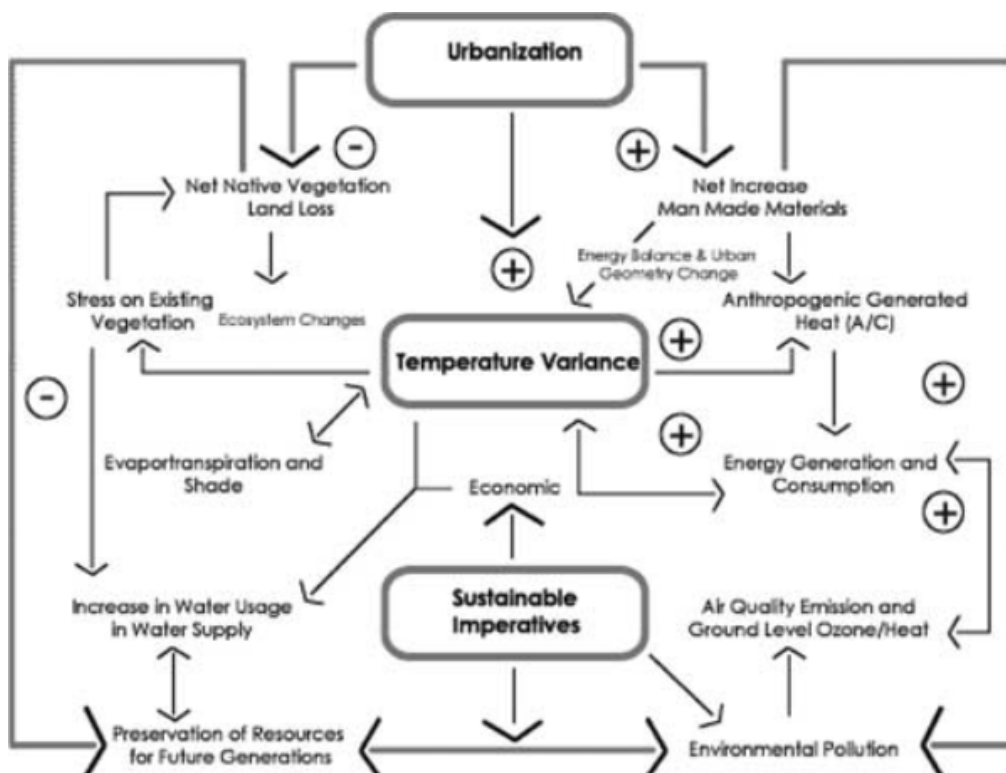

Figure 5: The influence of the engineered environment and urbanization. [Golden, 2004]

This phenomenon is directly and indirectly related to serious energy, environmental, health and economic problems, showing the multitude of its dynamics. The increased ambient temperatures cause a serious impact on the cooling energy consumption, peak electricity demand, heat related mortality and morbidity, urban environmental quality, local vulnerability and comfort.

To name a few, as depicted in the Figure below [Figure 6], with a focus on the ones related to the urban built environment and user's comfort, they can be summarized into the sub-categories below:

- **Commercial / Industry**:
    o Increased greenhouse gas emissions contribute to global climate change, which can impact the length and severity of the UHI effect.
    o Increased energy demands increase power plant emissions: CO2, NOx, VOC's.

- **Urban**:
    o Increased demands for water resources.
    o UHI increases anthropogenic heat and pollutants from elevated use of air conditioning and use of vehicles as a mode of transportation.

- **Residential**:
    o Heat related health risks and mortality rate increase.
    o Increased costs for energy and water demands which affect families and the competitiveness in a region [Golden, 2004].

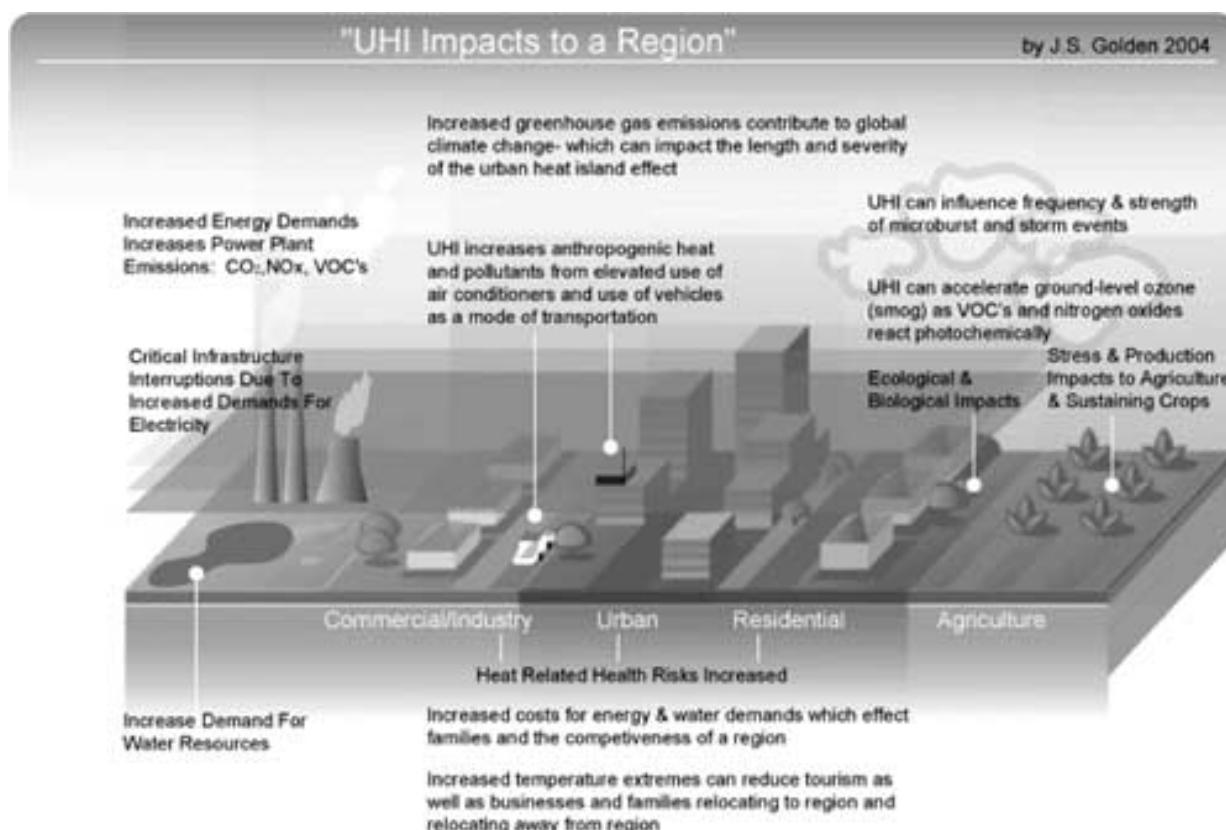Figure 6: The potential impacts associated with UHI. [Golden, 2004]

2.1.2. EXISTING MITIGATION STRATEGIES

The existing mitigation strategies so far can be roughly divided into two categories: increased vegetation (trees, landscaping, and green spaces) and changes to building practices (materials for higher albedo and/or modified thermal properties, alternative paved surfaces designs, building types, and other materials selections) [Santamouris, et al., 2018]. Other strategies are also common, such as decrease of the anthropogenic heat, solar control of open spaces, use of environmental heat sinks and increase of the wind flow in the canopy layer [Karlessi, et al., 2011].

Here, the focus will be placed on the second category, the strategies related to the building component. These include mainly the implementation of cool pavements and green roofs, controlling albedo with a reflective surface for unshaded areas and shading design for buildings and open spaces. The last one is of the most relevance for the objective of the current thesis, in combination with the increase of the reflective surfaces of the proposed building component to reduce the absorbed and transmitted solar radiation in the building's thermal mass. Apart from that, a strong connection will be added to mitigate the indirect impact of the building's energy performance to the UHI effect, by reducing the cooling demands, by means of shading and, consequently, both decreasing the anthropogenic heat and enhancing the inner comfort levels.

2.2. CLIMATIC CONTEXT – MEDITERRANEAN CLIMATE, ATHENS CASE STUDY

The Urban Heat Island (UHI) effect is particularly concerning in the Mediterranean zone, as climate change and UHI scenarios foresee a fast growth of energy consumption for the next years, due to the widespread of air conditioning systems and the increase of cooling demand [Salvati et al., 2017].

For the purposes of the current research, the city of Athens, Greece, will be considered as a case study for the development of the proposal. Located at the southernmost part of the Greek mainland and hosting approximately 3.8 million residents, it is a densely populated coastal area of the eastern Mediterranean, ranking among the eight largest urban zones in Europe. Athens has been experiencing pronounced warming during the last decades, which in summer amounts to approximately +1°C/decade since the mid-1970s, attributable to both global/regional warming and intensifying urbanization.

The UHI intensity was first investigated in Athens in the early 1980s and since then, the characteristics of the UHI in this area have been the focus of numerous studies based both on ground measurements and satellite observations. These studies have shown that the phenomenon exists during both the summer and winter periods, with its spatial and temporal pattern strongly controlled by the unique characteristics of the area. The UHI phenomenon in Athens is characterized by much higher ambient temperatures in densely built and populated areas compared to the surrounding suburban and rural areas. More recently, Giannopoulou et al. [Giannopoulou et al., 2010] reported a variation of the UHI intensity in Athens between 3.0°C and 5.3°C during the daytime and between 1.3°C and 2.3°C during the nighttime [Salvati et al., 2017] [Papamanolis et al., 2015]. Therefore, it is among the cities, where the phenomenon has a significantly strong intensity and impact and forms part of its climatic context.

2.2.1. SYNERGY OF GLOBAL CLIMATE CHANGE, HEAT WAVES AND URBAN HEAT ISLAND EFFECT IN THE MEDITERRANEAN CLIMATE

As a phenomenon of the recent decades, UHI develops in conjunction with global climate change, resulting in an even greater increase of hot periods in urban areas than in their rural corresponding parts [Santamouris et al., 2018]. At the same time, one of the major concerns nowadays is to reduce the energy consumption and environmental footprint of cities and buildings. In the Mediterranean climate, this issue is more and more associated with the summer season. The widespread use of air conditioning in residential buildings has led to a fast increase of electricity consumption over the last few decades. In effect, the predicted climate scenarios for the next 100 years foresee an increase of tropical nights (>20°C) and hot days (>35°C). In this sense, the combination of global warming with the UHI effect makes the energy issue particularly concerning in the Mediterranean basin [Salvati et al., 2017].

This situation affects the urban environment in a direct and indirect way. Higher urban temperatures act as a catalyst and speed up the photochemical reactions that result in the formation of tropospheric ozone, while the UHI affects the air flow and turbulent exchanges, resulting in higher pollutant concentration. In parallel, higher energy consumption during the summer period causes an increased emission of atmospheric pollutants generated by the electricity power plants, expands

the ecological footprint of the cities and results to a higher consumption of resources. In fact, estimation of the additional ecological footprint of the city of Athens necessary to compensate the global impact of the local UHI showed that this is equivalent to 1.5^{-2} times the city's political area and may extend up to 110.000 ha. [Founda et al., 2017].

At the same time, as a result of the climate change, Heatwaves (HW) are becoming more frequent and longer and, based on a recent study [Founda et al., 2017], a synergetic relationship was developed between UHI and HW, taking as an example the heatwaves taking place in Athens in 2012. Based on the outcomes, an intensification of the average UHI magnitude by up to 3.5°C during HWs was found, compared to summer background conditions, leading to increasing energy building demands, thermal risk in cities and vulnerability of urban population. It was also reported that an increase in the mean air temperature is coupled with a simultaneous, vast increase in HW frequency. The last decade has been marked by a number of record-breaking heat related events, as for instance the highest temperature ever measured since the mid 19th century (in 2007), the warmest summer ever recorded (in 2012), and the early heat waves in 2007, 2010 and 2016 [Founda et al., 2017].
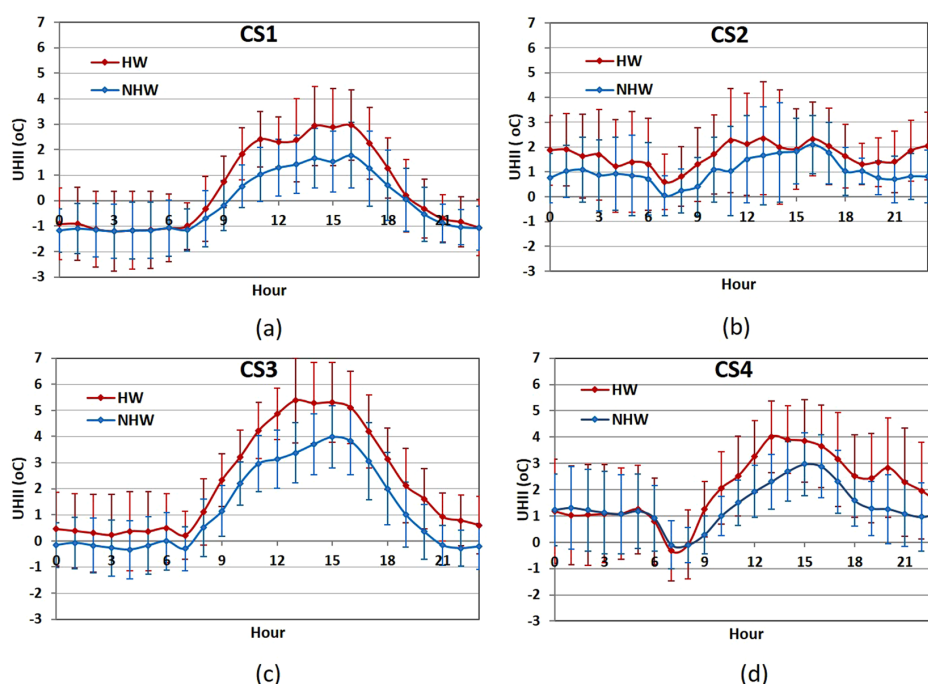

Figure 7: Diurnal patterns of average UHI intensity along with standard deviations at CS1-CS4, under HW and NHW conditions, over the study period (July-August 2012). [Founda et al., 2017]

2.2.2. URBAN HEAT ISLAND AND ITS ENERGY IMPACT ON BUILDINGS

It can be concluded that the combination of UHI and HWs in a continuous rise of temperature due to the global climate change is strongly affecting the energy performance of the built environment, especially in the Mediterranean area. The effects of the UHI on the energy consumption of buildings have been widely investigated, documenting a significant increase of the cooling loads and electricity consumption in the building sector. The heat dissipated from buildings to the external environment by the use of air conditioning systems, in return, increases the UHI phenomenon [Guattari et al., 2018].

More specifically, studies performed by Santamouris et al. [Santamouris et al., 2001] have found that the cooling energy demand of a typical office buildings located in the central area of Athens is almost two times higher than the one of a similar building located in suburban areas, with peak electricity loads almost tripled. Moreover, existing studies correlating the energy consumptions of similar buildings located in urban and rural areas have revealed an average increase of the cooling load of about 13%, with an annual global energy penalty for unit of city surface and degree of UHI intensity of 0.74 $kWhm^{-2}$ K^{-1} [Santamouris et al., 2018].

Through these studies, it can be estimated that a decrease of the magnitude of the anthropogenic heat released in the urban environment may drop down the ambient temperature and decrease the amplitude of the UHI. This may be achieved, among others, with an improvement of the energy efficiency of the building sector in the cooling-dominated areas, such as Athens. As such, the objective of the thesis is focused on those mitigation strategies that can promote a certain level of climatic responsiveness to extreme heat changes in an energy-efficient way, in order to reduce the building's energy consumption and cooling demands in this cause-effect relation. This gives way to the following chapter, which is related to the chosen mitigation strategy as a research field, to study and develop an autoreactive adaptive facade system, which is favored due to the real-time response potential to the above-mentioned also dynamic and unpredictable environmental changes.
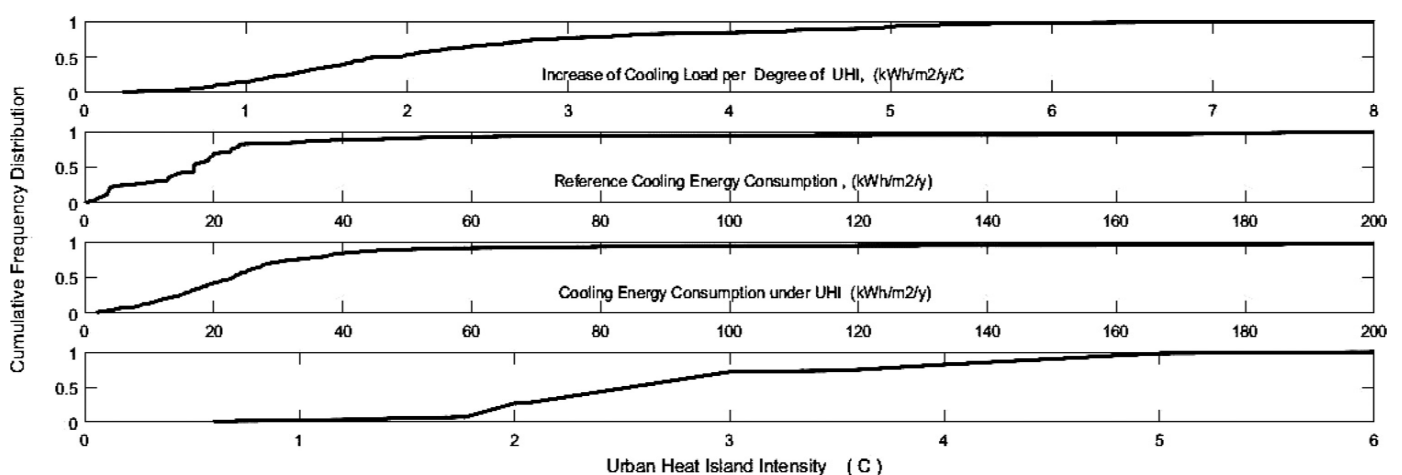
Figure 8: Impact of urban overheating on reference – typical buildings. a) Cumulative frequency distribution of the increase of the Cooling load of the buildings per degree of UHI. b). Cumulative frequency distribution of the cooling energy consumption of the buildings under reference climatic conditions. c). Cumulative frequency distribution of the cooling energy consumption of the buildings under urban –UHI conditions. d). Cumulative frequency distribution of the UHI intensity for all considered cases. [Santamouris, 2020]

2.3. DYNAMIC ADAPTIVE FACADES

The future of the sustainability of buildings is influenced by three challenging factors. From a social perspective, there is a need to achieve a high level of user well-being and indoor environmental quality. At the same time, from an environmental perspective, there is a need to reduce building energy consumption and neutralize building-related environmental impacts. Particularly, the integration of passive and active design technologies in the building envelope is gaining attention as a solution with high potentials to improve indoor comfort conditions and reduce the environmental impact during the life cycles of buildings. In this framework, the dynamic facades or adaptive facades, as defined by the European COST (European Cooperation in Science and Technology) Action TU1403 (Adaptive Facades Network (2014-2018)), have a significant effect on achieving the three performance requirements, by adapting to changing boundary conditions in the form of short-term weather fluctuations, diurnal cycles, or seasonal patterns [Luible, 2015].

Another important aspect concerns the potential reduction of energy demand in buildings, heat regulation and CO_2 emissions with the conversion of building envelopes from passive to active regulators of energy balance, which is promoted as part of the Climate and Energy Action Plans (Directive 2010/31/EU). In order to work effectively as a surface-regulator, the building skin must adopt different physical features at different times of the day, requiring different levels of environmental intelligence [Persiani et al., 2016].

In addition to this, what is relevant as well is to contribute with some knowledge as part of the framework commissioned to the Adaptive Facade Network set by the EU COST in 2014. The main aim of this COST Action is to harmonize, share and disseminate technological knowledge on adaptive facades at a European level [Luible, 2015]. By harnessing this knowledge, it will contribute to the generation of new ideas and concepts at a fundamental and product/system development level.

Considering the emergent issue of the UHI phenomenon and its foreseen increasing intensity in the Mediterranean region over the next years, the current thesis entails a challenge with scientific and societal relevance, aiming to achieve sustainability targets in the built environment.

2.3.1. MAIN CHARACTERISTICS AND PRINCIPLES

As a general definition, *"a climate adaptive building shell has the ability to repeatedly and reversibly change some of its functions, features or behaviour over time, either passively or actively, in response to changing performance requirements and variable boundary conditions, and does this with the aim of improving overall building energy performance and/ or inner comfort."* [Attia et al., 2020][Juaristi et al., 2020].

What distinguishes this type of facade technologies is the capability of the adaptive facades to adapt physical properties in a reversible way as a response to and/or to adjust to transient boundary conditions (either external, such as climate, or internal, such as occupants' requirements), in order to respond to changing priorities (i.e. minimizing the building energy use, maximizing the use of natural light, etc.). The term 'adaptive' is often synonym to 'responsive', 'dynamic', 'switchable', 'smart', 'active' etc. [Loonen et al., 2016].

Moreover, in the context of nearly Zero Energy Buildings (nZEB) these facades also need to collect and convert available surrounding energy (mainly solar) in an adaptive way, in order to correspond as much as possible to building energy needs. They are thus considered as a viable alternative for achieving low energy building operation with high indoor environmental quality [Loonen et al., 2015].

Adaptive facades are often related to designing dynamic envelope models, which, with the help of sensors, system components and smart materials, contribute towards reducing the building's energy demand and building's environmental impact. They are capable of managing energy flows by altering the properties of fixed devices (smart materials) or by controlling (manually or automatically) moving parts (e.g. sunshades, windows, ventilation outlets, etc.) in relation to the type of user and complexity of the building. This envelope typology is marked by dynamic anisotropy, where a change in the structure modulates the various environmental flows according to the climatic conditions of the place, including external climatic-environmental conditions [Aelenei et al., 2018]].
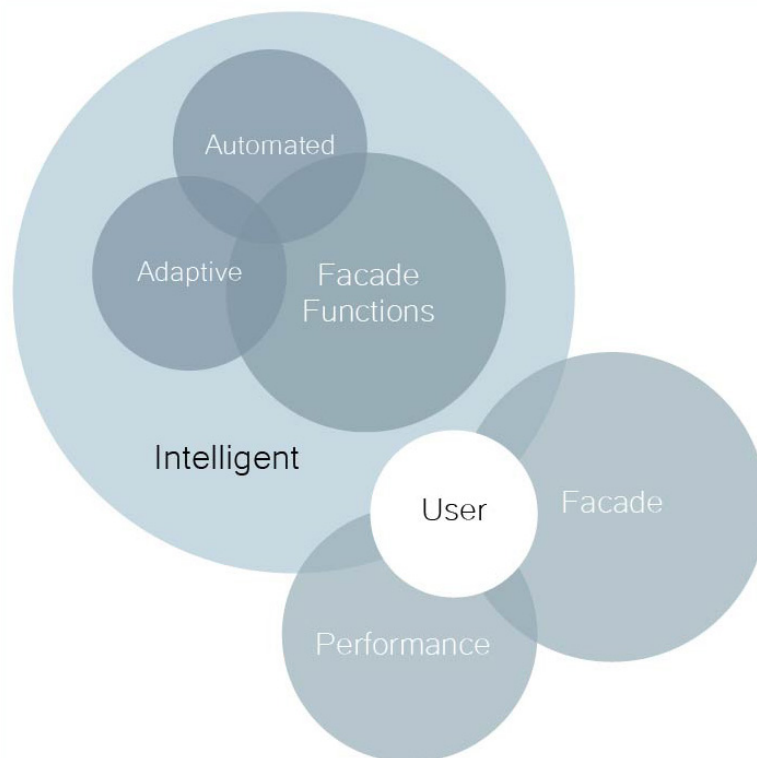

Figure 9: Visualization of the 'Intelligent facades' section context. [adapted from Böke et al., 2018]

2.3.2. CLASSIFICATIONS AND AVAILABLE TECHNOLOGIES

There are several classifications developed from different sources to categorize the available adaptive facade technologies, many of which are overlapping in certain areas, depending on the spectrum of the division each time. As an example, which is based on the collaborative frame of COST Action TU 1403 [http://tu1403.eu], a characterization was carried out in terms of technologies and purpose, depending on different factors, such as the purpose of facade/components with adaptive capacity, which can be related with thermal comfort, energy performance, indoor air quality (IAQ) and visual and acoustic performance, among other requirements, as can be seen in Figure 10 [Aelenei et al., 2018].

Purpose	Responsive function	Operation	Components (materials and systems)
– Thermal comfort	– Prevent	– Intrinsic	– Shading
– Energy performance	– Reject	– Extrinsic	– Insulation
– Indoor Air Quality (IAQ)	– Modulate		– Switchable glazing
– Visual performance	– Collect		– PCM
– Acoustic performance			– Solar tubes
– Control			– Integrated Solar Systems

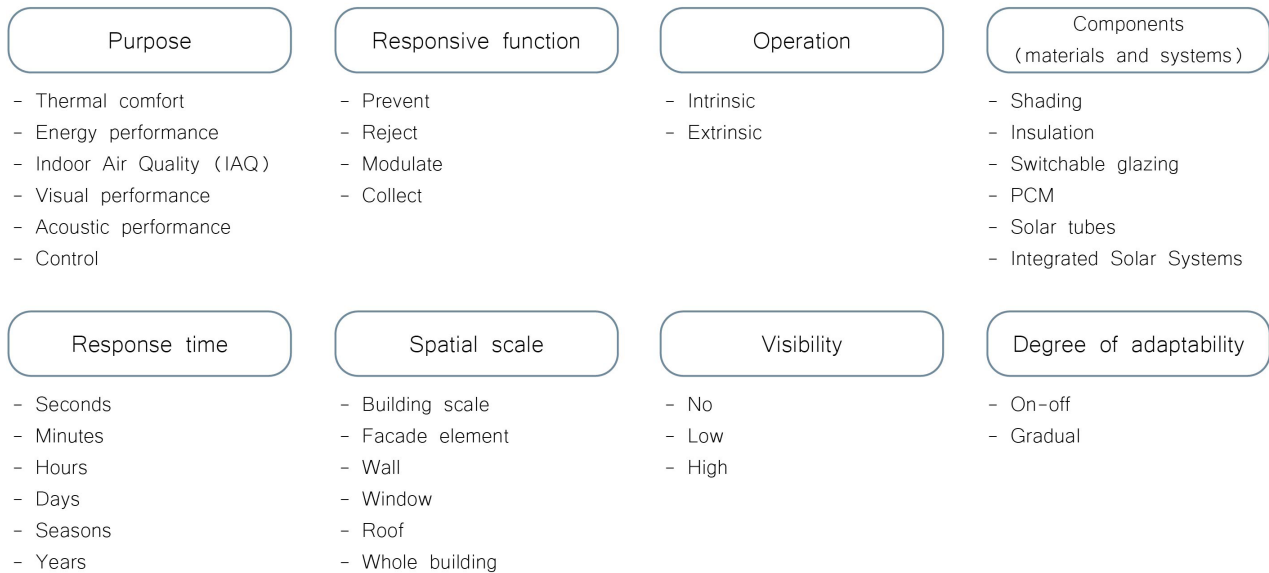| Response time	Spatial scale	Visibility	Degree of adaptability
– Seconds	– Building scale	– No	– On-off
– Minutes	– Facade element	– Low	– Gradual
– Hours	– Wall	– High	
– Days	– Window		
– Seasons	– Roof		
– Years	– Whole building		

Figure 10: Adaptive facades classification. [adapted from Aelenei et al., 2018]

Apart from that, another classification can be realized by subdividing the facade in terms of system, component and material level, based on the scope of interest and scale of the dynamic mechanism.
This can be seen in the Figure below [Figure 11] [Aelenei et al., 2018].

Adaptive Facade Classification

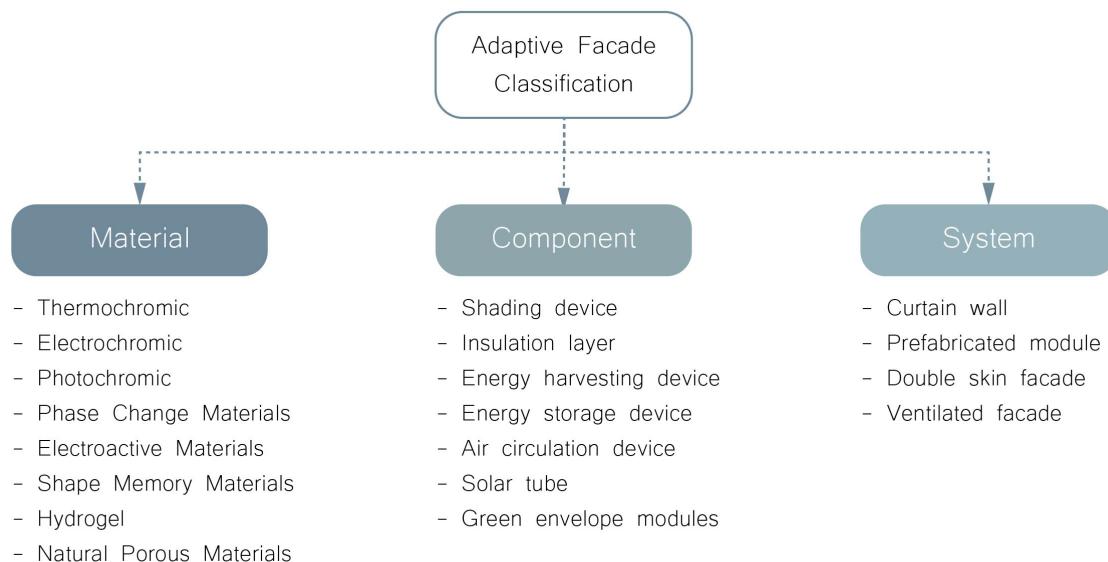| Material	Component	System
– Thermochromic	– Shading device	– Curtain wall
– Electrochromic	– Insulation layer	– Prefabricated module
– Photochromic	– Energy harvesting device	– Double skin facade
– Phase Change Materials	– Energy storage device	– Ventilated facade
– Electroactive Materials	– Air circulation device	
– Shape Memory Materials	– Solar tube	
– Hydrogel	– Green envelope modules	
– Natural Porous Materials		

Figure 11: Adaptive facades classification based on material, component and system scale. [adapted from Aelenei et al., 2018]

The above classifications provide a general overview of the possibilities and applications of the available adaptive facade technologies and show the potentials for implementation and the range of parameters that can be exploited to achieve the desired building performance and environmental response. Of particular interest are these technologies that can achieve the dynamic effect at the lowest scale of the facade system, which is the materials themselves, due to their inherent feature to reach significant levels of climatic responsiveness by minimizing external energy resources and complex mechanisms.

2.3.3. RESPONSE SYSTEMS AND TYPES [CASE STUDIES]

More particularly, based on the applied response systems and types, adaptive building envelope systems can be further subdivided into:

1. **responsive** devices: adaptive systems embedded in the core elements of the building's skin that measure the environmental conditions through a system of sensors in communication with a central control system which adjusts the form, shape, colour or character of the building through actuators.

2. **reactive** or **adaptive** devices: decentralized systems with local impact as action-reaction is managed by the one and same device.

3. **interactive** devices: a kind of Artificial Intelligence, having a centralized or decentralized multiple-loop control system allowing it to adjust or "learn" from the precedent experiences giving different output though stimulation might be of the same nature.

4. **autoreactive** systems: an evolution of reactive systems, using latent unused energy from their surrounding environment to achieve physical change through mechanical transmission or use of adaptive materials undergoing dynamic change in response to an external change of specific conditions.

5. **adaptronic** systems: which combine the characters of a centralized and a decentralized system, integrating a conventional centralized sensor-brain system and at least one functional material that allows localized embedded action and reaction to a specific modulus [Persiani, 2020].

The last two response system types are chosen for further exploration and will be analyzed more extensively throughout the research and design implementation.

To provide a better insight on the autoreactive systems, which introduce the next more specific section of the material study, these have the following characteristics:
- autonomous reaction
- kinetic output
- leftover energy
- functional purpose
- reaction to more than one input
- embedded materials with autoreactive properties, whereas the main parameters of auto-reaction can be divided into:
- System type:
    o type of change: change in degree and in kind
    o control center: centralized or decentralized
- Geometry:
    o structure: rigid or deformable
    o scale: small, medium, big
    o symmetry: bilateral, radial, asymmetric
- Energy:
    o radiant (temperature, light)
    o potential (humidity and precipitations)
    o kinetic (atmospheric turbulence and touch)
- Motion: motion strongly depends upon the geometry of the elements it is made of and co-evolves in natural systems as morphology is exploited energetically and mechanically. Furthermore, the material proprieties of a device (especially those of smart materials), can be used for counter-movements when not used as actuators [Persiani, 2020].

No matter how promising these systems are, the search for more dynamic and responsive technology tends to have increased most solutions' dependency on technology and energy rather than their independence. When smart, complex and expensive building technologies are subject to disproportioned amounts of resources in comparison to the achieved performance, the objective to exploit smart technological potentials is undermined. To counteract this downside, the present exploration also includes an effort towards minimizing complexity in mechanisms, actuators and number of mechanical parts of the adaptive facade systems.
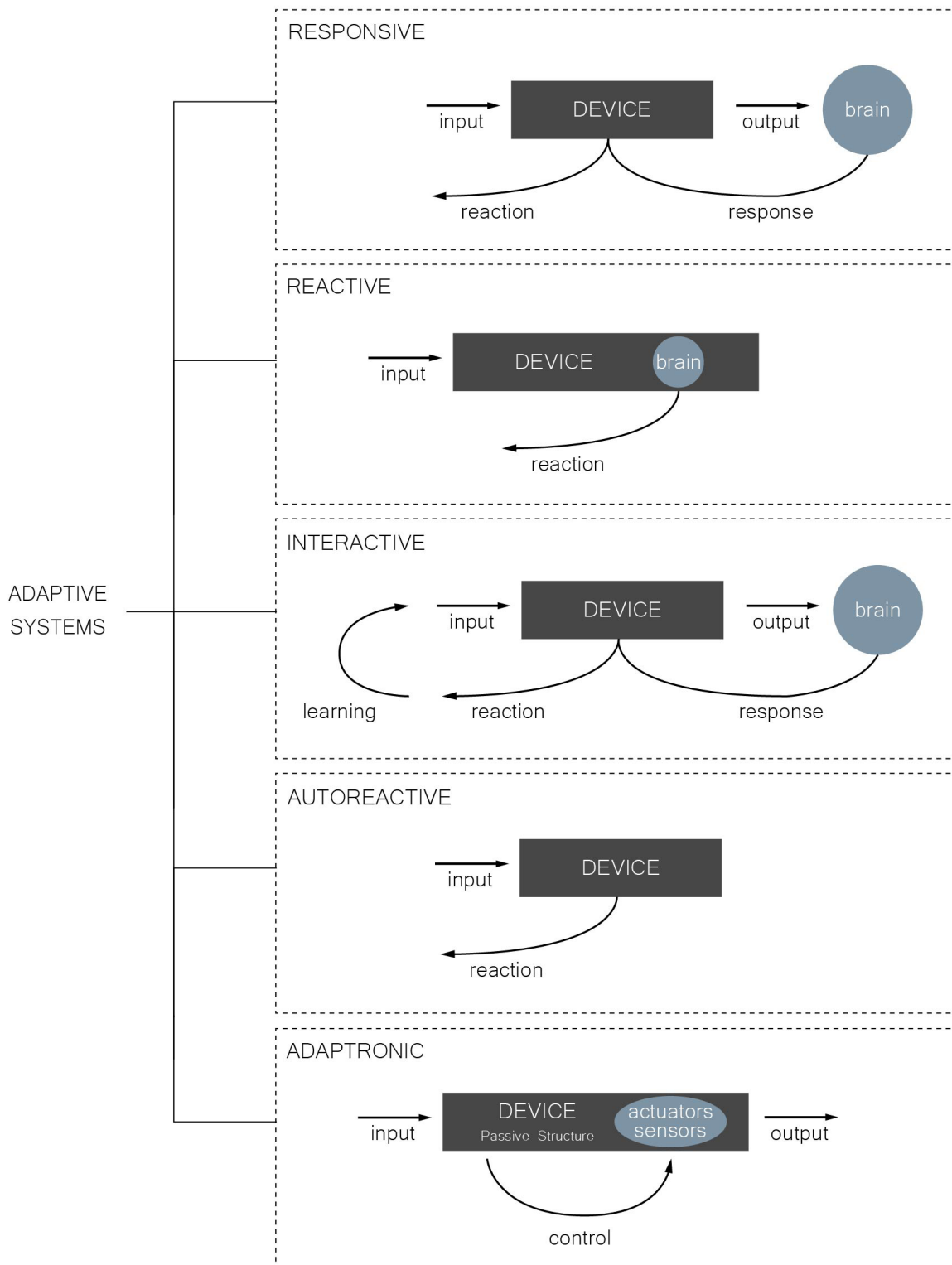
Figure 12: Scheme representing the adaptive systems' family. [adapted from Persiani, 2020]

A few representative examples showing the main principles in practice of some of the systems above are briefly explained below [Persiani, 2020]:

The facade of the Arab World Institute (AWI) in Paris is considered as the forerunner of the family of adaptive facade technologies. The double-glass facade integrates a metallic kinetic sunscreen system that adjusts the indoor light patterns depending on the outdoor light conditions. The kinetic system, which reinterprets the traditional Arabic "Moucharabieh" sunscreens, is realized as a multitude of motor-controlled camera-like metal diaphragms of different sizes and is considered a responsive system.

The "Kinetic Wall" is an interactive installation using kinetic petals that react to the presence of users by opening up dynamic windows on the wall and is triggered by a detection system that reacts to movements.

The "Hygroscope" installation explores the potential of a hygroscopic (humidity-sensitive) material to achieve kinetic response and is therefore considered a fully autoreactive system. The kinetic parts are thin triangular surfaces made of a maple veneer and synthetic composite, which is programmed to react differently depending on the fiber direction, the length, thickness and geometry. Absorption of humidity causes the distance between the fibers of the wood to increase, resulting in a swelling and lengthening of the material in the direction of the fibers.

The "Homeostatic" facade system is made of thin stripes integrating an electro-active polymer (EAP) wrapped around a flexible core, allowing the section of the stripes to bend with the expansion or contraction of the polymer. The actuation of one surface of the plates creates a bending and a deformation effect similar to that of a bi-metal, which is used to gradually shade the facade for light, solar and heat control. The movement in this system is directly controlled through a sensor-brain system integrating a functional material and the system can be considered to be an adaptronic one, with a kinetic mechanism that can also be employed in many autoreactive systems.
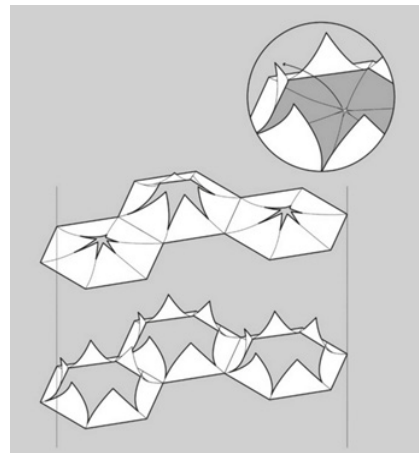

Figure 13: Scheme of the curling veneer flaps in the hygroscope system. [Persiani, 2020]
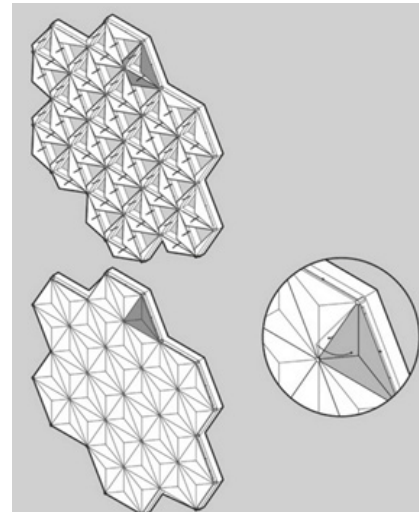

Figure 14: Scheme of the opening and closing of the kinetic wall (left) and a detail of the flaps performing the movement. [Persiani, 2020]
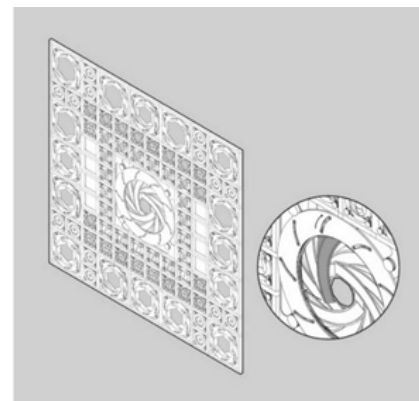

Figure 15: Scheme of the moucharabieh shutters and detail of one of the plates in the shutters that are rotated. [Persiani, 2020]
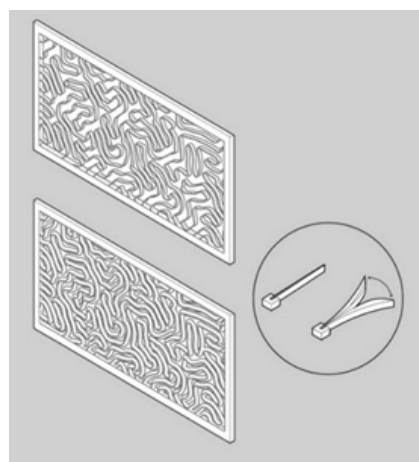

Figure 16: Scheme of the homeostatic facade kinetic transformation (left) and sectioned detail of the strips achieving the kinetic change (right). [Persiani, 2020]

BACKGROUND RESEARCH - MATERIAL AND MECHANISM

3.1. THERMO-RESPONSIVE AUTOREACTIVE SMART AND MULTIFUNCTIONAL MATERIALS

At a material scale, smart materials and structures are supposed to be able to respond to environmental changes at the most optimum conditions and adapt their own functions according to the changes, that is, they can respond in a pre-determined manner in an appropriate time with an environmental stimulus and then revert to their original states as soon as the stimulus is removed [Wei et al., 1998]. They are designed materials that have properties that can be significantly changed in a controlled way by an externally applied field value, such as stress, temperature and electric or magnetic fields. This behaviour enables them to fulfill actuation and sensing in one component. An advantage compared to conventional systems is their high integration and reduced complexity of mechanical parts, as they are the system itself combining sensing, actuation and mechanical functions. This favours their application in lightweight structures and development of dynamic systems [Drossel et al., 2015].

In the case of architecture and dynamic facades, even though adaptive facades show strong potential to exploit environmental resources through their dynamic behaviour, there is still more research needed in this respect. The cost-intensive and mechanical complexity natures of such systems of the past decades directed researchers' interest towards passive material-based actuation systems [SimAUD, 2017]. Aligned to this direction, one of the objectives of the current thesis is to achieve a balance between sophistication and benefit, by employing these innovative facade systems with a high and passive response to environmental changes.

Consequently, to trigger the response of the envelope, no external actuator or complex software management would be necessary. Nevertheless, these materials do not fulfil all the facade requirements by themselves. Thus, they need to be combined with other adaptive technologies and building elements, in order to be functional and feasible. Some of their promising potentials when applied in the external layer of the envelope, include the dynamic temperature change of the external cladding through the solar reflectance change and the enhancement or prevention of thermal losses through shape-changing ventilated facades [Juaristi et al., 2020].

This adaptiveness can be in favour of both reflecting the solar radiation and enhancing the building's energy performance, by reducing its cooling demands, and in both ways contributing directly and indirectly to the UHI reduction in a self-regulating and autoreactive manner. In the current context, the thermo-responsive smart materials are chosen to be studied further and implemented in a facade system design, in order to exploit the increased heat and solar radiation, caused by the UHI effect and HWs, which act as triggering environmental stimuli for the dynamic activation of the material system and its resulting response mechanism. Due to the fact that they are activated by a difference in temperature, these are promising candidate materials for activating smart morphing solar shadings with the thermal effect of incident solar radiation [Fiorito et al., 2016].

Even though their use could reduce the construction complexity in a dynamic adaptive facade implementation, their analysis in the facade industry is still underdeveloped and makes it difficult to retrieve relevant technical information, especially when researching on the properties of the material. Due to the difficulty to estimate the facade's performance well in advance, part of the study is also to reflect on the design implications that possible facade applications of such advanced materials could entail.
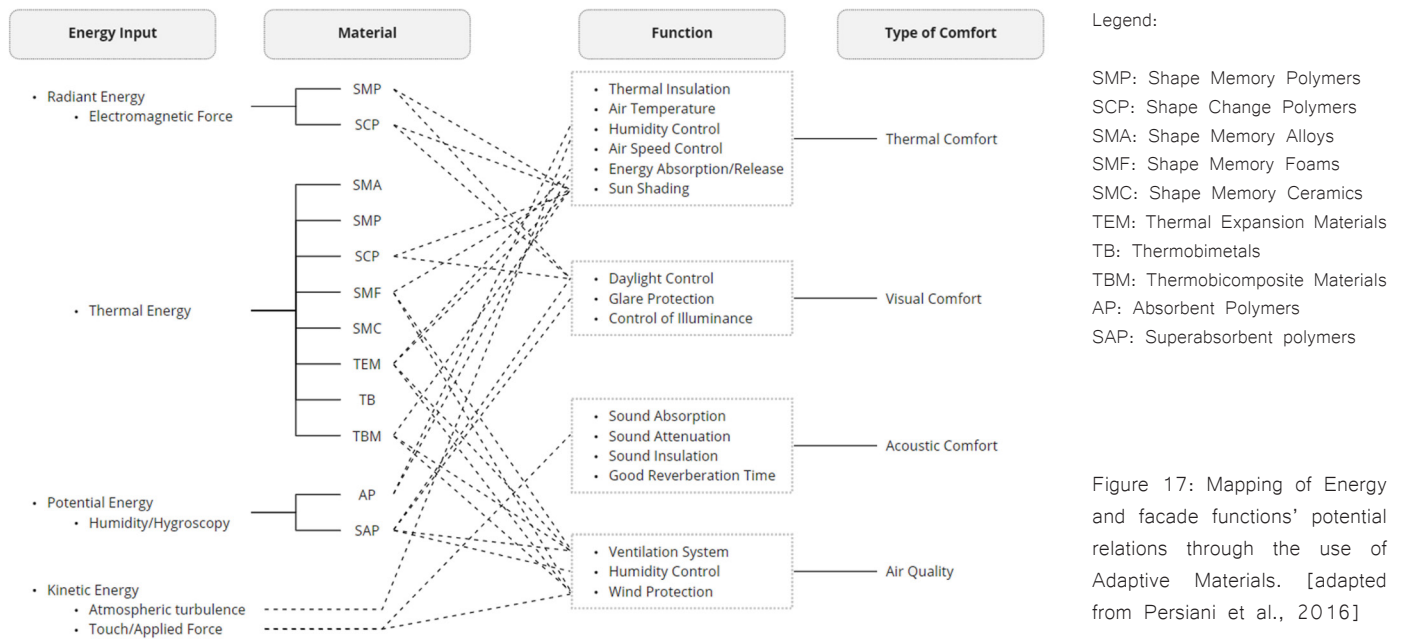
3.1.1. STAGES OF INTELLIGENT PROCESS

Figure 17: Mapping of Energy and facade functions' potential relations through the use of Adaptive Materials. [adapted from Persiani et al., 2016]

Legend:

SMP: Shape Memory Polymers
SCP: Shape Change Polymers
SMA: Shape Memory Alloys
SMF: Shape Memory Foams
SMC: Shape Memory Ceramics
TEM: Thermal Expansion Materials
TB: Thermobimetals
TBM: Thermobicomposite Materials
AP: Absorbent Polymers
SAP: Superabsorbent polymers

In a general spectrum, this type of materials belongs to the broader family of smart and multifunctional materials, also known as information materials. "Smart" implies notions of an informed response, with associated qualities of alertness and quickness and also an association with an intuitive or intrinsic response. Smartness in a material or system is determined by one or two mechanisms, which can be applied directly to a singular material, and conceptually to a compound system. If the mechanism affects the internal energy of the material by altering either the material's molecular structure or microstructure, then the input results in a property change of the material. If the mechanism changes the energy state of the material, but does not alter the material per se, then the input results in an exchange of energy from one form to another [Addington, 2012].

The five fundamental characteristics that were defined as distinguishing a smart material from the more traditional materials used in architecture are transiency, selectivity, immediacy, self-actuation and directness. These can be described as follows:

– **Immediacy**: real-time response

– **Transiency**: responsive to more than one environmental state

– **Self-actuation**: internal intelligence to rather than external to the 'material'

– **Selectivity**: the response is discrete and predictable

– **Directness**: the response is local to the "activating" event

[Addington, 2012]

There are various ways to describe the intelligent process of a system, depending on the different points of view and with a strong relevance to studies on natural systems. By using a functional approach, which is based on biological and psychological observations, this process is divided into three main linear stages:

perception → reasoning → action

These steps can be used to enable adapting the creative process of building envelopes to be designed following suitable steps for a given objective, as in this case, high performance through adequate climate approaches.

The first stage, perception, deals with the acquisition of information about the surrounding environment and its transformation into the communication format that the intelligent system uses for collecting such information, in this case the material itself. The information caused by the stimulus is translated, organized and interpreted to be used for the second stage. The second stage, reasoning, is a problem-solving procedure and implies a pre-defined set of actions. Data can be interpreted on different levels, such as environmental data, and logical rules might indicate an almost automatic action. Action, the third step, is the triggering of an activity as response to the initial stimulation that was detected by the perception system. It executes the conclusions reached by the logical system, performing a change in the physical properties of the intelligent system with no external energy for the activation.

As described by the steps and feedback mechanisms, intelligence is a concept with inherent dynamism and long-term adaptability towards maintaining a given goal. Changing conditions are answered by a set of responses which use the least energy possible and are always being adjusted according to information provided by external conditions, and this is one of the core challenges for sustainable design of responsive building envelopes [Capeluto et al., 2016].

Similarly, in the case of the adaptive facades, a certain level of automated self-regulation may also be considered [Macias-Escriva et al., 2013]. Such a self-adaptive and intelligent system involves the recording of information, data processing and control, and its transference in adaptations of the construction. Important component is, therefore, an existing sensing system, which determines relevant information about conditions (e.g. environmental) and other requirements. Furthermore, a control system processes the recorded information and transmits impulses to actuators, which then perform the adjustments of the construction [Böke et al., 2018].
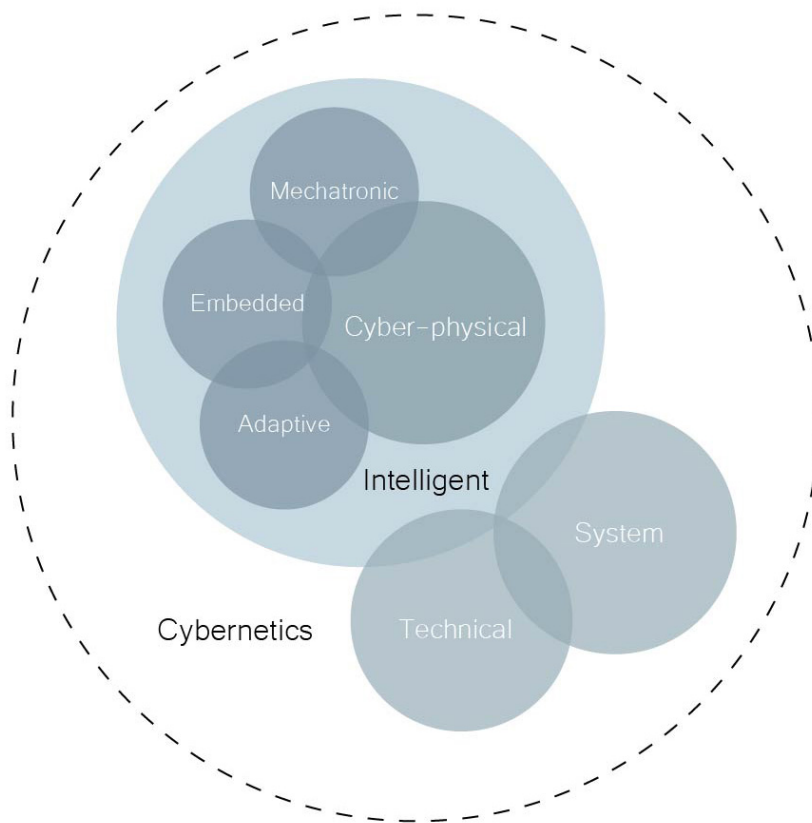

Figure 18: Visualization of the 'intelligent technical systems' section contexts. [adapted from Böke et al., 2018]

3.1.2. THERMO-RESPONSIVE SHAPE MEMORY MATERIALS (SMMs)

3.1.2.1. INTRINSIC FEATURES AND INHERENT DYNAMIC BEHAVIOUR

Narrowing down the focus even further, Shape Memory Materials (SMMs) belong to the energy-exchanging smart materials and are one of the major elements of intelligent composites because of their unusual properties, such as the Shape Memory Effect (SME), autoreactivity, large recoverable stroke (strain) and adaptive properties which are due to the (reversible) phase transitions in the materials. Superelasticity (in alloys) or visco-elasticity (in polymers) are also commonly observed under certain conditions [Otsuka et al., 2018].

More specifically, thermo-responsive SMMs can sense thermal stimulus and exhibit actuation or some pre-determined response, making it possible to tune some technical parameters such as shape, position, strain, stiffness and other static and dynamical characteristics [Wei et al., 1998]. An input of thermal energy (which can also be produced through resistance to an electrical current) alters the microstructure through a crystalline phase change, which enables multiple shapes in relationship to the environmental stimuli [Addington, 2012].
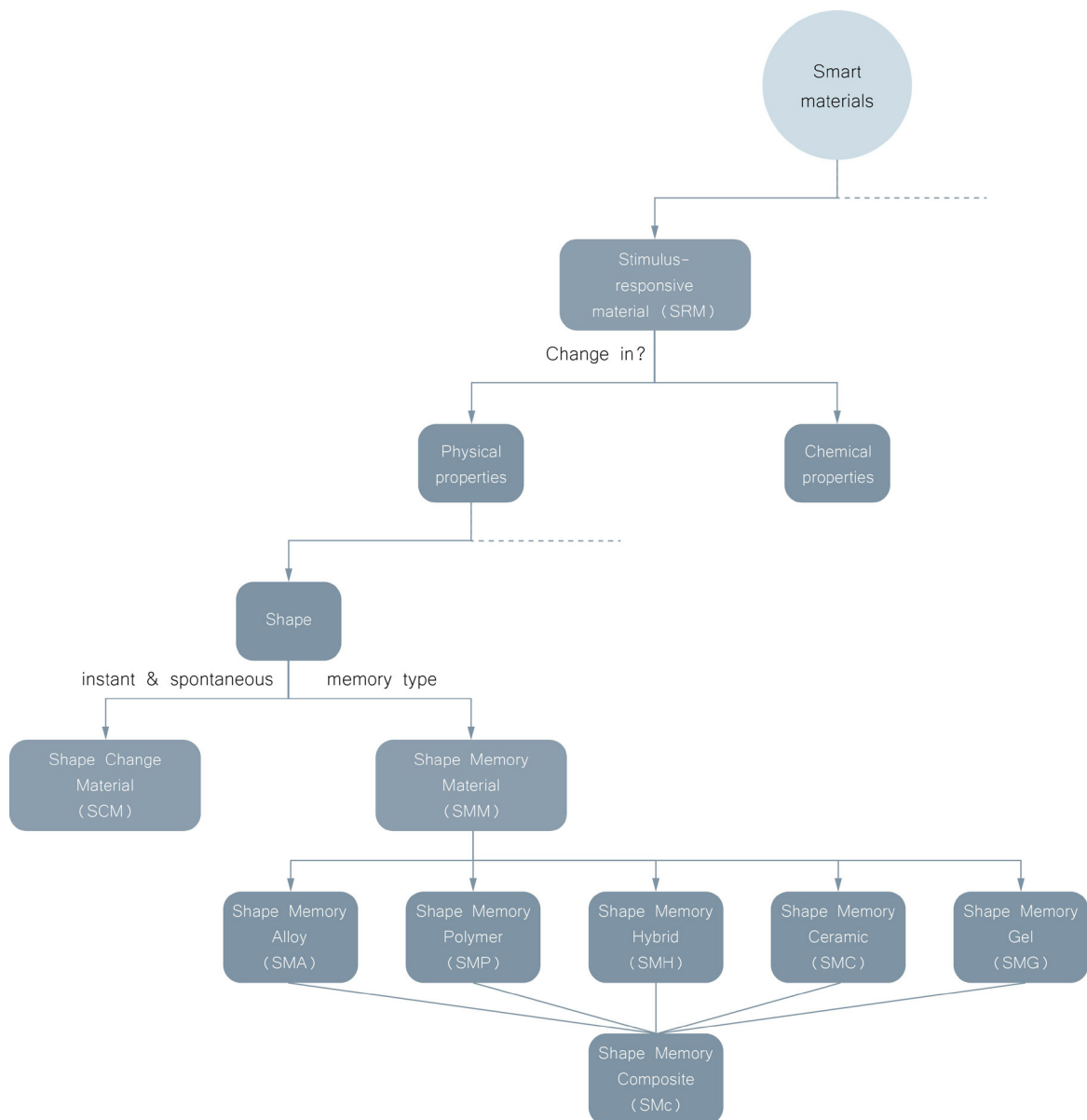

Figure 19: Location of various types of SMMs within the world of materials. [adapted from Sun et al., 2012]

3.1.2.2. CLASSIFICATIONS AND MATERIAL EVALUATION

There is a number of types of SMMs, which have been developed so far. Among them, Shape Memory Alloys (SMAs) and Shape Memory Polymers (SMPs) are the most developed ones at present, while there is a newly emerging type of SMMs, namely Shape Memory Hybrids (SMHs), which enable non-professionals in materials science to design SMMs with tailored properties/features for a particular application in a "do-it-yourself" manner [Fiorito et al., 2016][Huang et al., 2010].

Shape Memory Alloys

Thermo-responsive SMAs are featured by the four characteristic temperatures, namely austenite start temperature (A_s), austenite finish temperature (A_f), martensite start temperature (M_s) and martensite finish temperature (M_f). Upon cooling from high temperature austenite phase, the martensitic transformation starts at M_s and finishes at M_f. Upon heating from low temperature martensite phase, the reverse martensitic transformation starts at A_s and finishes at A_f. While at low temperatures, SMAs have the SME, at high temperatures, recovery can be achieved instantly and simultaneously upon releasing the applied load [Sun et al., 2012].
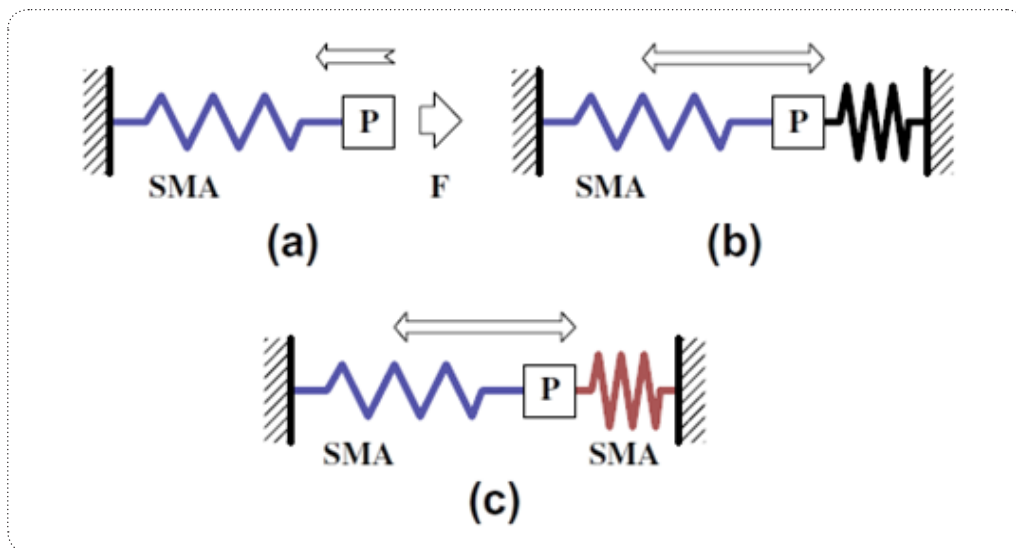

Figure 20: Three basic types of SMA actuators based on the one-way SME. (a) One-way actuator; (b) biased actuator and (c) two-way actuator. [Sun et al., 2012]
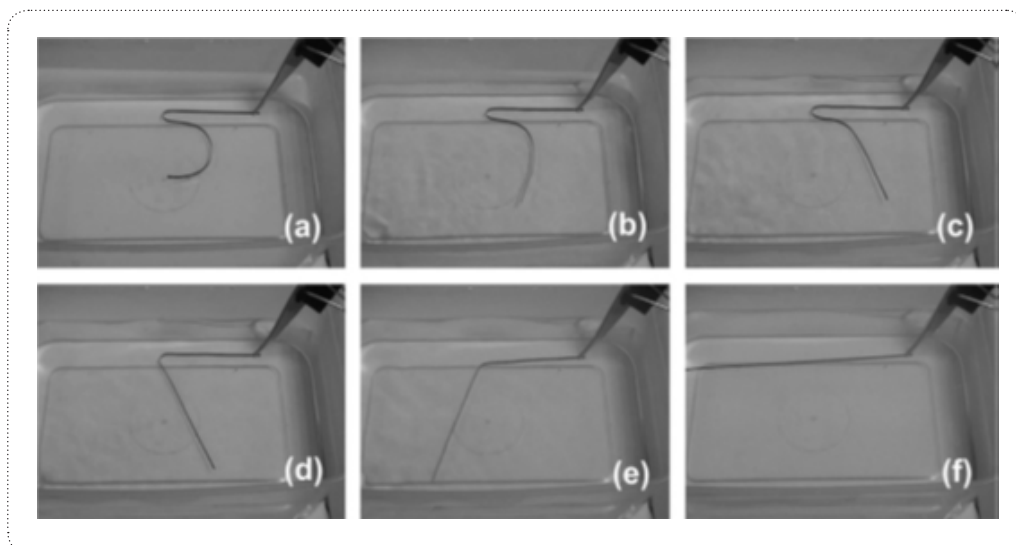

Figure 21: Triple-SME upon heating after local bending to introduce a gradient transition temperature field. [Sun et al., 2012]

Shape Memory Polymers

As a general concept, the Shape Memory Effect is not an intrinsic property of the SMPs, meaning that polymers do not display this effect by themselves. Shape Memory results from a combination of polymer morphology and processing and can be understood as a polymer functionalization [Behl et al., 2011]. The SME in SMPs is based on a totally different mechanism. Regardless of the types of the stimuli, there are two basic segments/domains in a SMP, one is elastic segment, and the other is transition segment. While the elastic segment always maintains high elasticity within the whole SME cycle, the transition segment does change its stiffness significantly at the presence of the right stimulus. SMPs normally are hard at low temperatures and become soft at high temperatures [Fiorito et al., 2016]. Shape memory polyurethanes

（SMPUs）remain one of the main classes of SMPs studied. Their attractiveness mainly lies in their ease of processing, low cost and high thermal and mechanical performance [Behl et al., 2011].

There are certain advantages of the SMPs over the SMAs which make their application appealing. To name a few, they have a lower density, lower cost of raw material and fabrication, while they can be easier programmable and 3D printable. Apart from that, the recoverable strain is normally higher, it is easier to tailor the thermo-mechanical properties of SMPs, the shape recovery temperature range can be easily altered within a wide range and even gradient and they have a higher potential for recycle and reuse at low cost. However, they may require a higher level of material understanding to program to the desired dynamic performance.
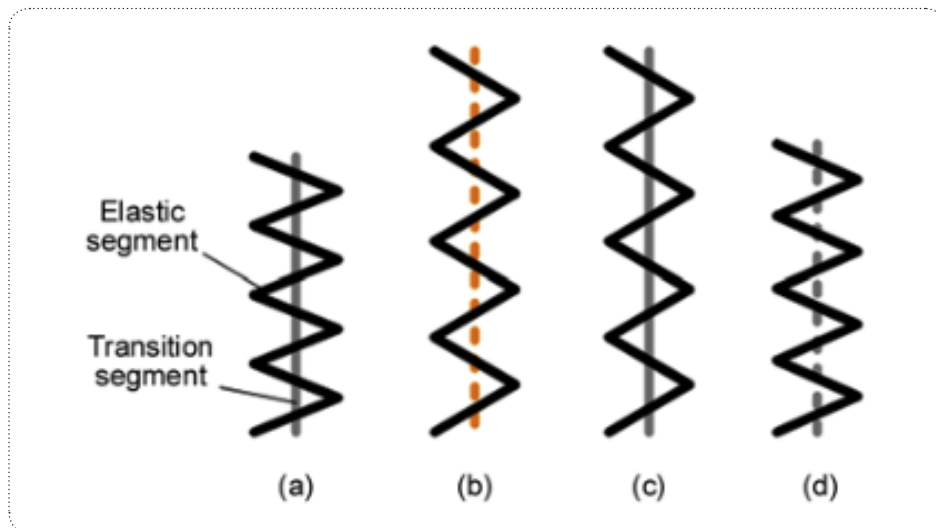

Figure 22: Illustration of the Shape Memory Effect: normal state（a）, deformed state（b）, preserved state（c）, recovered state（d）. [Fan et al., 2011]
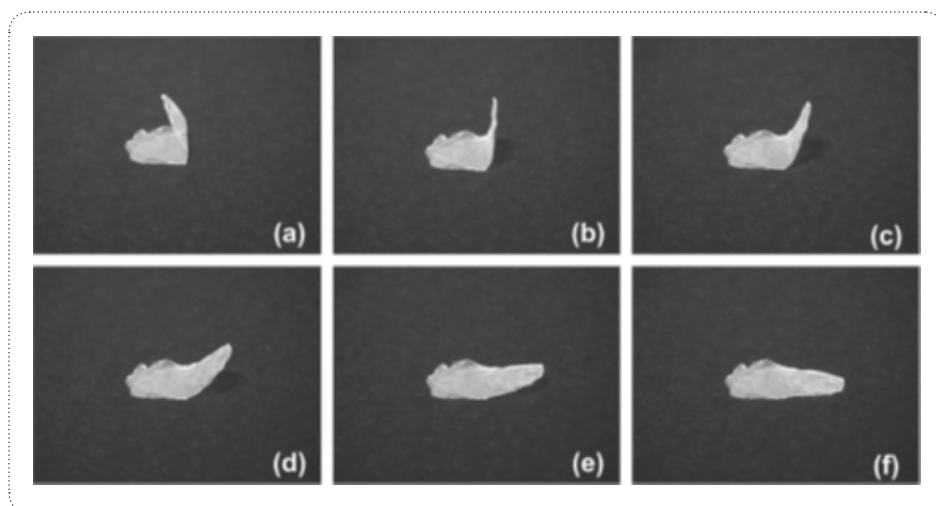

Figure 23: Shape recovery in a 300 nm thick PU SMP film upon heating. [Sun et al., 2012]

Shape Memory Hybrids

Despite the fact that the properties of SMPs can be more easily tailored than SMAs, the successful synthesis of a particular SMP for a special application normally requires strong chemical/polymer background, years of experience and great efforts in trial and error. This is not readily accessible to even every materials researcher. SMHs can provide an alternative solution that is based only on some simple concepts and utilizes only ordinary materials, which have well understood properties but do not have Shape Memory as an individual. Thus, the design of a SMM for a particular application turns out to be a routine which is easily accessible by ordinary engineers and even non-professionals in a do-it-yourself（DIY）fashion.

The mechanism behind the Shape Memory phenomenon in SMHs is the elastic-transition segment/domain system. An example would be silicone and wax, which both are biocompatible, as the elastic matrix and the transition inclusion, respectively. Ideally, in a SMH, there is not any chemical interaction between the matrix and the inclusion, so that the properties of the individual materials are largely maintained. Therefore, the properties of the SMHs can be well predicted from the very beginning. For instance, the transition temperature of the SMH is the softening temperature of original inclusion material. Aging, relaxation, and fatigue etc. can also be well controlled [Sun et al., 2012].
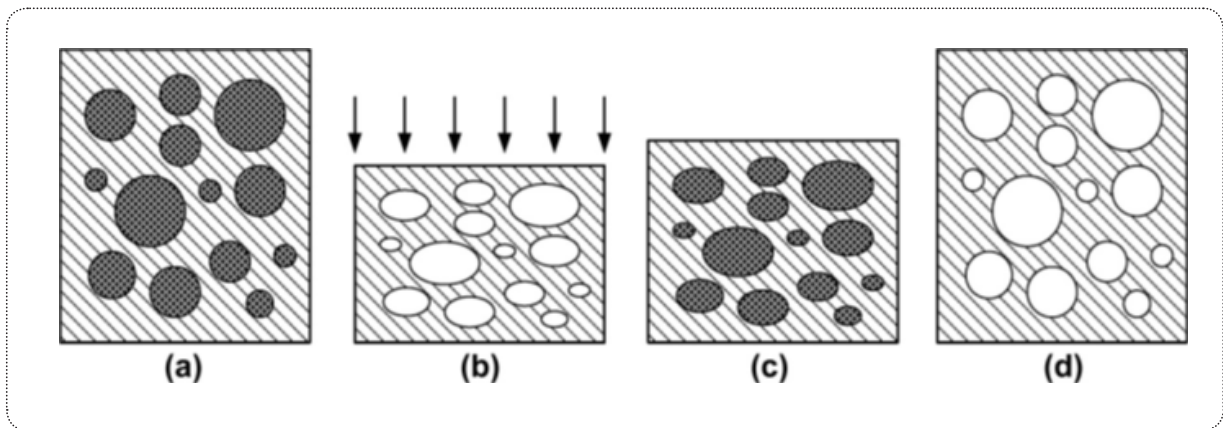

Figure 24: Illustration of mechanism for the SME in SMH. [Sun et al., 2012]
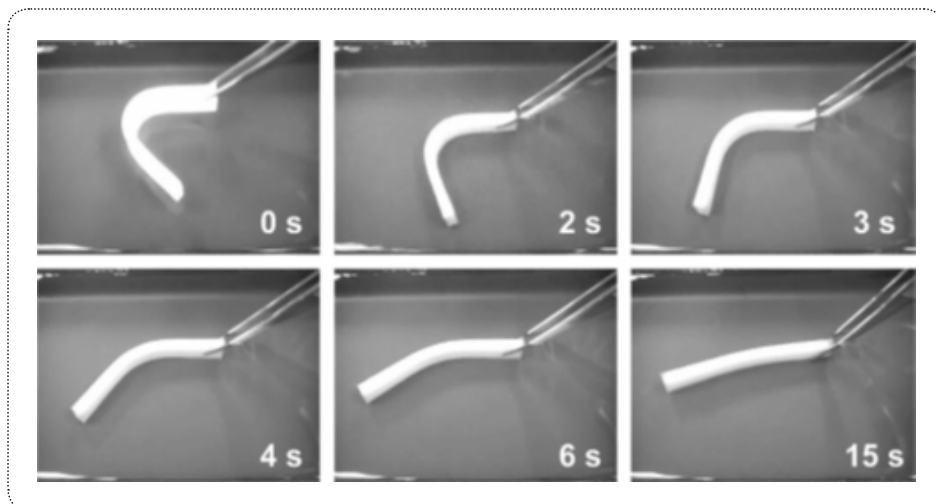

Figure 25: Shape recovery in a silicone/wax SMH upon immersing into hot water. [Sun et al., 2012]
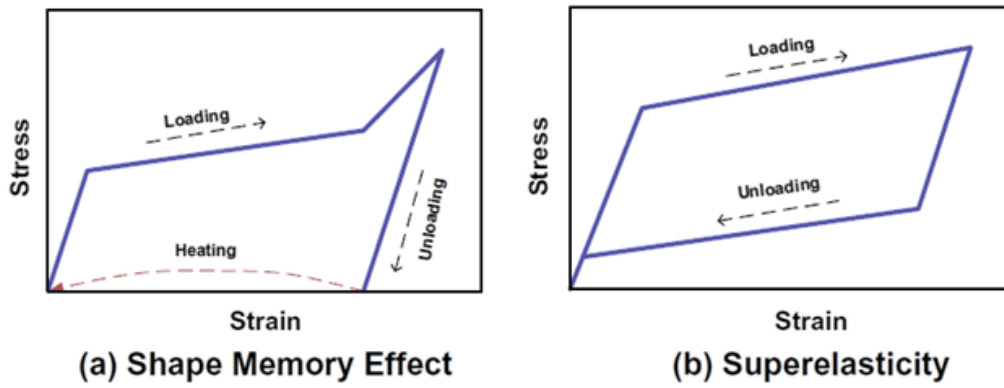
Figure 26: Shape Memory Effect (a) and Superelasticity (b) in SMA. [Sun et al., 2012]
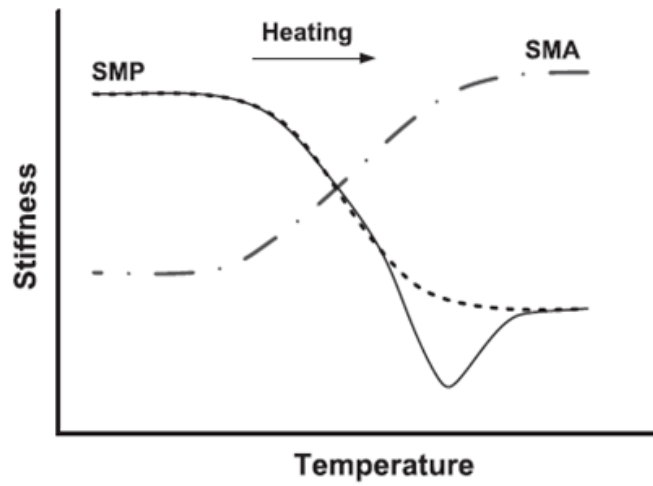

Figure 27: Change of stiffness in thermo-responsive SMMs upon heating. [Sun et al., 2012]
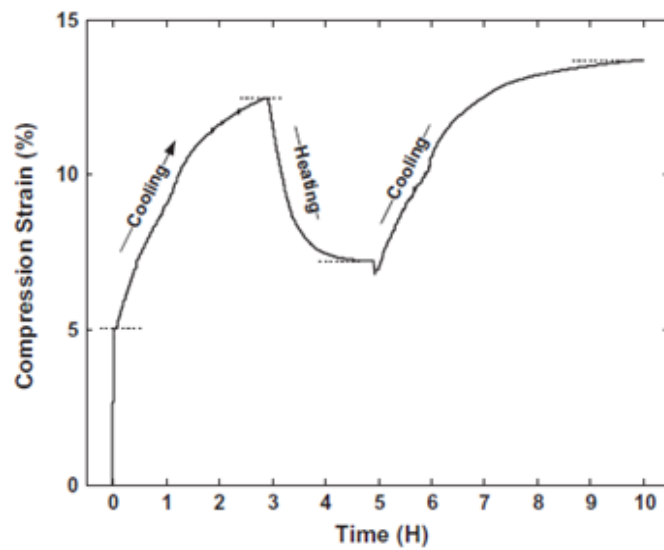

Figure 28: Compression strain against time (in hour) in a SMH during thermal cycling against a constant stress of 176 kPa. [Sun et al., 2012]

A brief overview and comparison of the three available Shape Memory Material families can be found in the tables below (these and some additional tables can also be found in the Appendix):

Table 1: SMA features [information retrieved from Fiorito et al., 2016]

SMA					
+	–	Mechanism	Alloy-based classification		
As an actuation material, SMAs are more powerful than SMPs. The actuation stress in SMAs is 10s MPa and above, while that in SMPs is a few MPa at the most	The difficulties in working with SMAs are related to their different behaviour and characteristics due to many different possible martensitic configurations	Thermo-responsive SMAs are featured by the four characteristic temperatures, namely austenite start temperature (As), austenite finish temperature (Af), martensite start temperature (Ms) and martensite finish temperature (Mf). Upon cooling from high temperature austenite phase, the martensitic transformation starts at Ms and finishes at Mf. Upon heating from low temperature martensite phase, the reverse martensitic transformation starts at As and finishes at Af. While at low temperatures, SMAs have the SME, at high temperatures, recovery can be achieved instantly and simultaneously upon releasing the applied load. This is called the super-elasticity (SE). According to the definition above, the SME is the characteristic of the SMM, while the SE is that of the SCM.	NiTi based	Cu-based	Fe-based
Biocompatibility, high corrosion resistance and high electrical resistance	Possible change in the mechanism properties after programming		+ Higher recoverable strain (around 7%), generated force and corrosion resistance		
Super-elastic behaviour			+ High actuation stress (up to 500 MPa)		
			+ High biocompatability		
			– Higher costs		

Table 2: SMP features. [information retrieved from Sun et al. (2012), Leng et al. (2011)]

SMP								Market diffused SMPs		
+	–	Mechanism	Chemical architecture classification					Base Material SMP	Ttrans [°C]	Company / Producer
Lower density PU SMP: 1.25 g/cm3 NiTi SMA: 6.4 g/cm3	More difficult to predict the behaviour of the polymers precisely due to significant relaxation, degradation, etc	The SME in SMPs is based on a totally different mechanism. Regardless of the types of the stimuli, there are two basic segments/domains in a SMP, one is elastic segment, and the other is transition segment While the elastic segment always maintains high elasticity within the whole SME cycle, the transition segment does change its stiffness significantly at the presence of the right stimulus. Carefully examining the mechanism behind the SME reveals that opposite to that in SMAs, SMPs normally are hard at low temperatures and become soft at high temperatures. Therefore, SMPs alone are normally not applicable in cyclic actuation, unless there is a V-shape in the stiffness vs. temperature curve upon heating, which has been found in a couple of SMPs	chemically cross-linked glassy thermosets	chemically cross-linked semicrystalline rubbers	physically cross-linked amorphous thermoplastics	physically cross-linked semicrystalline block copolymers		Styrene butadiene	60-70	Asahi company
Lower cost in fabrication and processing	The SME in SMPs may be affected by the programming conditions							Styrene-based (Veriflex®)	60-70	Cornerstone research group
Easily produced with high quality into almost any specified shapes at different scales using various traditional and advanced polymer processing technologies	Possible change in the mechanism properties after programming							One part epoxy	90	Cornerstone research group
Recoverable strain is normally an order higher than that in SMAs	The successful synthesis of a particular SMP for a special application normally requires strong chemical/polymer background, years of experience and great efforts in trial and error							Two parts epoxy	104	Cornerstone research group
It is easy to tailor the thermo-mechanical properties of SMPs by means of, for instance blending with different types of fillers or varying the compositions	Current understanding of the thermomechanical behaviour of SMPs is limited to one-dimensional deformation							Cyanate ester	135-230	Cornerstone research group
It is possible to be always transparent								Thermosetting epoxy	113	Composite technology development
Shape recovery temperature range can be easily altered within a wide range and even gradient								Thermolastic polyurethane	40-55	Mitsubishi heavy industry
Damping ratio in particular within the transition range is higher										
The potential for recycle and reuse at low cost is higher										
Many SMPs have excellent chemical stability, biocompatibility and even biodegradability										
SMPs are more flexible in surface patterning for different patterns at different scales, and the resulted surface patterns are more permanent										
SMPs can be integrated into mechanical/ structural design as one part or parts of a structure for load carrying under normal working situation										

Table 3: SMH features. [information retrieved from Sun et al., 2012]

SMH			
+	–	Mechanism	Matrix/inclusion structure
Based on simple concepts and ordinary materials with well-understood properties	Not enough research carried out to beeter understand their thermo-mechanical properties	The mechanism behind the shape memory phenomenon in SMPs is the elastic-transition segment/domain system. For example, if silicone and wax are selected, both are biocompatible, as the elastic matrix and the transition inclusion, respectively. While silicone normally keeps its high elasticity characteristic within a wide range of temperatures, wax melts upon heating to its melting temperature, and becomes very soft. As such, the sample can be easily compressed. The silicone matrix is elastically deformed, so that an elastic energy is stored in it. When the sample is cooled back to room temperature, wax becomes solid again, which can effectively prevent the release of the elastic energy in the silicone matrix. Consequently, after the constraint is fully removed, the sample largely maintains its deformed shape until it is heated again to above the melting temperature of wax.	Silicone/wax
The accessibility, flexibility in design and fabrication of SMH provides an easy access to ordinary people, even without much chemical/ polymer background	Due to the different composition of SMHs, their modelling requires a specific applied study, even if SMHs can be modelled in similar ways to SMPs		Silicone/water
Can be biocompatible			
Both the matrix and inclusions are not limited to polymers only, but can be selected from any materials			
There is not any chemical interaction between the matrix and the inclusion, so that the properties of individual materials are largely maintained			
The properties can be well predicted from the very beginning by means of materials selections and simple estimation			
Aging, relaxation, and fatigue etc. can be well controlled			
They are convenient to be tailored to meet the exact requirement(s)			
Proven ability of silicon-wax SMH for cyclic actuation			
Similar shape memory effect to the SMPs' one			

Table 4: SMM families comparison. [information retrieved from Sun et al., 2012]

	SMAs	SMPs	SMHs
Description / Composition	Most diffused are NiTi-based alloys. Classified in Ni-Ti based, Cu-based and Fe-based	More than 20 different types of SMPs. Most common are thermoplastic polyurethanes and epoxy SMPs	Composed of materials with no shape memory effect on their own. They are "custom made". The most studied are Silicon-Wax Hybrids
Movement / Morphing effect	Stress recover and original shape recover. Small contraction (up to 10%) and deformation. A force is required to re-establish the original shape	Stress recover and original shape recover. High deformation (up to 800%). A force is required to reestablish the original shape	Stress recovery and original shape recovery. Small reversible strain (up to 6-8%). A force is required to reestablish the original shape
Durability issues	More than 200,000 cycles for NiTi alloys. In NiTi alloys high resistance against corrosion and external weather	Up to 200 cycles for SMPU tested. Can be affected by external weather conditions	Currently no experimental data. External weather condition resistance related to composition
Recovery temperature	-10 °C to +200 °C NiTiCu alloys can be tailored for shading devices, As ~ 45-60 °C	+25 °C to +200 °C Can be tailored at lower temperatures Tg ~ 60-90 °C	Vary with the components: silicon-wax hybrids have an activating temperature of ~ 45 °C
Density	6000-8000 kg/m3	900-1100 kg/m3	Variable
Elastic Modulus E above Ts	70-100 Gpa	0.5-4.5 GPa 1.24 GPa (Polystyrene SMP)	Variable
Elastic Modulus E below Ts	28-41 GPa (NiTi SMAs)	2-10 GPa (Polystyrene SMP)	Variable
Transformation strain	6-8%	250-800% 50-100 % (Polystyrene SMP)	~6% (Silicone-Wax)
Actuation stress	150-300 MPa ~100 MPa (NiTi SMAs)	2-10 MPa	Variable
Market availability and shape	Wires (different diameters, already educated in range from few μm to 1 mm) Springs Plates/Sheets	Easily customized shape	Mainly derived from DIY approach User's desired shape
Sustainability	Biocompatible	The potential for recycle and reuse at low cost is higher Many SMPs are biocompatible and even biodegradable	Can be biocompatible Organic materials can be used

3.1.3. APPLICATIONS – CLIMATIC RESPONSIVENESS AND FACADE INTEGRATION

SMMs have been broadly used in a wide range of fields, with a large interest in aerospace and automobile industry, with applications that include hinges, trusses, optical reflectors and morphing skins, exploiting the deformability and elasticity of SMAs the most. In addition, SMPs also present additional potential in the areas of biomedicine, smart textiles and self-healing composite systems due to their autoreactive response mechanisms and shape reversibility in biodegradable ways. In architecture and engineering, the application of SMMs is still in an initial stage, however, there are already developments and interest in this direction as well. Most common examples are self-healing systems, actuators, sensors and vibration control systems, as well as smart and solar morphing envelopes to enhance the building's thermal comfort and energy performance and saving, which is towards where the current study is directing the research scope [Li et al., 2018].

In facade applications, there is still more research needed for the implementation of SMM technologies to be able to exploit the material's inherent dynamic behaviour in a holistic functional system. However, the autoreactive feature of these materials to the environmental changes would enable a low-energy and low-tech control of the thermal behaviour of the building envelope. In the Table below [Table 5] some potential applications are shown with their corresponding principles in SMM integration in the built environment in an energy-efficient way [Li et al., 2018].

Table 5: Potential applications of shape memory polymers in built environments. [adapted from Li et al., 2018]

|	Potential application	Principle	Reference
1	Active building facades with self-regulating sun protectors	A broad melting temperature range of temperature memory polymers based on crosslinked copolymer networks	[Behl et al., 2013]
2	Self-shading articulated surfaces	Two-part SMP filaments with different Tg values, forming variable stiffness tiles that respond to different incident solar heat levels	[Clifford et al., 2017]
3	Smart building envelopes	Integrated conventional one-way shape memory (SM), two-way reversible SM, and one-way reversible SM in semicrystalline SMPs	[Zhou et al., 2014]
4	Adaptive building envelopes	Significant reversible elongation resulting from crystallization of crosslinked poly (cyclooctene) films under tensile loads and induced cooling or heating	[Chung et al., 2008]
5	Functional smart architecture	Under various constant stresses, phase-segregated polyester urethanes (PEUs) with two-way shape changes between $-20°C \sim 60°C$	[Bothe et al., 2012]
6	Convertible roofs	Using a layering technique to combine the SMP and elastic polymer, which forms novel polymer laminates with a two-way shape-memory effect (two-way SME)	[Chen et al., 2008]
7	Interactive kinetic walls	Reversible actuation of ultrathin semicrystalline polymer films	[Stroganov et al., 2015]
8	Changeable architecture	The design and fabrication of polymer particles with two-way SMP abilities between $0°C \sim 43°C$ under stress-free conditions	[Gong et al., 2014]
9	Thermally comfortable buildings	Copolymer networks from oligo (ε-caprolactone) an n-butyl acrylate that enable a reversible bidirectional SME at human body temperature	[Saatchi et al., 2015]
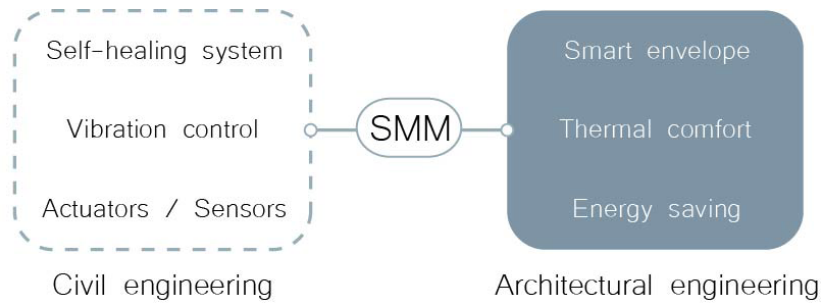
Figure 29: Applications of SMPs in civil and architectural engineering. [adapted from Li et al., 2018]
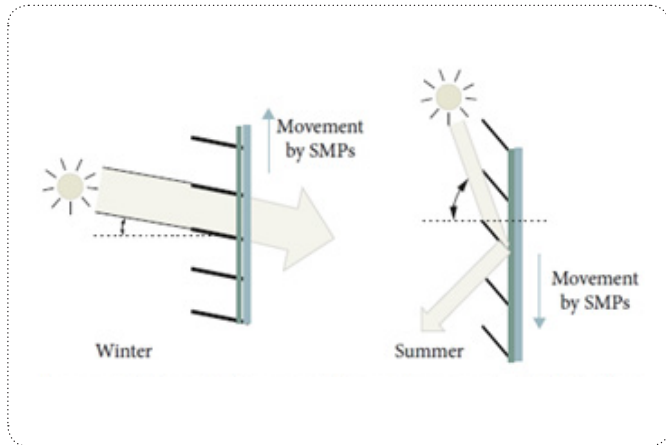

Figure 30: Schematic diagram of thermally responsive SMPs in heat controls of window blinds. [Li et al., 2018]
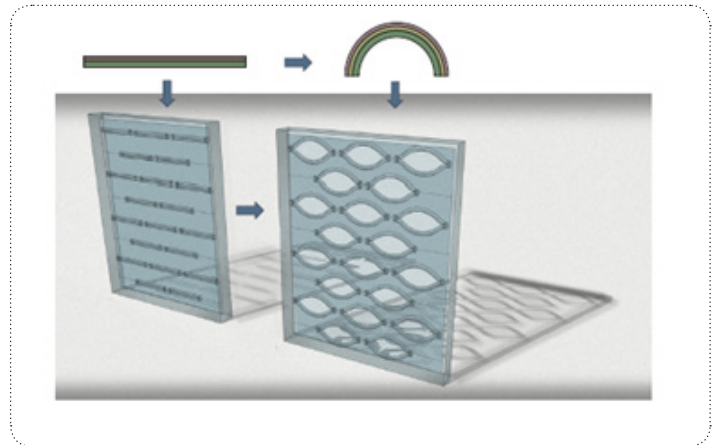

Figure 31: Schematic diagram of composite SMPs in shading controls. [Li et al., 2018]

3.1.4. "SMM FACADE INTEGRATION – UHI EFFECT" HYPOTHESIS

The above research on the material properties and behaviour already highlights some of the advantages and potentials of thermo-responsive SMMs to be implemented in adaptive facade applications due to their high level of direct responsivess and adaptation to real-time environmental changes, while they become attractive thanks to the ability to program their behaviour and, therefore, predict their dynamic performance and deformation. Of special attention are the inherent abilities of these materials, by applying the Shape Memory Effect to control the thermal transmission at the building envelope, increase the solar radiation reflectivity and reduce the thermal transfer. At the same time, some of the applied existing UHI mitigation strategies include reflective and undulated surfaces (either through the material's

thermal capacity or through the roughness level of the envelope's surface) with a direct impact on the reflection of the incoming heat and solar radiation, as well as the reduction of warm air-emissions from air conditioned buildings and the reduction of the inner operational energy through means of (self-) shading as an indirect intervention. Within this frame, the thesis' research objective attempts a connection between the two and lies on a hypothesis having both scientific and societal relevance. The hypothesis developed is *"whether, how and to what extent the implementation of SMMs in an integrated passive adaptive solar morphing facade system can contribute to the reduction of the building's impact on the UHI effect in an energy-efficient and autoreactive way".*

3.2. BIO-INSPIRED DESIGN APPROACH

At the same time, during the material literature study on the inherent characteristics of SMMs and their dynamic response mechanisms to external stimuli, there is a relevance and connection found to nature's strategies and principles for climatic adaptiveness. This led to a further exploration of existing bio-inspired mechanisms and their potentials to be interpreted in a facade design, by combining material and mechanism in a passive adaptive system. This gives way to the development of an approach towards responsive, adaptable facade systems by means of hingeless, energy-efficient and bio-inspired systems.

3.2.1. NATURE'S RESPONSE STRATEGIES AND PRINCIPLES FOR CLIMATIC ADAPTIVENESS

Biomimetics is a term coined by Otto Schmitt in 1969 [Schmitt, 1969]. It is known as the science that studies the replication in humans' design of natural methods and processes. Jeronimidis and Atkins defined also biomimetics as *"the abstraction of good design from nature"* [Jeronimidis et al., 1995]. The applications of biomimetics in research follow two different approaches: "bottom-up" and "top-down", with a multidisciplinary approach in both cases [Speck et al., 2008]. In a bottom-up process, research starts from biology and then it is transferred to other disciplines like engineering, whereas in the top-down approach, also known as bioconvergence, research starts from the engineering side of disciplines, where technical problems are accurately defined prior to finding a solution and nature is considered as a source of inspiration for possible solutions to be interpreted to obtain the technical solution.

An important characteristic of natural systems is a multilayered, finely tuned and differentiated combination of basic components which lead to structures that feature multiple networked functions [Knippers at al., 2012]. In relation to architectural applications and the replication of nature's strategies for climatic adaptiveness, Knippers and Speck [Knippers et al., 2012], proceeded to an identification of four main principles by classifying natural systems:

- **Heterogeneity**: characterized by different geometries for different elements and local adaptations of their physical or chemical properties.
- **Anisotropy**: nature shows the use of composite fiber reinforced materials, where the orientation of fibers and their spatial distribution are key factors.
- **Hierarchy**: In natural systems, hierarchy is multi-leveled and present at different scales, each level consisting of similar molecular components, but giving rise to different and, to some extent, independent functional properties and adaptions. This principle has not been already fully explored in architecture and engineering fields.
- **Multifunctionality**: characterized by the integration of monofunctional components into a single element, such as the integration of sensors and actuators in adaptive composite structures or elements for generation, transmission and storage of energy in facade elements.

Top Down

6. bionic product

5. technical implementation

4. abstraction, detachment from biological model

3. understanding the principles

2. biomechanics, functional morphology, and anatomy

1. biological research

Bottom Up

1. technical problem

2. search for biological analogies

3. identification of appropriate principles

4. abstraction, detachment from biological model

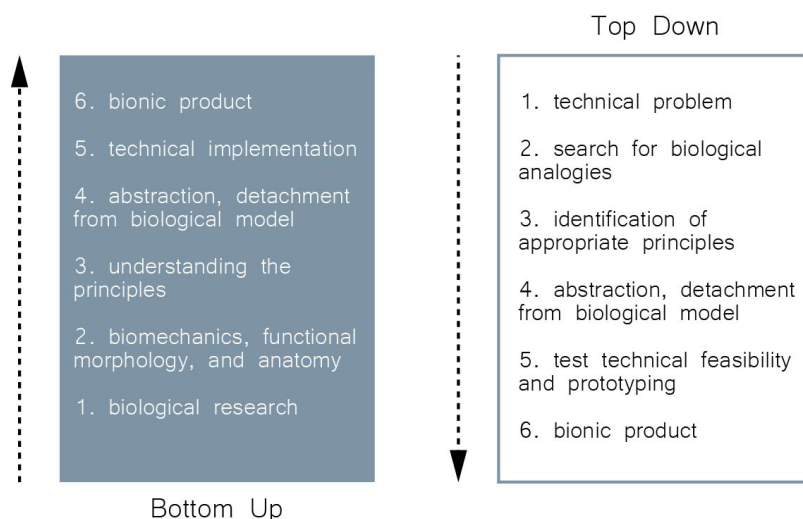5. test technical feasibility and prototyping

6. bionic product

Figure 32: Bottom-Up and Top-Down approaches of biomimetics. [adapted from Knippers at al., 2012]

Table 6: Design path matrix of the biomimicry pinnacles. [Kadri, 2012]

| Challenges	Processes	Flow	Adaptation	Scale	Environmental context	Morphological features	Structural features	Material features	Other features
Air									
Exchange	Diffusion	passive	Morphological	micro	Tropical Arid Temperate Cold	Fractals	Valves Conduits	Elastic	Counter-current unidirectional flow enlarged surface area
Move	Pressure variations	passive	Morphological	meso		Funnels Mounds	Conduits	Porous Elastic conductive	contracting expanding unidirectional flow
Heat									
Retain	Increase insulation Counter-current flow Reduce cold stress	passive	Morphological Behavioural	micro meso	Cold Polar	Adjacent Cluster		Conductive	Reduce surface area
Dissipate	Enhance convection Enhance conduction	passive	Morphological	meso	Tropical Arid	Branching Conduits		Conductive elastic	Peripheral flow Unidirectional flow Enlarged surface area
Water									
Gain	Condensation	passive	Morphological	micro	Arid	Bumpy	Channels	Hydrophilic	
Transport	Capillary action	passive	Morphological	micro	Arid	Hexagonal Fractal	Tubes Grooves Channels	Hydrophobic	overlaps folding
Lose	Evaporation	passive	Physiological	micro	Tropical Arid Temperate Cold				Asymmetric expansion Porous
Conserve	Control permeability	passive	Physiological	micro	Arid	Thorns	Grooves	Elastic Waxy	
Light									
Manage intensity	Exposure Inclination		Morphological	meso	Temperate Cold	Dense Monolayer			Elongation Inclination Rotation
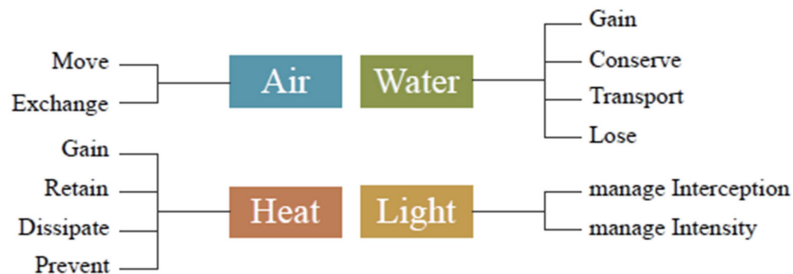
Figure 33: Key functions of adaptive building envelopes and their analogies found in nature. [Kadri, 2012]

3.2.2. NATURE'S INTRINSIC FEATURES AND SMM'S INHERENT BEHAVIOUR

Similarly, smart materials, e.g. alloys and polymers, have intrinsic features that share common features with the nature's responsiveness strategies and homeostatic mechanisms. More specifically, they have shown to possess the characteristics to work as actuators with minimum or no external energy and without the need for complex mechanisms, either separated or integrated, into shading components as an example. Through their Memory Shape Effect and speed of actuation, these actuators are able to produce ranges of movement and responsiveness suitable to be applied in dynamic shading facade systems. Although there are a few examples of applied use of smart materials in shape morphing solar skins, there is much research being developed in this direction for the design of future environmentally responsive facades. The use of shape memory actuators in building sector is still to a limited extent, especially concerning their solar activation, life cycles and resistance to external weather conditions. From the available materials, Shape Memory Alloys have been extensively tested and used, and can be currently considered as suitable materials for shading applications, whereas Shape Memory Polymers and Hybrids can present future interesting opportunities, due to their enhanced dynamic performance and user-friendly customization.

Focusing on architectural applications and the design of shape morphing solar shadings, the principles of anisotropy and multifunctionality are the most relevant ones, if the design is approached following the principles of biomimetics. Anisotropy would define how deformation, and therefore movement, can be achieved through the distribution and orientation of material's fibers. Multifunctionality is then related to the capacity of embedding different functions into one single element (as sensing and actuating functions of smart materials). In this sense, the connection to phytomimetics and the study of nastic structures is of great relevance. Main feature of plants is their flexible movements with high reversibility, which forms the triggering movement and constitutes an inspirational model to reduce complexity of moving parts in buildings and to develop deployable structures. Apart from that, they also show anisotropic arrangement of material and fibers to reduce material stresses in an energy-efficient way.

Nastic structures in general present three important characteristics interrelated with kinetic building systems, which are also present in smart materials. Firstly, movement is triggered by an external stimulus, secondly, motion is carried through volume change (shape) and, lastly, their anisotropy is derived from an unequal distribution of material in the cells. Nastic movements respond to an external stimulus regardless the direction of the stimuli inducing movement and predominantly reversible, for instance the folding/unfolding and raising motion of leaves [Schleicher et al., 2015].
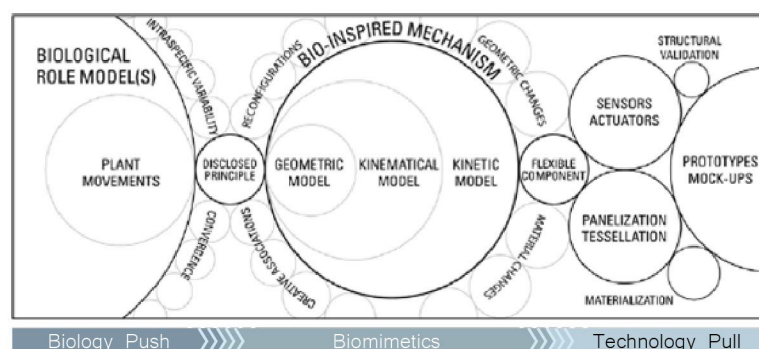

Figure 34: Mapping the key aspects of transferring bio-inspired motion principles into technical kinetic structures. [Schleicher et al., 2015]
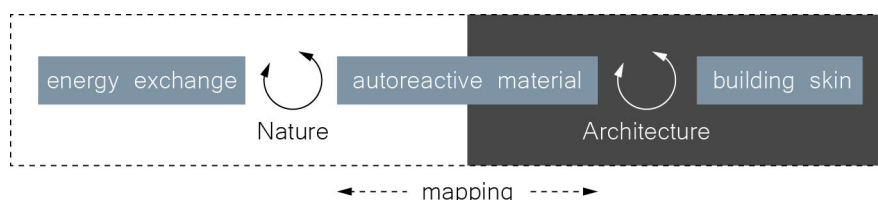

Figure 35: Conceptual mapping pattern between the three topics. [adapted from Persiani et al., 2016]

3.2.3. BUILDING'S THERMAL BEHAVIOUR AND ENVIRONMENTAL RESPONSE WITHIN A BIO-INSPIRED FRAMEWORK [CASE STUDIES]

The abovementioned features and inherent behaviours can be replicated by incorporating material and mechanism in an integrated passive adaptive facade system. In both cases, the aim is to respond to complex but limited ranges of environmental conditions by changes in geometric configuration through the ingrained properties of the material itself, without the need for external energy or complex mechanical parts, and by means of movement which is produced using the elastic properties of the materials working at high strain.

In this direction, architectural envelopes can be designed to move dynamically by reacting automatically as decentralized energy independent systems rather than being controlled by sensor-brain systems [Persiani et al., 2016]. By following nature's priority principles for self-regulation, passive adaptive facade systems can incorporate dynamic material systems and mechanisms with inherent autonomic response. The integration of material systems with intelligence and life features intrinsic in their microstructure can, therefore, produce adaptive functionality to the building envelope and better climatic responsiveness by means of mass and energy regulation.

Biomimicry, after all, attempts to learn from the most fit solutions in nature and borrow ideas for solving many anthropologic issues (technological, social, environmental etc.) As evolution has favoured fit organisms over obsolete ones, these are an enormous inspiration pool for evolving new technologies [Persiani et al., 2016].

Case studies

The inherent directness and climatic responsive mechanisms explained throughout the literature study of materials and response mechanisms are attractive to architects and engineers and there are already some realized projects which have been developed and show promising potentials for further exploration in implementing SMM and/or a biomimetic approach in integrated facade applications. Most of the examples concern kinetic shading systems, while solar morphing shading skins are not broadly explored. Where an actuator is required, this can be completely embedded into the device or strategically located to trigger a specific action [Dakheel et al., 2017]. Some of these applications can be summarized in the overview table below [Table 7], based on the actuator systems, material and mechanism selection and possible relation to bio-inspired approaches.

Table 7: Case studies. [information retrieved from Fiorito et al. (2016), Dakheel et al. (2017)]

|	Project name	Motion	Smart actuator	Stimulus	Scale	Biomimetic approach	Reference
1	Flectofin®	Three-dimensional movement (swivel motion - Both in the same axis)	–	External mechanical forces	Component	Bottom-up	[Lienhard et al., 2011]
2	Solar Kinetic	Three-dimensional movement (swivel motion - Both in the same axis)	Shape Memory Alloys (SMA)	Heat source provided through electrical current	Sub-component	Bottom-up	[Suralkar, 2011]
3	Blind	Three-dimensional movement (swivel motion - around a different axis)	Shape Memory Alloys (SMA)	Heat source provided through electrical current	Sub-component	Top-down	[Khoo et al., 2011]
4	Air Flow(er)	Three-dimensional movement (swivel motion - around a different axis)	Shape Memory Alloys (SMA)	Heat source provided through electrical current	Component	Top-down	[Payne et al., 2013]
5	Sun Shading	Three-dimensional movement (swivel motion - around a different axis)	Shape Memory Alloys / Shape Memory Polymers (SMA/SMP)	Heat source provided through electrical current	Component	–	[Lignarolo et al., 2011]
6	Smart Screen	Bi-Dimensional Movement (Translational Movement by overlapping layers)	Shape Memory Alloys (SMA)	Heat source provided by solar radiation	System	–	[Decker et al., 2010]
7	Piraeus Tower	Bi-Dimensional Movement (Translational Movement by overlapping layers)	Shape Memory Alloys (SMA)	Heat source provided by solar radiation	System	Top-down	[Doumpioti et al., 2010]
8	Lily Mechanism	Three-dimensional movement (swivel motion - Both in the same axis)	Shape Memory Hybrid (SMH)	Heat source	Component	Bottom-up	[Schleicher at al., 2015]
9	Kinetic Solar Skin	Three-dimensional movement (swivel motion - around a different axis)	Shape Memory Alloys (SMA)	Heat source provided through electrical current	Component	–	[Pesenti et al., 2015]
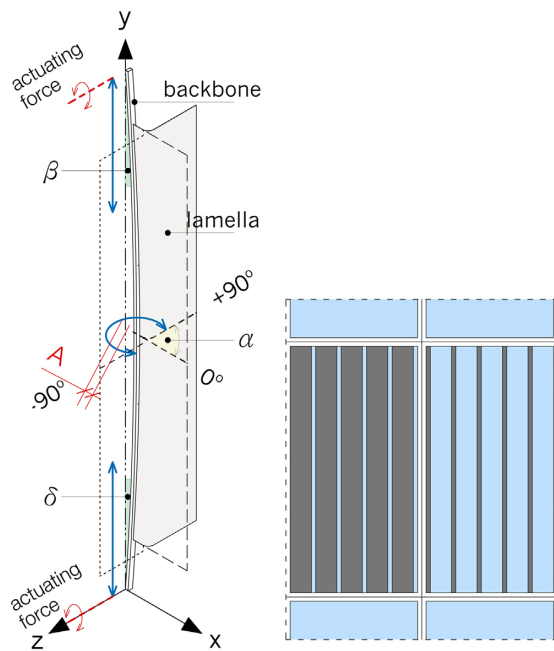
Figure 36: Project (1): Flectofin®. Scheme of operation and example of facade's integration (closed and open configuration). [Lienhard et al., 2011]
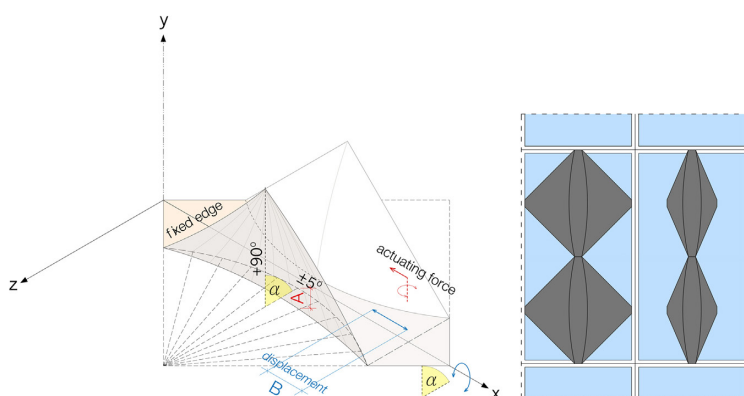

Figure 37: Project (2): Solar Kinetic. Scheme of operation and example of facade's integration (closed and open configuration). [Suralkar, 2011]
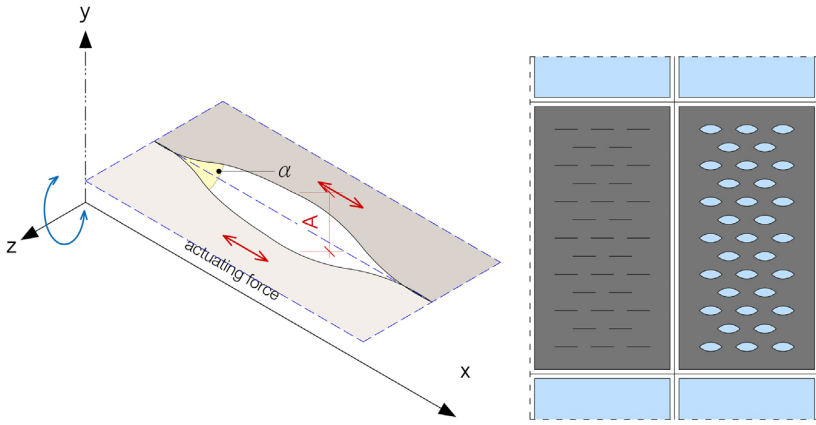
Figure 38: Project (3): Blind. Scheme of operation and example of facade's integration (closed and open configuration). [Khoo et al., 2011]
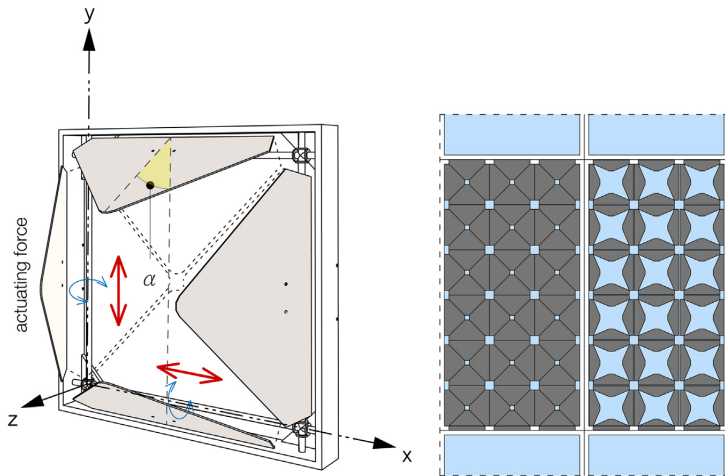

Figure 39: Project (4): Air Flow(Er). Scheme of operation and example of facade's integration (closed and open configuration). [Payne et al., 2013]
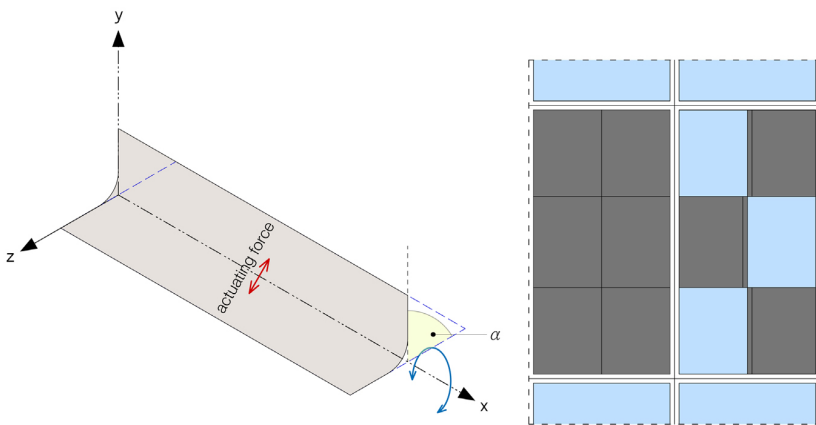

Figure 40: Project (5): Sun Shading. Scheme of operation and example of facade's integration (closed and open configuration). [Lignarolo et al., 2011]
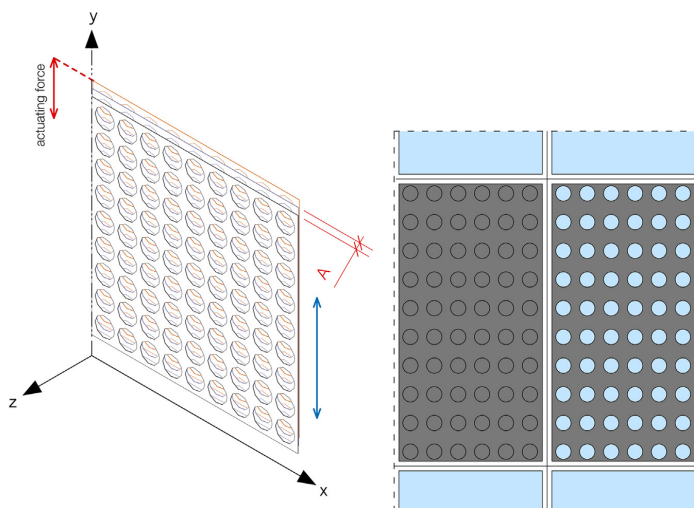

Figure 41: Project (6): Smart Screen. Scheme of operation and example of facade's integration (closed and open configuration). [Decker et al., 2010]
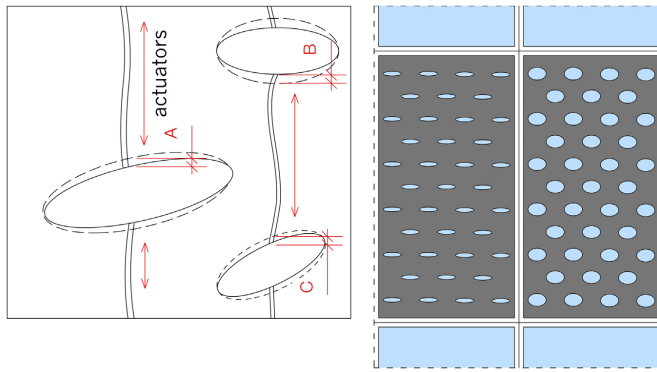
Figure 42: Project (7): Piraeous Tower. Scheme of operation and example of facade's integration (closed and open configuration). [Doumpioti et al., 2010]
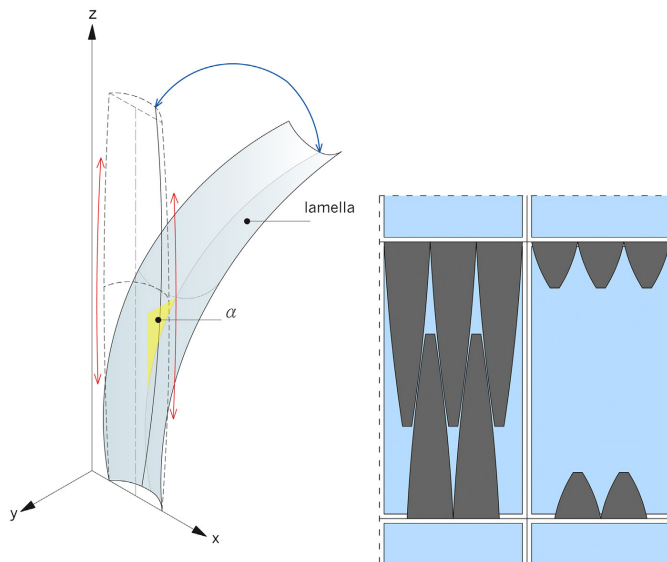

Figure 43: Project (8): Lily Mechanism. Scheme of operation and example of facade's integration (closed and open configuration). [Schleicher et al., 2015]
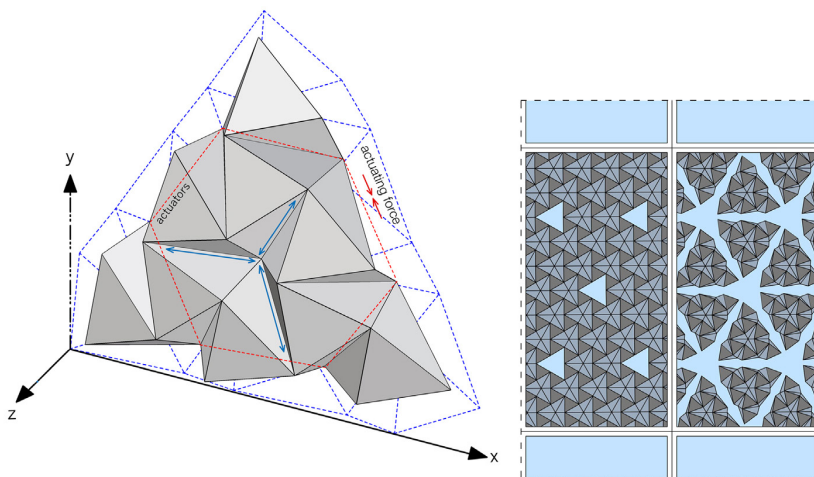

Figure 44: Project (9): Kinetic Solar Skin. Scheme of operation and example of facade's integration (closed and open configuration). [Pesenti et al., 2015]

All the selected projects present one or two degrees of freedom in the desired movement, varying between two extreme positions, open and closed modes, with continuous transition between the two positions. Where movement is three-dimensional, a constrained swivel motion produced by bending and buckling of elastic materials characterizes rotation. An exception is the case of the Air Flow(er) project, in which hinges are used to rotate stiff wings. Most of those performing three-dimensional movements have also been developed either at component or subcomponent scale, due to

the discrete sizes and capabilities of smart materials as actuators. On the contrary, translational movements are more suitable for larger scale projects.

As for the biomimetic approaches, anisotropy can be classified as a bottom-up approach aimed at taking into abstraction reversible and repeatable movements found in nastic structures, by means of materials properties and distribution within the component, like in the Flectofin®, Solar Kinetic and Lily Mechanism projects. Movement is produced from the material elasticity and

from the fibers' arrangements, while minimizing stress when movement is produced. Based on research following a biomimetic bottom-up approach, they are characterized by means of an iterative process, starting from the reproduction of movement, and followed by the optimization of shape and by the selection of materials. These projects were inspired by existing studies in plant movement, by exploring the nastic properties of *Strelitzia Reginae* flower, *Aldrovanda Vesiculosa* carnivorous plant, and *Lilium Casablanca* flower, respectively. The three examples can perform fast actions and are, therefore, suitable for applications responsive to the continuous changing position of the sun. In the contrary, a top-down approach can be identified in the Blind, Air Flow(er) and Piraeus Tower projects, using analogies from various natural sources, but not related to movement in all cases. However, multifunctionality is considered a predominant feature in all projects, mainly incorporating smart materials for sensing and actuating the systems.

These projects also experiment with the use of polymers as constituent materials for their components, mostly thanks to their elastic properties in tension and low stiffness in bending. Formed and amorphous polymers were used, with layered compositions to reproduce anisotropy of plants. A second material can be found either as protective layer or as actuator, like glass fiber reinforced polymers (GFRP), silicones and elastomers.

In the studied examples, common feature is also the integration of SMM materials as triggering actuators for the shading movements. In most of the cases, thermal triggering has been the most widely researched and developed method for changing shape of the solar shadings, by exploiting a temperature gradient, which is directly provided by direct sunlight exposure. Different activation temperatures have been tested in the analyzed projects. For instance, in the Piraeus Tower project, action would occur between 35°C and 40°C, whereas in the Sun Shading one, SMAs would move when reaching more than 90°C. In the Lily Mechanism project, a Shape Memory Hybrid was implemented, by combining two materials with different thermal expansion behaviors, like GFRP and PMMA, capable to trigger the movement when the materials' temperature exceeds 70°C.

However, one of the limitations of such automated systems, is the dependency on the environmental conditions, where variable external conditions could limit the efficiency of any system intended to produce movement by means of heat and solar exposure. Because of that, it is not always possible to establish a holistic relationship between devices' temperature and solar irradiance. Consequently, sometimes heat needs to be instead generated directly or indirectly from electricity, for example produced by a photovoltaic converter, as in the cases of the Solar Kinetic, Sun Shading and Blind projects. This means that, although control is considered to be automated and responsive to outdoor conditions without any central brain to control the whole facade system, in practice, occupants' control is preferred to be potentially available, mainly for ventilation purposes. However, such applications are not explored in much extent in the built environment, and this highlights at the same time the challenges of such completely automated systems for future facade implementations [Fiorito et al., 2016].

Most of above case studies exploit the dynamic movement for sun-control purposes which can be produced at component scale through lightweight and elastic structures to form solar morphing and shading devices for building applications. The adoption of these materials allows fabrication of components with an anisotropic composition, like differentiated thicknesses and a predominant fiber distribution in a desired direction. The optimization of movement, through the reduction of material's stress and the use of innovative low-energy triggering methods, such as smart materials actuators, are some of the additional benefits [Fiorito et al., 2016]. In those projects, where a biomimetic connection to natural systems' mechanisms is additionally present, this originates by either a bottom-up or top-down approach.

04   FACADE DESIGN INTEGRATION

4.1. ADAPTRONIC SYSTEM: AUTOREACTIVE MATERIAL & ACCLIMATED KINETIC ENVELOPE

Based on the objectives and research approaches, the thesis aimed to develop a solar morphing kinetic facade system, which can achieve motion using latent energy in an energy-efficient and autoreactive way, with optimal use of sensors and actuators, where material, form, function, structure and motion are independent in a fit combination [Persiani et al., 2016]. The intention was to use the research's background information and study to couple the autoreactive inherent features of the material within an acclimated kinetic system, which provides the desired climatic adaptiveness, by replicating strategies and principles found in nature. As such, the term "acclimated" is from biology and refers to a process in an individual organism adjusting to a gradual change in its environment through its morphological, behavioral or physical changes [Wang et al., 2012]. The end result is a combination of both systems and leads to an adaptronic system, which is able to modify its behaviour to create an envelope of utility and have as objective to instill intelligence in the microstructure to perform adaptive functions [Rogers et al., 1999].

On one hand, the advanced rate of technological advancement can help simplifying the design of moving components through the use of smart materials, reducing consistently the number of operating difficulties. On the other hand, biomimicry can improve the design process by individuating the best combination of geometry, motion type, motion transmission and actuating parameters. [Persiani et al., 2016].

To elaborate further, the adaptronic systems can be defined based upon a technology paradigm as *"the integration of actuators, sensors, and controls with a material or structural component"*. Multifunctional elements form a complete regulator circuit resulting in a novel structure displaying minor complexity, low weight and high functional density. However, they can also include the notion of biologically inspired materials and mechanisms by addressing the goal of the material system as follows: *"material systems with intelligence and life features integrated in the microstructure of the material system to reduce mass and energy and produce adaptive functionality"* [Rogers et al., 1999].

The integration of material and systems is holistic in the same way that biological structural systems do not distinguish between materials and structures. The design and development of natural organisms is an integrated process in which component functions are multiple, and result in a cost-effective and durable structure whose performance matches the living system. Likewise, the distinction between adaptronic structures and intelligent structures is vague. Each of the systems requires a hybrid approach to integrating the technologies that synergistically combine life functions and intelligence. The distinction between material systems and structures can then be defined in terms of the scale of their microstructures [Rogers et al., 1999].

Figure 45: Characteristics of mechatronic and adaptronic systems [adapted from Drossel et al., 2015]

4.2. FACADE DESIGN GUIDELINES

The goal was to propose a "living" envelope, a low-energy and low-tech facade system capable of predictably changing in shape in response to heat changes through the ingrained properties of the material it is made of, without the need for external energy or complex mechanical parts and by optimizing the use and number of actuators required to achieve the desired result. In this way, by applying the Shape Memory Effect of the material, a control of the thermal transmission of the building envelope can be achieved, as well as a reduction of the thermal transfer through an optimal dynamic performance of the facade skin.
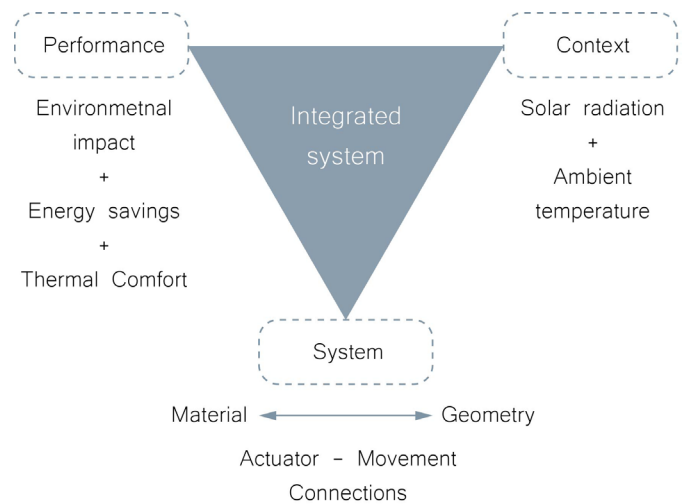

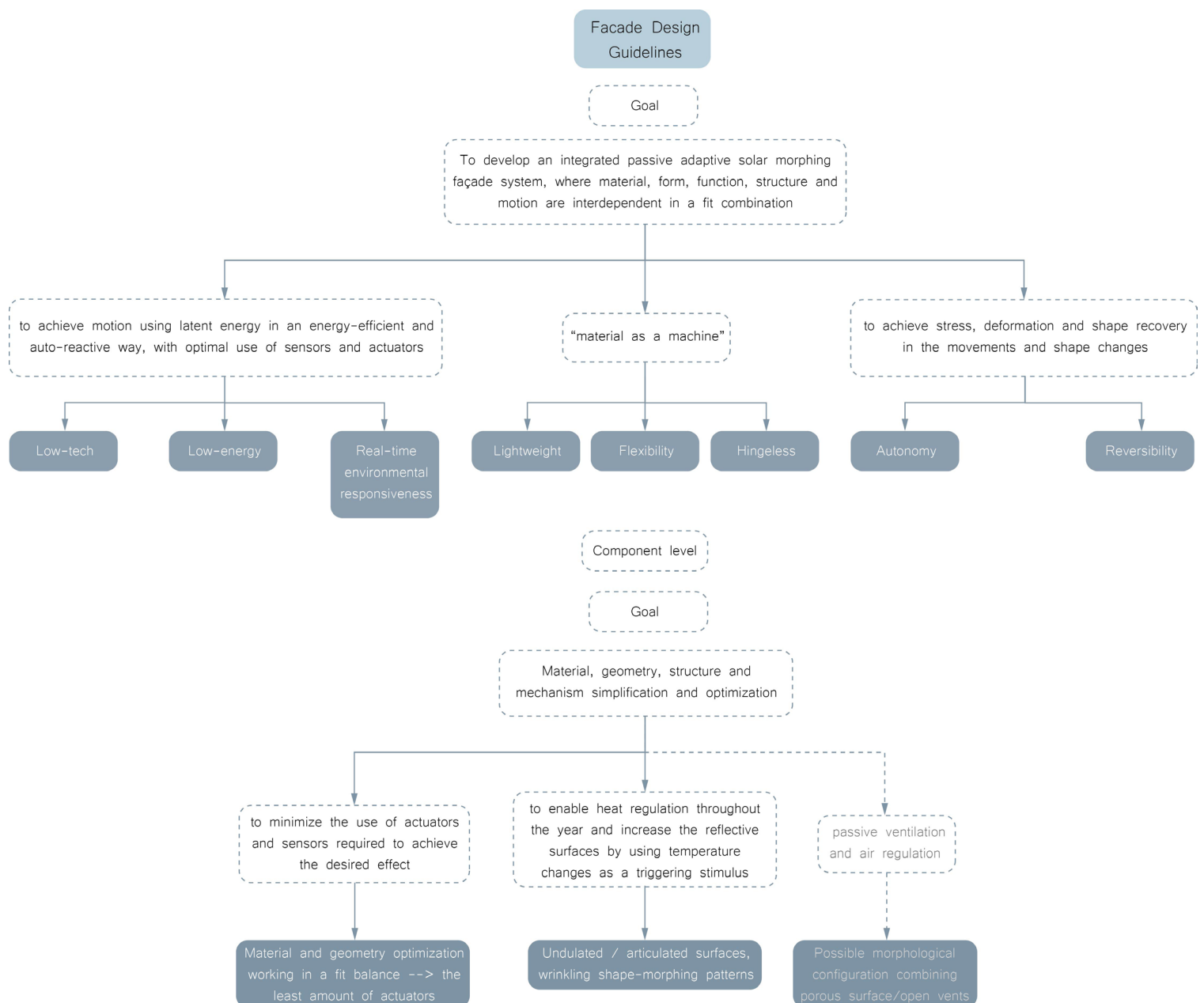Figure 46: Diagram of integrated design principles [own work]

Figure 47: Diagram of facade design guidelines [own work]

4.3. APPROACH AND PRELIMINARY IDEAS

The facade design proposal concerns the development of a self-shading skin integrated in a exterior facade system, aiming to regulate the heat exposure in both the cooling- and heating-dominated periods. The base of the idea is that the double layer consists of an inner solar absorbing coating layer and the outer SMM-based shape-morphing skin layer, which forms a dynamically responsive and reflective articulated surface. During the summer months, the SMM skin, triggered by the temperature rise, expands and creates undulated and dense surfaces, increasing the reflectivity of the building envelope. In the contrary, during colder periods, the skin retracts to its originally programmed form, revealing the inner heat absorbing layer that is exposed to solar radiation. In both states, the goal is to minimize the cooling demands of the building during hot periods and the heating demands during the cold seasons, acting in an opposite logic than in a regular shading system (covered during summer-open during winter). In the end, the aim is to passively minimize the energy needs and, consequently, the building's footprint on the UHI effect in an indirect way. However, since a fully automated system might not reach the maximum possible effect, the possibility to override the function could potentially be incorporated as a design option to enable the user's freedom of operational control.

Besides that, there has been a research on bio-inspired strategies for heat regulation in natural organisms. The focus was placed mostly on the articulated morphology of the succulent plants' surfaces to reflect the solar radiation by means of their geometry, which is then used as bio-inspiration for the development of an undulated shape morphing facade skin, to increase the angle and area of reflecting surfaces. At the same direction, the layered structure of butterfly wings with their ridges and cross ribs are acting mechanisms to minimize the acceptance of solar heat. As for ventilation strategies, the dynamic opening and closing movement of the "stomata" on the leaves' surfaces to regulate the air intake and exhaust of the plant is an additional strategy used as background inspiration to promote adaptiveness through passive dynamic shape changes.

Additionally, the articulated effect of the self-shading skin depends to a certain degree on the material choice and the origin of the actuating element, which can be a point, a line or a surface. Translated to the facade component, this can result in considering the actuating force acting either in the form of the connecting joint, the edge or the surface of the self-shading skin structure, such as a nodal trigger forcing the movement, a linear elongation-deformation or a surface expansion-shape recovery. This led to various design options, translational movements and degrees of freedom, with SMAs and SMPs having different potentials. For example, SMAs are more commonly used in edge deformations, while SMPs provide mostly surface shape changes. However, SMAs or SMPs can both be applied to control the deformation by control of the joint element, as well. Therefore, the available options could be flexibly optimized based on either a material-driven or a design-driven choice, and therefore, as a starting point, options in both directions were considered to be further evaluated.

Figure 48: Cacti fractal cooling system during day and night and articulated reflecting surfaces. Source: Eastgate. (2017, November 08). Retrieved from https://blogs.uoregon.edu/bioform/2017/11/08/1067/
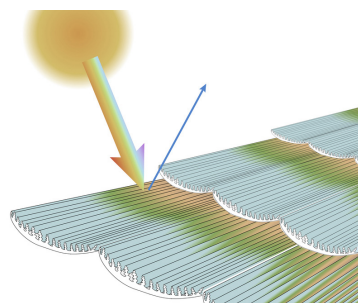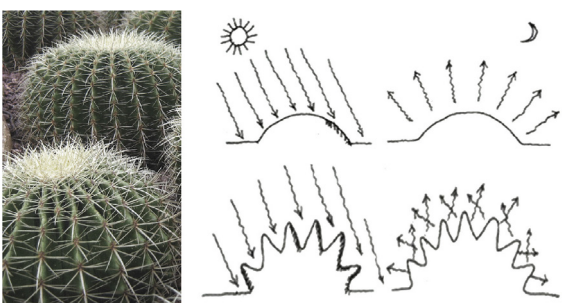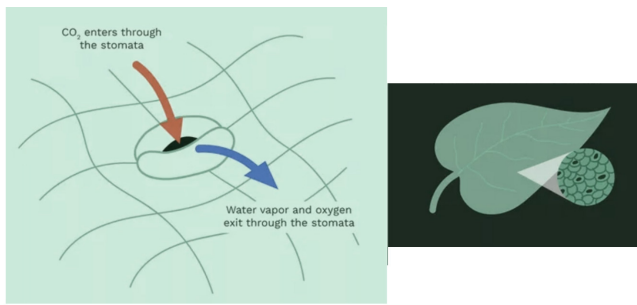
Figure 49: Scheme of butterfly wing's tiny scales covered with microscopic ridges, cross ribs, and other structures. Source: Vukusic, P., Yoshioka, S., Prum, R. O., Vukusic, P., Kinoshita, S., Team, A., & Sherry. (2002, July 26). Wing scales cause light to diffract and interfere : Morpho. Retrieved from https://asknature.org/strategy/wing-scales-cause-light-to-diffract-and-interfere/

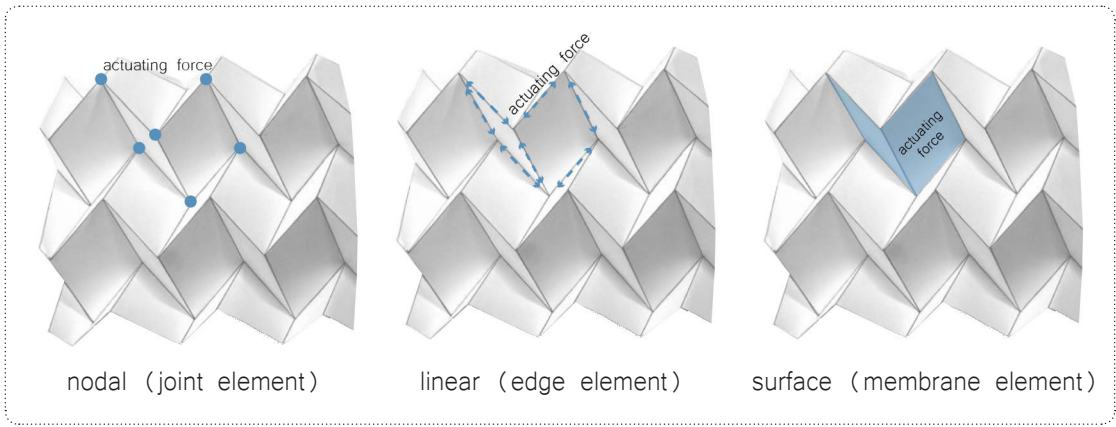Figure 50: Leaves' stomata principal function. Source: Bailey, R. (n.d.). What's the Function of Stomata in Plant Tissue? Retrieved from https://www.thoughtco.com/plant-stomata-function-4126012

nodal（joint element） linear（edge element） surface（membrane element）

Figure 51: actuation force placement [own work]

References
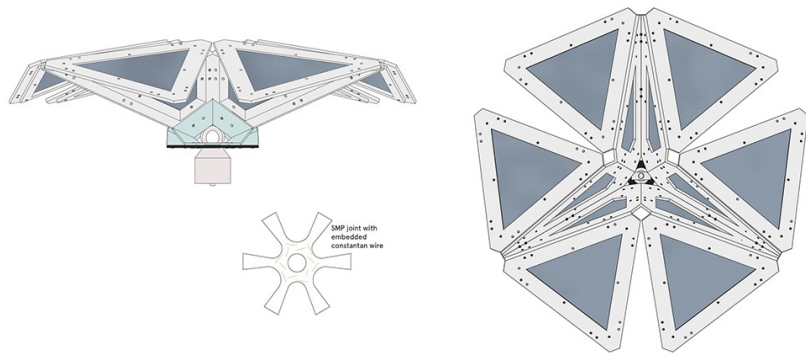
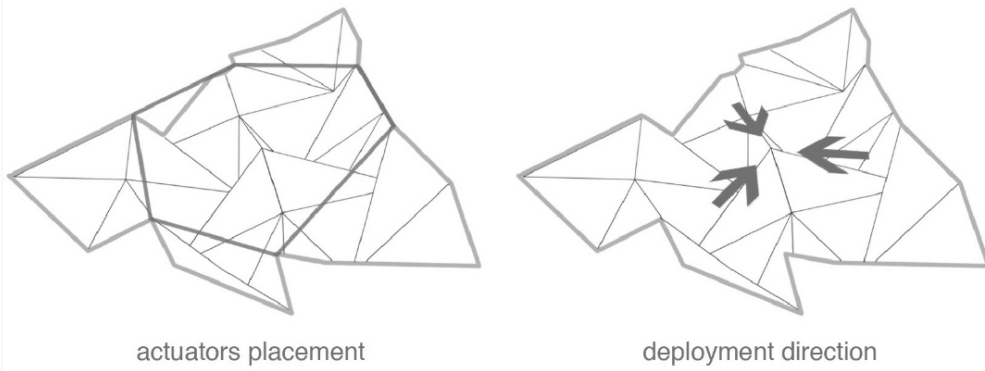Figure 52: SMP joint [Rawn, 2014]

actuators placement deployment direction
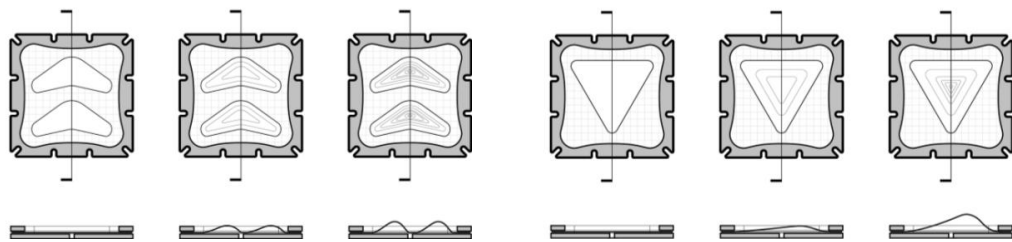
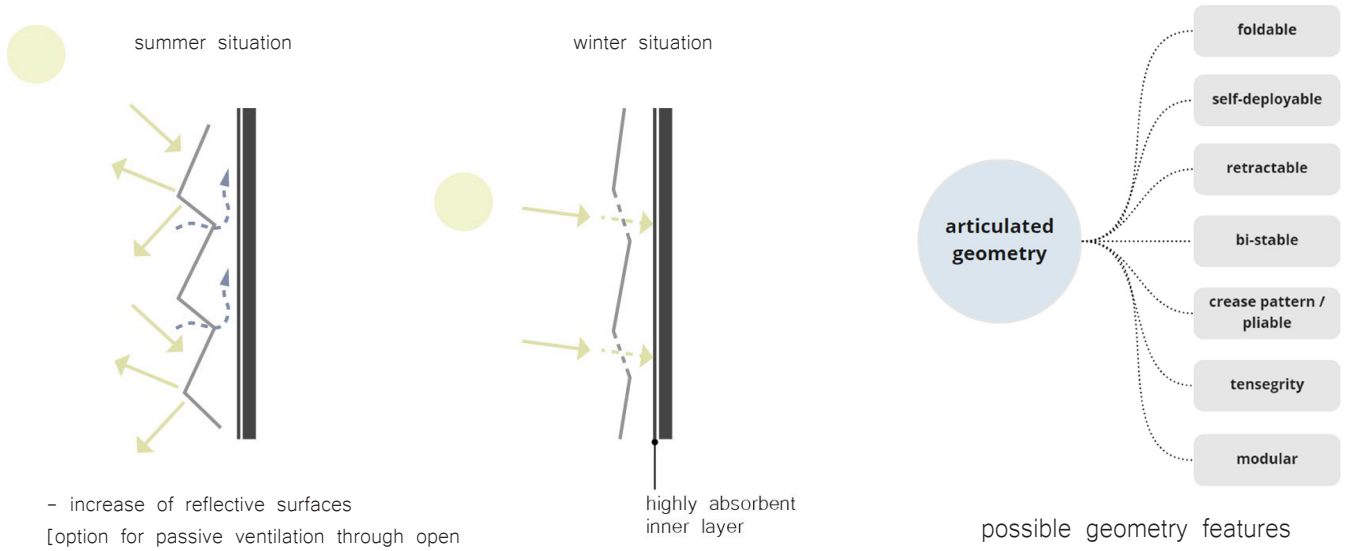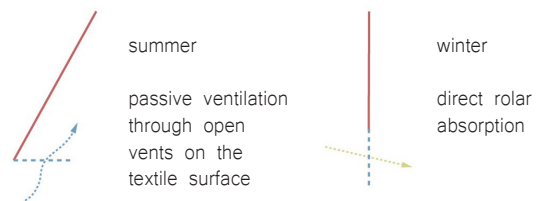Figure 53: SMA edge wire [Dakheel et al., 2017]
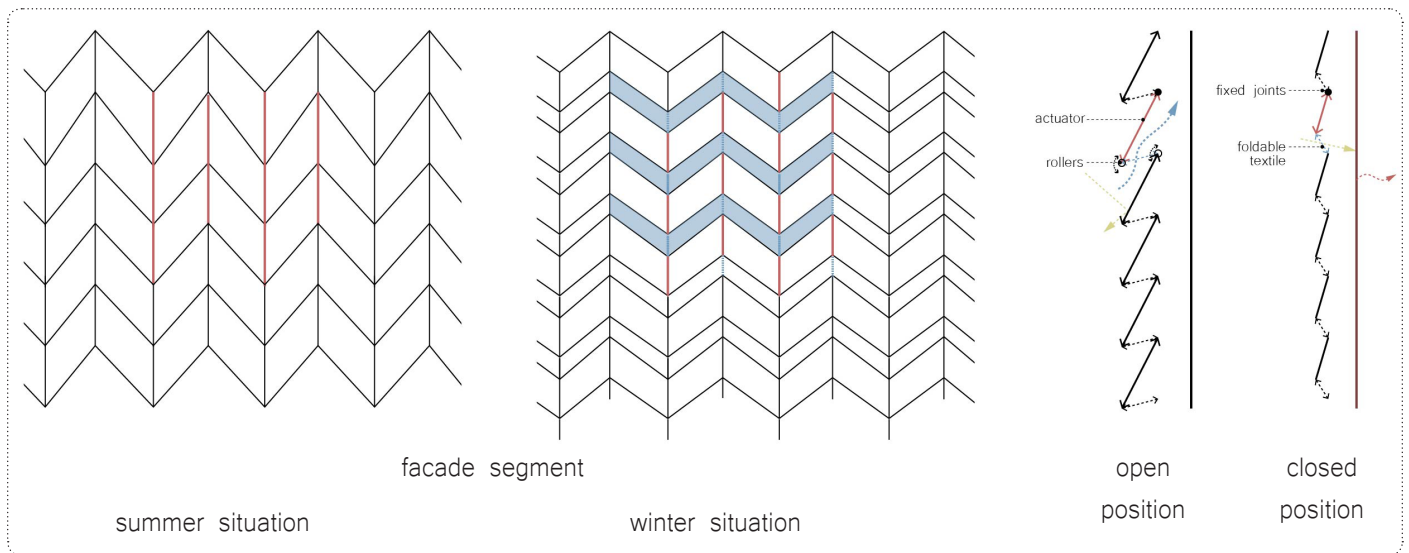

Figure 54: SMP 3D-printed surface tiles [Clifford et al., 2017]

Facade design ideas

summer situation

winter situation

highly absorbent
inner layer

– increase of reflective surfaces
[option for passive ventilation through open
vents of the membrane]
– retractable / foldable membrane or textile as filling
"breathing" skin with a translucent and fritted surface

articulated
geometry

- foldable
- self-deployable
- retractable
- bi-stable
- crease pattern / pliable
- tensegrity
- modular

possible geometry features

design option #1

facade segment

summer situation

winter situation

open
position

closed
position

actuator
rollers

fixed joints
foldable
textile

summer

passive ventilation
through open
vents on the
textile surface

winter

direct rolar
absorption

design option #2

facade segment

summer situation

winter situation

dynamic movement options

design option #3

component

open position   closed position

facade segment

design option #4

fritted textile surface

highly absorbent inner layer

facade segment

summer situation   winter situation   open position   closed position

design option #5 (SMP surface)

undulated surfaces in both   summer situation   winter situation   alternative geometry
directions (inverted components)   after actuation   before actuation
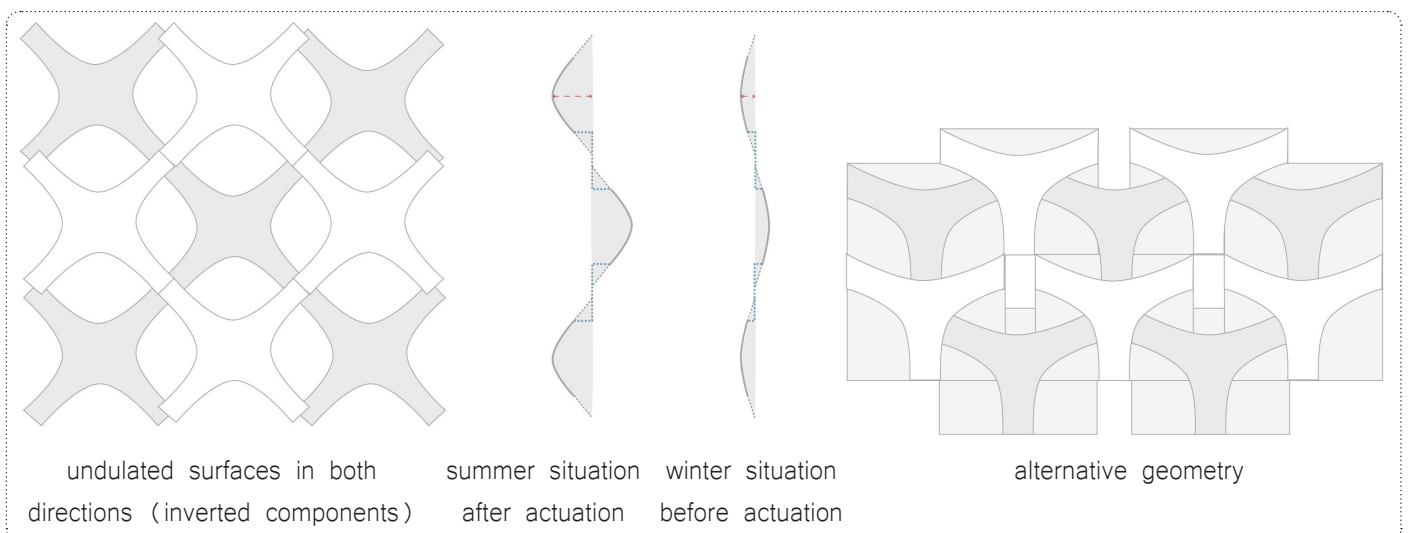
4.4. DESIGN METHODOLOGY & WORKFLOW

The design methodology can be divided into three distinct stages, which were realized either in a linear chronological sequence or in parallel. The first phase consisted of the literature study, where the background information was accumulated to be applied in the design integration. This included also studies on the material properties and dynamic behaviour to enable a better understanding of its inherent performance. After setting a theoretical base, the following stage involved the design phase, which was informed in parallel by research and iterative performance evaluation studies in a feedback-loop process, where material and geometrical explorations were conducted.

In the performance analysis and evaluation phase, parametric simulations and design optimizations were realized to fine-tune the selected shading prototype design. This was assisted by the feedback from the performance validation, to provide parametrical design variations in conjunction with energy and environmental simulations throughout the design process. These simulations received weather and solar radiation data and attempted a connection to the UHI and its impact on the microclimate and surrounding environment. Besides that, a thermal behaviour modelling under targeted conditions was realized in a CFD simulation software, as well as energy, radiation and daylight simulations in different operation periods of the SMM-based shading device.

The above iterative process was based on an interoperability toolchain workflow, where most of the digital tools were integrated in the same parametric software environment (Grasshopper). This approach allowed for a better data interchange and modelling compatibility between the various energy simulation engines, a more direct comparison of the different simulations and results, while optimizing the overall workflow in a systematic and comprehensive way. Figure 55 provides an overview of this digital toolchain analyzed for the purpose of each analysis study.
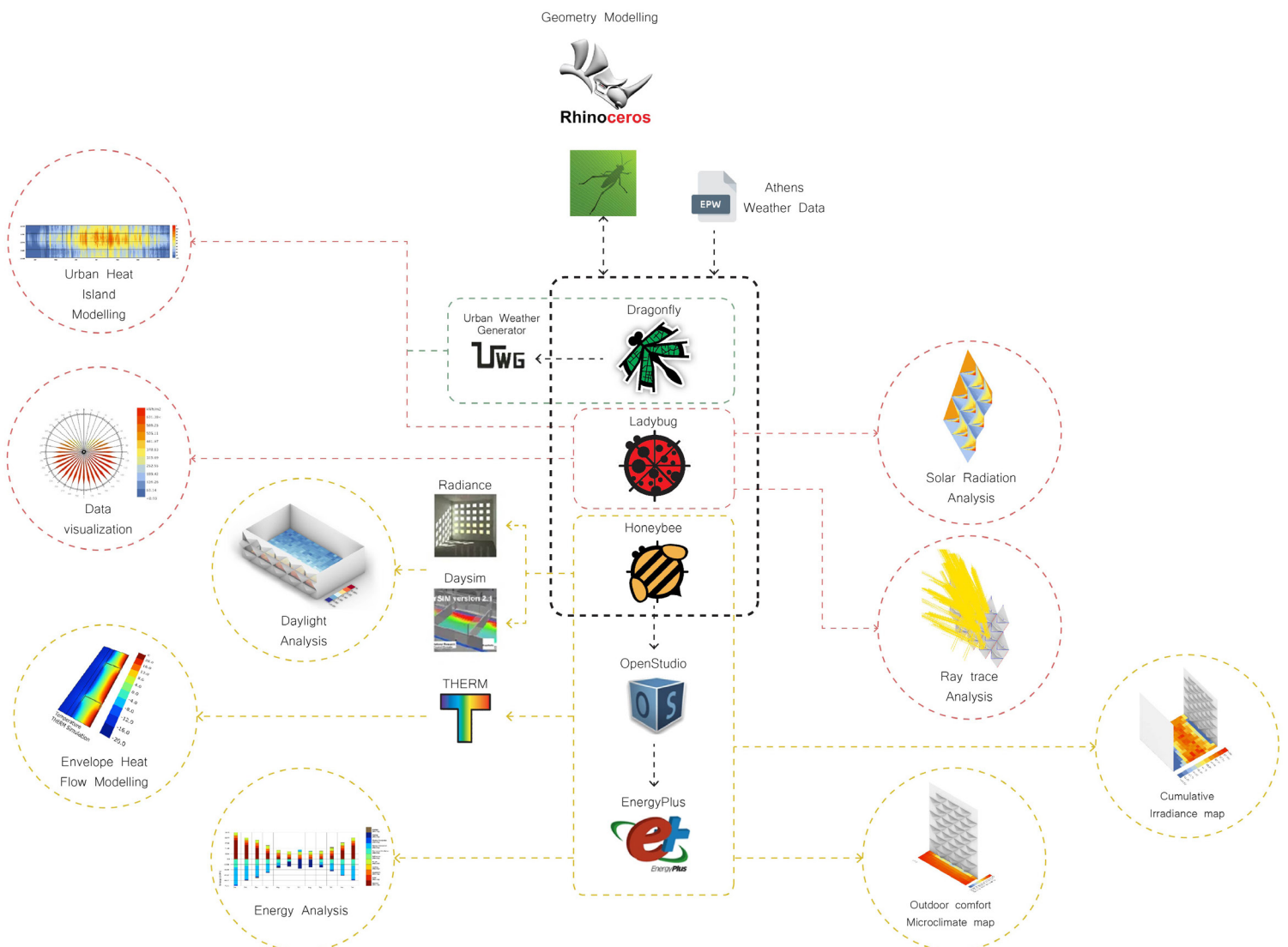

Figure 55: Overview of the digital tools workflow. [own work]

4.5. EVALUATION METHODOLOGY

Based on the above workflow, the evaluation methodology consisted of assessing the SMM adaptive facade system's performance, based on the mentioned performed energy and environmental simulations. The objective was to estimate the impact of the system on the urban microclimate from the reflection of the solar radiation, as well as the effect on the reduction of the building's cooling demands. Besides that, a feasibility assessment was conducted, by evaluating these smart technologies based on certain criteria, involving cost effectiveness, technical feasibility and physical integration, among others, in order to reflect on their potentials for facade applications, also in comparison to similar technologies. These evaluations provided with both a quantitative and a qualitative overview of the challenges, restrictions and potentials of future SMM-based facade developments, as well as a feedback to the proposed hypothesis of the thesis on the level of contribution, feasibility and consideration of this approach as a UHI mitigation strategy.

05   INFORMED DESIGN BY RESEARCH

5.1. LAYERS OF EVALUATION

Since the UHI is a multi-layered problem, a similar research approach was followed, by creating a series of layers of parameters [Figure 56] for the decision-making process which function in a feedback-loop logic. More specifically, the preliminary design explorations were initially evaluated based on certain general qualitative design criteria which were guided by the overall preliminary design goals. Some of these options that satisfied to an extent the first exploration round, proceeded to a feasibility control check in terms of the operability of the SMM mechanism, which is the primary condition for the design to be realized. The next step related to the direct UHI impact, which evaluated the percentage of sun rays reflected towards the atmosphere and was influenced mostly by the geometrical features and the arrangement of the facade. Once a minimum threshold for this requirement was met, the next evaluation criterion concerned the indirect impact, which related to the building's energy performance and, more specifically, its cooling load demands. This stage set the minimum of requirements that would give a design which would have undergone enough optimization phases to provide satisfactory information and results for an overall reflection and performance evaluation of the facade system.

However, due to the complexity of the context in question, more factors are intertwined, as for example the passive operation of the facade mechanism on either a daily or a seasonal basis, as well as the impact of the facade orientation. In an ideal operational scenario, all the requirements would have to be satisfied to achieve an optimal adaptive environmental and energy performance. In practice, though, since the facade design was focused on a fully passive operation, the above ambition would lead to a mechanism too complex and unrealistic to operate. The objective of these feedback-loop workflow and optimization stages was, therefore, to identify the sweet spot where the system is as little complex as possible with minimal presence of mechanical and structural parts to maximize at the same time the building's environmental performance in relation to the UHI effect.

Figure 56: Diagram of layers of parameters that determine the responsive performance of an SMA-based passive adaptive facade envelope with the aim to reduce the building's impact on the UHI effect. [own work]
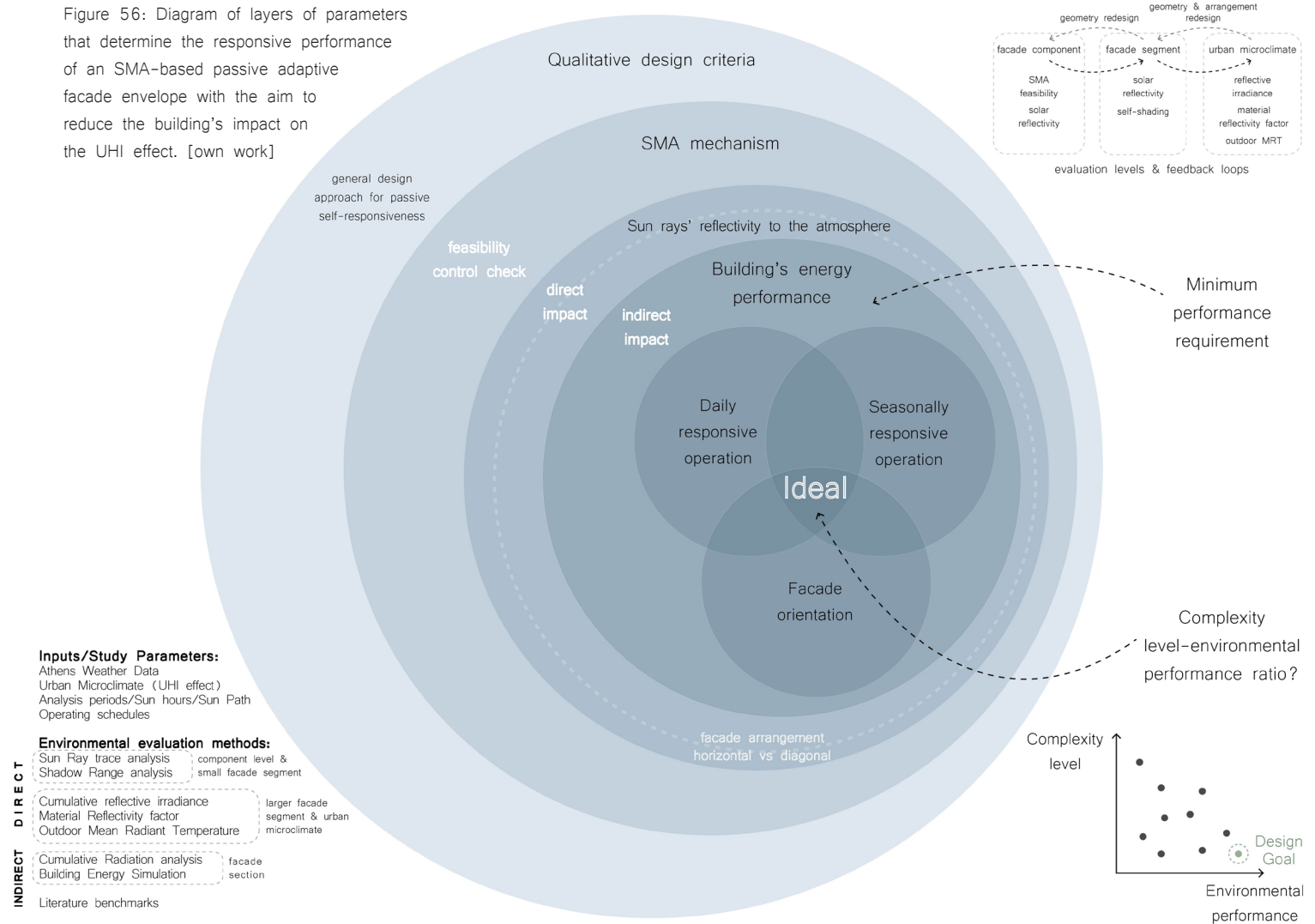
5.2. ABSTRACT GEOMETRY DESIGN EXPLORATIONS

As a starting point, a set of benchmark criteria was defined to guide the geometrical explorations, based on the design guidelines. The focus was concentrated on the self-deployable structures as a principle of the self-folding geometries, which would feature undulated surfaces. This type of structures has similarities with the working mechanisms of the SMMs, because with minimal material use, they can achieve reversible, lightweight structures with improved strength-to-weight ratios, while they can lead to an automation of the construction of complex geometries at large or small scales. Similarly to the biomimetic approaches explored in the first chapters, these structures are also frequently found in nature, which exploits them for rapid and efficient lightweight fabrication. Manufactured systems typically require complex, expensive, and time-consuming 3-D fabrication processes, and require complicated infrastructures for assembly and deployment. Nature, on the other hand, is often able to rapidly fabricate lightweight structures using self-folding strings or sheets, with references found in biology at length scales from nanometers to meters,

such as organic molecules, winged insects, brains, and tree leaves [Tolley et al., 2014]. Another key point for the evaluation process was the design of an elegant and intelligible actuation system with minimum use of actuators for reduced complexity, ease of fabrication and avoidance of operation complications, while taking into consideration the architectural impact in terms of facade aesthetics, since it is directly exposed to the urban fabric.

In summary, the abstract geometrical explorations had the objective to:
- minimize actuation mechanisms, increase deployability and reversibility,
- maximize reflective surfaces and reflection angles,
- simplify the geometry to avoid complex mechanisms, allow for actuator placement to be exposed to solar radiation, minimize fabrication intensiveness,
- achieve a maximum effect with minimum energy and movement,
- enable reversible movements.

The abstract geometries were then evaluated according to their folding behaviour, the variation of dynamic movements, the actuation characteristics and the feasibility level, based on the score barriers and values summarized in the table below [Table 8].

Table 8: Main identified barriers for abstract geometry explorations and score system for the evaluation. [own work]

Barriers	Description	Score values		
		–	+	++
Folding behaviour	The relation between the crease pattern of the element and its folding behaviour. Evaluation based on: – Articulation / undulation level (degree of mountains and valleys) – Self-shading effect – Degree of unhindered actuation – Degree of reflectivity	No undulated geometries, very smooth and flattened surfaces, showing no self-shading effect. Possible placements of the actuators are obstructed or create conflicts with neighboring geometries.	A certain degree of self-shading is allowed through a higher level of undulated geometries present. More possibilities for unhindered actuation through integration of the actuators within the façade geometry.	The folding pattern can result to a significant level of articulation that has at the same time a high self-shading effect, without resulting to geometries conflicts or overlapping that would hinder the dynamic behaviour.
Range of intermediate states	A certain transformation capacity, in relation to the applicability of the element and its folding process. Evaluation based on: – Reversibility of deformation – Variation of dynamic movement	The geometry deformation is irreversible or causes material deterioration. The dynamic movement is limited to a start and end position with no flexibility for intermediate stops.	The geometry deformation requires force and effort to be reversed. The intermediate stops are either too complex that need additional control or still too limited and stiff.	The geometry deformation allows for an easy enough reversible movement. There is enough variation in the dynamic movement with a certain transformation capacity.
Actuation characteristics	The characteristics of the design and dynamic movement that relate to the actuation mechanism. Evaluation based on: – Speed of actuation/folding effect – Minimal energy needed for actuation – Number of actuation points – Degrees of freedom (DoF) – Required displacements – Actuation forces	There is a lot of force and points of actuation required in the mechanism. The DoF are either too many (too flexible) or too little (too rigid) and the displacement is either too little or too large.	There is already good enough relation between the energy required, the speed of actuation and the resulting deformation with a reasonable number of actuation points. It still has some limitations on the optimal flexibility and DoF.	There is good balance between the energy of the actuation forces and the resulting displacement with less actuation points required. There is enough elasticity in the system to allow the dynamic deformations, keeping at the same time a certain degree of rigidity.
Feasibility	Overall feasibility to integrate systems into façade components, considering functional and physical constraints for integration. Evaluation based on: – Ease of fabrication and manufacturing / Assembly / Costs (Real-scale building applicability factors) – Maturity of technology and material integration – Complexity level (in processing, manufacturing, assembly)	Too complex to be realized in a real-scale building application or too expensive for its erection. The technology required is not mature enough to allow an easy processing and fabrication.	The complexity of the components is reduced and they can be easier combined for a better integration. The materials and technology are already applied in practice, but there are still some limitations in terms of know-how or costs.	The fabrication and assembly process is better facilitated, the technology is mature enough and there is already knowledge for large scale applications. The investment required is also within reasonable limits.

Based on these benchmark criteria, a distinction was made on certain geometry traits and possibilities of the geometry and actuation to select those with potentials for further development. Some of these categorizations are further elaborated as follows:

Folding technique

The actuation of the folding elements has a major influence on the applicability of self-deployable structures and should be taken into account already in the early phases of the design, involving the number of actuation points, the required displacements and the actuation forces.

From the available self-folding mechanisms, the ones explored here used as a starting point existing self-folding techniques, namely the origami, kirigami and line-crease ones. The materiality of origami mechanisms, that

can be generalized as material hybrids, afford properties, such as structural rigidity across the planar faces, hinged flexibility along the fold lines, and possible embedded actuation between adjacent folded planes, which make them good candidates to be used in combination with passive self-actuators [Felton et al., 2013]. Additional advantages relate to the process of folding, which allows to quickly achieve three dimensional shapes with enhanced structural properties directly defining an envelope, separating in- and outside [Peraza-Hernandez, 2014, cited in Lebée, 2015]. During the folding process, they also exhibit properties, such as shape-changing, negative Poisson's ratio and bistability [Liu et al., 2018]. These folding kinematic properties make them versatile and suitable for implementation on deployable structures with the capacity to transform and adapt to multiple predetermined configurations and offer benefits when considering ease of transportation, erection and material efficiency [Greevenbroek, 2018].

Research has showed that origami structures show potentials in the field of smart structures, where projects have been developed that seek methods to create self-folding origami with potential application for morphing wings, micro-robots, and medical devices, as well as space structures. In the work of Hawkes et al., the development of a composite material sheet that can fold itself by electrical heating of a Shape Memory Alloy (SMA) hinge was investigated. Additionally, Liu et al. proposed a self-fold origami made of sheets of optically transparent, pre-strained polystyrene that shrinks in-plane when heated uniformly [Saito et al., 2015].

Kirigami, which is a variation of origami that includes cutting of the paper rather than only folding the paper, has also been recently used in research in the development of metamaterials with kinematic properties [Chen et al., 2020]. The challenge in this case is that its potentials in real structures are still in an exploratory stage, while the degrees of freedom and flexibility are significantly increased to be reliably used in large structures with a certain degree of controlled behaviour.

Function type

Typically, origami-like foldable structures work in a surface topological logic, where each crease adds a degree of freedom (DoF) and increases the dimensionality of the configuration space. Each crease intersection, or vertex, generates geometric constraints and limits the available portion of configuration space, whereas the coupling between folding angles and configuration-space topology allows for kinematic phenomena to emerge. However, a type of energetic bistability can be exhibited from structures assembled from rigid panels and torsional springs by introducing constraints on folding angles, which alter the connectivity of the configuration space topology. Such structures have their mechanics arising from both topological and energetic considerations [Liu et al., 2018], allowing a more individual movement to happen in a component scale by isolating fragments of the tessellation pattern. As an example, Figure 57 shows the traditional square twist, whose crease pattern has zero degrees of freedom (DoF) and therefore should not be foldable, can nevertheless be folded by accessing bending deformations that are not explicit in the crease pattern. These hidden bending DoF are separated from the crease DoF by an energy gap that gives rise to a geometrical mono- and bistability [Silverberg et al., 2015].

Stiffness level

Similarly, origami-based structures are usually designed following rigid folding techniques, where the facets and fold lines of origami can be replaced with rigid panels and ideal hinges, respectively. Designing such a deployment mechanism has a significant meaning in an engineering context, particularly in architecture for the following reasons:

1. The structure based on a watertight surface is suitable for constructing an envelope of a space, a roof, or a facade.
2. Purely geometric mechanism that does not rely on the elasticity of materials can realize robust kinetic structures in a larger scale under gravity.
3. The transformation of the configuration is controlled by smaller number of degrees of freedom. This enables a semi-automatic deployment of the structure [Tachi, 2010].

However, applying rigid origami to actual designs of architectural space in practice is hard to achieve, because the model cannot sufficiently adapt functional and environmental conditions required by an actual design context [Tachi, 2010]. Ideal rigid folding is, therefore, impossible in real structures, since every act of folding and unfolding is accompanied by elastic deformations. These deformations emerge as stretching and shrinkage of fold lines, fold line drifts, and out-of-plane deformations of facets [Saito, 2015]. Especially in the case of intentional deformations initiated by the SMMs, a certain level of flexibility is intended to be accommodated in the design.
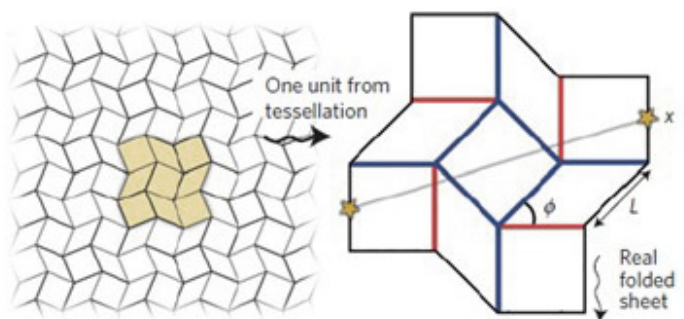

Figure 57: The square twist's essential geometric properties and mechanical characteristics. [Silverberg et al., 2015]
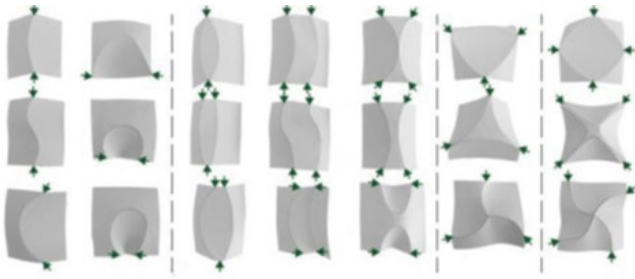
Figure 58: Overview of patterns created by configurations of respectively one, two, three and four creases. The green arrows indicate the orientation of actuation [Vergauwen et al., 2013]
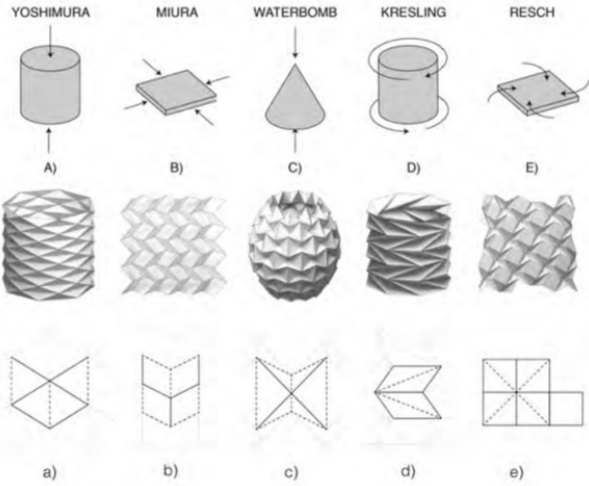

Figure 59: Natural Folding: Top: Illustration of Force + Matter. Middle: Expression of Folded Form. Bottom: crease patterns. a/A) Yoshimura-ori, b/B) Miura-ori, c/C) Waterbomb-ori (pinecone-ori/ananas-ori) d/D) Kresling-ori, e/E) Resch4-ori. [Gardiner et al., 2018]
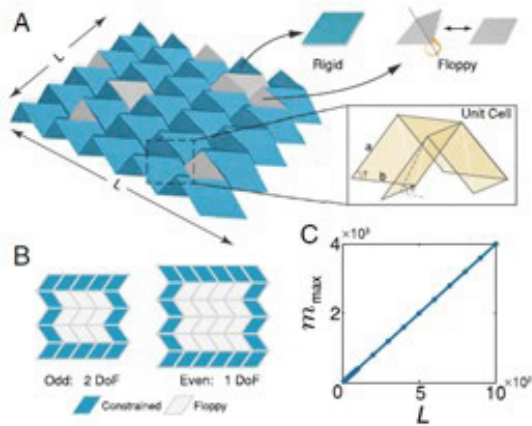

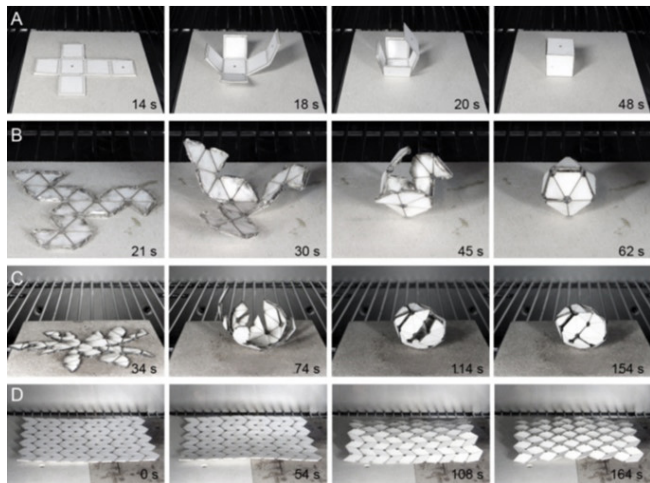Figure 60: Floppy origami as an example of a partially elastic geometry [Chen et al., 2019]

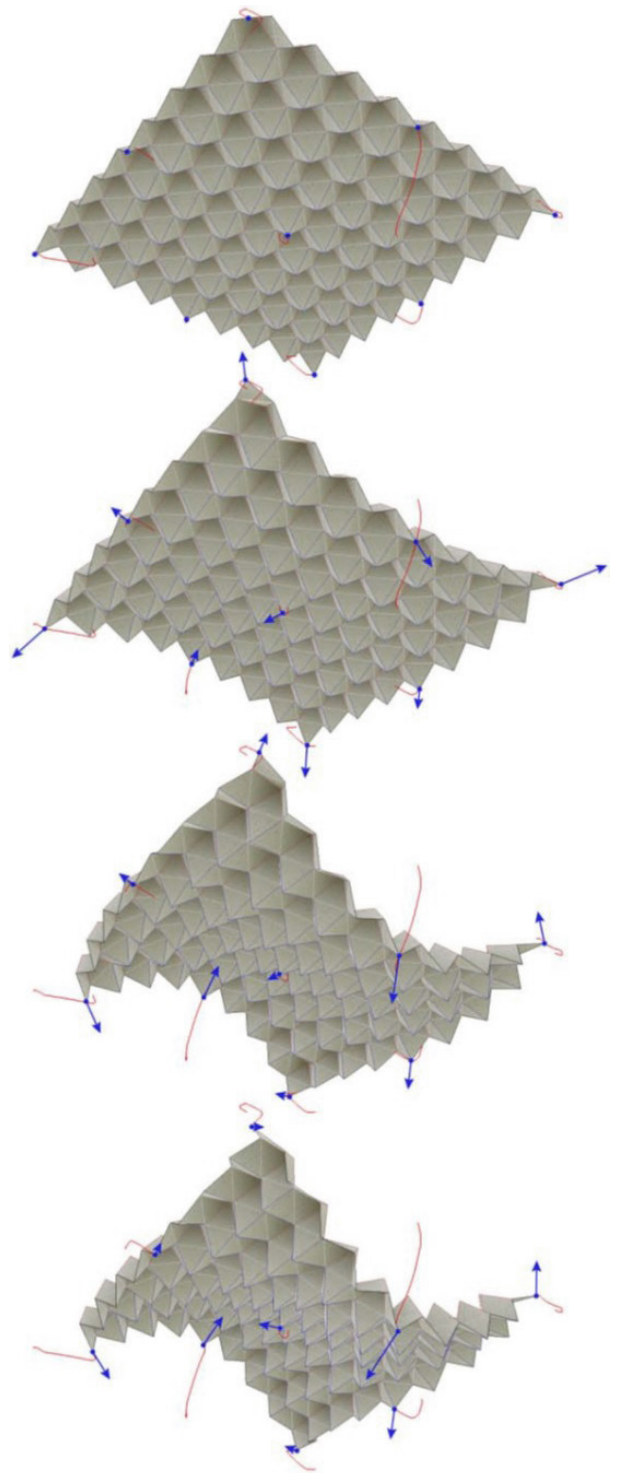Figure 61: Self-folding experiments with Shape Memory Polymers [Tolley et al., 2014]

Figure 62: Kinematic surface actuated by controlling the positions of 9 points (reaction force drawn in blue). [Tachi, 2010]
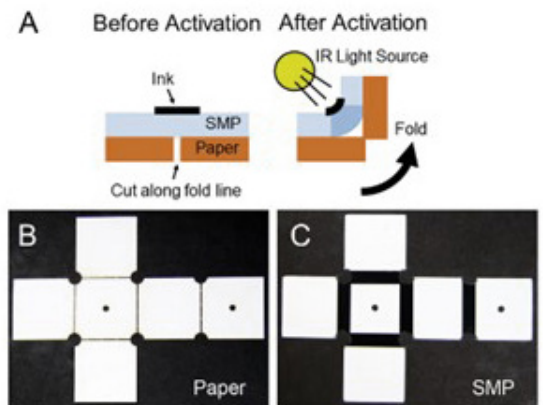

Figure 63: Light activated self-folding example of a 20mm long cube with SMPs. [Tolley et al., 2014]

This introduces the notion of partially elastic self-folding structures, where the facets of origami are replaced with not only rigid plates, but also elastic ones, creating a one degree of freedom（DoF）mechanism. These models are not rigid foldable, but can be folded down to a compact stack of plates with only a small amount of strain. Even if these partial strain rates are minimal, they can achieve full folding or unfolding in the entire structure and can help expand the origami into a new method of designing morphing structures. These mechanisms provide also with effective ways to use small-displacement actuators such as SMA actuators in morphing structures, because they enable to arbitrarily select energetically stable points in one origami folding process [Saito, 2015].

Facet geometry

The facet geometry of self-deployable structures can be divided into the triangular and quadrilateral ones. If no singularity is assumed, the degrees of freedom are represented as:

$$DoF = N_{E0} - 3_{NL} - 3$$

In this case, the kinetic motion of a mesh is controlled by the boundary configuration.

Another approach for designing a rigid-foldable structure is to use a quadrilateral mesh, such as Miura-ori. A quadrilateral mesh origami is normally not rigid-foldable since the degrees of freedom is given as:

$$DoF = N_{E0} - 3_{NL} - N_{facets} + 3 + N_S$$

Here, the number of facets N_{facets} basically increases proportional to the square of N_{Eo} for a normal two-dimensional mesh [Tachi, 2010]. The differences are that triangular patterns produce kinetic structures whose degrees of freedom are determined by the number of elements on the boundary, whereas quadrilateral ones can produce one-DoF kinetic motion based on redundant constraints. From these, the most flexible design originates from a triangular mesh.

Actuator self-folding mechanism

In continuation of the material background research in the first chapters, the actuator mechanism, which can be replace either a node, a folding edge or a face of the self-deployable geometry, can also work in different mechanism manners, related to the mechanics of the system. One example would be to act in a muscle-like movement, which, however, could add more complexity to the mechanical parts involved in the kinetic system. More simple and equally efficient ways would be to work in a linear shrinking deformation, causing a movement as part of a lever system or attached to a torsion axle, and in both ways reducing the input force required from the actuator to provide a greater output force.
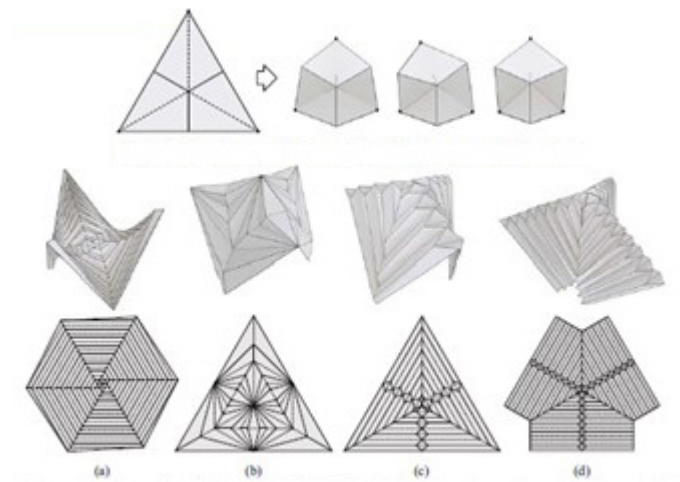

Figure 64: Examples of triangulated tripods. Quadrilateralpanels are all triangulated. [Tachi, 2010]
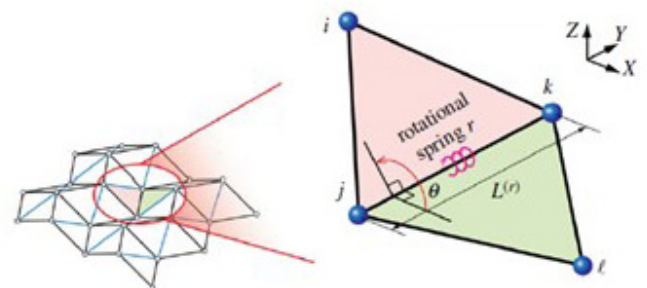

Figure 65: Examples of triangulated tripods. Quadrilateral panels are all triangulated. [Liu rt al., 2017]
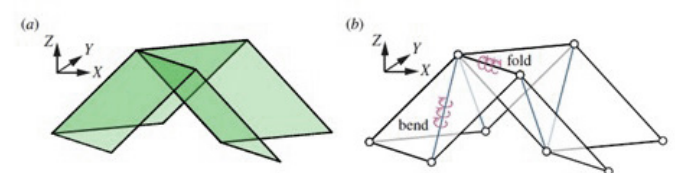

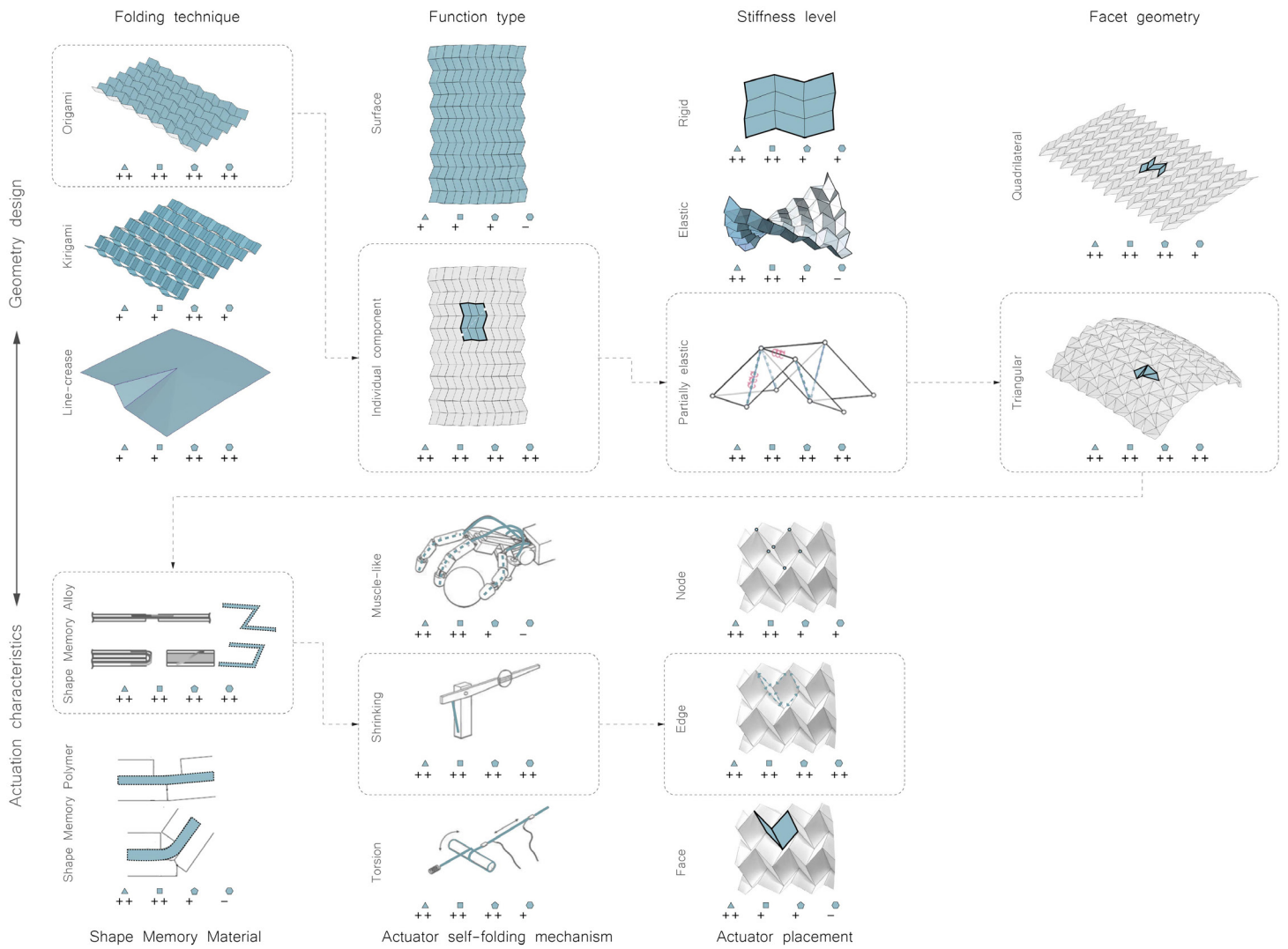Figure 66: Components of a rotational spring element, which is part of an origami assemblage. [Liu rt al., 2017]

5.3. MATERIAL & GEOMETRY SELECTION

From the above explorations, a series of geometrical traits was selected and design decisions were taken to proceed to a geometry concept for further development. Below is a summary overview [Table 9] of the main takeaways from each sub-category and the decision-making tree process [Figure 67], based on a balance and trade-off between desired geometry design and allowable actuation characteristics, following the previous research. Starting with the folding technique, the origami logic was a better candidate, because of its structural rigidity, while allowing some flexibility along the fold lines that could be used as the actuation edges. Additionally, even though the origami is usually seen as a surface, the responsive system would work better as an individual component, because it would be less complex and energy intensive. When it comes to the stiffness level, in real structures it is practically impossible to achieve ideal rigid structures and since the SMMs would by default cause certain deformation, a partially elastic system would be more adequate, while a triangular facet geometry would be more flexible and better controlled by the boundaries. As for the actuation technology, the SMAs were more promising, due to their maturity and accessibility, while they can be easier integrated in a folding geometry. They also function better in linear deformations through shrinking, thus reducing additional mechanical parts. For these reasons, a position along the edges would be, consequently, a more appropriate and integrated solution.

Table 9: Overview of the chosen design approaches and the argumentation factors behind the decision. [own work]

Design approach	Argumentation
Origami structures	– Structural rigidity across the planar faces – Hinged flexibility along the fold lines – Embedded actuation between adjacent folded planes
Individual working components	– Easier to manipulate individual movement and reactions to the environmental stimuli, less conflict to neighboring ones – Less complicated, less energy- and actuator-intensive
Partially elastic	– Ideal rigid folding impossible in real structures --> folding and unfolding accompanied by elastic deformations – Allows small-displacement actuators such as SMAs actuators to be embedded in morphing structures
Triangular facet geometry	– Most flexible design – Kinetic motion of mesh controlled by boundary configurations – More stable as an individual component
Shape Memory Alloys	– Change in configuration can be constrained by length preserving rigid bars or SMA wires along edges – More mature technology and wider use of applications
Shrinking actuator mechanism	– Simpler and more efficient way – Better integration in the edges of the geometry – Minimal mechanical parts
Edge actuator placement	– Better integration in a folding geometry – Minimal mechanical parts

Figure 67: Overview of the decision-making tree and the corresponding benchmark criteria. [own work]

Geometry design

Folding technique
- Origami: ++ ++ ++ ++
- Kirigami: + + ++ ++
- Line-crease: + + ++ ++

Function type
- Surface: + + + −
- Individual component: ++ ++ ++ ++

Stiffness level
- Rigid: ++ ++ + +
- Elastic: ++ ++ + −
- Partially elastic: ++ ++ ++ ++

Facet geometry
- Quadrilateral: ++ ++ ++ +
- Triangular: ++ ++ + ++

Actuation characteristics

Shape Memory Material
- Shape Memory Alloy: ++ ++ ++ ++
- Shape Memory Polymer: ++ ++ + −

Actuator self-folding mechanism
- Muscle-like: ++ ++ + −
- Shrinking: ++ ++ ++ ++
- Torsion: ++ + + +

Actuator placement
- Node: ++ ++ + +
- Edge: ++ ++ ++ ++
- Face: ++ + + −

Benchmark criteria

△ Folding behaviour: the relation between the crease pattern of the element and its folding behaviour
 - Articulation / undulation level (degree of mountains and valleys)
 - Self-shading effect
 - Degree of unhindered actuation
 - Degree of reflectivity

■ Range of intermediate states: a certain transformation capacity, in relation to the applicability of the element and its folding process
 - Reversibility of deformation
 - Variation of dynamic movement

⬠ Actuation characteristics:
 - Speed of actuation/folding effect
 - Minimal energy needed for actuation
 - Number of actuation points
 - Degrees of freedom (DoF)
 - Required displacements
 - Actuation forces

⬡ Feasibility:
 - Ease of fabrication and manufacturing / Assembly / Costs (Real-scale building applicability factors)
 - Maturity of technology and material integration
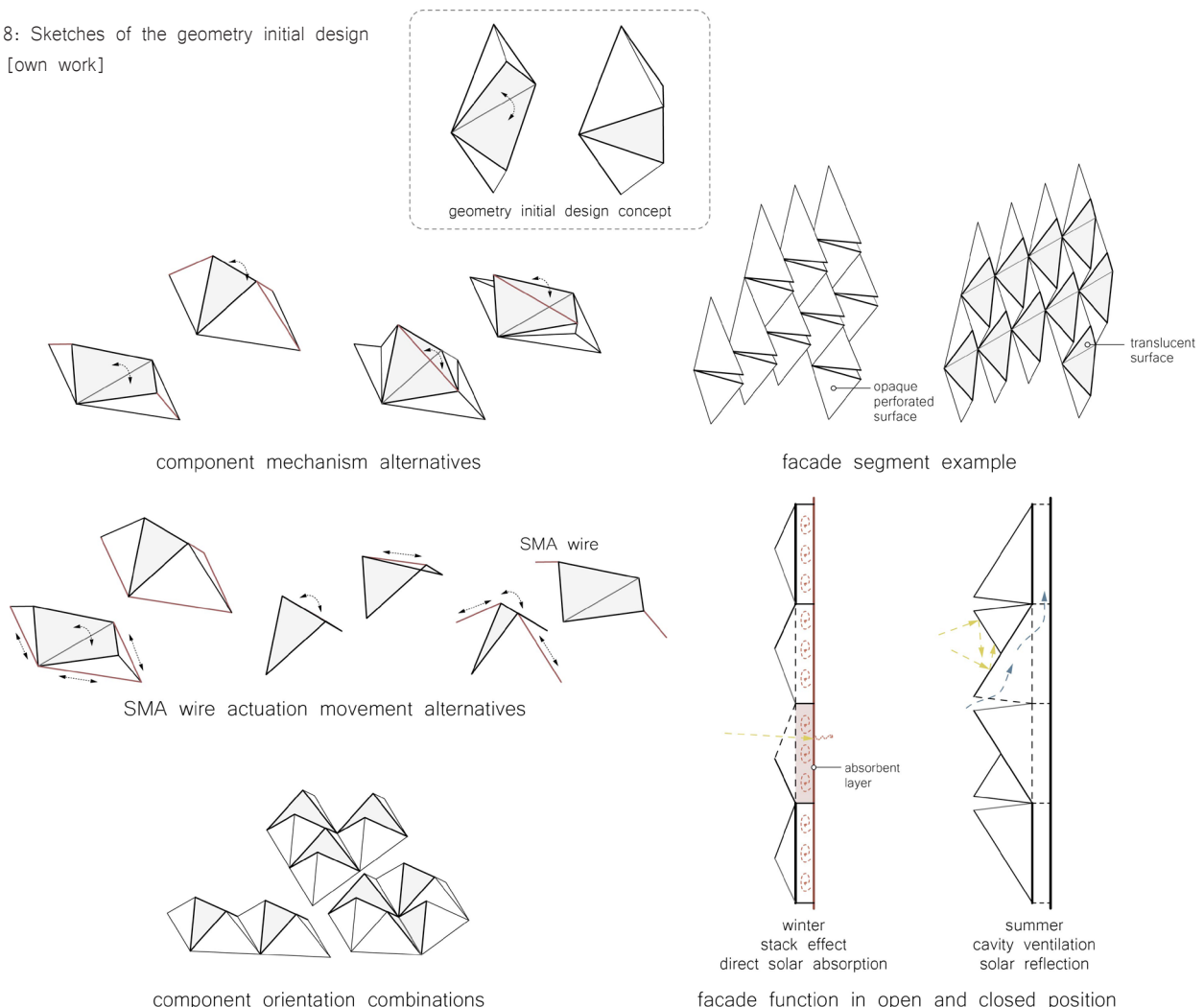 - Complexity level (in processing, manufacturing, assembly)

5.4. GEOMETRY DESIGN CONCEPT

During this iterative process, some of the preliminary design geometries that were originally proposed were evaluated based on the extent that they featured the above criteria. From these, the one highlighted in Figure 68 was the selected geometry concept to be investigated further, which is composed by two inverted pyramids, rotating around their common edge. This concept was selected because of its simplicity and flexibility to accommodate different arrangements and kinetic deformations with a minimal amount of geometries involved and enabling a high degree of undulation. Apart from that, it offered the possibility for coordination of the movements, allowing at the same time a certain component autonomy in relation to the neighboring units to avoid complications and enable individual stimuli triggering. The component also showed flexibility in terms of the different options for placement of the actuation mechanism aiming for a high integration level of the SMA wires in the same geometry, minimizing additional structural and mechanical elements.

To approve this initial geometry design concept, its potential on complying to the design guidelines in terms of facade functionality was also addressed at this early stage. In the same conceptual diagrams, the double facade function is illustrated, where during the winter the component adopts an open position with retracted and more flattened geometries that allow sun exposure and at the same time, works in a multiple closed-cavities system to increase the stack effect and solar absorption by exposing high absorbent surfaces in the interior. On the contrary, its actuated rotational movement leads to a closed summer position, allowing for a higher solar reflection and scattering of the incoming solar radiation in combination with an opened-air cavity system. The same logic follow the materials that compose each geometry face, switching from opaque reflective surfaces to translucent and perforated ones, adjusting to each ventilation and shading seasonal demands. This concept was then further developed to examine the energy and environmental performance by evaluating to what extent these design intentions satisfy the addressed research objectives.

Figure 68: Sketches of the geometry initial design concept. [own work]

geometry initial design concept

component mechanism alternatives

facade segment example

translucent surface

opaque perforated surface

SMA wire

SMA wire actuation movement alternatives

absorbent layer

component orientation combinations

winter
stack effect
direct solar absorption

summer
cavity ventilation
solar reflection

facade function in open and closed position

06   ENERGY & ENVIRONMENTAL PERFORMANCE EVALUATION

6.1. GOALS

Important part for the energy and environmental performance evaluation of the design was to first establish a set of goals in alignment with the early design geometry explorations and overall guidelines of the previous chapters. These are used as benchmark criteria for better understanding and evaluation of the design decisions. More specifically, they can be divided in the two distinct facade performance operations, during cooling- and heating-dominated periods, and how they address both the direct and indirect UHI impact in each case. This distinction is enabled by the dynamic movement of the facade component, which passively allows for the dual movement and transition throughout the seasons to adapt to the different heating, ventilation and shading needs.

In the first situation and in relation to the facade geometry deformation, the goal is to increase the undulated shading surfaces. By doing so, the self-shading is increased, reducing the direct solar radiation that is absorbed on the facade surface, while increasing the number of surfaces that are positioned perpendicular to the solar rays and reflect the radiation back to the atmosphere. In relation to the indirect impact, the undulated surfaces also act as primary shading devices that obstruct the direct sunlight to the interior of the building from the south, but also from east-to-west. When it comes to the air cavity function, the goal was to have an opened-air cavity ventilation that works as a heat attenuation zone, which exhausts and helps circulate the hot air that is accumulated inside.

On the contrary, the situation is reversed during wintertime, when the increase of the incoming solar radiation is desired to reduce the building's heating demands. To achieve this, the movement is more focused on decreasing the undulated shading surfaces, to admit more sunlight to the interior and to increase the solar radiation, which is being absorbed through the outer surface layer. At the same time, considering the lower position of the sun during the cold months, the top surface which tracks the sun's seasonal movement should also be lowered to be in a perpendicular position, similarly to the summer situation, and to switch the top side to a more absorbent one in terms of materiality. In accordance to the energy performance, there should be an increase of exposed surfaces that can absorb heat, such as the inner glazing or a highly absorbent coating in the opaque building surfaces inside the cavity, in combination with a closed-air cavity ventilation system, which functions as a heat buffer with multiple amplification zones.

The above goals show the desired performance and design intention and were used as guidelines to assess the compliance of the proposed facade system on these boundary conditions and to what extent they are satisfied. This was conducted based on quantitative and qualitative performance analyses and studies, which were later used to evaluate and reflect on the possibilities and limitations of the design, also in relation to similar facade technologies.
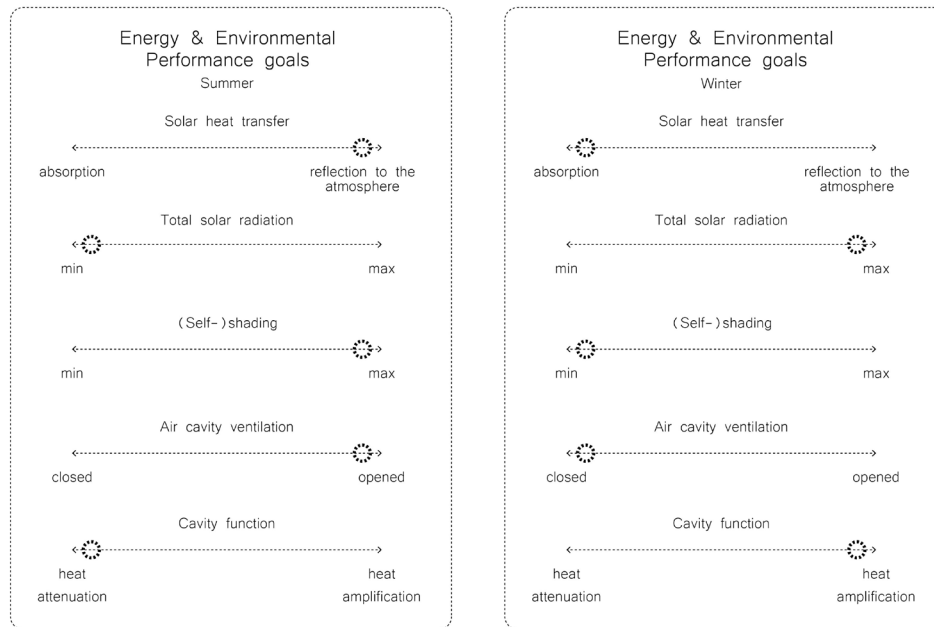
Figure 69: Diagrams of the energy and environmental goals during the summer and winter situation. [own work]

6.2. CLIMATE DATA - OPERATING SCHEDULE

Since the objective of the thesis is concentrated around the UHI effect, the environmental analyses also considered the urban environmental conditions in the simulations. This was realized by using the Dragonfly plug-in inside the Grasshopper environment, which enables the modelling and estimation of large-scale climate phenomena, such as the Urban Heat Island. This is accomplished with the help of the urban thermodynamic engine Urban Weather Generator [76], which can be connected to the rest of the digital simulation tools as a starting point by morphing the climate data of the studied location to reflect the conditions within an urban street canyon. The workflow of the climate information base set-up can be seen in the flowchart below [Figure 70], where

the EPW Weather file for Athens is imported from the EnergyPlus online database [29] and is then connected to the Dragonfly plug-in components to generate and include the urban climate data and conditions. Some of the additional inputs are, among others, the albedo of walls, streets and roofs, vegetated and paved surfaces, anthropogenic heat related to traffic, typical building typologies and envelope parameters. These values are set based on literature [Bradley et al., 2002] and an estimation according to general guidelines. The above values are gathered in the Tables 10 and 11.
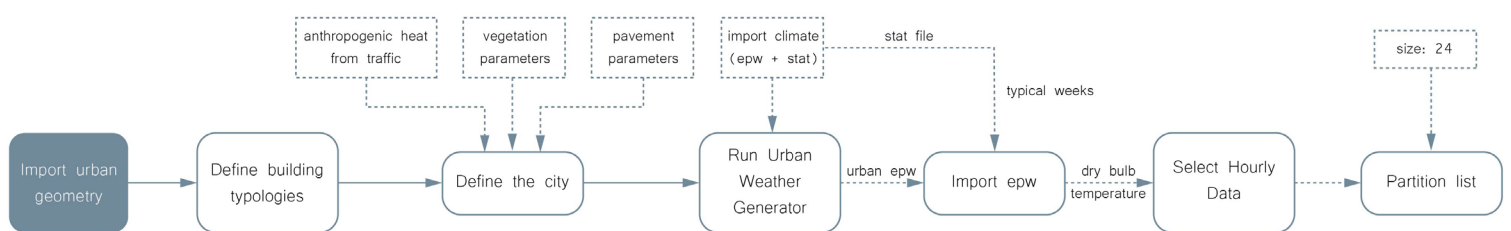

Figure 70: Flowchart of the Urban Weather Generator (UWG) workflow. [own work]

Tables 10, 11: Overview of the input urban parameters assigned in the UWG workflow. [own work]

Urban parameters	Values	Remarks
traffic sensible heat	8 W/m²	typical mixed use part of the city
vegetation albedo	0.25	typical vegetation albedo
pavement albedo	0.1	typical fresh asphalt

Building Typologies: Mixed use buildings		
Envelope Parameters	glazing ratio	0.5
	SHGC	0.35
	wall albedo	0.2 (light grey finish)
	roof albedo	0.3 (white gravel)

Based on the above data, the Annual Weather Data was plotted to estimate the activation temperatures of the SMA and the operating schedule of the adaptive facade system throughout the year. Apart from the climate set-up as explained before, the clear-sky situation was chosen to be used in the simulations, as it exhibits the worst-case scenario for the incoming solar radiation and the temperature increase. In the graphs below, the rural and urban conditions in terms of the impact on the dry bulb temperatures can be seen in comparison, where

there is a clear increase in the summer temperatures, especially during the evening hours, when the UHI is more intense because of the accumulated heat that is being released from the urban environment [Figure 71]. Next to them, a few more graphs of the solar radiation rose and the annual sunlight hours are used to get a better understanding and overview of the weather and climate conditions in the area [Figures 72, 73].
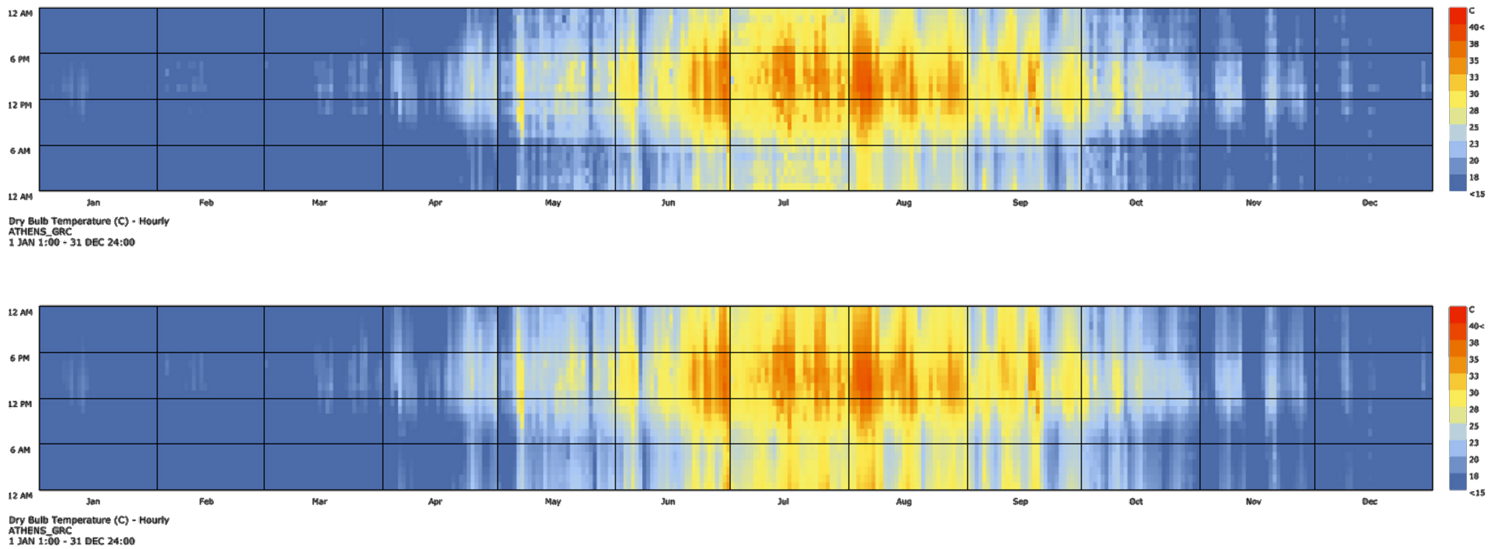

Figure 71: Annual dry bulb temperatures chart. Top: Rural temperatures, bottom: Urban temperatures after the UWG modification. [own work]
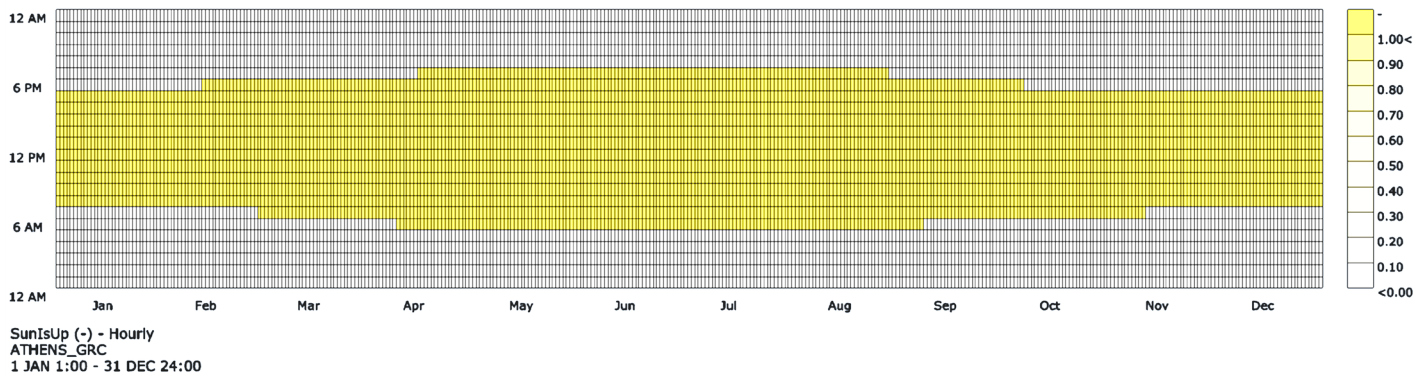

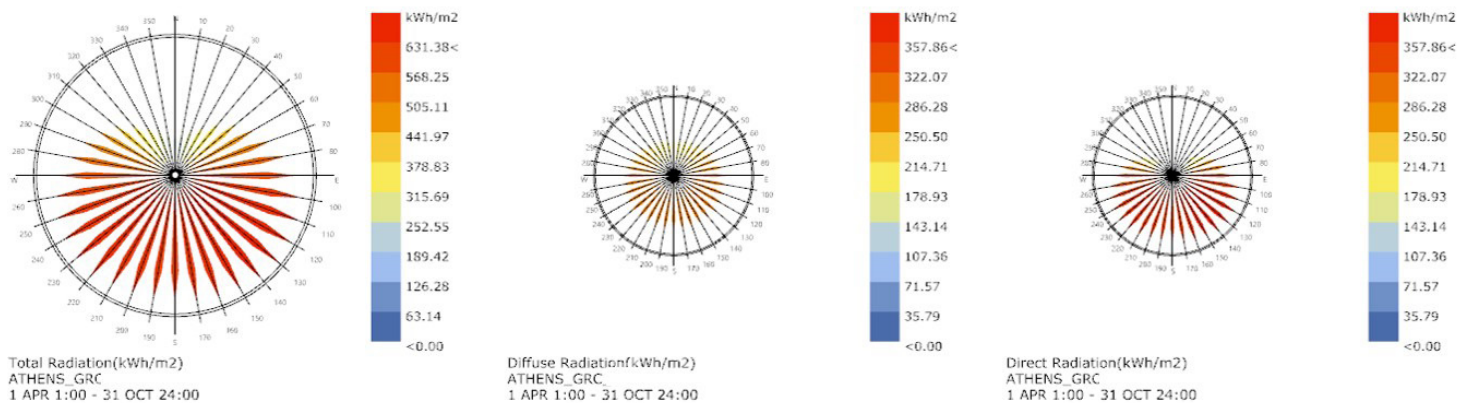Figure 72: Annual sunlight hours chart. [own work]

Figure 73: Radiation rose charts for the period April-October. From left to right: Total, diffuse and direct radiation values in kWh/m². [own work]

For the scope of the analyses, three representative periods were chosen to be used for the environmental studies, which were derived from the imported weather file. These were a typical spring week (05/04–11/04), a typical summer week (29/06–05/07) and an extremely hot summer (03/08–09/08). In the tables below, the hourly dry bulb temperatures were analyzed for each period, where the highest, lowest and average temperatures are highlighted and the time range for each case. As it can be seen, during the summer, the temperatures range approximately between 23°C and 35°C, with a peak around noon, while in the spring, the temperature ranges between 12°C and 17°C. It can also be observed that the temperature fluctuations happen in a quick and not distinct pace during the day, which could be translated that a gradual seasonal movement of the proposed facade system can be more straightforward and durable than a daily operation, especially when relying only on a passive mechanism to avoid operating complications and malfunctions. Based on this temperature analysis, the responsive facade system can be estimated to be active approximately between April and October with a total working temperature range of 15°C–35°C. More specifically on the operating schedule of the SMA mechanism, it can be programmed to have an activation set temperature at 23°C (A_s), when the SMA starts shrinking causing the deformation towards the summer end position with a peak at 35°C (A_f). At this state it is stabilized and afterwards gradually recovers back to the original state at 20°C (M_s), as the temperature starts decreasing, and is finally stabilized to the winter situation at 15°C (M_f).

Table 12: Hourly daily dry bulb temperatures for the typical spring week (05–11/04). [own work]

Typical Spring week 05/04-11/04							
	Day of week						
Hour of day	1	2	3	4	5	6	7
0	15,1	16,6	14,8	15,6	14,6	8,4	11,4
1	15,1	16,2	14,5	15,6	14,4	8,5	11,3
2	14,8	15,8	14,3	15,5	14,2	8	11,2
3	14,4	15,4	14,2	15,3	14,1	7,7	11,1
4	14	15,1	14,1	15,1	14	7,2	11
5	13,9	15	14,1	15	14,2	7,4	11
6	13,8	15,1	14,2	15	14,4	7,8	11
7	14,1	16,4	14,4	15	14,6	8,2	11,1
8	14,6	15,9	14,8	15,3	15,4	9,4	11,6
9	16,4	15,8	15,9	15,9	16,3	10,8	12,6
10	19	16,1	17,3	17	17,2	12,2	14
11	20,1	16,6	18	17,6	17,8	12,8	14,7
12	20,5	17,3	18,3	17,9	18	13,2	14,9
13	20,6	18	18,4	18,1	18	13,7	15
14	20,5	18,1	18,3	18	17,6	14	15
15	20,4	17,8	18	17,7	16,8	14,2	15
16	20,2	17,5	17,4	17,3	15,7	14,4	14,9
17	20	17	17,2	16,9	14,6	14	14,6
18	19,3	16,6	17	16,6	13,9	13,1	14,4
19	18,8	16,2	16,7	16,3	13,2	12,7	14,1
20	18,4	15,9	16,5	16,1	11,8	12,3	13,8
21	17,9	15,7	16,2	15,8	10,3	12	13,5
22	17,5	15,4	15,9	15,3	9	11,7	13,2
23	17	15,1	15,7	14,9	8,6	11,5	12,9

									Time Range	Average
maximum	20,6	18,1	18,4	18,1	18	14,4	15		13:00-14:00hrs	17,5
minimum	13,8	15	14,1	14,9	8,6	7,2	11		04:00-05:00hrs	12,1
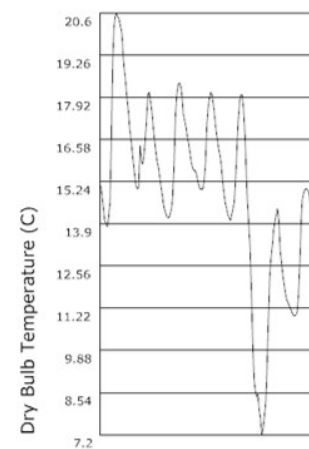
ATHENS_GRC

Typical Summer week 29/06-05/07							
	Day of week						
Hour of day	1	2	3	4	5	6	7
0	22,9	31,4	25,9	24,8	24,5	25	25,3
1	22,6	30,9	24,9	24,2	24,2	24,8	24,9
2	22,4	30,2	24,3	24,2	24	24,6	24,8
3	22,1	29,3	24,1	23,9	23,8	24,3	24,6
4	21,8	28,5	23,9	23,5	23,5	23,9	24,2
5	22,4	30	23,5	23,5	23,4	23,8	24,2
6	23,3	30,2	23,6	24	24	24,5	24,8
7	25,3	30,3	24	23,8	24,1	24,6	25
8	28	31,1	25,2	24,6	24,8	25,5	25,7
9	30,8	32,1	26,6	25,8	26,3	26,6	26,1
10	33,4	33	27,3	27,5	26,8	27	28,2
11	34,6	33,4	27,9	27,3	27,1	27,2	28,9
12	35,3	33,8	28,1	27,9	27,2	27,9	29,1
13	35,8	34,1	27,6	29,1	27,4	28,4	29,1
14	35,2	34	25,2	28,8	27,3	28,3	29,2
15	34,4	33,8	27,4	28,4	27,2	28,2	29,2
16	35,3	33,6	27,8	27,5	26,9	28	28,7
17	34,9	32,6	27,5	26,9	27	28,8	27,5
18	34,3	31,4	26,8	26,5	26,3	28,3	26,6
19	33,4	30,3	25,8	25,7	25,9	26,7	26
20	33	29,7	26	25,3	26,1	26,4	26,1
21	32,6	29,4	25,7	25,2	25,8	26	26,1
22	32,1	28,2	25,3	24,9	25,4	25,6	25,7
23	31,8	27,2	25	24,6	25,3	25,5	25,5

	1	2	3	4	5	6	7	Time Range	Average
maximum	35,8	34,1	28,1	29,1	27,4	28,8	29,2	12:00-14:00hrs	30,4
minimum	21,8	27,2	23,5	23,5	23,4	23,8	24,2	04:00-05:00hrs	23,9

ATHENS_GRC

Table 13: Hourly daily dry bulb temperatures for the typical summer week (29/06-05/07). [own work]
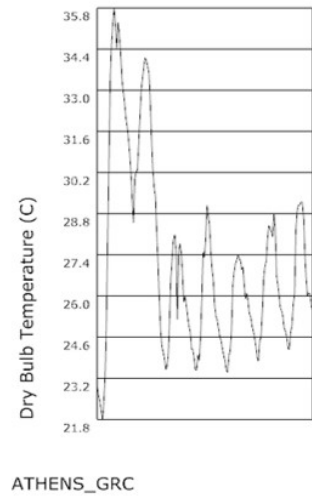
Extremely Hot week 03/08-09/08							
	Day of week						
Hour of day	1	2	3	4	5	6	7
0	27,6	29,5	29,9	30,2	31,2	27,4	29,4
1	27,5	29,1	29,5	29,8	30,7	27,2	29,1
2	27,4	28,7	29,1	29,6	30,3	27	28,8
3	27,2	28,4	28,8	29,2	30	26,8	28,5
4	27	28,2	28,5	28,8	29,6	26,6	28,2
5	27,6	28,7	29	28,6	29,5	26,7	28,2
6	28,7	29,4	29,7	28,7	29,5	27,1	28,2
7	29,9	30,2	30,6	29,1	30,7	27,5	28,4
8	30,5	31,6	30,9	30,6	30,2	28,4	28,9
9	30,7	33,2	32,5	32,6	30,4	29,6	29,3
10	30,7	34,8	34,3	34,7	31,5	31	30,2
11	32,2	35,5	35,1	35,6	32,5	32	31,2
12	34	36	35,7	36,4	33,3	32,7	32,3
13	36	36,5	36,2	37,1	34,1	33,2	33,3
14	36,2	36,3	36,3	36,9	33,6	33,3	32,5
15	36,2	36,1	36,1	36,4	32,8	33,3	31,2
16	36,1	35,8	36	35,7	31,7	33,2	30
17	35	35	35,3	35	30,8	32,6	28,7
18	34	33,8	34,3	34	29,6	31,7	27,1
19	32,7	32,9	33,5	33,4	28,8	31,1	25,8
20	31,9	32,1	32,7	33	28,3	30,8	25,1
21	31,2	31,5	31,9	32,6	28	30,5	24,6
22	30,5	30,9	31,1	32,1	27,8	30,1	24,4
23	30	30,4	30,5	31,7	27,6	29,8	24,1

	1	2	3	4	5	6	7	Time Range	Average
maximum	36,2	36,5	36,3	37,1	34,1	33,3	33,3	13:00-14:00hrs	35,3
minimum	27	28,2	28,5	28,6	27,6	26,6	24,1	04:00-05:00hrs	27,2

ATHENS_GRC

Table 14: Hourly daily dry bulb temperatures for the extremely hot week (03-09/08). [own work]
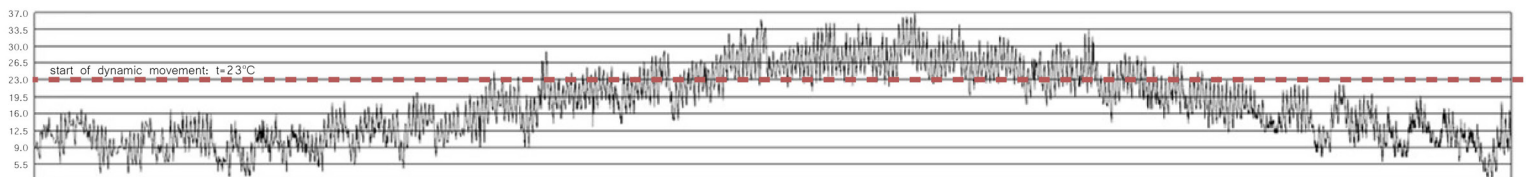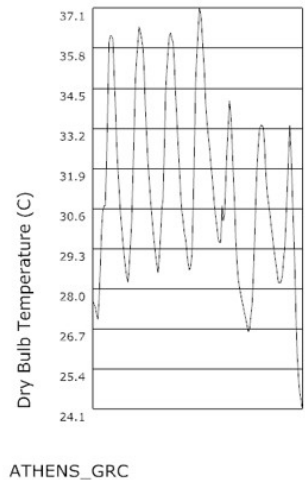

start of dynamic movement: t=23°C

Figure 74: Annual dry bulb temperatures diagram and threshold of the SMA's operating schedule (23°C: start of dynamic movement). [own work]
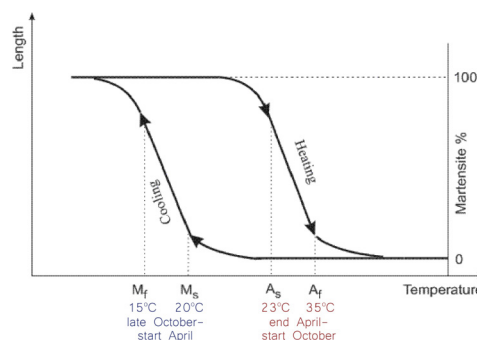

Figure 75: The hysteresis curve of the SMA and its actuation temperatures. [own work]

6.3. UHI DIRECT IMPACT EVALUATION

Workflow & Methodology

The evaluation of the UHI direct impact followed a systematic and step-by-step feedback-loop workflow, where each design decision underwent a series of design iterations and control checks. Similar to the preliminary explorations, the starting point of the shape and geometry was informed by the design guidelines, which received a first feasibility confirmation to proceed to the environmental performance evaluation, starting with the UHI direct impact. For this, the main assessment method in relation to the component geometry was the ray trace analysis, with the condition that at least 75% of the incoming solar rays to the facade should be reflected back towards the atmosphere and not directed to the urban environment. Once this condition was met, the second level of evaluation was realized on the facade level and arrangement with the same condition criteria. After several iterations and when the general facade geometry and arrangement fulfilled these requirements, the performance assessment was realized on an urban level to assess the impact of the facade design on the microclimate conditions, by simulating and visualizing the cumulative radiation heat maps in an urban canyon street scenario, in relation to the surrounding environment and in comparison to a typical facade. These results could then lead to an additional optimization of the component geometry or the facade arrangement. All the performance observations in the end helped to reflect on the overall direct impact on the UHI effect and potentially update and refine some of the preliminary design guidelines.
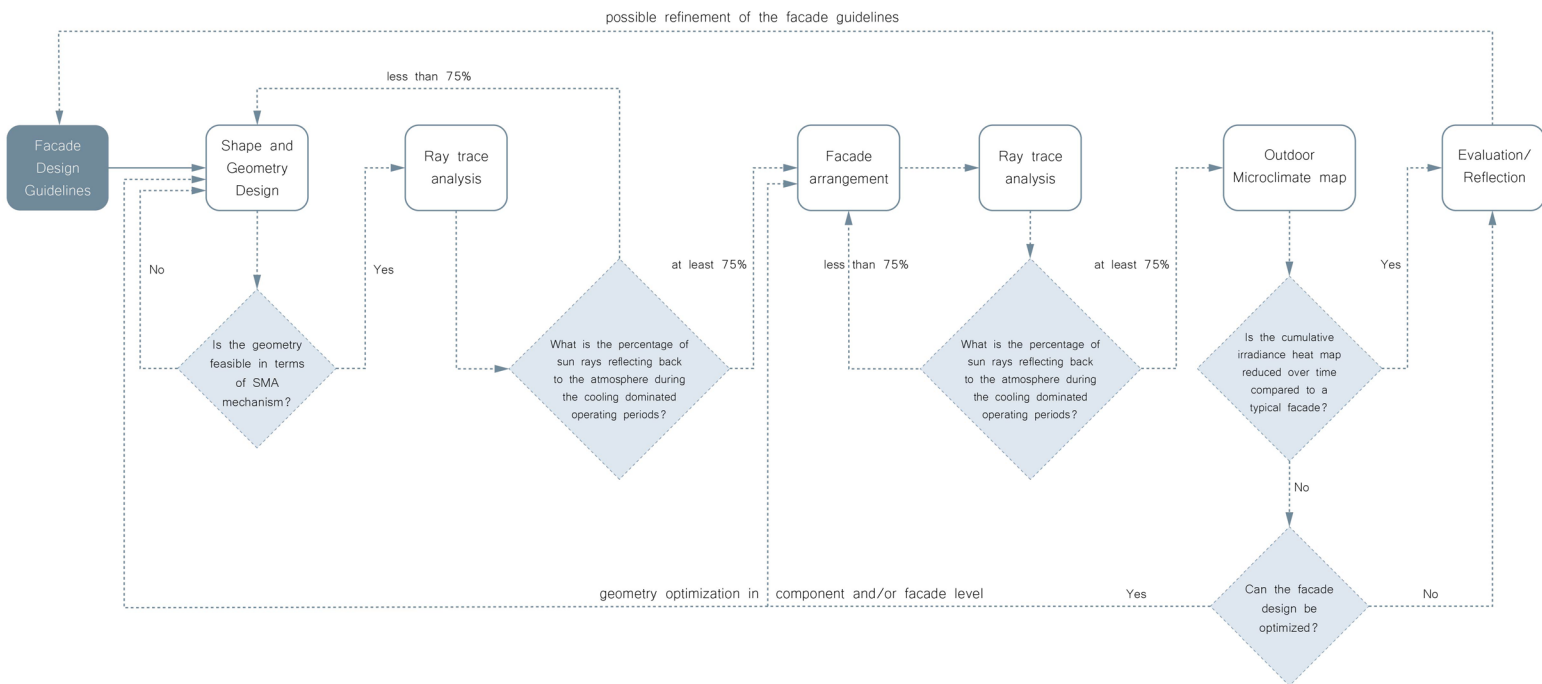

Figure 76: Flowchart of the feedback-loop iterative process of the UHI's direct evaluation workflow. [own work]

6.3.1. COMPONENT AND FACADE LEVEL – SUN RAY TRACE ANALYSIS STUDIES

6.3.1.1. PRELIMINARY GEOMETRY AND ENVIRONMENTAL STUDIES

The first explorations of the initial geometry concept were based on the proportions of the component and how these relate to their environmental performance in terms of solar radiation, to receive a first indication on the impact of the self-shading effect and how the proportions affect the overall scale and performance, as seen on the table below [Table 15]. However, by following the methodology explained in the previous flowchart [Figure 76] and since the most important factor to evaluate the direct impact was the reflectivity of the sun rays back to the atmosphere, a first round of sun ray trace analyses on a segment of the facade was realized using the

Honeybee "Bounce from Surface" component, which will be elaborated further later in this chapter. The first results already showed that the original geometry reflected only about 10% of the rays. This was mostly due to the rays reflected from the top pyramid downwards and led to a geometry refinement, having a more flattened pyramid on top with a rotation of 10° from the z axis, slightly open for ventilation. Apart from that, the rotation of the bottom pyramid was optimized to have the top surface perpendicular to the sun rays from June to December as a first case, which provided as an output a range of 30°–75° rotation.

Table 15: Overview of the various geometry alternatives based on proportions and sizes and a first solar radiation study. [own work]
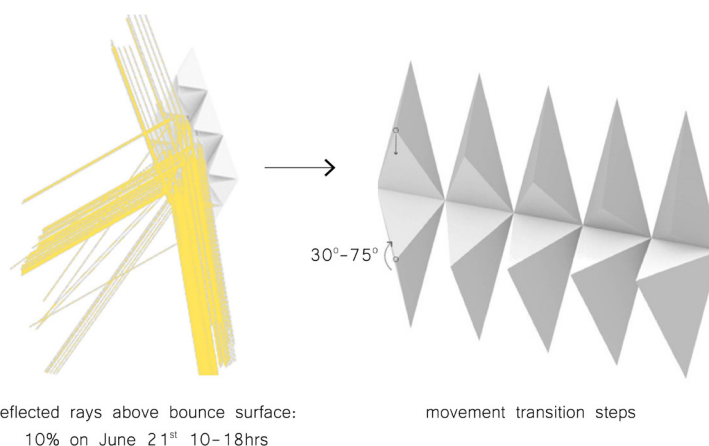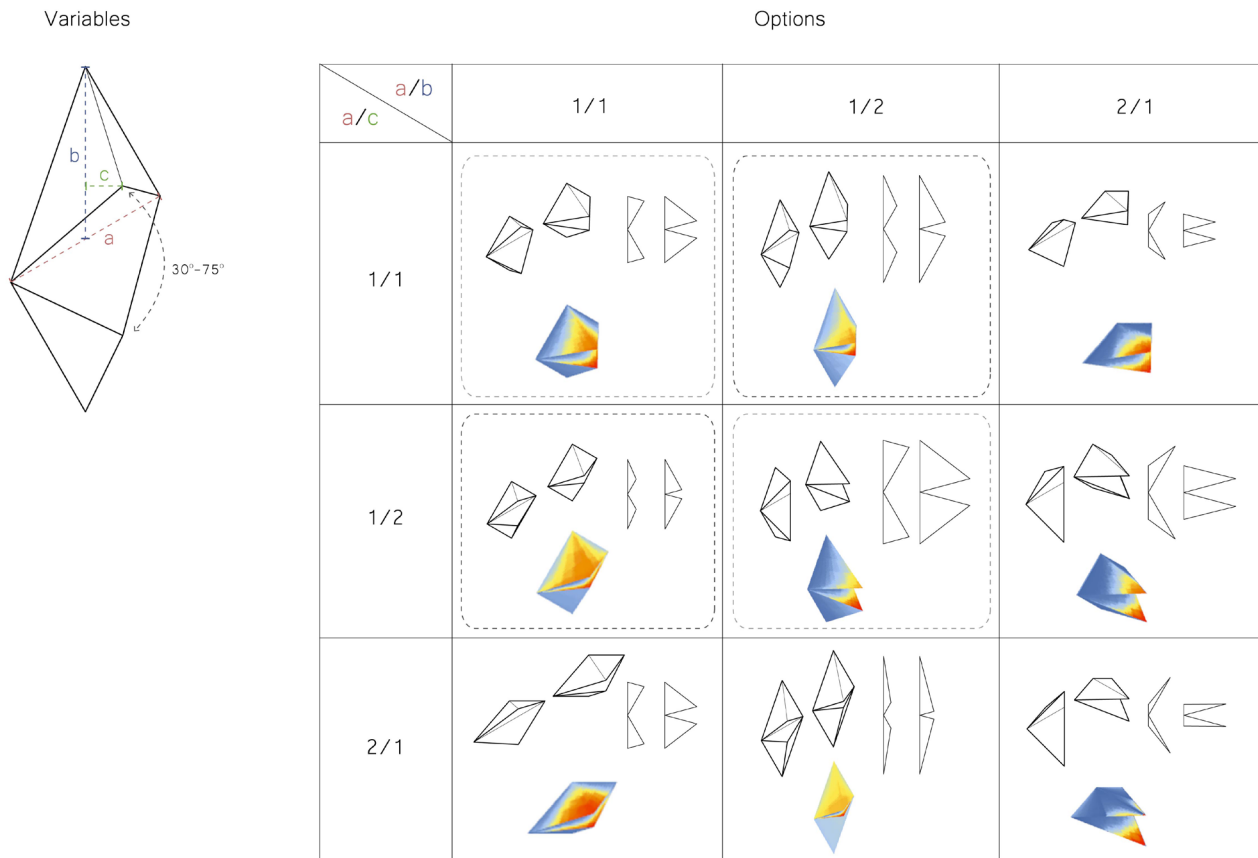

Figure 77: Geomtery design optimization stages based on the environmental performance. [own work]

reflected rays above bounce surface:
10% on June 21st 10-18hrs

movement transition steps

6.3.1.2. SMA'S FEASIBILITY DESIGN CONTROL GUIDELINES

As explained in the workflow process, the first step before evaluating the environmental performance of the facade design is the feasibility of the proposed system, which in this case involved the SMA operation and workability, since it is the critical parameter for the system to be realized and integrated in practice. For the early design stage of the geometry explorations, certain rules of thumb were taken into consideration to follow a design decision, which were based on literature [Lobo et al., 2015] and guidance from experts in the field [Rouven-Denz, P., Priedemann Facades] and SMA manufacturers [Ingpuls]. The main concerns were that the SMA strain ratio should be kept within 3-5% of the original wire length, to achieve better dynamic performance and to ensure the wire's durability after a certain number of cycles. In accordance to that, the wire should not reach large total lengths, because this would also compromise its durability and longevity over time and in addition, it would require a larger diameter due to the higher strength demands.

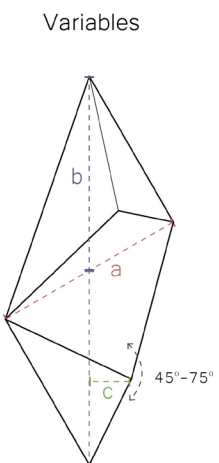## 6.3.1.3. GEOMETRY REFINEMENT STAGES – PERFORMANCE IMPROVEMENT

Based on the abovementioned general guidelines, the initial studies were continued on different component sizes and proportions and similarly to the first explorations, the edge "a" was taken as a reference dimension and the dimensions "b" and "c" were variables, as seen in the table below [Table 16]. Some further parameters that were considered were the desired degree range that was set to the minimum of 45°-75°, to satisfy at least the assumed operating schedule from April to October, considering the sun's azimuth angle at these end positions. From these end values, the summer angle was the most critical one to be satisfied and it was set as a benchmark for the initial evaluation round. In the same table, the first candidates that met the above conditions are highlighted and were selected to be further studied on their allowable rotational range, including a small tolerance to allow space for possible marginal geometry improvement.

Table 16: Overview of the various geometry alternatives based on proportions and sizes in relation to the SMA's design guidelines. [own work]

Strain ratio (limit: **3-5%**)
desired rotational degree range:
start: 45°   **end: 75°**
(perpendicular to sun rays on October/November 12hrs and June 21st 12hrs)

Variables	a/b ╱ a/c	1/0.5	1/0.75	1/1	1/1.5	1/2
	1/0.5	9%	7% A	5.5% B	3.8% C	2.8%
	1/1	16%	14%	11.5%	8% D	6% E
	1/2	18%	21%	20%	16%	12.5%

Table 17 shows an overview of the relation between the sizes of the candidates from the previous table and the allowable rotational range. The rotational range was calculated assuming the bottom two edges of the bottom pyramid to be replaced with SMA wires in their total length, which would share the force needed for the rotation. In this way, additional material would also be avoided and the working mechanism would be better integrated in the facade system. This approach was meant to be the first intention in alignment with the design guidelines. As seen from the table, it can be observed that cases with small rotational range reduce in the end the advantage of having a dynamic system, since the movement is negligible and there would not be much increase in performance compared to an equivalent static system. At the same time, large deviations between proportions could compromise the SMA's durability and workability, as explained before, which would lead to an increase in the complexity of the system and the required forces to realize the dynamic deformations. From those options, the ones highlighted proceeded further to be studied on their environmental performance based on the ray trace analysis.

Table 17: Overview of the relation between the sizes and allowable rotational range to be further studied on their direct environmental performance. [own work]

A (1/0.75, 1/0.5)

end angle \ start angle	40°	45°	50°	55°
70°	x	x	**4.8%**	**3.5%**
75°	x	7%	6%	**4.8%** (1)

B (1/1, 1/0.5)

end angle \ start angle	40°	45°	50°	55°
70°	x	**4.6%**	**3.7%**	x
75°	6.3%	5.5%	**4.7%** (2)	x

C (1/1.5, 1/0.5)

end angle \ start angle	40°	45°	50°	55°
70°	x	x	**2.6%**	x
75°	**4.3%**	**3.8%**	**3.2%** (3)	x

D (1/1.5, 1/1)

end angle \ start angle	40°	45°	50°	55°
70°	x	x	5.4%	**4.1%**
75°	x	8%	6.8%	5.4%

E (1/2, 1/1)

end angle \ start angle	40°	45°	50°	55°
70°	x	**5%**	5.4%	**3.1%**
75°	x	6%	**5.1%**	**4.1%**

In the next stage, during the ray trace analysis, a backward raytracing method was followed using a combination of a Forward Ray Trace analysis and the "Bounce from Surface" component of the Honeybee plug-in, which starts with the geometry in question to examine the direction of the sun vectors after bouncing off the surface and automatically generates start points of the sun rays based on a grid size or density of the sun vectors. The advantage of the latter method is that it also enables the visualization of the sun rays after several bounces, considering the rays reflected from the neighboring surfaces before bouncing off to the atmosphere or the urban environment. In this study, the analysis considered 2-3 bounces and evaluated the reflectance both between the different options from the previous table and between a horizontal and a diagonal arrangement. The flowchart including both the sun ray trace and the radiation analyses is illustrated on the combined flowchart in Figure 79, since the workflow shares similar

steps to a certain point. A summary of the results can be found in Figure 78, where it was concluded that the Option 2 showed a good enough performance with both a larger rotational range with a starting angle between 45°-50° and a strain ratio within allowable limits. Some further observations were the existence of a "blind" angle, which corresponds to the rays being reflected from the top pyramid downwards through the in-between geometry gaps in certain time periods, as also seen in the diagram below. The analyses also showed that the bottom pyramid's size and arrangement had the most impact on obstructing the sun rays from the top ones with a wider geometry being more efficient towards this goal. In this respect, the diagonal facade arrangement exhibited a better performance as well, because those rays were reflected back to the atmosphere by the neighboring components and the ones below, as a result of the more scattered component distribution, while the horizontal one had a negligible impact.

1a)
top pyramid 15° rotation
reflected rays above bounce surface:
60% on June 21st 12hrs
60% on June 21st 10-18hrs

1b)
top pyramid 10° rotation
reflected rays above bounce surface:
85% on June 21st 12hrs
90% on June 21st 10-18hrs

2)
top pyramid 10° rotation
reflected rays above bounce surface:
75% on June 21st 12hrs
80% on June 21st 10-18hrs

3)
top pyramid 10° rotation
reflected rays above bounce surface:
60% on June 21st 12hrs
85% on June 21st 10-18hrs

Horizontal arrangement
top pyramid 15° rotation
reflected rays above bounce surface:
75% on June 21st 12hrs
85% on June 21st 16hrs

Diagonal arrangement
top pyramid 15° rotation
reflected rays above bounce surface:
85% on June 21st 12hrs
70% on June 21st 16hrs

"blind" angle

Horizontal arrangement
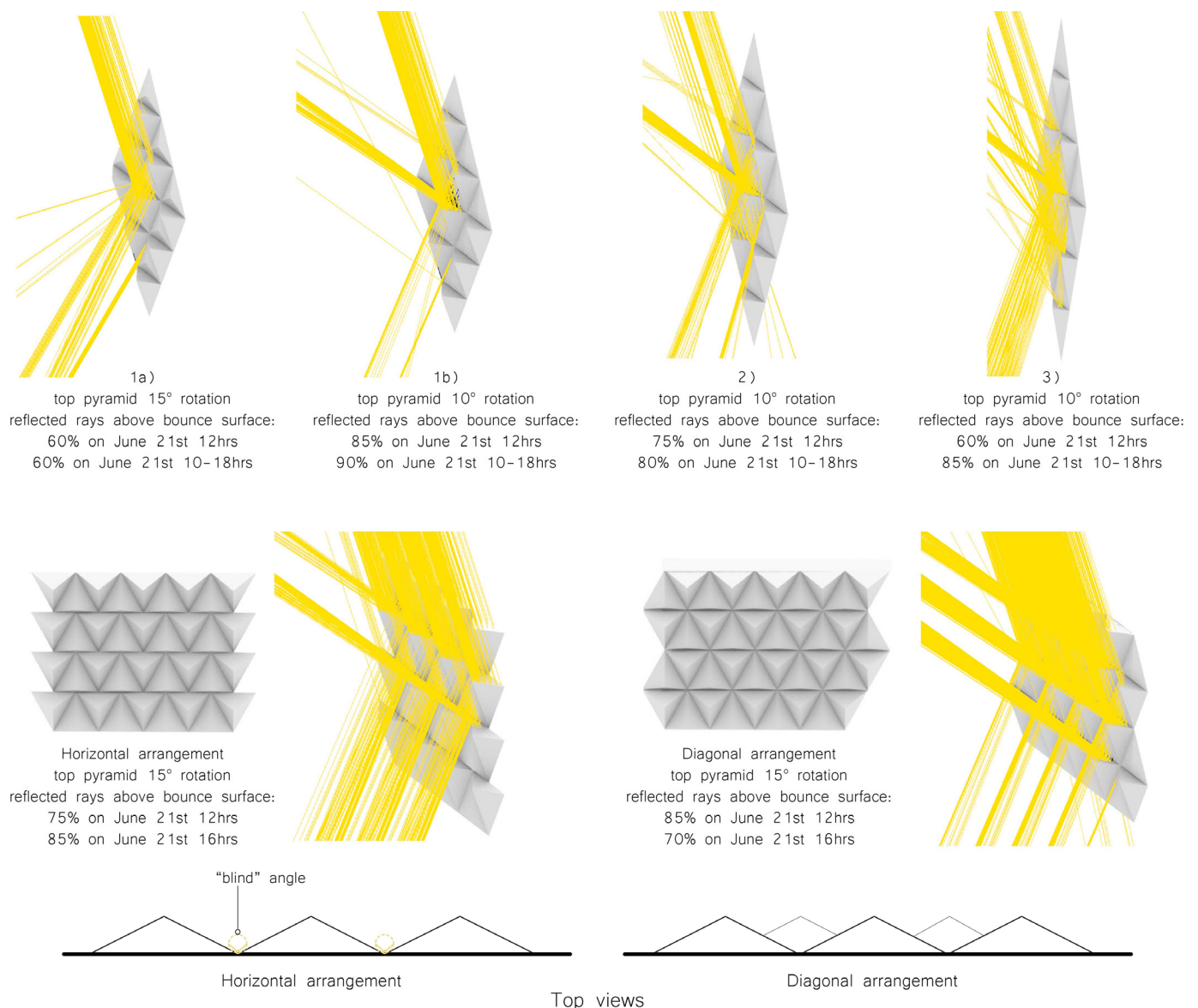
Diagonal arrangement

Top views

Figure 78: Summary of the sun ray trace analysis studies for each option and in comparison to the facade arrangement. Bottom: The impact of the "blind" angle impact and the difference between the horizontal and diagonal arrangement. [own work]

Forward Ray Trace Analysis

Base Analysis Set-up

Bounce from Surface

Radiation Analysis

Forward Ray Trace Analysis section:
- Generate test points
- domain start / domain end → Construct Domain
- Create Number Range in X / number of steps / Create Number Range in Y
- Construct Test points → Flatten points → Evaluate Surface
- Reparameterize surfaces → Brep faces → Deconstruct Brep → context Brep
- set context that will reflect the sun rays
- Geometry → Move points / Motion / Multiplication
- Start points → Forward Ray Tracing → additional context Brep / number of bounces / last bounce length
- 2 bounces → **Sun Rays traced forward through the analyzed geometry**

Base Analysis Set-up section:
- epw file path → Import epw file
- month range / hour range → Set analysis period → Create sun path / sun center point & scale factor
- clear sky → Generate Cumulative Sky Matrix → Select Sky Matrix

Bounce from Surface section:
- context Brep → Deconstruct Brep → Brep faces → Flip Normals of the Faces → Source surfaces
- sun positions / sun vectors
- Context / Groft / Sun vectors → Bounce from Surface
- grid size / number of bounces / first bounce length / last bounce length

Radiation Analysis section:
- analyzed geometry / analyzed context / grid size / distance from base → Radiation Analysis → **Radiation Mesh** / **Total Radiation**
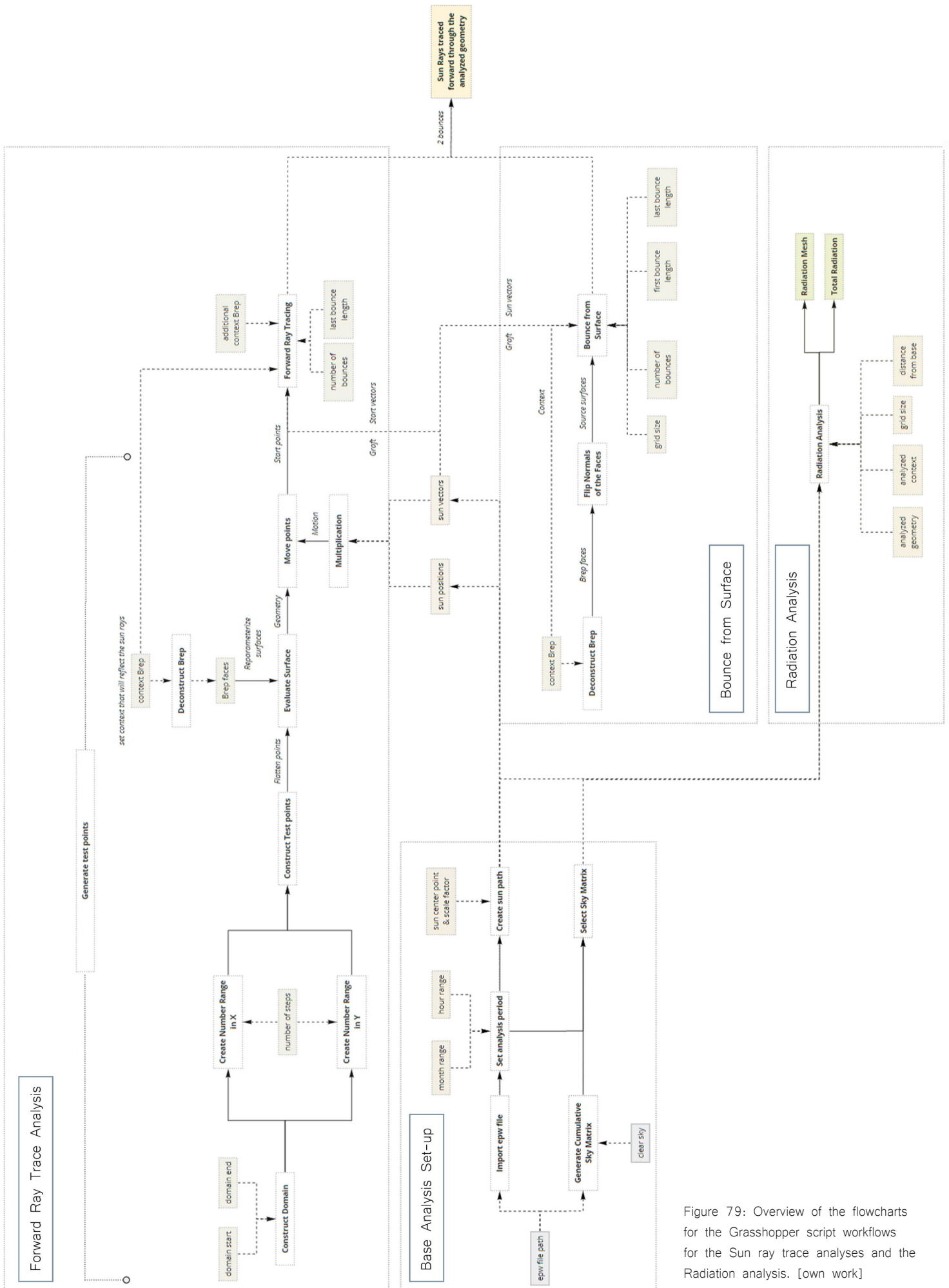
Figure 79: Overview of the flowcharts for the Grasshopper script workflows for the Sun ray trace analyses and the Radiation analysis. [own work]

6.3.1.4. DYNAMIC RESPONSE OPERATION BASIS

At the same time, an exploration was realized in relation to the dynamic response operation basis, comparing the geometrical and performance requirements between a daily and a seasonal operation, considering the scenario of a south-facing opaque facade. The assumption in this case was that the bottom pyramid that is mainly responsible for the reflection of the incoming sun radiation should have a sun-tracking function. This meant that the critical difference between a daily and a seasonal operation would be the direction of the rotational movement, from east-to-west or south-to-north respectively, as shown in Figure 80. During this analysis, several geometrical iterations and variations were studied to examine the feasibility and limitations ranging from daily to seasonal operation and dynamic movements to satisfy these conditions accordingly.

It was estimated that a dynamic response on a daily basis would lead to a system with high complexity level to be able to provide a precise dynamic response in a complete passive manner in such a short time frame and with so many unpredictable parameters involved. As it was shown with the operation temperature schedule, the changes happen too fast and within a small range. This scenario would not be able to achieve efficient reversible movements, compromising, as a result, the durability of the SMA and would work more accurately with a mechanically controlled mechanism. Apart from that, the sun rays were still reflected towards the urban environment to a great extent, not showcasing enough additional benefits and arguments in favour of this option. In contrast, a more gradual movement within a seasonal operation basis could account better for the tolerances expected from the SMA's dynamic deformations, following more gradient temperature changes and a range spread throughout a larger period. Furthermore, as shown with the previous sun ray trace analyses, the geometry and movement have good environmental performance concerning the direct impact, while a seasonal movement would mean a slight independence from the inner comfort's demands and more flexibility to slightly diverge from accurate movement not directly affecting the user's comfort to a great extent.

In relation to the geometry, even though a fully daily operation was not intended, a slight refinement was still followed to meet some of the daily sun-tracking requirements. This was realized by creating an inwards "valley" folding line on the top surface of the bottom pyramid, and thus reflecting some of the east-to-west sun rays throughout the day in an optimized "static" version, while the whole bottom pyramid rotates from south-to-north with an optimal upward rotation during the high peak seasons. Through these studies illustrated in Figure 81, it was also observed that a wider facade component works better in terms of reflecting upwards the rays bouncing from the down-facing surfaces of the bottom pyramid, which led to the final refinement set of component proportions for each pyramid to be used for the next studies, which were: length-to-height: 1/0.5 and base-length-to-pyramid-height: 1/0.5, with an overall component proportion of 1/1 and with the top pyramid having a 10° rotation from the z axis.
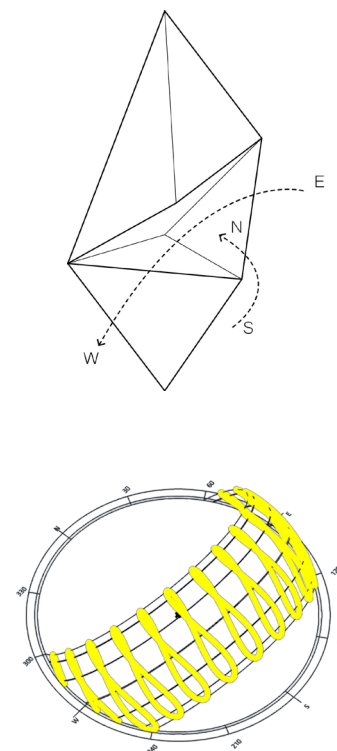

Figure 80: Top: The south-north and east-west responsive dynamic movement directions of the facade component.
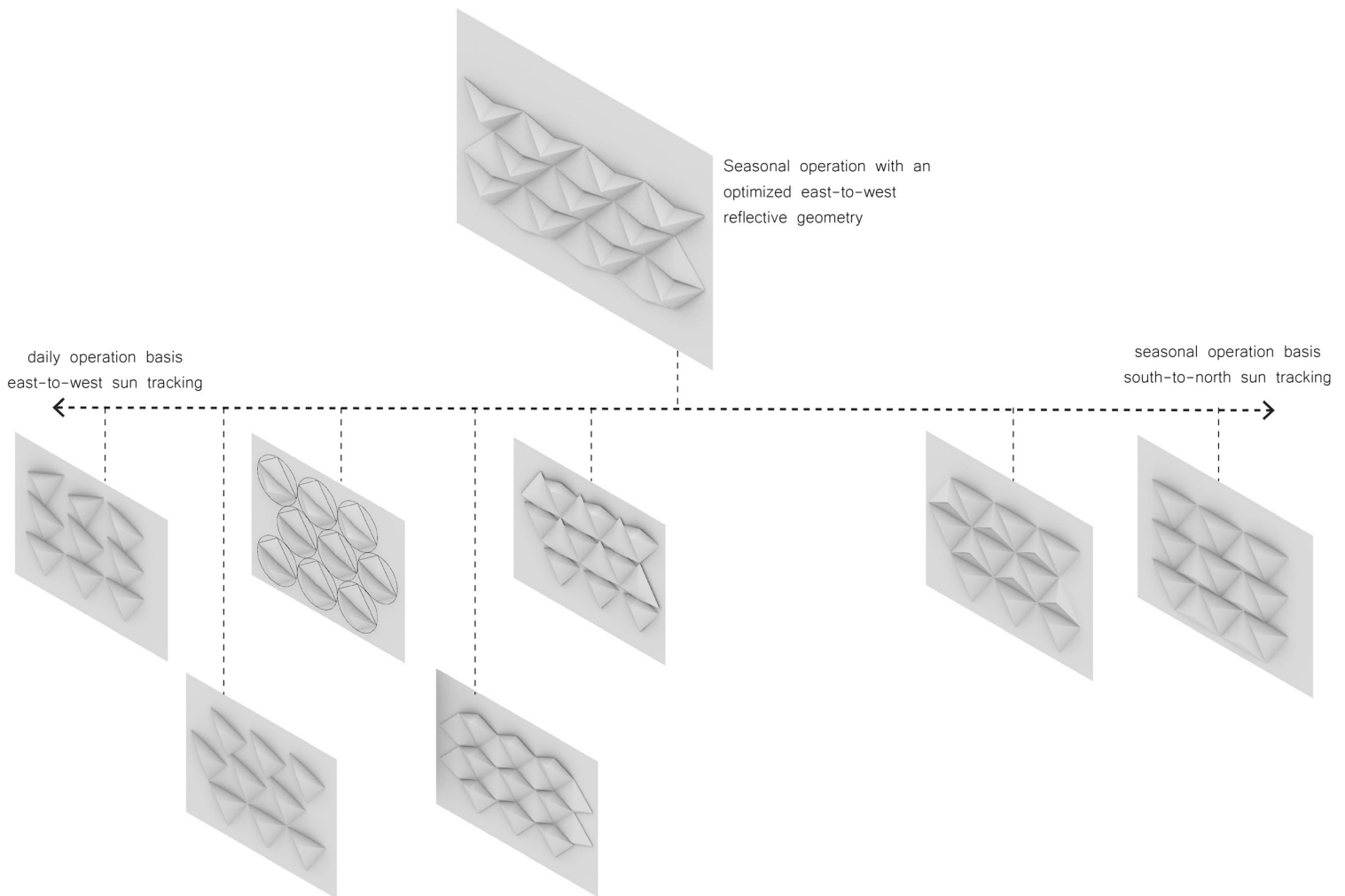Bottom: The annual sun path diagram. [own work]

Figure 81: Diagram of the dynamic response basis scale ranging from daily to seasonal operation with examples of the different geometry adjustments and movement alternatives. [own work]

6.3.2. URBAN LEVEL – OUTDOOR MICROCLIMATE STUDIES

6.3.2.1. CUMULATIVE IRRADIANCE HEAT MAPS

The first layer of evaluation of the direct UHI impact on the urban level was to simulate and visualize the cumulative irradiance on the urban environment, assuming a scenario of an urban street canyon in Athens with the proposed south oriented facade design. The most important part of this study laid on quantifying the reflected part of the solar energy and assessing the effect of the facade geometry on its reduction on the street level and the neighboring buildings, in comparison to a typical facade surface, different surface types and window-to-wall ratios.

For this study, two approaches were followed, in accordance with the design tool's possibilities. In the first case, the Honeybee Daylight Analysis component was used to calculate the cumulative irradiance on the street level, which accounts for direct, diffuse, horizontal

infrared and reflected solar radiation from the surrounding surfaces. In this case, it was also possible to include information of the surface types, ranging from fully absorbent (R:0, G:0, B:0) to fully reflective ones (R:1, G:1, B:1) and the glazing ratio, comparing a fully opaque (0%) to a curtain wall (85%). The analysis was conducted for the extremely hot week (03-09/08) as the worst-case scenario.

The results can be seen in the overview Table 18, where with highly absorbent surfaces there was negligible impact between the facade types, since most of the radiation is absorbed and is irrelevant to the facade geometry. This case, however, would lead to undesired effects on the overheating of the building's interior and, thus, increasing the resulting indirect impact. On the other hand, when reflective surfaces were involved, the

proposed design's impact was slightly more apparent, but still showing a mere 3% reduction of the total radiation. What is perhaps more important was that the radiation was reduced mostly near the facade surface, avoiding unpleasant comfort situations to pedestrians walking nearby, as would occur in the case of large thermal masses during the evening hours due to the exhausted heat that is being accumulated throughout the day.

However, even though the first methodological approach provided with an indication of the cumulative radiation on the street level, the distinction between the different types of radiation and the contribution of the reflected part was not entirely clear. For a more comprehensive understanding, a second complementary approach was followed, using the Ladybug Radiation Analysis component this time. The difference in this case was that the radiation accounts only for the direct and diffuse radiation (the infrared radiation is included by default in both

cases). By decoupling these two analyses, it could then be possible to extract the value of the reflected radiation and compare the results, allowing for small divergence in the values due to possible slight differences in the two calculation processes. The flowcharts of the workflow for these two approaches are illustrated in Figure 82. The results in Table 19 show that the percentage of the cumulative radiation that is responsible for the reflected radiation from the facade and the surrounding surfaces was reduced by around 40% with the proposed design, with again a reduced radiation close to the facade surface. However, that portion still accounted only for 6% of the total radiation, which is a relatively small amount and, therefore, would lead to the conclusion that even though the direct impact could be minimized with the proposed facade geometry to reduce the overheating of the urban microclimate, the overall impact on this regard is not significantly large.
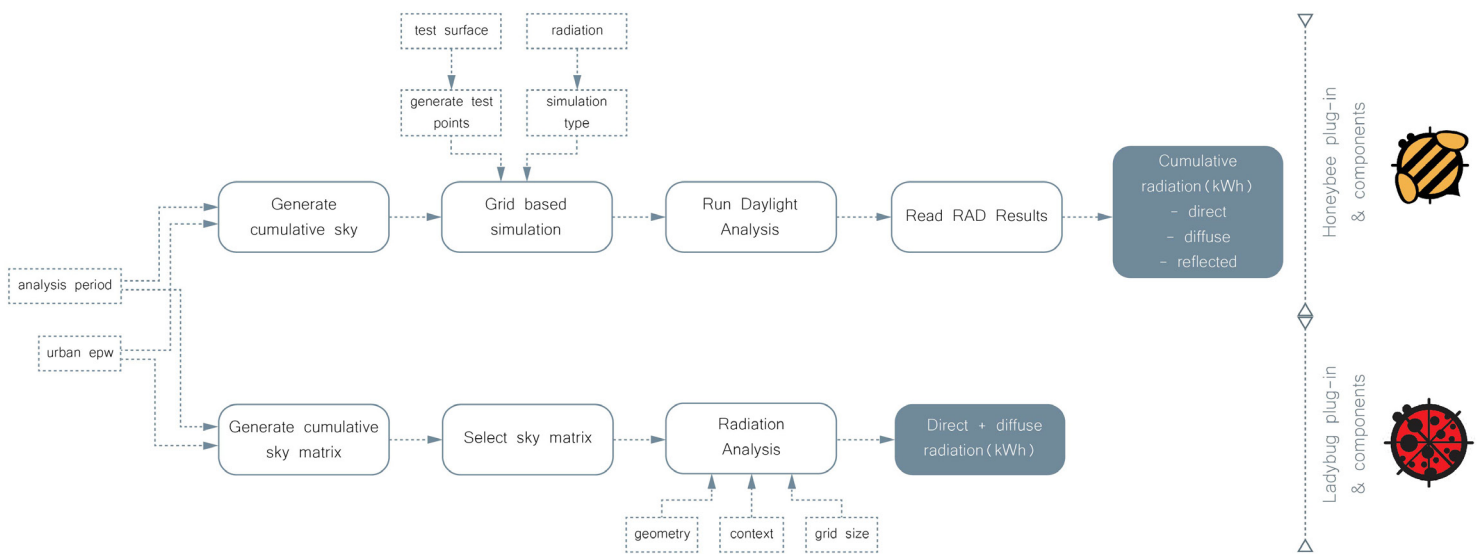

Figure 82: Flowchart of the two workflow approaches for the radiation analysis study and the design tools used for each case. [own work]

Table 18: Cumulative radiation values on street level in an Athens urban canyon
(cumulative radiation: direct, diffuse and reflected radiation from all the surrounding surfaces). [own work]
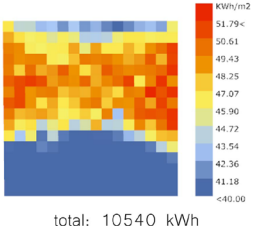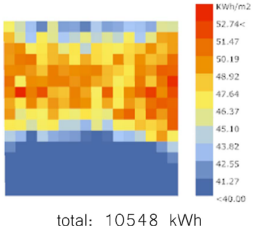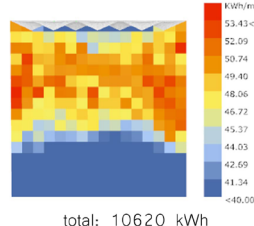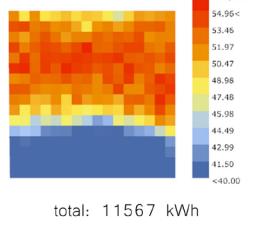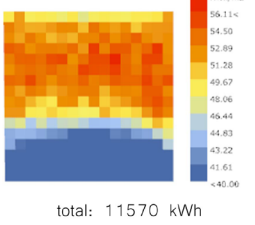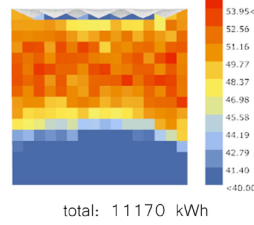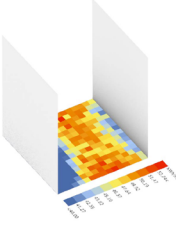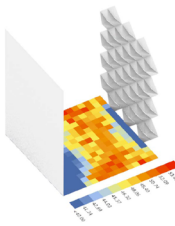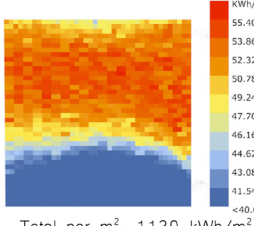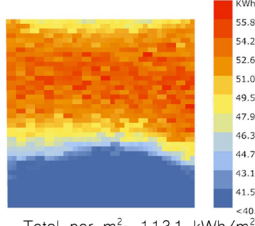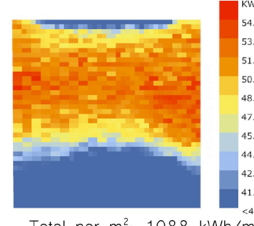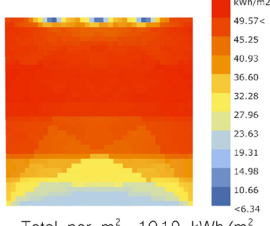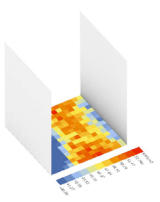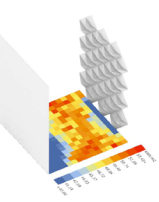
Facade type	Standard facade		Facade design	Observations / Difference in %
Glazing ratio / Diffuse reflectance	0% fully opaque	85% curtain wall		
	Top view grid results			
R:0 G:0 B:0 highly absorbent surfaces	total: 10540 kWh	total: 10548 kWh	total: 10620 kWh	– negligible impact – reflected radiation reduced due to low material diffuse reflectance factors, large part of heat is being absorbed
R:1 G:1 B:1 highly reflective surfaces	total: 11567 kWh	total: 11570 kWh	total: 11170 kWh	– 3% reduction – reduced radiation near the facade surface
Axo view grid results				Other input parameters – Athens Weather Data, including urban conditions – South orientation – Analysis period: Extremely Hot Week (03–09/08) – Direct normal radiation – Diffuse horizontal radiation – Horizontal infrared radiation – Reflected radiation from surrounding surfaces

Table 19: Analysis and partial values of the total cumulative radiation on street level in an Athens urban canyon
(cumulative radiation: direct, diffuse and reflected radiation from all the surrounding surfaces). [own work]

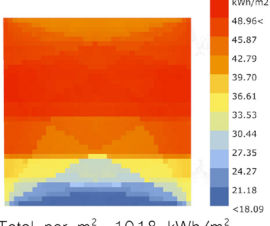| Facade type	Standard facade		Facade design	Observations / Difference in %
Glazing ratio / Radiation values	0% fully opaque	85% curtain wall		
	Top view grid results			
Cumulative radiation (1) (direct, diffuse and reflected)	Total per m²: 1129 kWh/m²	Total per m²: 1131 kWh/m²	Total per m²: 1088 kWh/m²	– ~4% reduction of total radiation on street level – reduced radiation values near the facade surface
Direct and diffuse radiation (2)	Total per m²: 1018 kWh/m²		Total per m²: 1019 kWh/m²	– ~40% reduction of the reflected radiation from the facade and the surrounding surfaces that adds up to the cumulative radiation values – reduced radiation near the facade surface
Reflected radiation (1)–(2)	Total per m²: **113 kWh/m²**		Total per m²: **69 kWh/m²**	Other input parameters
Axo view grid results				– Athens Weather Data, including urban conditions – South orientation – Analysis period: Extremely Hot Week (03–09/08) – Direct normal radiation – Diffuse horizontal radiation – Horizontal infrared radiation – Reflected radiation from surrounding surfaces

6.3.2.2. UNIVERSAL THERMAL COMFORT INDEX (UTCI)

An additional analysis concerned the Universal Thermal Comfort Index (UTCI), which is a thermal comfort indicator based on human heat balance models and designed to be applicable in all seasons and climates and for all spatial and temporal scales [Bröde et al. 2012]. There are 10 UTCI thermal stress categories and the ones related to heat stress are defined as follows: above +46: extreme heat stress; +38 to +46: very strong heat stress; +32 to +38: strong heat stress; +26 to +32: moderate heat stress; +9 to +26: no thermal stress. This indicator was then used to produce the outdoor comfort microclimate maps and assess the impact of the facade on the heat stress near the facade surface.

For this analysis, the flowchart can be seen below [Figure 83], where the change in the Mean Radiant Temperature values due to the urban conditions were added to the Dry Bulb Air Temperature hourly values

and it was again realized for the extremely hot week (03-09/08). Additionally, the calculation took into account additional parameters that influence the outdoor comfort temperature, such as the wind speed, relative humidity and ground reflectivity, which was set to 0.4, considering a concrete paved surface. The results in Table 20 show a negligible overall average temperature difference between a typical facade and the proposed geometry, with a reduction of 5% of the minimum temperature near the facade surface, whereas the UTCI thermal stress category was in the boundaries between strong and moderate heat stress. Because of the small differences between the two cases, the results from this analysis didn't provide much feedback or insight for further consideration, but were more useful as an additional tool to understand the overall performance on the urban microclimate.
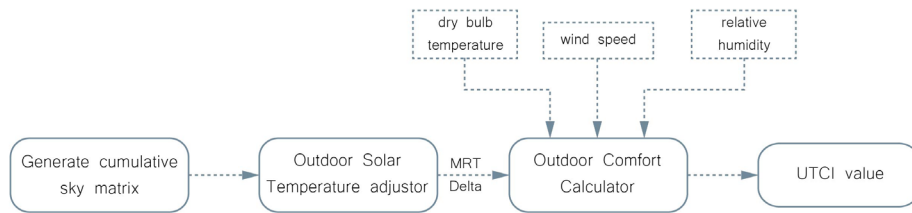
Figure 83: Flowchart of the workflow for the simulation of the UTCI value. [own work]

Table 20: Universal Thermal Comfort Index (UTCI) near the facade surface
(change in Mean Radiant Temperature Values added to the Dry Bulb Air Temperature hourly values). [own work]

Facade type	Top view grid results	Axo view grid results	Observations / Difference in %	Input parameters
Standard facade			average: 31.8 °C minimum: 31.4 °C	– Athens Weather Data, including urban conditions – South orientation – Analysis Period: Extremely Hot Week (03-09/08) – Dry Bulb Temperature – Relative humidity – Wind speed – Direct normal radiation – Diffuse horizontal radiation – Horizontal infrared radiation – Ground reflectivity: 0.4
Facade design			average: 31.7 °C minimum: 29.9 °C – negligible average temperature difference – 5% reduction of the minimum temperature – reduced temperature near the facade surface	

6.3.2.3. COMPARATIVE SUN RAY TRACE ANALYSES

Lastly, a final validation check on the direct environmental impact of the facade was conducted in relation to the direction of the reflected sun rays as a full building facade and not as isolated component or segment and in the context of the urban street canyon with surrounding buildings opposite to the analyzed one. Since the facade is south-oriented, the study concerned only the rays reflected from the proposed facade to the surroundings and not from the opposite-facing building. The analysis considered the date of 21st of June between 12:00-13:00, when the sun is at its highest peak, and the comparison was then realized between the current design and a typical flat facade. The results can be seen in the Figure below [Figure 84].

In accordance with the radiation analysis grid results, the ray trace analyses showed that a typical facade reflected the sun rays downwards towards the street level, if no other obstacles were obstructing the rays'

direction. On the contrary, the proposed design, as also demonstrated in the previous chapters with the studies on the individual components, reflected most of the sun rays upwards back to the atmosphere. In addition to this, the small number of rays which did not fall in that category and deviated by bouncing more horizontally due to the reflection on the different angles of the geometry surfaces, still did not bounce towards the street level, but to a much higher level above the ground. They were also scattered throughout the opposite building's length and height thanks to the convex outer geometries, avoiding undesired and increased solar focus points, as well as concentrated heat areas in the surrounding urban environment.

June 21st 12-13hrs

June 21st 12-13hrs
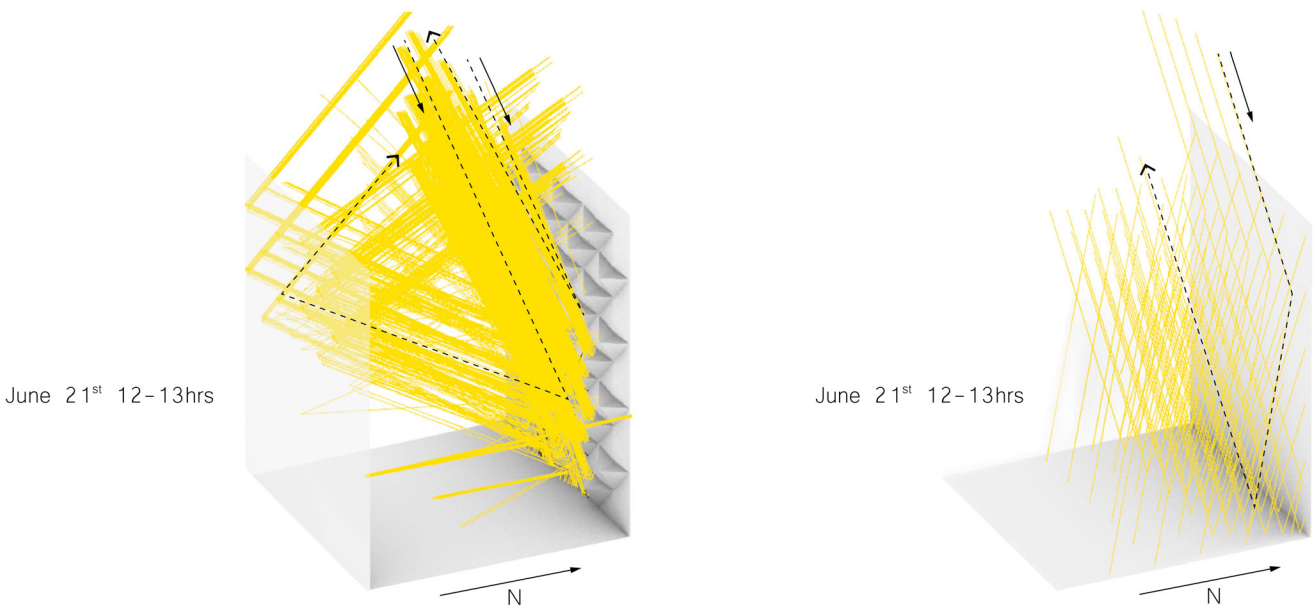
Figure 84: Comparative sun ray trace analyses of the proposed facade (left) and a typical facade in an urban street canyon, including the reflection towards the opposite building. [own work]

6.3.3. CONCLUSIONS

As a summary from the above evaluation studies on the direct impact of the facade design on the UHI effect, it can be concluded that the proposed geometry does show a reduction on the reflected solar radiation at the street level and on the urban heat intensification at a microclimate level. This is more apparent especially close to the facade surface and through dissipating the incoming solar rays from being reflected and accumulated inside the urban canyons. The part of the reflected solar radiation on the urban surroundings that the building is responsible for is, therefore, significantly reduced. However, the direct impact on the overall building's share on the UHI effect still remains relatively small compared to the cumulative solar radiation that is caused by other sources and is not obstructed by other mitigation strategies. In this sense, it can be assumed that a reduction on the building's direct contribution is not as impactful as the indirect one could be, which concerns the building's energy performance and is the objective of study and evaluation of the following chapters.

building's direct UHI impact footptint based on the reflective radiation to the street level

cumulative solar radiation distribution in the urban microclimate

Figure 85: Charts summarizing the direct impact evaluation conclusions. [own work]

6.4. FACADE SURFACE LEVEL — SOLAR RADIATION ANALYSIS STUDIES

Part of the evaluation process of the current research thesis is also to assess to what extent such a dynamic seasonal response offers additional benefits to the building's environmental and energy performance, which is an aspect related to both the direct and indirect UHI impact. For this study, the primary goals that were initially set to this regard and were further el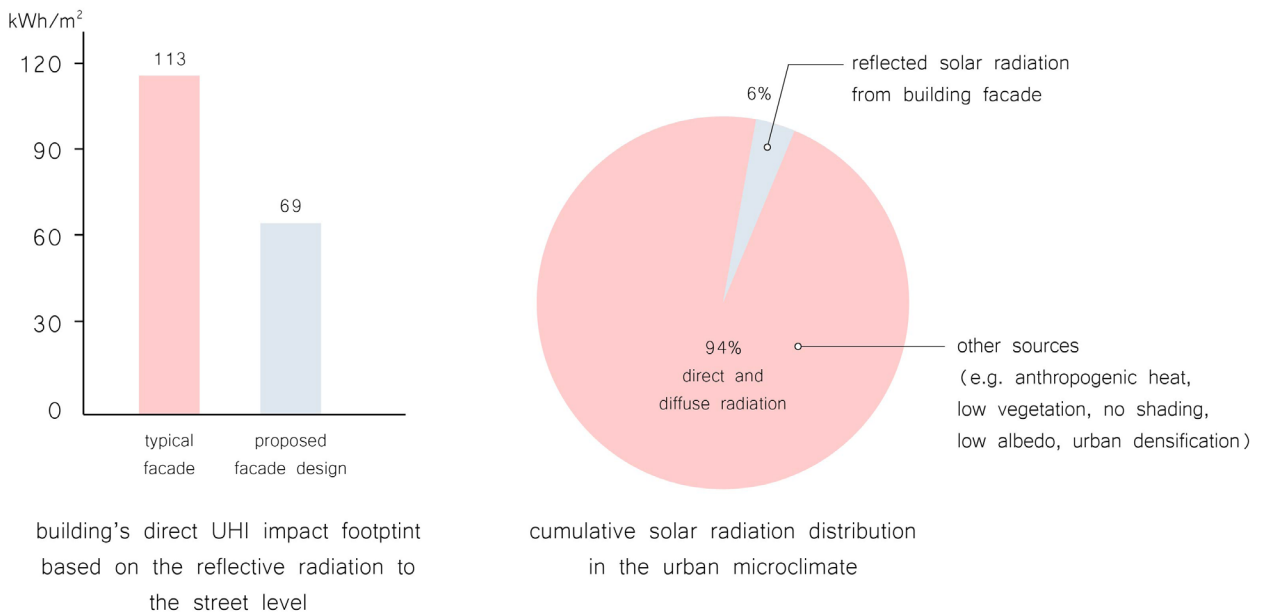aborated to respond to the summer and winter optimal performance benchmark criteria are used as reference points for the evaluation.

Taking these boundary conditions in consideration, solar radiation analyses were conducted on a segment of the facade surface, which was extracted from a centered region, so that the self-shading of the neighboring components could also be considered in the simulations as part of the shading geometry context. The analyses were realized using the Ladybug Radiation analysis component in Grasshopper for the three typical weeks as analysis periods and compared the proposed facade design with its alternated dynamic positions throughout the seasons with two equivalent static versions, replicating in the first case the summer position and in the second one the winter position. In this way, the goal was to estimate to what extent a dynamic responsive movement could be justified and the performance goals could be achieved. Similarly, a radiation analysis was realized to compare the proposed facade to a typical south-facing one with

a 45% window-to-wall ratio during the extremely hot period and with a clear sky.

From the overview comparative tables below [Tables 21, 22], the results showed that a dynamic system could achieve about 3% reduction of the total solar radiation compared to its static versions during the cooling-dominated periods and a 4.5% increase during the heating-dominated periods. In relation to the standard facade type, the proposed design could achieve around 20% reduction in kW/m^2 of the received solar radiation on its surface. This was significantly due to the number of undulated convex geometries and the resulting self-shading, which led to the dissipation of the incoming solar radiation, in contrast to the fully exposed flat facade. It could also be estimated that these dynamic deformations respond better to the objectives of the performance goals related to the positioning towards the sun, the admittance or obstruction of the solar radiation and the areas where it is concentrated the most. These aspects, however, could not be directly quantified in this study, because the analyses could not account for all the parameters involved, since these were more related to the indirect impact and studies on the inner energy performance would give a better insight to evaluate the effect of the design geometry and dynamic function.

Table 21: Solar radiation analysis on facade level (axonometric views).
Existing facade (45% window-to-wall ratio) / New facade overcladding comparison. [own work]
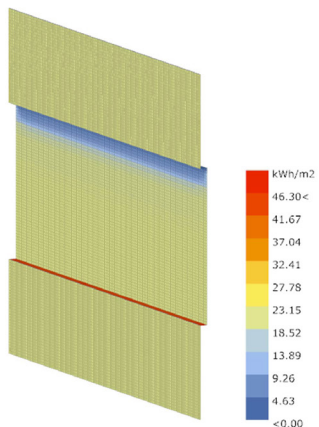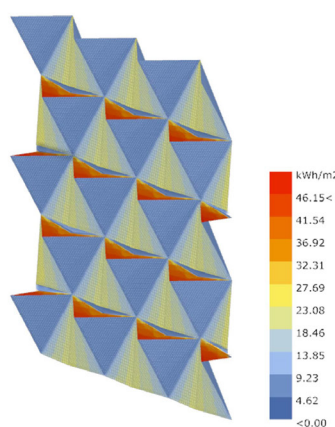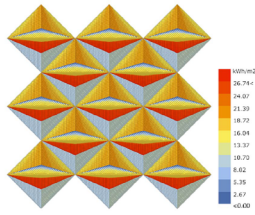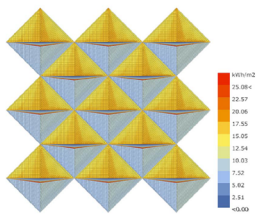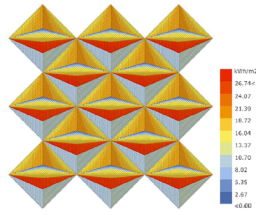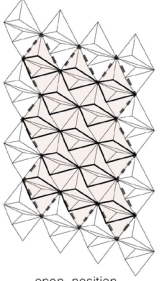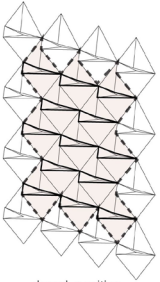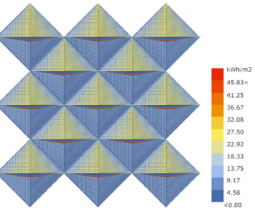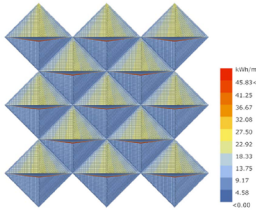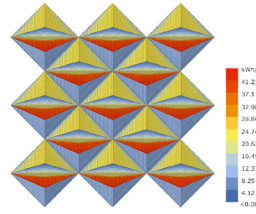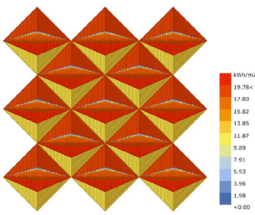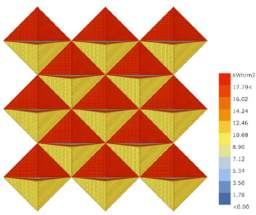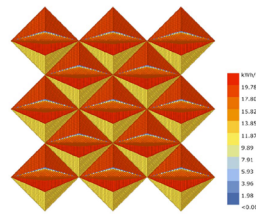
Analysis period / Facade type	Existing facade	New facade overcladding	Difference in %
Extremely Hot Week (03-09/08) (peak of dynamic facade movement)	Total radiation: 560 kWh 11.8 kWh/m²	Total radiation: 532 kWh 9.4 kWh/m²	5% reduction in total solar radiation 20% reduction in kWh/m² **Input parameters** – Athens Weather Data, including urban conditions – South orientation – One-floor facade segment – Clear sky

Table 22: Solar radiation analysis on facade level (front views).
Dynamic to static facade system comparison. [own work]

Analysis period \ Facade type	Dynamic facade	Static facade (closed)	Static facade (open)	Objectives / Difference in %	Input parameters
Typical Spring Week (05-11/04) (start of dynamic facade activation)	Total radiation: 441.5 kWh	Total radiation: 429 kWh	Total radiation: 441.5 kWh	Cooling-dominated periods: - increase of undulated (self-) shading surfaces - reduction of the solar radiation on the facade surface - top reflective surface of the bottom pyramid perpendicular to sun rays' direction and to receive the most radiation — 3% reduction in solar radiation with a dynamic facade system	- Athens Weather Data, including urban conditions - South orientation - Clear sky test facade segment
Extremely Hot Week (03-09/08) (peak of dynamic facade movement)	Total radiation: 503.6 kWh	Total radiation: 503.6 kWh	Total radiation: 519.5 kWh	Heating-dominated periods: - decrease of undulated shading surfaces - admit more sunlight to the interior - less self-shading to increase the solar radiation on the facade surface - increase of solar absorption to the inside layers - top surface of the bottom pyramid perpendicular to the lowered sun rays' direction - increase of surfaces that absorb solar radiation and more exposure to highly absorbent layers — 4.5% increase in solar radiation with a dynamic facade system	open position
Typical Winter Week (15-21/12) (end of dynamic facade movement)	Total radiation: 474 kWh	Total radiation: 452.7 kWh	Total radiation: 474 kWh		closed position

6.5. FACADE COMPONENT'S MECHANISM & FUNCTION CONCEPT

At this stage, it needs to be additionally mentioned that apart from the distinction between the seasonal dynamic performance and response to the direct and indirect UHI impact, there is also a distinction in the function of the different parts of the facade component and the role of the SMA mechanism to coordinate the movements. In this respect, the top part of the facade system is responsible for the indirect impact and has a role as a secondary shading device and direct sunlight filter, regulating the building's cooling demands, evenly dispersing the daylight and controlling the glare to a certain allowable degree. On the other hand, the bottom part is responsible for the direct impact and works as the primary shading device. More specifically, its function aims for the reduction of the reflective sun rays to the urban environment, by tracking the sun, positioning the top surface perpendicular to the sun rays' angle during the seasonal sun movement and, by doing so, obstructing the direct sunlight. Along this dual operation, the SMA mechanism coordinates both with a single linear deformation that initiates the double dynamic movement. The diagram in Figure 86 with the facade component's mechanism and function concept, highlights the two distinctions and performance features.
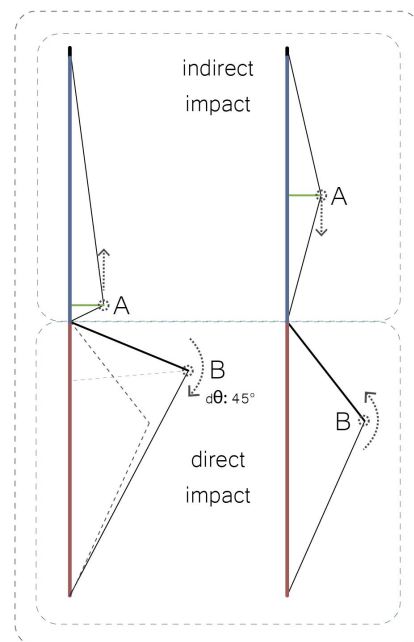
Figure 86: Diagram showing the distinction of the component's top and bottom parts in relation to their function and the direct and indirect response. [own work]

6.6. APPLICATION POSSIBILITIES

The above distinction helped to explore the facade application possibilities further and to assess the applicability conditions and distinctions in materiality and performance. This is more relevant in relation to the indirect impact, where the materiality and the inner facade situation have a more critical role, whereas the direct impact study was mostly concerned with the outermost facade geometry, which was the primary driving force. For this purpose, an overview of the possible facade types was realized based on the window-to-wall ratio of the inner facade type, ranging from fully opaque facade (0%) to a curtain wall one (85%) with various intermediate glazing ratios. In Table 23, an exploration was realized on the inner-to-outer facade relation and on various combinations of materiality and proportions to study how the outer facade system could adapt based on the inner facade type and what the possible variations could be in each case. The different options vary mostly on the different transparency levels depending on the inner facade's wall type and also the overall scale of the component could be adjustable in relation to the floor-to-floor height.

Based on these general studies, Table 24 includes a summary overview of some observations on the function of the double facade. One of them is that the level of responsiveness moves to a more hybrid system with a combination of active and passive function once the window-to-wall ratio increases, because the user's wish to override the system increases and the requirements for inner comfort and control are more demanding. However, this could also be partly satisfied by proper performance-driven selection of the materials and textiles with solar control properties that can achieve satisfactory emissivity and transparency values to avoid undesirable effects. As an example, Figure 88 shows some features of how the facade application would work in terms of materiality, where the bottom part can be a perforated mesh, which would have the vents open when stretched during summer and partially closed during winter to increase the convection effect. Its top surface could also potentially as a concept have a pleated double-coloured textile moving in an accordion-like fashion to reveal either a light reflective side or a dark absorbent one when expanded during winter and stretched during summer.

facade surface
window-to-wall ratio

| 0% | 15% | 25% | 45% | 85% |

opaque   varying window-to-wall ratio   curtain wall
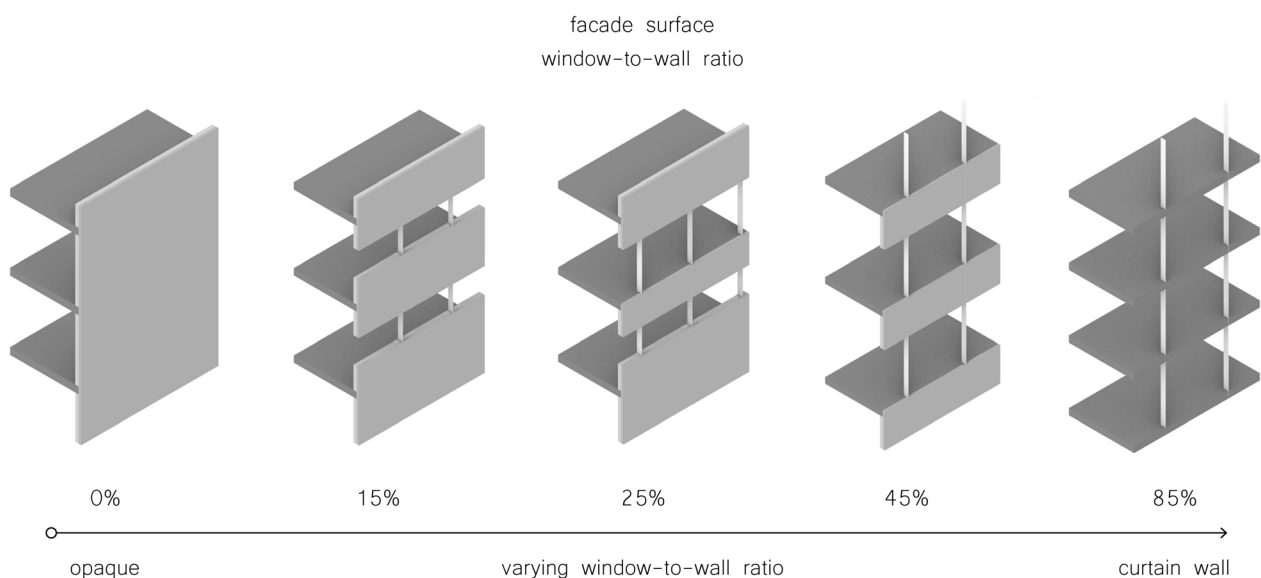
Figure 87: Diagram showing the inner facade's window-to-wall ratio range. [own work]

Tables 23, 24: Top: Facade design's applicability to various building typologies.
Bottom: Facade type characteristics observations summary. [own work]

- ·············· slab level
- ·············· opaque part top level
- ·············· translucent part top level
- △ translucent ETFE textile surface
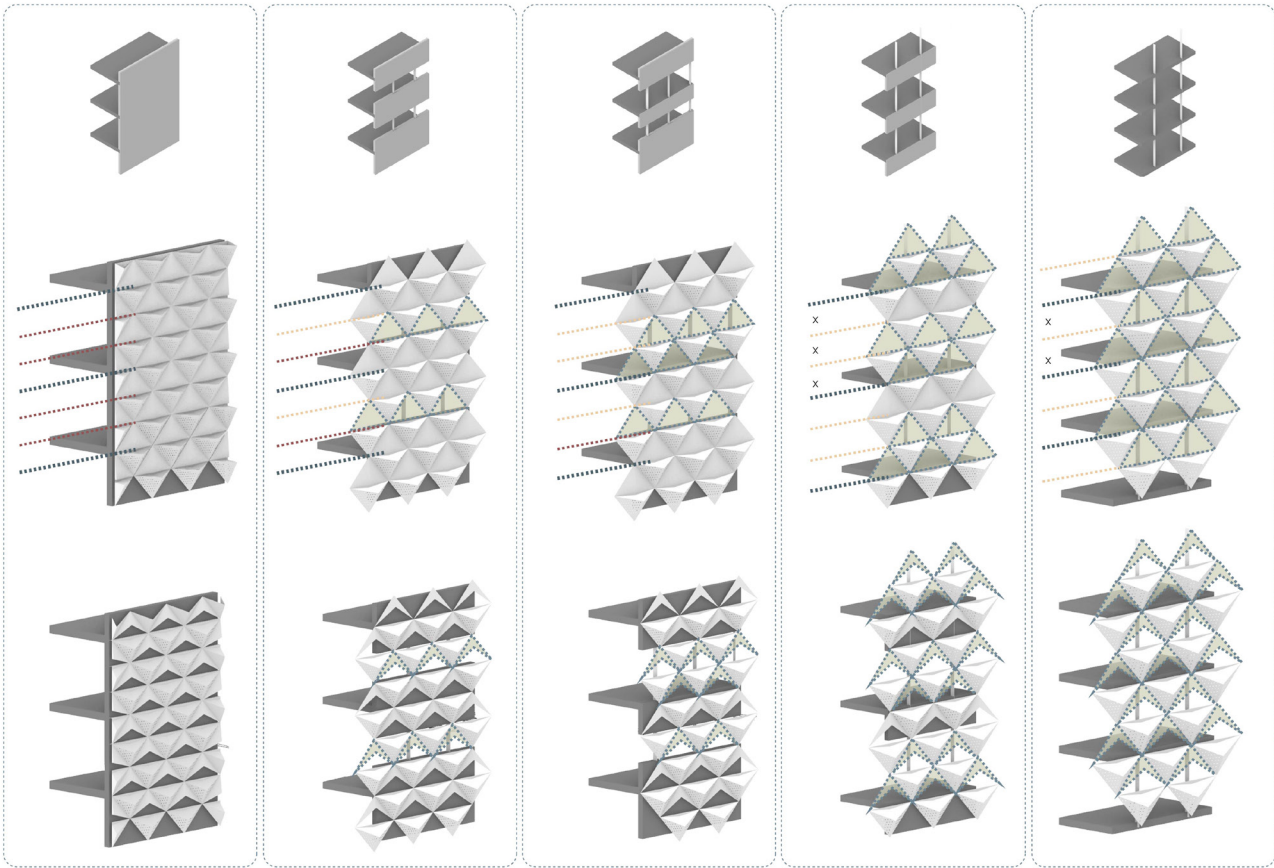
Façade type			
Façade characteristics	Opaque ventilated double façade	Double Façade with varying glazing ratio on the inner layer	Double façade with a curtain wall on the inner layer
Responsiveness	fully passive	hybrid (active and passive)	hybrid (mostly active during sunny periods, passive by default)
Operating schedule	seasonal with no option to manually override the movement	seasonal by default with the possibility to manually override the movement of the top part	seasonal by default with the possibility to manually override the movement of the top part
User's inner comfort	not affected	daylight and glare control, shading and natural ventilation demands	daylight and glare control, shading and natural ventilation demands
Effect on building's cooling demands' reduction (UHI indirect impact)	probably negligible due to little direct exposure to sun radiation (thermal studies are required)	thermal studies are required	thermal studies are required
Textile characteristics	opaque, light-coloured, reflective	light-coloured, reflective, bottom pyramid opaque (maybe perforated for diffuse sunlight to enter the cavity), top part translucent	light-coloured, reflective, bottom pyramid opaque (maybe perforated for diffuse sunlight to enter the cavity), top part translucent
Inner cavity	highly absorbent coating	highly absorbent coating on the opaque parts of the envelope construction between the floors	highly absorbent coating on the opaque parts of the envelope construction between the floors
Other features	-	daylight and thermal studies to be made based on glazing ratio, cavity width and shading component's size and the impact on the building's cooling demands (which glazing ratio has the most impact)	flexibility on the opaque parts of the textiles which can be defined considering the full façade and not floor per floor, creating different overall shading patterns

floor slab

opaque membrane
surface in tension

air inlet

opaque PTFE highly
reflective membrane

cavity zone

opaque PTFE coated
fiberglass ventilated open
mesh to allow air and
some diffuse daylight in

cavity zone

translucent ETFE
membrane surface

-high reflectivity factor
-low-e and g-values
-helps to evenly disperse
daylight

floor slab

cavity zone

bottom part also acting as a
shading device to obstruct
east-to-west sunlight

cavity zone

air inlet

floor slab

pleated double-colored
textile
(summer: folded with
reflective light color visible
winter: expanded with
absorbent dark color
additionally revealed)

transparent ETFE
membrane to allow
clear views when no
sun-shading is needed

highly absorbent inner
coating layer

membrane in retraction to
allow direct solar radiation
enter the cavity and heat
up the glazed surfaces
and the absorbent inner
coating layer on the
opaque building
construction surfaces

Figure 88: Diagrammatic axonometric
views of an example illustrating the
facade application concept during the
summer (top) and the winter situation
(bottom). [own work]

opaque PTFE coated fiberglass ventilated
open mesh (vents are partially closed
when the mesh is not stretched during
winter situation to increase heat
convection inside the cavity)

6.6.1. CASE STUDY

In the current project and to apply the evaluation of the indirect impact of the system on a real building situation, a case study scenario from the above options was selected, which involved a retrofit intervention in Athens, in a typical south-facing office building with 45-85% window-to-wall ratio and built between 1960-1980. These buildings that account for a significant percentage of the building stock in the center of Athens [72] have low energy performance, because they consist of outdated and poorly maintained building components, resulting to an increase of the cooling demands and consequently increase of the building's indirect UHI impact. At the same time, they are composed of materials with either low albedo, such as concrete, or ones that reflect the direct sunlight to the urban environment such as glazing, increasing the direct impact. The goal is, therefore, to propose an overcladding retrofit strategy with a passive design, which involves the replacing of the windows and the outer facade system design addition and is focused on the combination of geometry, materiality and dynamic movement, resulting to a low-tech, -energy and -cost intensive solution, while increasing, at the same time, the building's environmental and energy performance.

[source: Ermou kai Kornarou - Syntagma. (2020, December 27). Retrieved from https://finders.co.il/en/portfolio/ermou-kai-kornarou-syntagma/]

[source: OTE Telecoms Central Building, Athens. (2020, July 06). Retrieved from https://cubusengineering.gr/en/projects/commercial-building/ote-telecoms-central-building-athens/]

[source: Lomholt, I., Welch, A. (2020, October 21). Athens Office Building: Greece Offices - e-architect. Retrieved from https://www.e-architect.com/athens/athens-office-building]

Figures 89: Photos of examples for the case study office buildings in the center of Athens.

6.7. UHI INDIRECT IMPACT EVALUATION – CASE STUDY BUILDING'S INTERIOR LEVEL

As explained in the previous chapters, the UHI indirect impact evaluation relates to the building's energy performance, as well as the effect of the facade skin and the cavity function primarily on the reduction of the cooling loads and, consequently, also on the inner comfort. The studies are further elaborated in the following sections.

6.7.1. HEAT FLOWS & VENTILATION STRATEGY DIAGRAMMATIC CHARTS

In the following diagrams [Figures 90, 91] the ventilation strategies and heat flows are schematically explained in both the summer and winter situation during the day and night operation. In the first situation, the cavity works as an opened air heat attenuation zone with a top air exhaust and in the winter as a heat amplification and buffer zone with multiple closed cavities that exploit the heat stack stratification effect. The top pyramid works mostly as air inlet with slightly open vents, to ensure a small ventilation inside the cavity, and the bottom one is reflecting the sun rays and works as a convection zone through its interior air volume. The intention was to explore and evaluate the different possibilities and options for ventilation strategies and amount of air circulation inside the cavity, as well as the combination with night ventilation during summer. The objective of the studies was to explore to what extent and in which circumstances the system could have a positive effect on the cooling demand's reduction and to avoid overheating and potential greenhouse effect during summer.

summer situation   winter situation
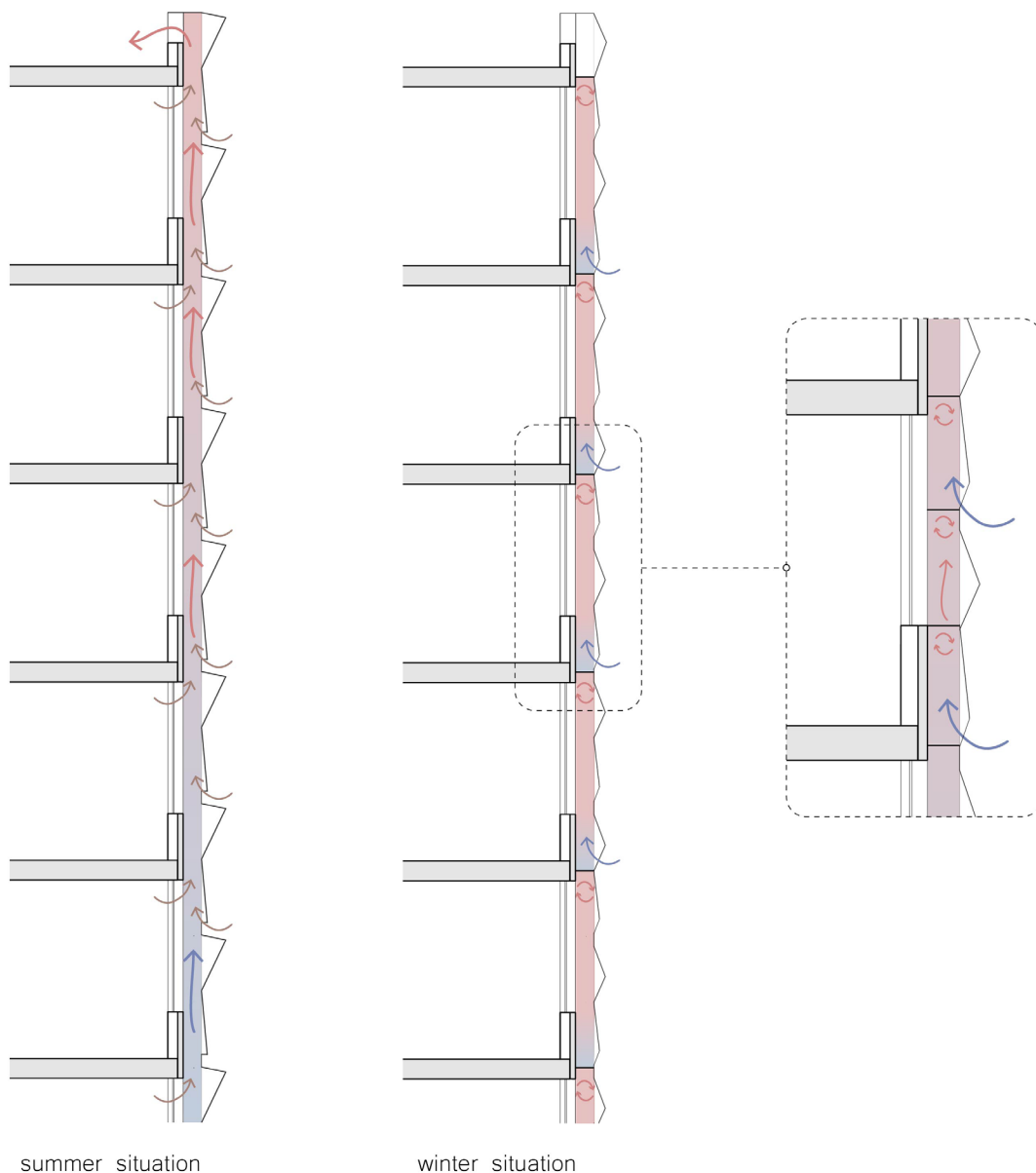
Figure 90: Diagrammatic sections of the ventilation strategy concept in the summer and the winter situation respectively. [own work]

summer situation

top air outlet

inside target temperature 21ºC

outside temperature 35ºC

conduction

air inlet

convection

heat radiation

solar radiation

reflected solar rays to the atmosphere

absorbed solar heat

day

top air outlet

inside target temperature 21ºC

outside temperature 20ºC

conduction

air inlet

heat radiation

night

heat attenuation zone:
opened air cavity ventilation

winter situation

inside target temperature 21ºC

outside temperature 10ºC

air inlet

conduction

convection

heat absorbent coating

reflected solar rays to the atmosphere

solar radiation

absorbed solar heat

day

inside target temperature 21ºC

outside temperature 5ºC

air inlet

conduction

heat absorbent coating

convection

night

heat amplification zone:
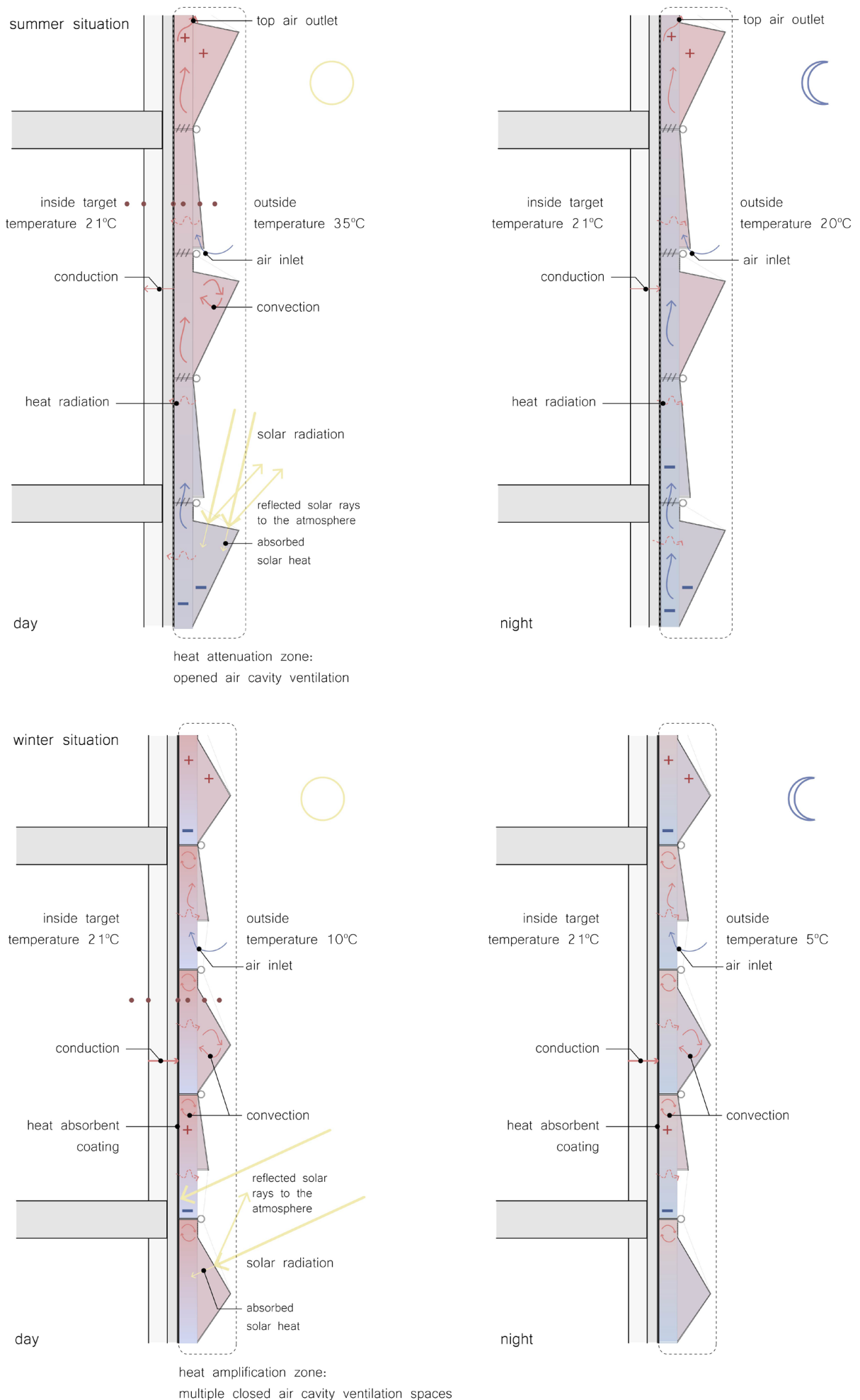multiple closed air cavity ventilation spaces

Figure 91: Diagrammatic sections of the heat flows in the summer (top) and the winter situation (bottom) during day and night. [own work]

6.7.2. BUILDING'S ENERGY PERFORMANCE EVALUATION STUDIES

For the evaluation process, the studies were focused mostly on the dual cavity function in the cooling- and heating-dominated periods, to simulate the dynamic air and heat flows throughout the day and to visualize the temperature fluctuations through the cavity section to the interior. For these purposes, the studies were divided into analyzing the summer and winter situation, with the summer one to be the most critical one for the evaluation of the proposed facade system on the indirect impact, and the winter one to work more as a validation control and understanding of the proposal for the cavity function. During the summer scenario, the focus was placed on estimating the cooling demands and assessing the parameters and boundary conditions that influence the performance and, in the end, compare the results to the existing single facade scenario. On the contrary, for the winter situation it was more insightful to simulate the heat and air flows inside the closed cavity zones and to visualize the temperature fluctuations from the exterior to the interior of the building to assess the effect of the thermal heat buffer zones and to make a comparison with different boundary conditions and cavity widths. Finally, as a side study, a daylight analysis was conducted to evaluate the shading effect in the interior of the building with different component scales, to what extent the inner comfort is affected and the percentage of reduction of the admitted daylight, in relation to the existing facade with no external sun-shading.

The study workflow for these analyses can be seen in the flowchart below [Figure 92]. The approach followed an interoperability and decoupling method, due to software limitations and to exploit the possibilities of the most suitable software for the requirements of each study. More specifically, for the cooling demands analysis, the Honeybee plug-in in Grasshopper was used, which enables the simulation of the different thermal zones, internal loads and ventilation options and can provide an estimation of the Energy Use Intensity (EUI) indicator for the analyzed periods. Since it is an early design stage, this approach provided with sufficient and accurate enough results to give a first indication of the building's energy performance.
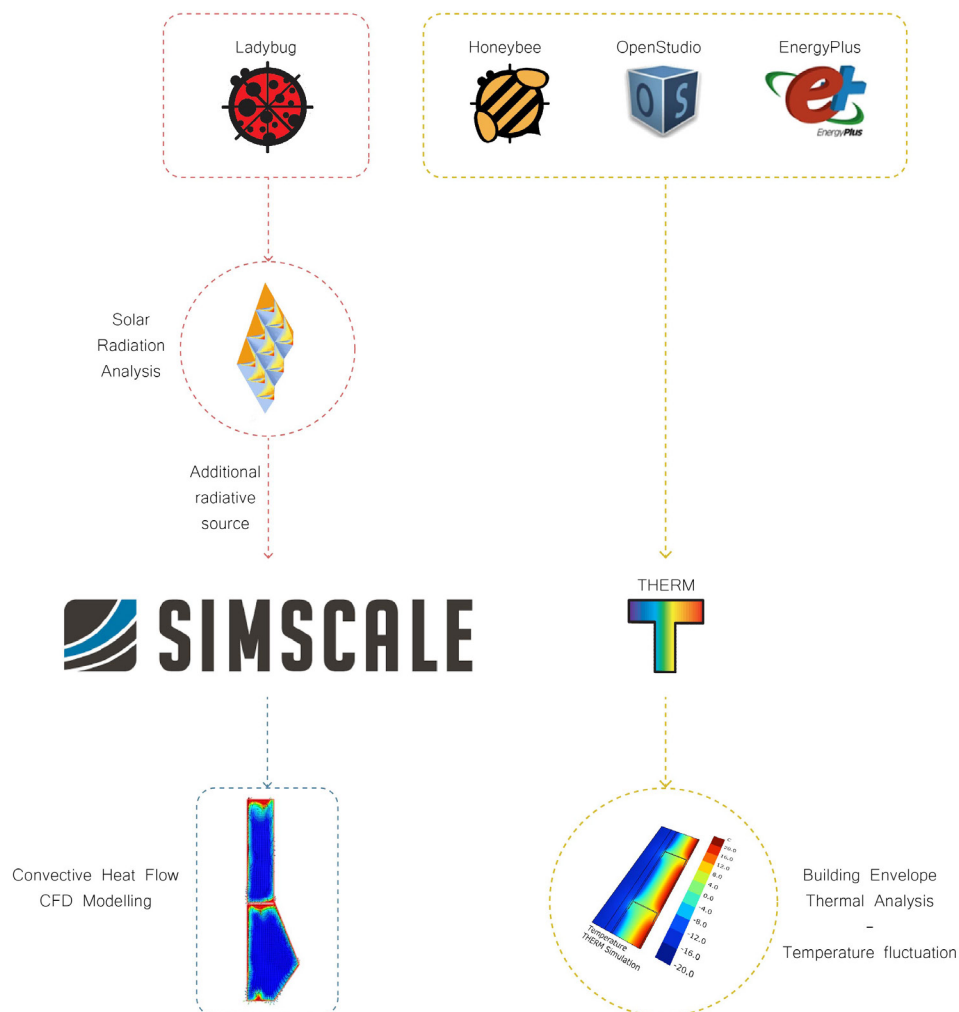

Figure 92: Overview of the toolchain and the data interchange between the different design tools used for the thermal simulation studies. [own work]

In parallel, since the cavity system functions in a more dynamic way, CFD simulations were also necessary. These were realized using the open source online digital software SimScale [103], which could be compatible with geometries imported from Rhino and, without necessarily requiring extensive experience in Fluid Dynamics and CFD modelling, it can provide satisfactory, yet with certain simplifications, results. This method was coupled with data provided by the Ladybug radiation analysis, which was used to retrieve the solar radiation value to be assigned as an additional radiation heat flux (W/m^2) on the facade surface during one day. The SimScale simulations were used to visualize the full height cavity flows during the summer situation and the impact of air inlets and outlets, but mostly to also visualize the winter cavity system.

Finally, for the winter situation and as a complementary analysis, the THERM plug-in in Grasshopper was also used, which can provide the temperature fluctuations from the outside to the inside boundary, by selecting material properties and boundary conditions, including the layer behind the cavity zone. Even though it is not a dynamic simulation, it could still provide sufficient results for a specific date and time condition.

In the next sections, the analyses above and their results are explained more in detail.

6.7.2.1. COOLING DEMANDS ESTIMATION STUDIES – ENERGY USE INTENSITY (EUI) INDICATOR

The conclusions from both the direct impact evaluation and the background literature research have indicated that the building's energy performance and the indirect impact of the cooling systems have eventually a stronger effect on the UHI intensification. On this section, studies on the Energy Use Intensity (EUI) indicator were realized to estimate the cooling demands per area in different scenarios and ventilation strategies of the proposed facade system and compared to the existing case study office building as a benchmark condition. The studies were focused on the cooling-dominated periods (April–October) of the facade system's operating schedule, with a focus on the summer peak.

The workflow followed is explained on the flowchart below [Figure 93] and, during the methodology, the Honeybee plug-in was used in combination with the integrated Energy Simulation engines EnergyPlus and OpenStudio. Due to some limitations of the software and the way the processing functions, certain simplifications were applied, which, however, had a negligible effect on the validity of the results. For example, the geometry needed to be slightly simplified to enable surface adjacencies and to avoid simulation errors when translating the geometries to the different boundary thermal zones. Another simplification included the solar distribution to only account for the exterior direct and blocked solar calculation, with the beam solar radiation to be assumed to fall on the floor without considering the interior reflections. This was due to the presence of convex geometries, which cause errors during the interior solar calculation, because of the many reflecting angles.
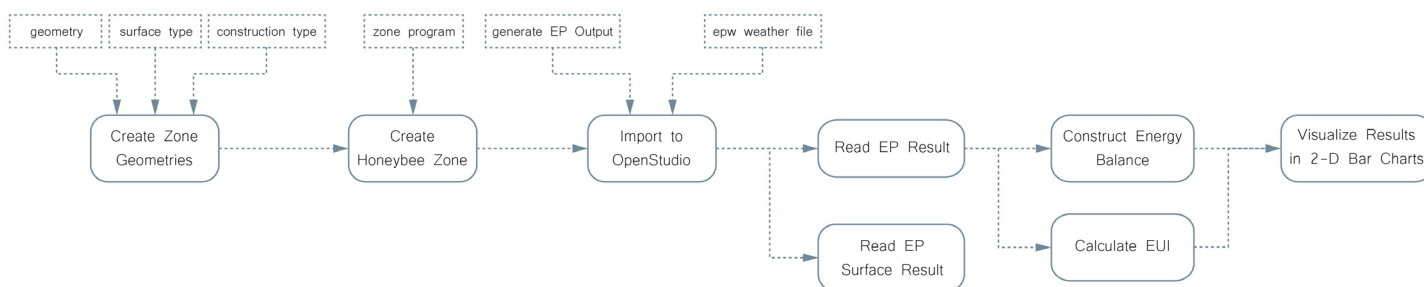

Figure 93: Flowchart of the Energy Use Intensity calculation workflow. [own work]
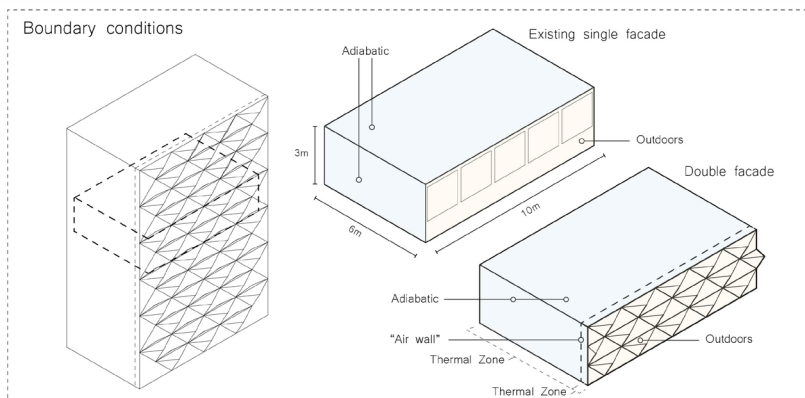
Additionally, one floor of the building was taken as the test geometry with dimensions of 10m (facade length) x 6m (room depth) x 3m (floor-to-ceiling height), which was divided into two thermal zones, the interior with the inner layer as one and the cavity zone with the outer layer as a second one. The outer boundaries of the interior were considered as adiabatic surfaces, whereas the inner layer, which was the interface between the interior and the cavity was assigned as an "Air Wall", which in EnergyPlus it is translated as enabling the air and heat exchange between the two zones [29]. The influence of this setting, however, was also tested in the following simulation cases to evaluate the different ventilation and air flow scenarios. Apart from that, the boundaries of the cavity zone were also assigned to be adiabatic and the outer facade layer, which involves the proposed design, was set to be an exterior boundary. The cavity was assigned as an unconditioned plenum zone and as a default dimension, it was assumed to be 400mm wide, which was a measurement proven to have efficient air and heat flow performance in double facade systems, based on literature research [Zhou et al., 2010], however, this was also chosen as a variable to be used for validity check. Lastly, since materiality had a meaningful role in the amount of solar radiation admitted to the interior, in relation to the properties of the opaque, but mostly the translucent textile part of the exterior layer, the specific energy performance values were also assigned to the corresponding materials. Here, also the option to adjust and assess various alternatives for the translucent part was left open, to explore the solar control possibilities with low-e integrated coatings or fritted patterns and different Solar Heat Gain Coefficient (SHGC) values, and their impact on the reduction of the cooling loads.

The input parameters for the evaluation studies can be seen in the overview table below [Table 25], including the interior and boundary conditions and the set-ups for air flow, internal loads and material properties, with a cooling setpoint at 24°C and a heating setpoint at 15°C [Matzarakis et al., 2004, Carlucci et al., 2021, Cartalis et al., 2001, Leonidaki et al., 2014]. The inputs highlighted in red are considered as variables.

Table 25: Overview of the input parameters and boundary conditions for the Energy Use Intensity calculation. [own work]

Existing single facade	
Window-to-wall ratio	0.45
Thermal Zones Thresholds	Cooling setpoint: 24°C Heating setpoint: 15°C
Internal Loads	Equipment Load: 15 W/m² Lighting Density: 10 W/m² Number of people: 0.05 ppl/m² Ventilation: 0.0008 m³/s∗m² 0.002 m³/person∗m²
Air Loads System	Conditioned (mainly mechanical ventilation)
Glazing type	Generic double pane window without low-e coatings

Boundary conditions

Double facade system					
Inner layer – Interior conditions		Cavity		Outer layer	
Window-to-wall ratio	0.45	Width	400mm	Opaque textile properties	Material: Single layer ETFE Roughness value: 0.1 (rough) Conductivity: 0.238 W/mK Density: 1740 kg/m³ Specific heat capacity: 0.002 J/kgK Thermal absorptance: 0.89 Solar absorptance: 0.3 Visible light absorptance: 0.8 RGB: white (255, 255, 255)
Thermal Zones Thresholds	Cooling setpoint: 24°C Heating setpoint: 15°C	Ventilation type	Stack ventilation		
Internal Loads	Equipment Load: 15 W/m² Lighting Density: 10 W/m² Number of people: 0.05 ppl/m² Ventilation: 0.0008 m³/s∗m² 0.002 m³/person∗m²	Operable effective area (1/sqrt((1/InletArea²)+ 1/OutletArea²))	~0.4m²	Translucent textile properties	Material: Single layer ETFE Roughness value: 0.1 (rough) Conductivity: 0.238 W/m∗K Density: 1740 kg/m³ Specific heat capacity: 0.002 J/kg∗K Thermal absorptance: 0.89 Solar absorptance: 0.3 Visible light absorptance: 0.8 RGB: (255, 255, 255) U-value: 5.6 W/m²K SHGC: 0.93 (with no solar control coating or fritted pattern) Visible transmittance: 0.85
Air Loads System	Conditioned (mainly mechanical ventilation)	Inlet-Outlet height	3m		
Glazing type	Generic double pane window without low-e coatings	Wind coefficient	0		
Energy Use Intensity calculation (Cooling loads kWh/m²) (Analysis period: April – October) – Input parameters		Stack discharge coefficient	0.65		
		Air Loads System	Not conditioned		

The cases examined are summarized in table 26 and relate to a great extent to the ventilation strategy and the material properties. More specifically, Case#1 assumed a small inlet and outlet opening, whereas the rest of the parameters remained unaltered with the default property of an ETFE textile with no additional treatment or coating. For comparison on the air inflow impact, Case#2 considered a larger operable effective area, to evaluate whether the air inflow resulted to a reduction of the cooling loads or led to overheating of the cavity, while in Case#3 the cavity was assigned as only slightly ventilated with minimized vents open (in reality, a fully sealed cavity cannot be achieved with the current design).

From Case#4 on, the SHGC of the translucent textile had a lowered value and in Case#5 a smaller cavity size was tested. Case#6 explored the ventilation scenario for an only night-time ventilation to aid the exhaust of the accumulated heat that is trapped inside the cavity during the day, with a scheduled air exchange between the thermal zones. In Case#7, no natural ventilation was enabled through the cavity, with no direct air exchange between the thermal zones, but allowing only heat exchange through the construction and some air flow through the cavity to the top exhaust. Lastly, Case scenario#8 explored the possibility to avoid the double skin function during the summer, eliminating the cavity effect and not allowing any natural ventilation or air exchange to the interior. In this case, the facade skin works only as an independent exterior shading device, without creating any in-between thermal zone.

As for the existing single facade case study, to avoid complications with natural ventilation strategies, which was an unknown variable in this case, and to make a comparison as objective as possible, the air loads system was assumed to be conditioned and mostly functioning through mechanical ventilation, while the glazing type was assigned as a generic double pane window without low-e coatings. Additionally, in the cases where natural ventilation was enabled, it was set to be activated with a delta temperature setpoint at -2°C in relation to the cooling setpoint.

Table 26: Overview of the case studies and test parameters for the EUI calculation studies. [own work]

Case	Test variables			
#	Operable effective area (w / w/o air exchange between the cavity and the interior)	Night-time ventilation	SHGC value (translucent part)	Cavity width
1	0.4m² (w air exchange)	–	0.93	400mm
2	1m² (w air exchange)	–	0.93	400mm
3	0 (slightly ventilated) (w air exchange)	–	0.93	400mm
4	0 (slightly ventilated) (w air exchange)	–	0.6 (solar control coating)	400mm
5	0 (slightly ventilated) (w air exchange)	–	0.6 (solar control coating)	150mm
6	0.4m² (w scheduled air exchange)	yes	0.6 (solar control coating)	400mm
7	0.4m² (no natural ventilation) (w/o direct air exchange)	–	0.6 (solar control coating)	400mm
8	w/o air exchange, no double skin function or natural ventilation (no cavity thermal zone), exterior facade skin only as sun-shading			

#1   #2   #3   #4   #5   #6   #7   #8
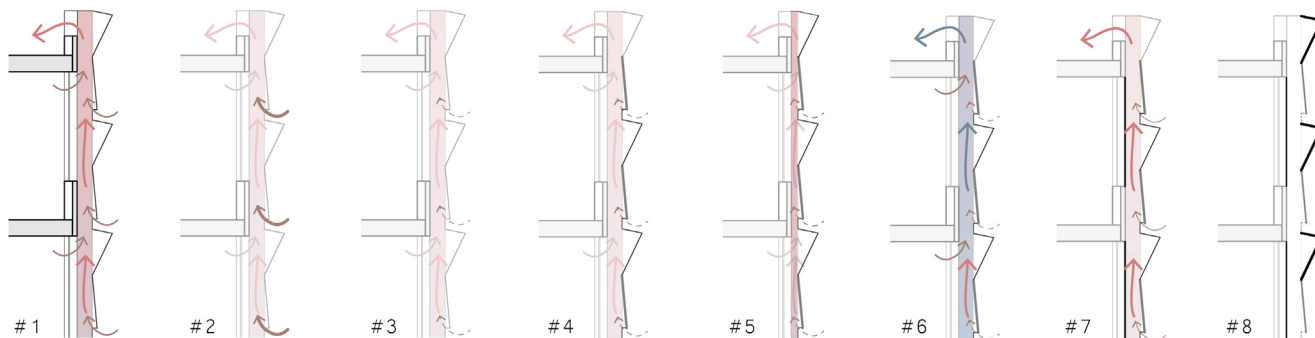
A summary of the results for the cooling loads per area can be found in Table 27, whereas the difference in percentage compared to the existing single facade was also calculated. The Energy Balance (in kWh) and the Floor-Normalized Cooling Load for the building (in kWh/m^2) charts for the analyzed period are shown below for each corresponding case [Figure 94].

Table 27: Overview of the cooling loads results for each case study and comparison to the existing single facade with no external sun-shading. [own work]

Case	Cooling loads per m^2 (Energy Use Intensity)	Difference in %
Existing single facade	**120 kWh/m²**	
#1	145.1 kWh/m^2	+21%
#2	188.7 kWh/m^2	+57%
#3	113.5 kWh/m^2	-5.4%
#4	104.4 kWh/m^2	-13%
#5	109.7 kWh/m^2	-8.5%
#6	102.3 kWh/m^2	-15%
#7	104.4 kWh/m^2	-13%
#8	95 kWh/m^2	-21%

Existing single facade

Case #1

Case #2

Case #3

Case #4
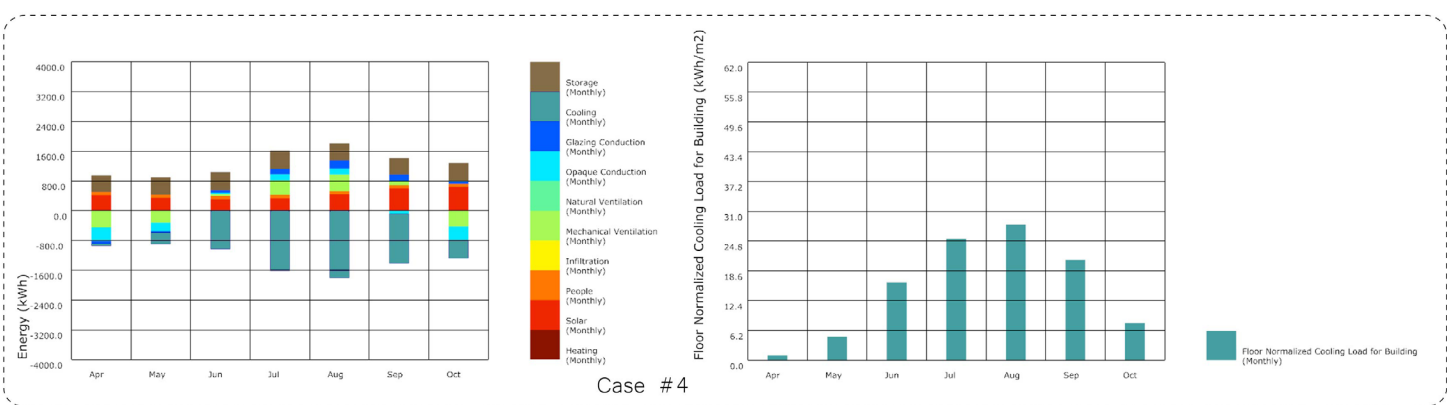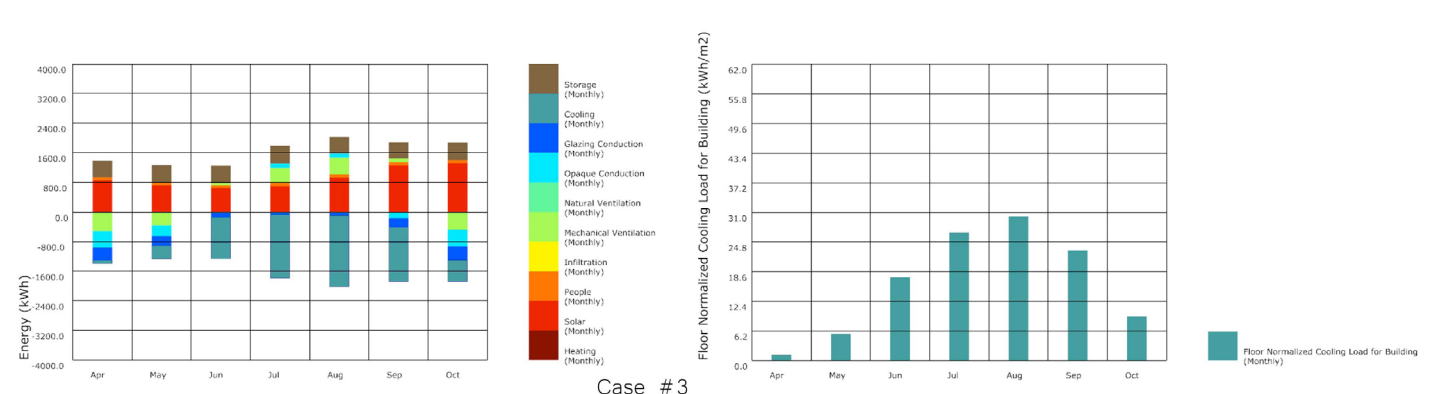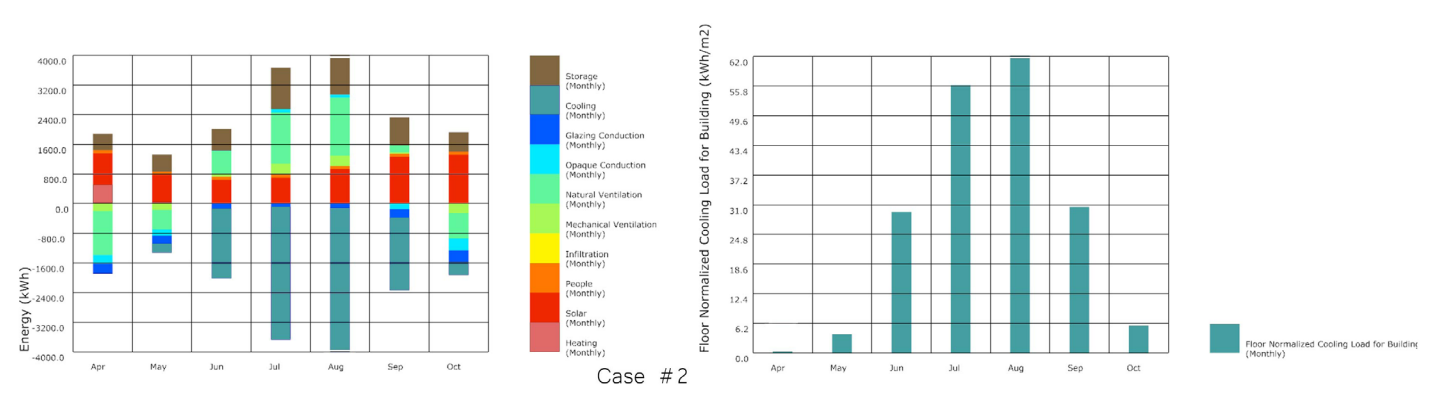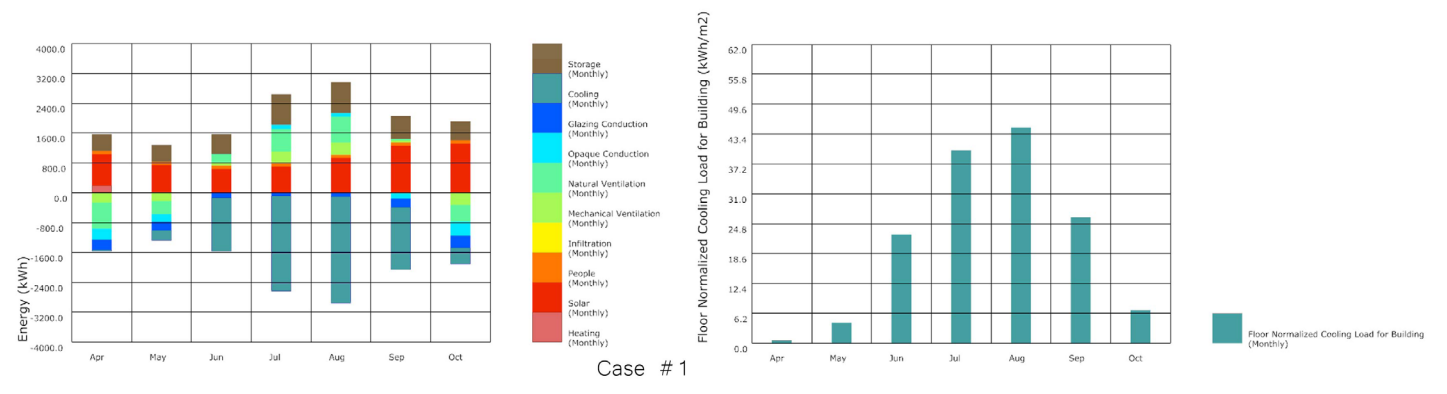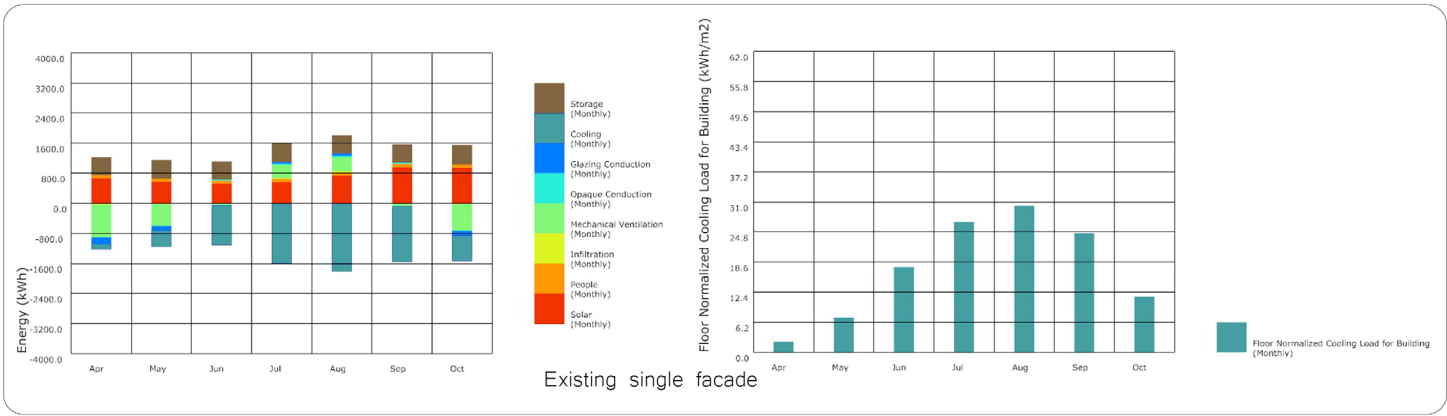
Figure 94: Energy balance charts (left) and EUI of the cooling loads charts (right) for each case study. [own work]

From the above studies it can be concluded that during the cooling-dominated periods, the air inflow inside the cavity led to an overheating of the building due to the greenhouse effect inside of it. A higher amount of air inflow resulted, therefore, to an increase in the cavity temperature, as can be seen in the Cases#1 and #2 with an increase of 21% and 57% of the cooling demands, respectively. The increase was also caused by the absence of additional solar control coatings on the textile surface, which is one of the variables that influenced the cooling demands value, as can be seen in the Case#4, with a reduction of -13%, as a result of the reduction of the SHGC coefficient value. A larger cavity also had a better impact than a smaller one in

that respect, because the smaller one would also lead to a faster increase in the air flow temperature inside the cavity. When it comes to the ventilation strategies, what can be estimated is that it would be more efficient to achieve a combination of night-time ventilation to exhaust the accumulated hot air during the non-operating times of the office building, when it is not occupied, and to minimize the air exchange between the different thermal zones during the day, to avoid discomfort and to minimize the need for air conditioning. More specifically, by comparing the cases #6,7 and #8, it can be concluded that the least interaction and air exchange between the interior and the exterior environment has the most beneficial impact for the reduction of the cooling loads, whereas the facade system would work better merely as an exterior shading device reducing the solar heat gains to the building's interior by 21%, without interfering as a double facade and as a result trapping warm air in the in-between space. There is, therefore, no other added benefit during the summer apart from the shading effect.

In this respect, a supplementary evaluation study involved the comparison of the shading effect of the proposed facade skin to other typical shading devices and their impact on the reduction of the cooling demands, taking as comparison the unshaded existing facade case and Case#8 from the previous study (here named as Case#1). The examples to be compared with were namely typical exterior horizontal venetian blinds and an exterior fabric roller shade or perforated metal screen. In both of these cases, it was assumed that the shading is on, if the outside temperature exceeds the cooling setpoint of 24°C and if the horizontal solar radiation exceeds the setpoint of 400 W/m^2.

The results summarized in Table 28 and Figure 95 showed no significant difference between the three shading examples, with even a marginally better performance of the typical shading devices. The effect of the facade skin could not outperform the rest during this comparison and make it competitive against more cost-efficient and simpler shading solutions, but at the same time it still showed a similar performance. The facade performance during the summer is, therefore, not sufficient on its own to justify such a design. However, this led to the next evaluation round, to assess whether the dynamic movement would bring additional benefits through its seasonal function and adaptation by creating the multiple-cavity double skin function during the winter.

Table 28: Overview of the cooling loads results for the shading type scenarios and comparison to the existing single facade with no external sun-shading and the corresponding cases in schematic graphs. [own work]

Case	Shading type scenario	Cooling loads per m^2 (Energy Use Intensity)	Difference in %
#	Existing single facade with no sun-shading	**120 kWh/m²**	
1	Proposed facade skin design only as sun-shading	95 kWh/m^2	-21%
2	Typical exterior horizontal venetian blinds*	92 kWh/m^2	-23%
3	Exterior fabric roller shade/perforated metal screen*	89.5 kWh/m^2	-25%

*Shading is on, if the outside air temperature exceeds the Cooling Setpoint of 24°C
and if the horizontal solar radiation exceeds the SetPoint of 400 W/m^2

Existing facade
(no sun-shading)   #1   #2   #3

Existing single facade with no sun-shading
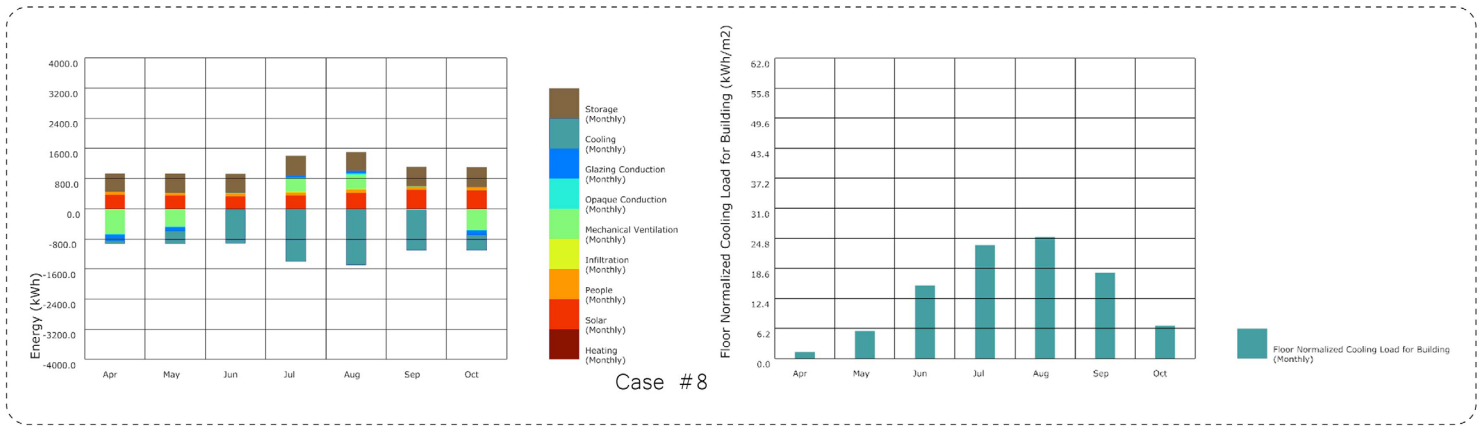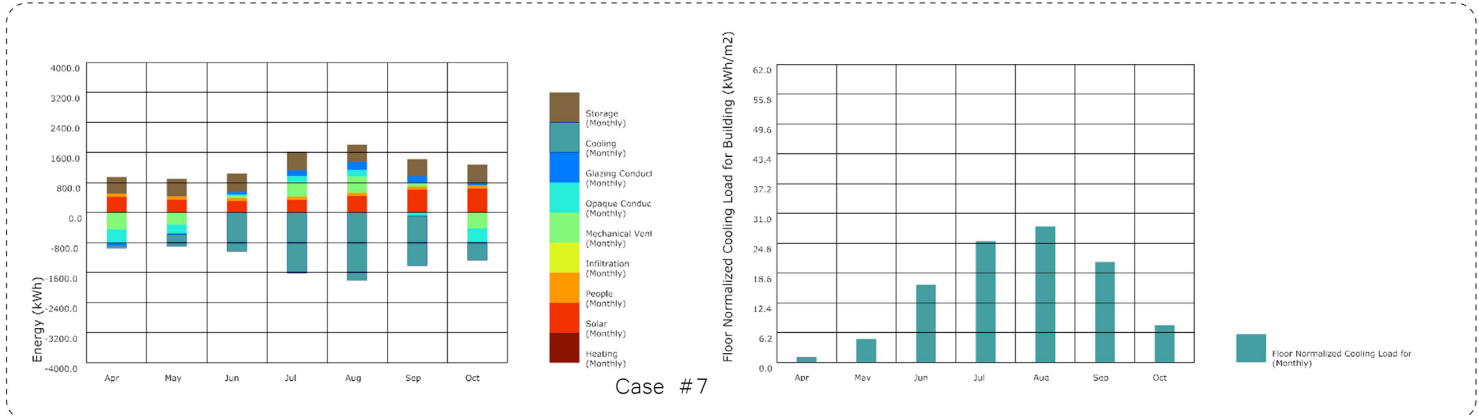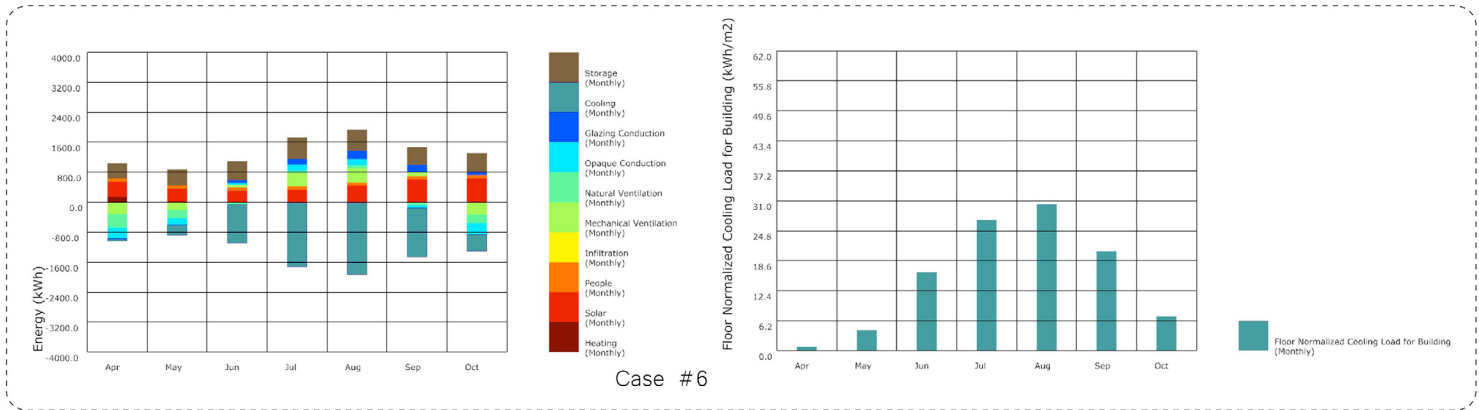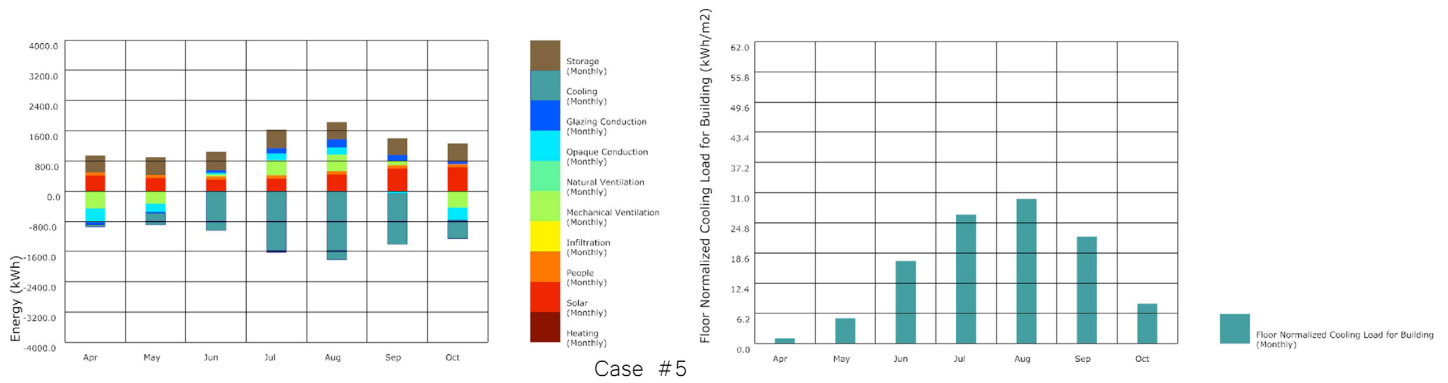

Case # 1

Case # 2

Case # 3
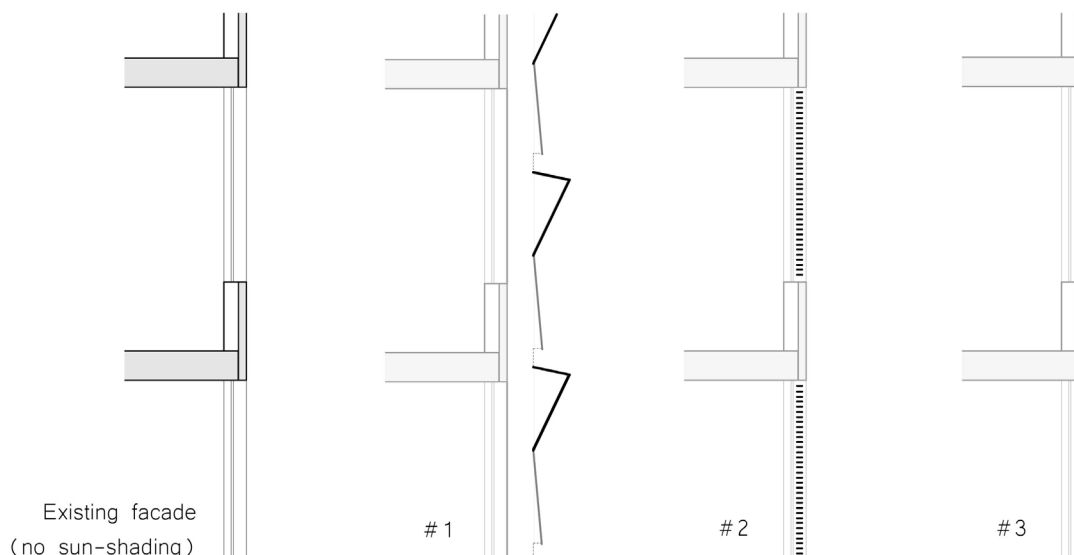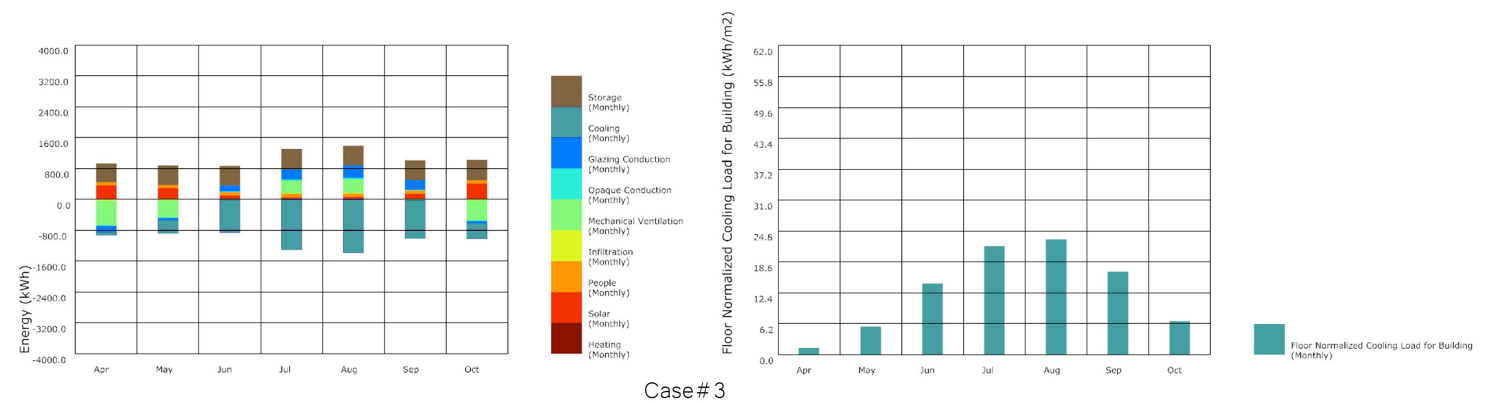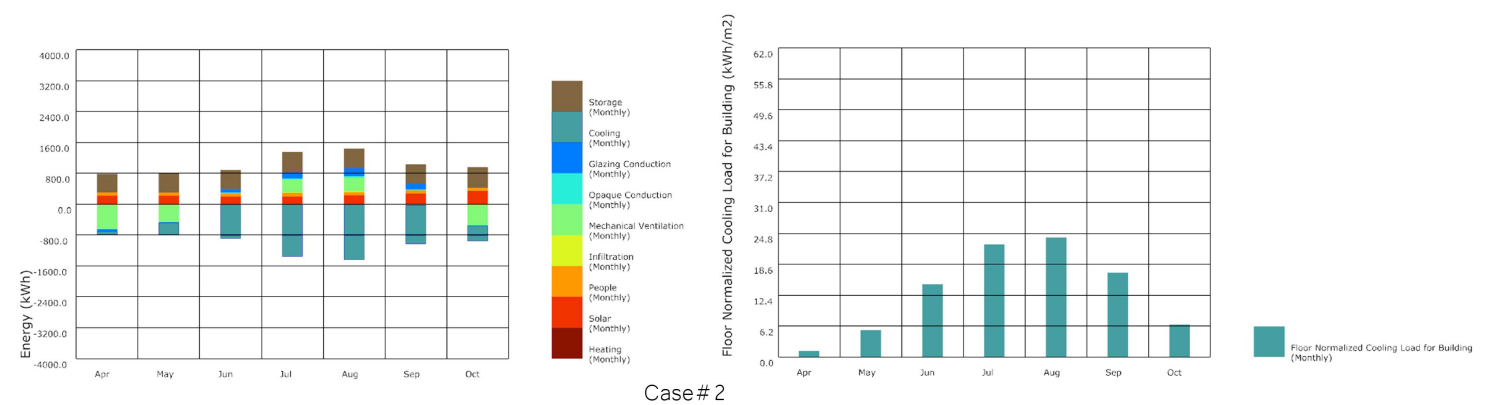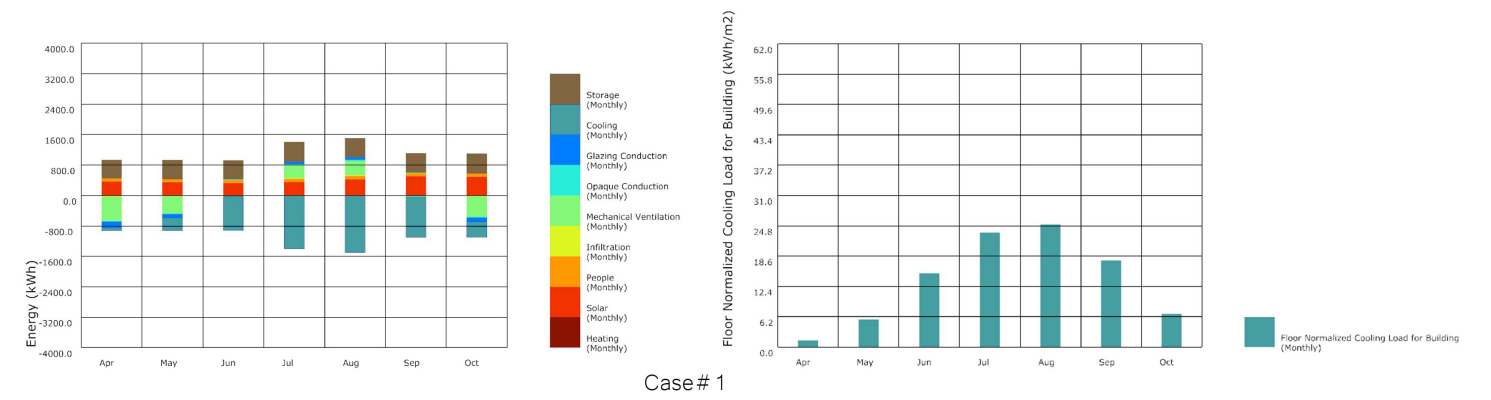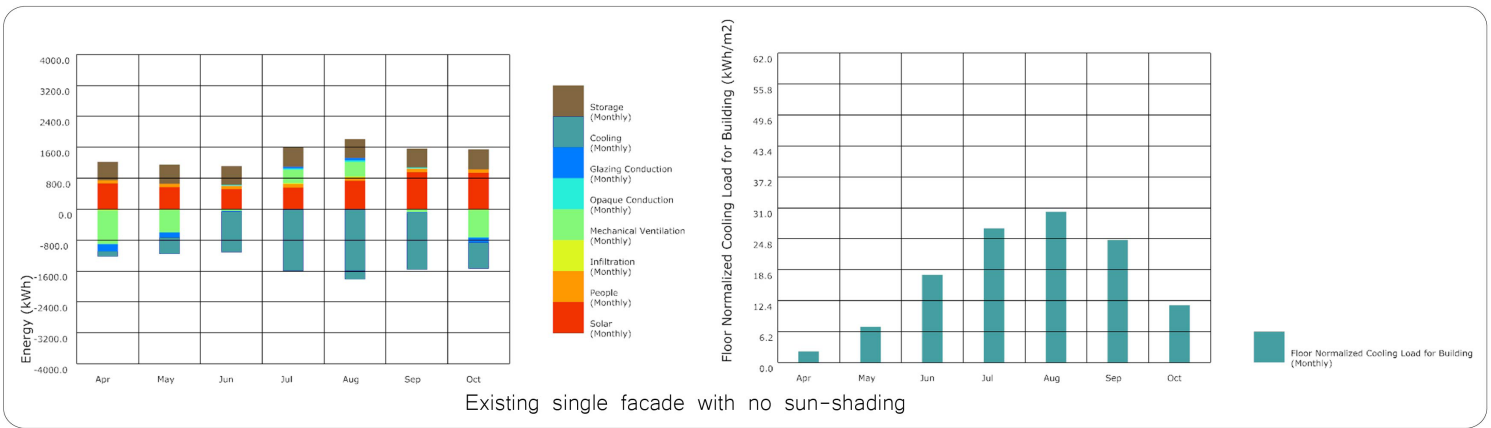
Figure 95: Energy balance charts (left) and EUI of the cooling loads charts (right) for each case study. [own work]

6.7.2.2. THERMAL ANALYSIS – HEAT AND AIR FLOWS SIMULATIONS

In parallel to the assessment of the cooling demands, thermal analyses were conducted to simulate and visualize the heat and air flows inside the cavity and to obtain an approximation of the temperature fluctuations between the outside and the interior boundary zones.

As explained before, for these studies an interoperable decoupling methodology was followed, combining radiation analysis and temperature surface output data through Ladybug plug-in to be used as input of the additional radiative sources for the SimScale convective heat transfer simulations. In this way, the convective and radiation heat transfer could be solved with the absorbed solar radiation treated as heating source on the facade skin surface. This is a compromised alternative due to the difficulty in accurately modelling the radiation heat transfer and the complex nature of this type of analysis. By using EnergyPlus to solve the radiation heat transfer, this step can provide surface temperatures and heat flux values under certain weather conditions to be assigned in the CFD simulation as boundary conditions. The CFD simulation can then return the air temperature distribution and the corrected convective heat transfer coefficient, as well as airflow rates in the cavity to update the heat transfer calculation by EnergyPlus. This decoupling method has been proved to be effective in predicting the thermal behavior of double skin facades and has already been tested in similar research projects [Fuliotto et al., 2010, He et al., 2011, Pappas et al., 2008]. A similar approach was, therefore, also followed in the current study.

At the same time, the results from SimScale were compared to the static temperature fluctuations calculated in the THERM plug-in and software environment. Even though the two approaches follow a slightly different process information logic and the thermal analysis in THERM does not include air flows, it helped as a complementary study to understand the temperature fluctuations, including the building envelope behind the cavity, and to give an indication of the thermal buffer effect of the cavity during the winter. Apart from that, it was also possible to assign additional material properties as inputs and in the end during the comparison of the two workflows, to complement each other and compensate for their possible limitations. The workflow, input parameters and boundary conditions for the THERM simulation are summarized in the overview Table 29 and in Figure 96.

Table 29: Overview of the input parameters and boundary conditions for the THERM analysis. [own work]
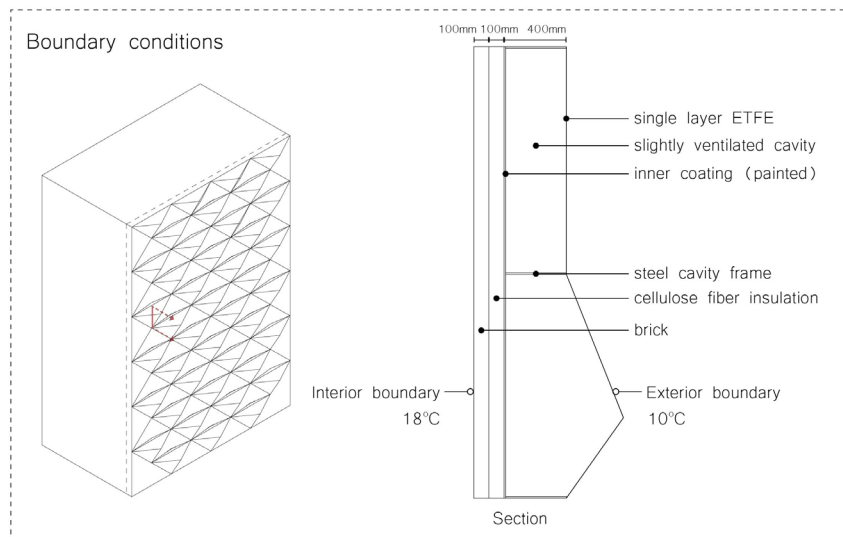
Thermal boundary conditions			Outer layer properties
	Exterior Boundary	Interior Boundary	Material: Single layer ETFE
Temperature	10°C	18°C	Roughness value: 0.1 (rough) Conductivity: 0.238 W/mK Density: 1740 kg/m^3
Additional heat flux	420 W/m^2	–	Specific heat capacity: 0.002 J/kgK Thermal absorptance: 0.89 Solar absorptance: 0.3
Emissivity	0.89	–	Visible light absorptance: 0.8 RGB: white (255, 255, 255)

As for the SimScale simulation set-up, a steady-state convective heat transfer analysis was realized for a duration of 3600s. This time duration, however, led to certain limitations, because it still simulated a fragmented time frame and could not show the full cavity function throughout a whole day, which would then cause an increase in computational time. The input geometries imported from Rhino were also simplified to be easily translated as one closed volume that was used for the air flow, where only the interior boundary surfaces were modelled. For example, the surfaces needed to be continuous and not intersecting, so areas where the multiple cavity zones were positioned needed to leave a small gap and not be fully sealed. Another limitation concerns the applied additional radiation heat, which was assigned as one average value distributed homogeneously on the outer boundary surface, whereas during the solar radiation analysis it was mostly concentrated on the top surface of the bottom pyramid, which was more exposed to the direct sunlight.

The simulation runs were grouped into the two seasonal scenarios, summer and winter one, with sub-cases in each situation. In the winter scenario, with an ambient temperature of 10°C and a surface temperature of 13°C (data from the Annual Weather and Radiation analyses), the interest was placed on the heat accumulation inside the multiple cavity zones, the increase in temperature that is caused due to the heat stack effect and the impact of the cavity width, as well as to visualize whether the interior volume of the pyramid worked indeed as a heat convection zone. The case studies in this set-up included one floor with two closed cavity zones, excluding the inner building, since there is no air exchange between the two thermal zones. Case#1 was

the basic set-up with a 400mm wide cavity and no air inlets or outlets as an ideal scenario, merely functioning as a heat amplification zone, Case#2 featured slight openings through small vents to evaluate the more realistic situation, and in Case#3 a more narrow cavity of 150mm was examined. In practice, there are certain differences in the amount of air inflow, which meant that certain divergence in the simulated results and reality was expected and taken into account.

On the contrary, the summer scenario, with an ambient outdoor temperature of 35°C and a surface temperature of 31°C (data from the Annual Weather and Radiation analyses), was modelled as a full height open cavity in the 6-storey building with a top outlet and the cases were related to the ventilation strategies explored in the previous section. Case#1 allowed air inlets from the outer layer and enabled the air exchange with the interior through air outlets, Case#2, reduced the air flow to only air inlets and flow through the cavity to the top exhaust outlet and Case#3 investigated the effect of an only slightly ventilated cavity and a top outlet. The summer scenario was focused mostly on the air and heat flows in relation to the impact of the different ventilation strategies on the air circulation inside the cavity.

In all the cases mentioned above, the outer layer was considered as an exterior boundary, while the cavity and interior surfaces were assigned an adiabatic boundary condition.

An overview of the initial and boundary conditions for both the summer and the winter situation can be found in the following tables [Tables 30, 31].
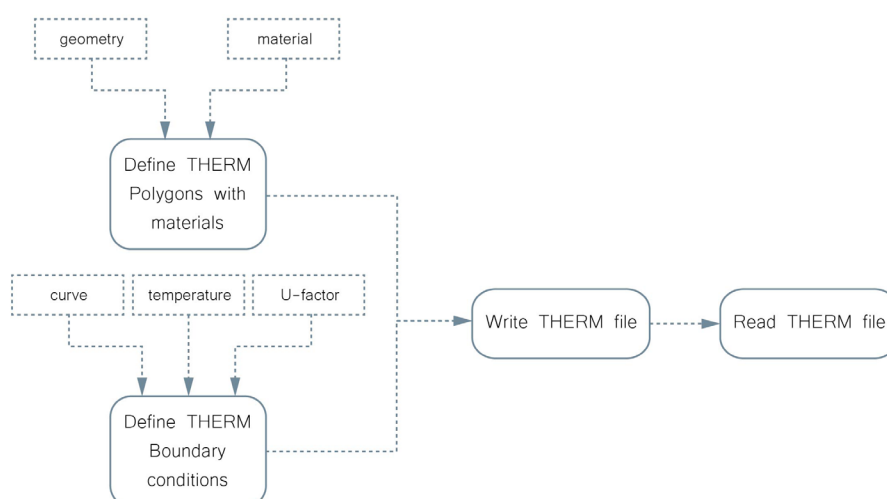
Figure 96: Flowchart of the workflow for the THERM analysis. [own work]

Table 30: Overview of the input parameters and boundary conditions for the SimScale CFD convective heat transfer analysis in the winter situation. [own work]

Initial conditions	Boundary conditions				
	Outer layer		Cavity sides – Inner layer	
Fluid: Air Kinematic viscocity: 1.529e-5 m²/s Density: 1.196 kg/m³ Thermal expansion coefficient: 3.43e-3 1/K Specific heat: 1004 J/(kg*K) Gravity: -9.81 m/s² Global temperature: 10°C Velocity: 0 m/s	Cavity width	400mm	Temperature type	Adiabatic
	Temperature type	External wall heat flux	Radiative behaviour	Opaque
	Heat transfer coefficient	5.6 W/m²K	Emissivity	0.9
	Ambient temperature	10°C [value from Annual Weather Data]	Winter situation (Analysis day: 21/12) – Multiple closed-air cavities system	
	Thermal conductivity	0.89		
Simulation control	Layer thickness	12.5mm		
Convective Heat Transfer simulation analysis Time dependency: Steady-state End time: 3600s Time step: 1s	Initial boundary temperature	13°C [surface temperature value from Solar Radiation analysis]		
	Radiative behaviour	Transparent		
	Additional radiative source	420 W/m² [value from daily Solar Radiation analysis on the facade surface on 21/12]		

Table 31: Overview of the input parameters and boundary conditions for the SimScale CFD convective heat transfer analysis in the summer situation. [own work]

Initial conditions	Boundary conditions			
	Outer layer		Cavity sides – Inner layer	
Fluid: Air Kinematic viscocity: 1.529e-5 m²/s Density: 1.196 kg/m³ Thermal expansion coefficient: 3.43e-3 1/K Specific heat: 1004 J/(kg*K) Gravity: -9.81 m/s² Global temperature: 35°C Velocity: 0 m/s	Cavity width	400mm	Temperature type	Adiabatic
	Temperature type	External wall heat flux	Radiative behaviour	Opaque
	Heat transfer coefficient	5.6 W/m²K	Emissivity	0.9
	Ambient temperature	10°C [value from Annual Weather Data]	Summer situation (Analysis day: 29/06) – Opened-air cavity system	
	Thermal conductivity	0.89		
Simulation control	Layer thickness	12.5mm		
Convective Heat Transfer simulation analysis Time dependency: Steady-state End time: 3600s Time step: 1s	Initial boundary temperature	31°C [surface temperature value from Solar Radiation analysis]		
	Radiative behaviour	Transparent		
	Additional radiative source	160 W/m² [value from daily Solar Radiation analysis on the facade surface on 29/06]		

The results from the winter situation [Figure 97] showed that there is an increase in the surface temperature around the inner boundary of up to 25°C with a further increase on the top surfaces of the cavity boundaries due to the air and heat stratification. Similar results were found through the THERM static temperature fluctuation simulation, which showed a heat buffer accumulated outside the insulation layer, reducing the heat losses and the temperature difference between the interior and the exterior during the cold months. It can also be noticed that the simulations realized through SimScale capture only an hour of operation and, in that way, show the effect in its starting moments when the cavity begins to heat up, while the THERM model shows the temperature fluctuations as a static building construction with no incoming airflow, which, however, receives a constant additional radiation heat on the outer boundary layer. In this sense, Case#1 and the THERM model can be approximate representatives of the two boundary conditions, the beginning and the peak of the thermal effect respectively, with the SimScale one to also highlight the reverse situation when the model slowly transcends back to its original cool state after the solar radiation intake is reduced during the late afternoon hours.

In addition, in Case#2, there is an increase in the temperature inside the cavity and also the convective effect of the inner pyramid volume is more evident, which can be justified by the increase in the heat flows induced by the increased air movement that is heated up when entering the cavity. However, this creates at the same time a constant air influx, which leads to heat losses at similarly high speeds, so the heat buffer effect is then being reduced. Lastly, in Case#3 the narrower cavity on top also led to an increase in temperature due to the less air volume requiring less time to reach a higher temperature. However, as seen by the cooling demands analysis and despite possible winter benefits, a narrow cavity would cause an overheating during the summer, which, is more critical to mitigate for the scope of the current thesis. It can, therefore, be concluded that the function during the cold seasons as a multiple-cavity system can have the potential to offer additional benefits as a thermal buffer zone for the reduction of the heat losses.
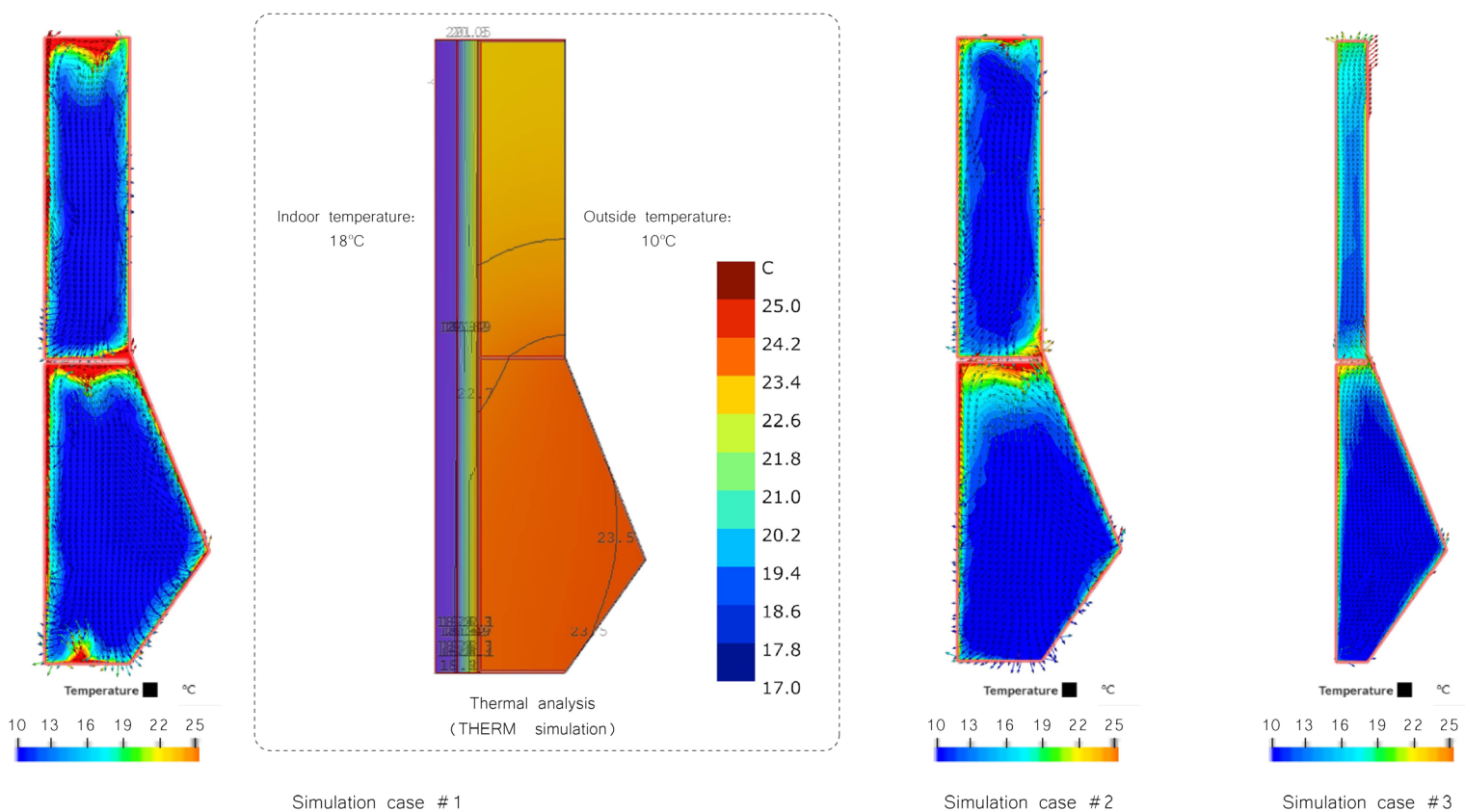
Figure 97: Convective heat transfer analysis simulation results for the winter situation. [own work]

Regarding the summer scenario, the results summarized below [Figure 98] showed similar behaviour inside the cavity, with higher temperatures on the boundary surfaces and in the narrow air volumes. What is different here, is that there is a slight reduction of accumulated heat when there are no air inlets between the interior building spaces and the continuous cavity zone, as in Case#2. In accordance to the conclusions from the cooling demands analysis, the air entering the cavity is warmer than the interior, causing overheating of the cavity and introducing hot air to the interior instead,

in a greenhouse manner. The temperatures reached are above the outdoor ambient temperature, ranging in average from 35°C–37°C, with some local intensified boundary areas that exceed those limits. This can also be seen in the areas around the air inlets, where there is a local increase in temperature. Case#3 showed negligible difference compared to Case#2 and needed to be also slightly modified to avoid continuity errors caused by excluding air inlets, so a minimum area of air inlets was also assigned at the bottom of the outer layer instead, to comply with the pressure outlet on top.
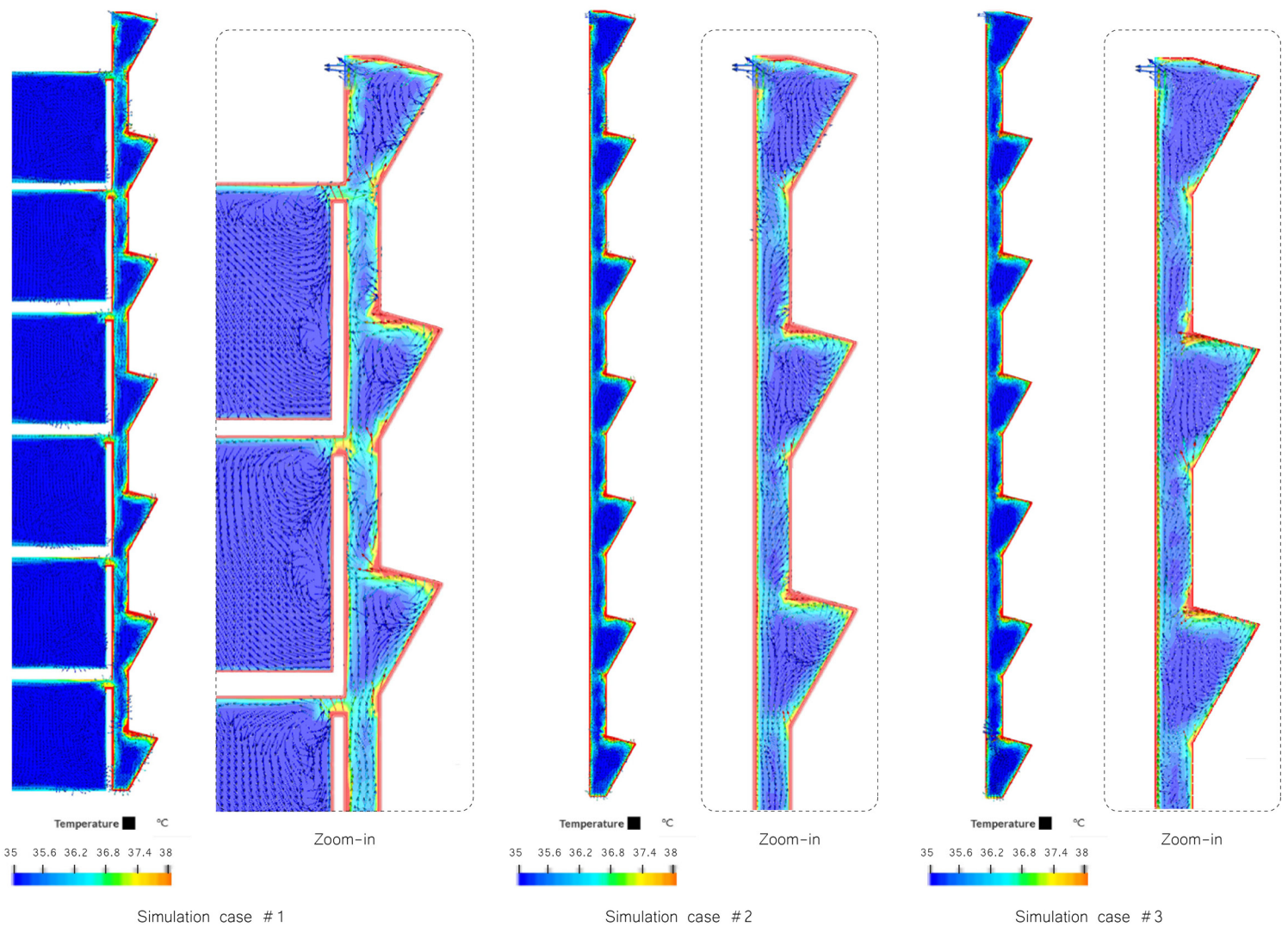

Figure 98: Convective heat transfer analysis simulation results for the summer situation. [own work]

6.7.2.3. DAYLIGHT ANALYSIS

The last analysis that was realized concerned the evaluation of the impact of the outer facade skin on the Daylight Factor (DF) in the interior, since the proposed overcladding retrofit inevitably affects the inner comfort and daylight conditions. Daylight Factor is a ratio that represents the amount of illumination available indoors relative to the illumination present outdoors at the same time under over-cast skies [23]. In this sense, this evaluation round is not directly related to the building's impact on the UHI effect, but relates mostly to the user's comfort to assess whether and under which conditions the facade design is within acceptable daylight limits in the non-opaque facade scenario.

The same base case study with a 45% window-to-wall ratio is also considered in this study as well, with room dimensions of 10m length, 6m depth and 3m interior height. The proposed facade design featured alternating opaque and translucent textile parts in the component's top part, depending on the construction of the inner facade, coupling opaque textile with the opaque wall and the translucent one in front of the windows, working mostly as a solar filter. The properties used were the ones discussed in the previous studies, with the optimized SHGC of 0.6, assuming solar control coatings.

The comparison was realized between the proposed facade design and the existing case scenario of the single facade with no exterior sun-shading. Apart from that, a few more cases were studied, to evaluate various alernatives of the same design in different component scales, how they could adapt to a larger window-to-wall ratio and to make an estimation on the allowable DF limits and room requirements that would result to a desired visual comfort level. For each assessment,

the BREEAM and DGNB standards were considered as benchmark criteria, which offer a list of requirements and rating levels on this regard [22, 23, 24, 25]. Based on BREEAM, for an office building, at least 80% of the area must comply to a minimum DF of 2% and at the same time a uniformity ratio of at least 0.4 or a minimum point DF of at least 0.8% must be reached. As for the rating, according to DGNB [24], the DF are ranked as follows: >3%: very good, >2%: medium, >1%: slight, <1%: none. These parameters and case studies are summarized in the tables below [Tables 32, 33].

In parallel, an additional index was also simulated, the Useful Daylight Illuminance Index (UDI), which provides a daylight availability metric that corresponds to the percentage of the occupied time when a target range of illuminances at a point in a space is met by daylight. Daylight illuminances in the range 100 to 300 lux are considered effective either as the sole source of illumination or in conjunction with artificial lighting. Daylight illuminances in the range 300 to around 2000 lux are often perceived as desirable. Recent examples have led to recommendations to achieve an average UDI in the range of 100-2000 lux for 80% of occupancy hours [25].

The DF and UDI analysis studies were conducted using the Honeybee Daylight Analysis component, which runs an annual Daylight simulation under a uniform sky of the input geometry on a test grid, which in this case consists of the interior floor, and calculates the average annual DF and UDI, respectively. The flowchart of the analysis workflow is shown in Figure 99.

Tables 32, 33: Overview of the case studies and test variables and the requirements for Daylight Factor (DF) and Useful Daylight Illuminance (UDI) Index [own work]

Case	Test variables		Room dimensions
#	Window-to-wall ratio	Component overall size	Length: 10m Depth: 6m Interior height: 3m
1	0.45	2000mm*2000mm	
2	0.45	3000mm*3000mm	
3	0.85	3000mm*3000mm	

BREEAM requirements			DGNB rating	UDI recommendations
DF required	Area to comply	Other requirements	>3% very good >2% medium >1% slight <1% none	100-2000 lux for 80% of occupancy hours
2%	80%	uniformity ratio >= 0.4 % or a minimum point daylight factor >= 0.8%		

The results found in Table 34 and visualized in Figure 100 showed that the existing single facade had a DF of 7.5% with no external sun-shading system and a value of 5.3% for 80% of the test points, which is already exceeding the limits to allow daylight throughout the whole room. However, in practice, some sort of shading would need to be added in the interior to avoid excessive daylight and glare that leads to visual discomfort. In comparison to that, Case#1 achieved a DF of 1.4% and 2.15% in all and 80% of the test points, respectively. Even though the 2.15% is within limits, with the default room size, the requirement for uniformity ratio or minimum point DF was not met.

After certain sizing iterations, it was found that in this case a dimension of 3.5m was the maximum depth that the room would have to reach to comply to all the requirements stated above. Case#2, which tested a larger facade component, showed slightly lower results with a DF of 1.3%, and 1.85% of the 80% of test points and the maximum room depth of 3m required. The reduction with a larger component can be justified by the larger depth of the bottom pyramid that increases the shading effect. When the same facade component was tested in front of a full curtain wall facade as in Case#3, the DF was increased to 1.95% and 3.2%

respectively and the room depth up to 3.7m. Apart from Case#3, Cases#1 and #2, which were related to the specific case scenario could achieve a close to medium visual comfort depending on the room dimensions, whereas the ones taken as default could only reach a slight visual comfort rating, which would not be sufficient enough. Additionally, the top translucent textile can also be used as an external solar control filter to evenly disperse the incoming daylight to the interior, by reducing the SHGC, which would have been the issue with the existing single facade.

As for the UDI values, the results showed that in the existing facade, in average only 56% of the occupancy time the UDI is between 100-2000 lux and this happens also only at the back of the room in a distance from the windows, due to the increased daylight caused by lack of shading that results to undesireably high illuminance values. The rest of the studied cases are approximately within the recommended range, however, it can be observed that similarly to the unshaded existing facade scenario, Case#3, which tested a higher window-to-wall ratio, also showed test points close to the facade which still received more than 2000 lux on average. This means that in such an office area a working space close to the window area would not have been recommended.
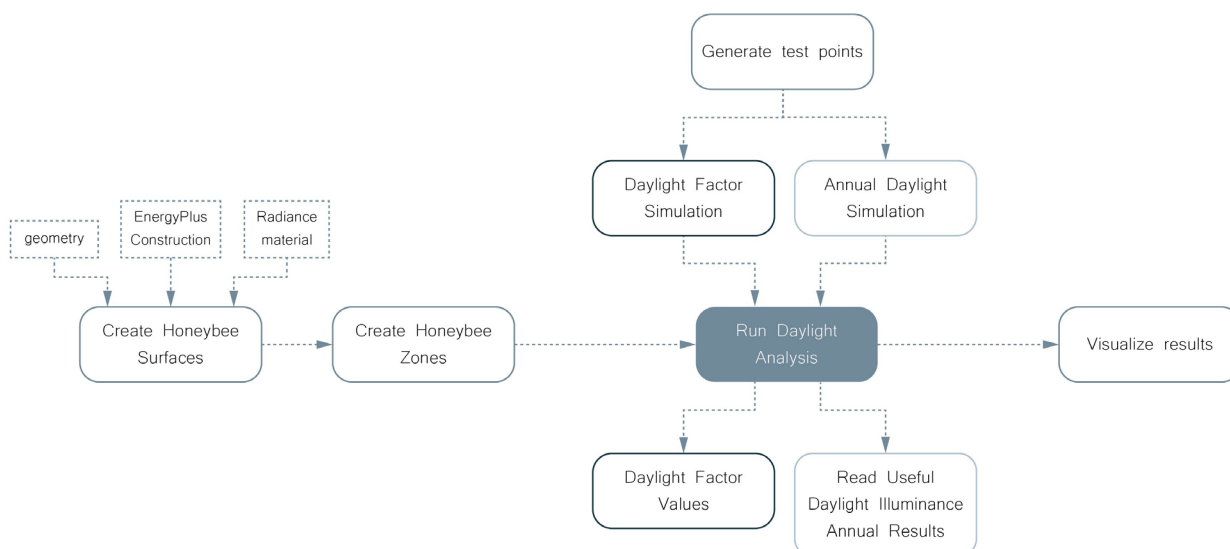
Figure 99: Flowchart of the Daylight Analysis workflow. [own work]

Table 34: Overview of the case studies results and the compliance to the requirements for Daylight Factor (DF) and Useful Daylight Illuminance (UDI) Index [own work]

Case	Daylight factor (DF)	DF of 80% of test points	room depth within DF BREEAM limits	average UDI within 100-2000 lux range
Existing single facade with no external sun-shading	**7.5%**	**5.3%**	**yes**	**56%**
#1	1.4%	2.15%	<=3.5m	80%
#2	1.3%	1.85%	<=3m	78%
#3	1.95%	3.2%	<=3.7m	84%

Existing single facade with no external sun-shading
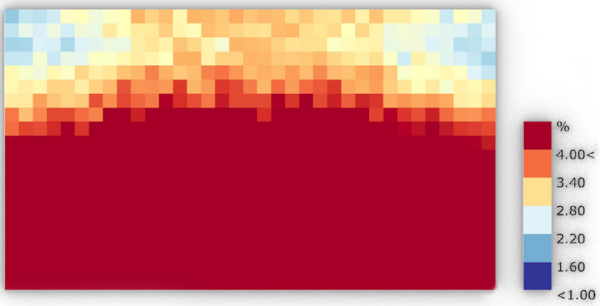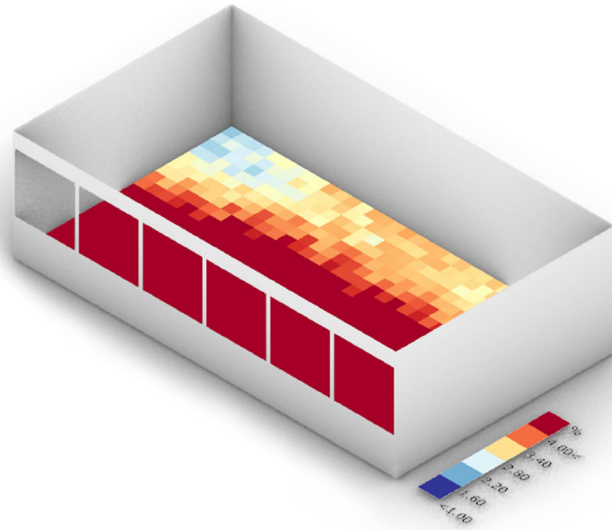
Daylight Factor（DF）
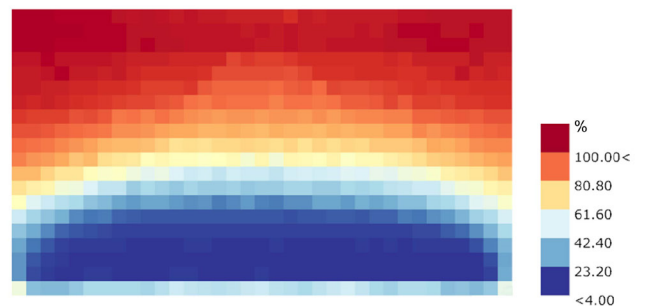
Useful Daylight Illuminance Index（UDI）100-2000 lux

Case#1
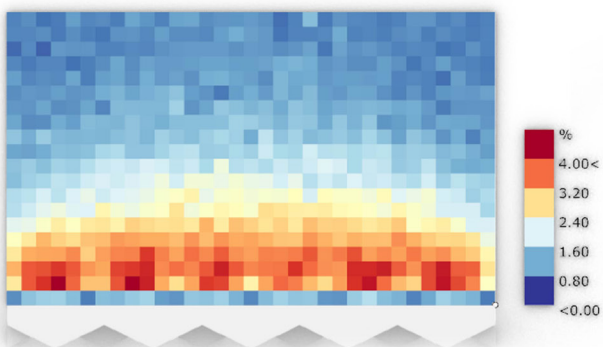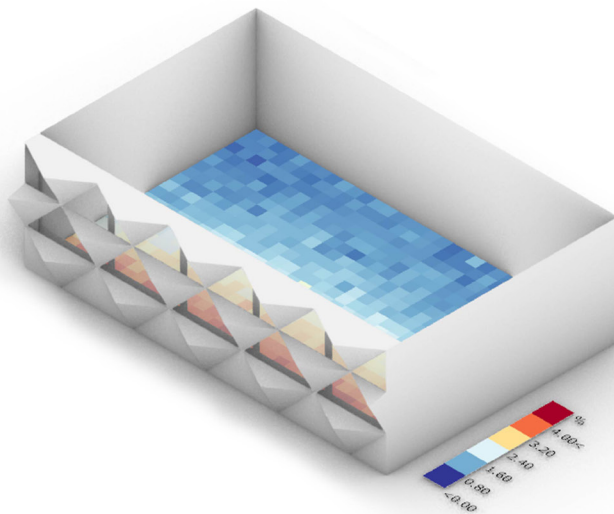
Daylight Factor（DF）
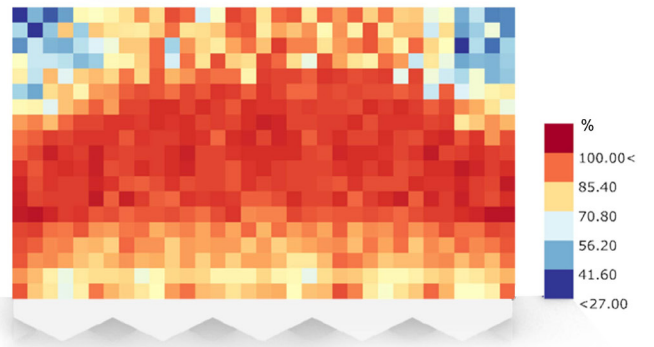
Useful Daylight Illuminance Index（UDI）100-2000 lux

Case#2
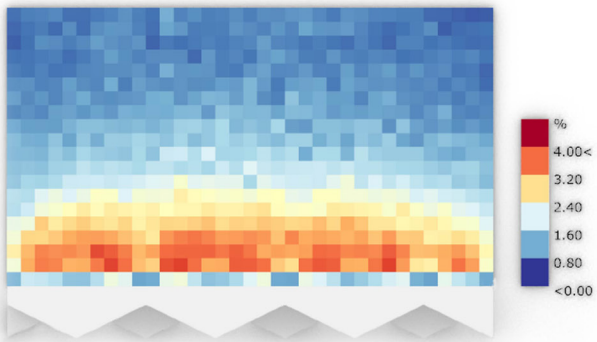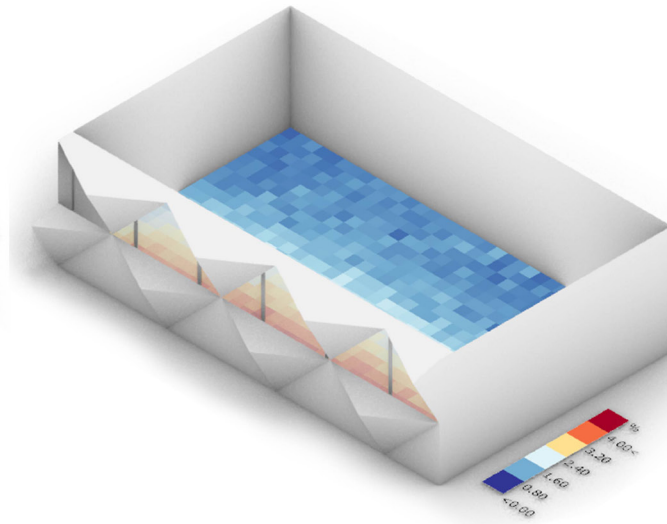
Daylight Factor (DF)
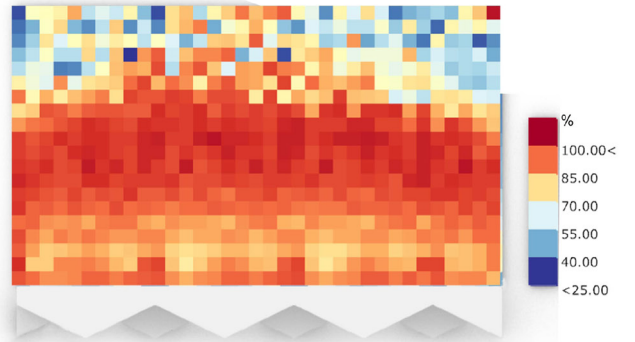
Useful Daylight Illuminance Index (UDI) 100-2000 lux

Case#3
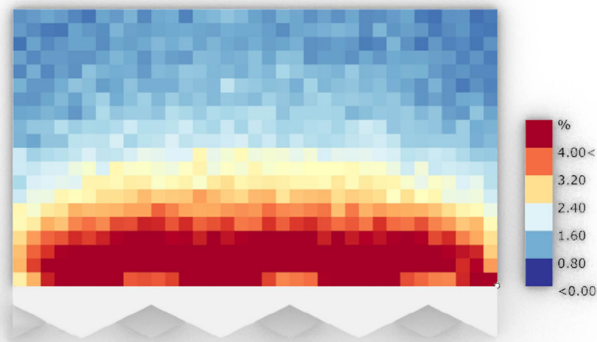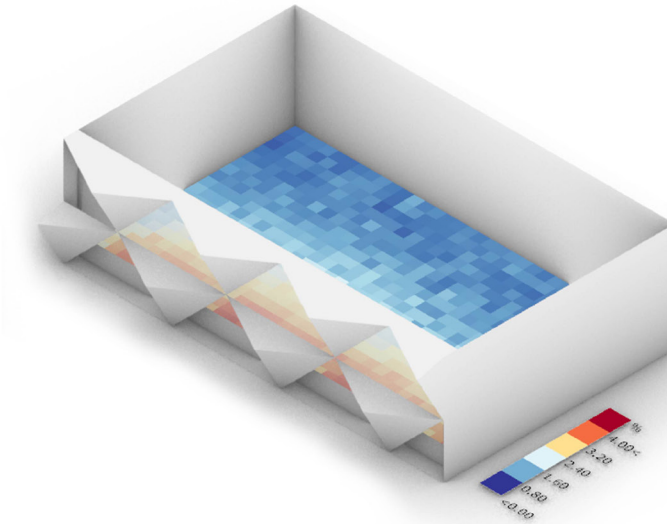
Daylight Factor (DF)
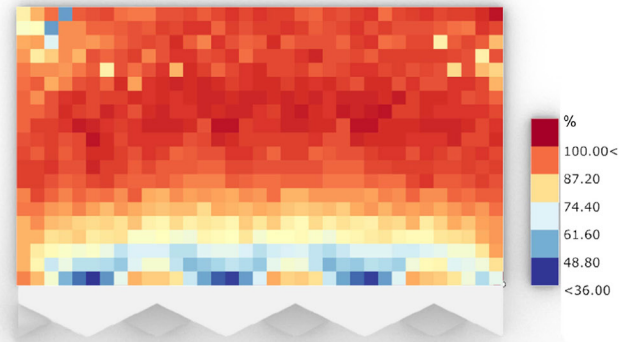
Useful Daylight Illuminance Index (UDI) 100-2000 lux

Figure 100: DF and UDI index results for each case study. [own work]

As a remark, the intention was to additionally evaluate the impact of the facade skin's shading effect on the reduction of the electric lighting energy use, and to assess whether there was a reduction on the building's overall energy consumption from this respect as well, compared to the existing situation. However, during the energy simulation process, certain "bugs" were encountered, related to the compatibility between the different versions of the OpenStudio simulation engine and the Ladybug environment, which were not fully supported with each other at the moment without calculation clashes, resulting to simulation errors that did not allow a complete data processing to provide the desired results for the lighting energy demands. It was found that this had been a common trouble-shooting problem in other users as well, and based on the discussions with the software developers in the allocated forums, for the time being, it had been a work-in-progress to be resolved in updated versions that would enable a more stable compatibility between the different versions of the simulation engines with no issues of this nature. This study is, therefore, recommended to be considered as a next step for further exploration in the future, once this issue is resolved, in continuation of the daylight analysis, for a more complete and comprehensive performance evaluation of the system.

Nevertheless, some assumptions can still be raised on the correlation of the daylighting and the energy savings, based on relevant research studies on that matter. In general, when cooling is needed in a space, both the use of electric lighting and the presence of daylight will each add to the cooling load. Especially in warmer climates, cooling may be needed for large parts of the annual operation. In pracice, during the building's occupancy, there are, therefore, more parameters involved and the daylighting could lead to a net increase in energy consumption, if the additional cooling load due to daylight exceeds the energy saved due to reduced electric lighting, or if the net heat gains and losses through the glazing do not compensate for the lighting energy saved.

For a better understanding, the study by Nabil et al. examined the correlation between UDI and electric lighting loads to assess the overall energy demands in buildings [Nabil et al., 2005]. By creating a number of electric lighting models, including windows without and with blinds and luminaire switching, it was found that for windows without blinds, there was a strong positive correlation between electric lighting usage and achieved UDI [Figure 101a]. This occured because, for the majority of the design variants, there was an over-provision of daylight, with values exceeding 2000 lux at one or more points for much of the year. However, illuminances higher than 2000 lux are likely to cause occupants to trigger shading mechanisms. Because of that, for example in fully glazed buildings, where the blinds are used to control glare and the lights are on, there is a combination of high solar gains, because blinds reject only a small part of the energy once it has passed through the glazing, and consequently no

a

b

Clear double glazing   AntiSun Green glazing   AntiSun Bronze glazing
      +   *   □
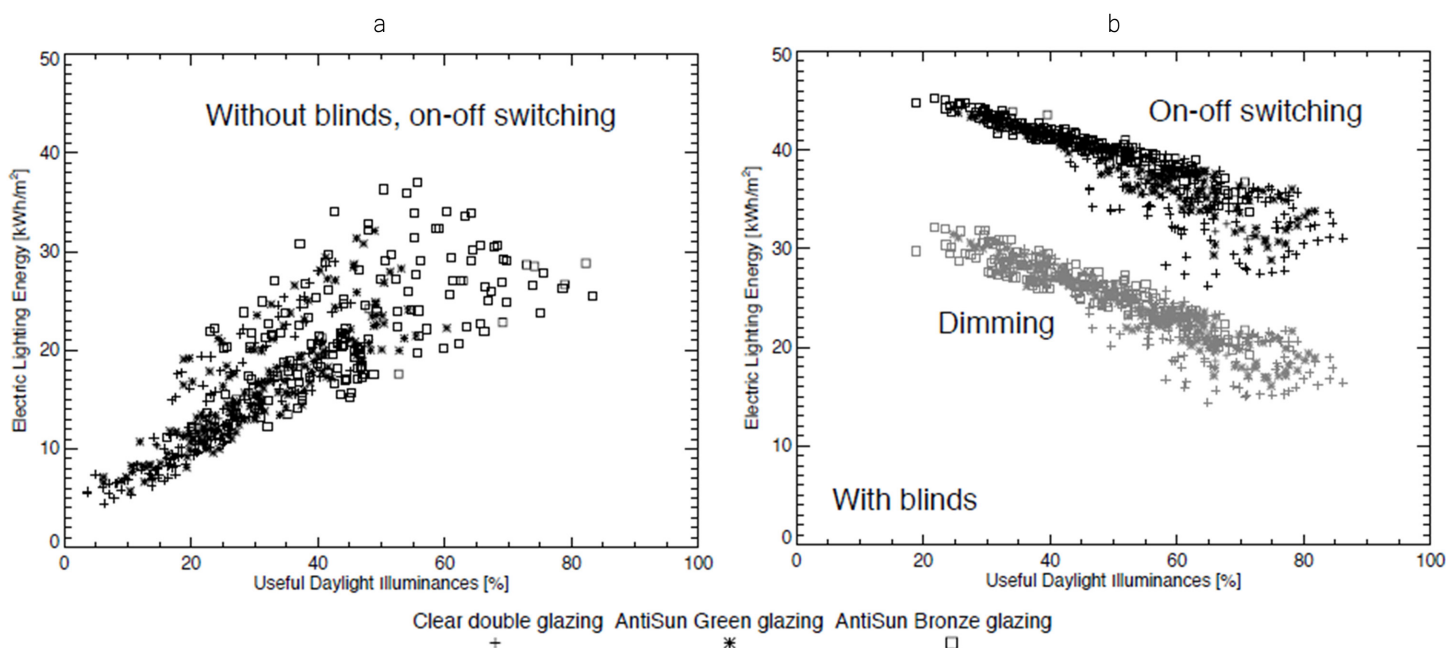
Figure 101: Annual electric energy consumption for lighting versus achieved UDI for all combinations of three glazing types in twelve orientations and fourteen climate types. a) Situation without blinds, b) Situation with blinds. [Nabil et al., 2005]

significant daylight benefit in terms of reduced lighting energy [Mardaljevic et al., 2009]. This is similar to the existing building scenario of the case study, where the daylight analysis resulted to an increased percentage of test points with illuminance values higher than 2000 lux. In this sense, even though the electric lighting use might seem to be reduced as a consequence of the increased daylight values, in practice this would be unattainable without blinds, due to visual and thermal discomfort.

In contrast, at the same study, there was an anti-correlation between annual electric lighting usage and achieved UDI for each of the luminaire switching models [Figure 101b], which suggest that high levels of UDI in offices with operable shading devices are associated with lower levels of electric lighting usage, while this relation is general and does not depend on the location or orientation of the building. High occurencies of UDI in the range between 100-2500 lux commonly fall in the category of UDI-autonomous, where it is assumed that additional artificial lighting will most likely not be needed.

In the current project, as it was shown before, the proposed shading design can achieve in average around 80% of its test points within the UDI-autonomous range. It can, therefore, be assumed that at this early design stage, this can provide an early indication of a low requirement for electrical lighting, and, as a result, a reduction of the building's overall energy consumption. In practice, however, a combination of passive and active control with the option to override the dynamic movement of the outer shading foils could potentially allow a much better and more reliable control of both the solar heat gains and the electrical lighting energy loads. In the end, it becomes a trade-off between the above two requirements with the goal to achieve the desired balance and optimize the building's overall energy performance. It can, therefore, be estimated also during this exploration, that once the number of involved parameters and operational requirements is increased with the parallel increase of the user's demand for inner comfort, then the passive operation of the facade system can hardly remain a self-sufficient solution anymore and would probably require the aid of an additional active operation and control mechanism to maximize both the building's energy performance and the user's comfort.

6.7.3. CONCLUSIONS

The indirect analysis studies and comparative evaluations provided some insights on the environmental and energy performance of the proposed design. It can be concluded that during the cooling-dominated periods, the facade skin has a higher performance when functioning only as an exterior shading device and not a double facade, without interfering with the air inflow, but working as a separate exterior structure obstructing the incoming solar radiation. By doing so, the solar heat gains can be reduced and, consequently, the building's cooling demands, while a reduction of the natural ventilation in the building's interior throughout the day is also beneficial with a combination of a more scheduled night-time ventilation strategy.

Nevertheless, the shading impact of the proposed design does not outperform other commonly used typical exterior shading systems, but still performs almost equally well.

What makes the difference in the current design is the dynamic performance of the facade's passive mechanism that shifts to the multiple-cavity double facade during the winter and leads to additional benefits in the reduction of the heat losses through the building construction. However, solely in relation to the UHI effect, this is a secondary function that is not directly related to the phenomenon and mitigation method, since the reduction of the cooling loads has the main and more impactful role. It can be, therefore, said that the overall energy performance of the building can, on one hand, be improved by integrating such a passive adaptive facade system, when being evaluated through an annual operation basis. On the other hand, the environmental performance merely in relation to the reduction of the building's indirect UHI impact is not much different than by simply implementing standard exterior shading systems.
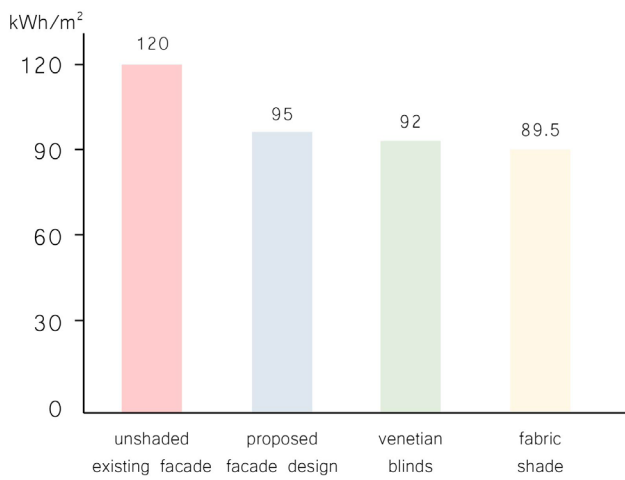
building's cooling loads per m² with different
exterior shading systems
(April-October)
[building's indirect impact mitigation method]

overall building's annual energy
performance improvement with the
proposed dynamic facade design

building's indirect UHI impact reduction
[building's annual environmental
performance improvement]
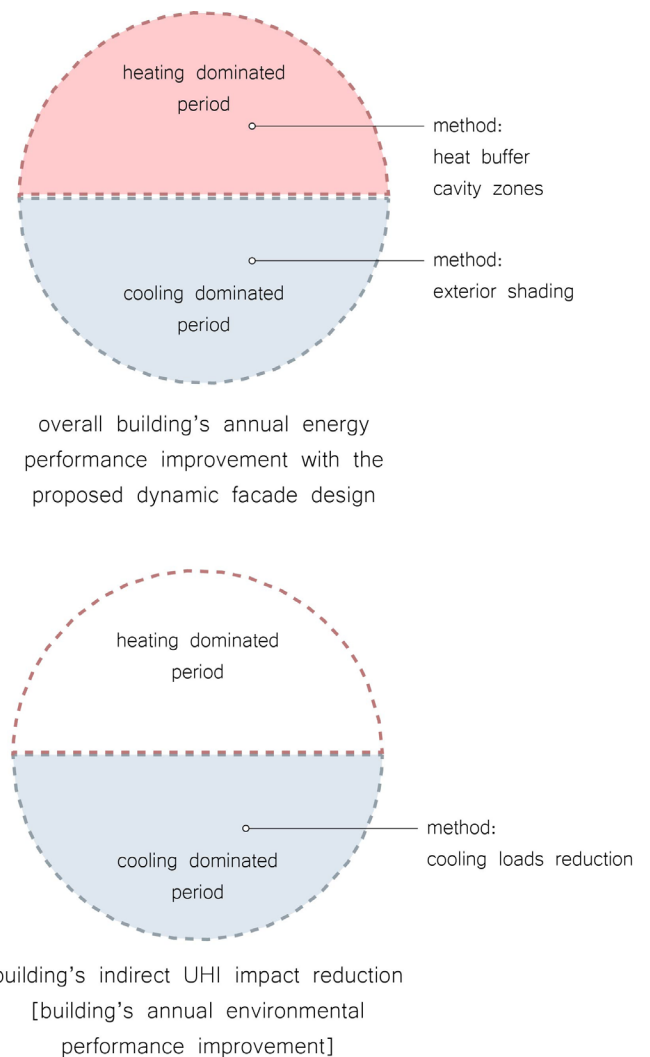
Figure 102: Charts summarizing the indirect impact evaluation conclusions. [own work]

FINAL DESIGN

The concept development of the final design is illustrated in Figure 103, where the main facade components and their function are explained. Briefly, the two SMAs are positioned on the bottom edges of the bottom pyramid and are connected to a pivot axle connected at the common edge of the top and bottom parts. The deformation of the SMAs initiates the rotation of the axle, which on its turn causes on one hand the rotation of the bottom pyramid and on the other hand the linear movement of the top part. At the same time, in the cavity, a series of lamellas act as a bias counterweight of the SMA forces and control the opening and closing of the cavity to shift from the summer to the winter situation. This is enabled by threads which connect the different moving components with the pivot axle. The rest of the geometry surfaces is covered with elastic textiles that can accommodate and adjust to these transformations and have different texture surfaces and properties based on their function, as it will be further explained in the next sections.
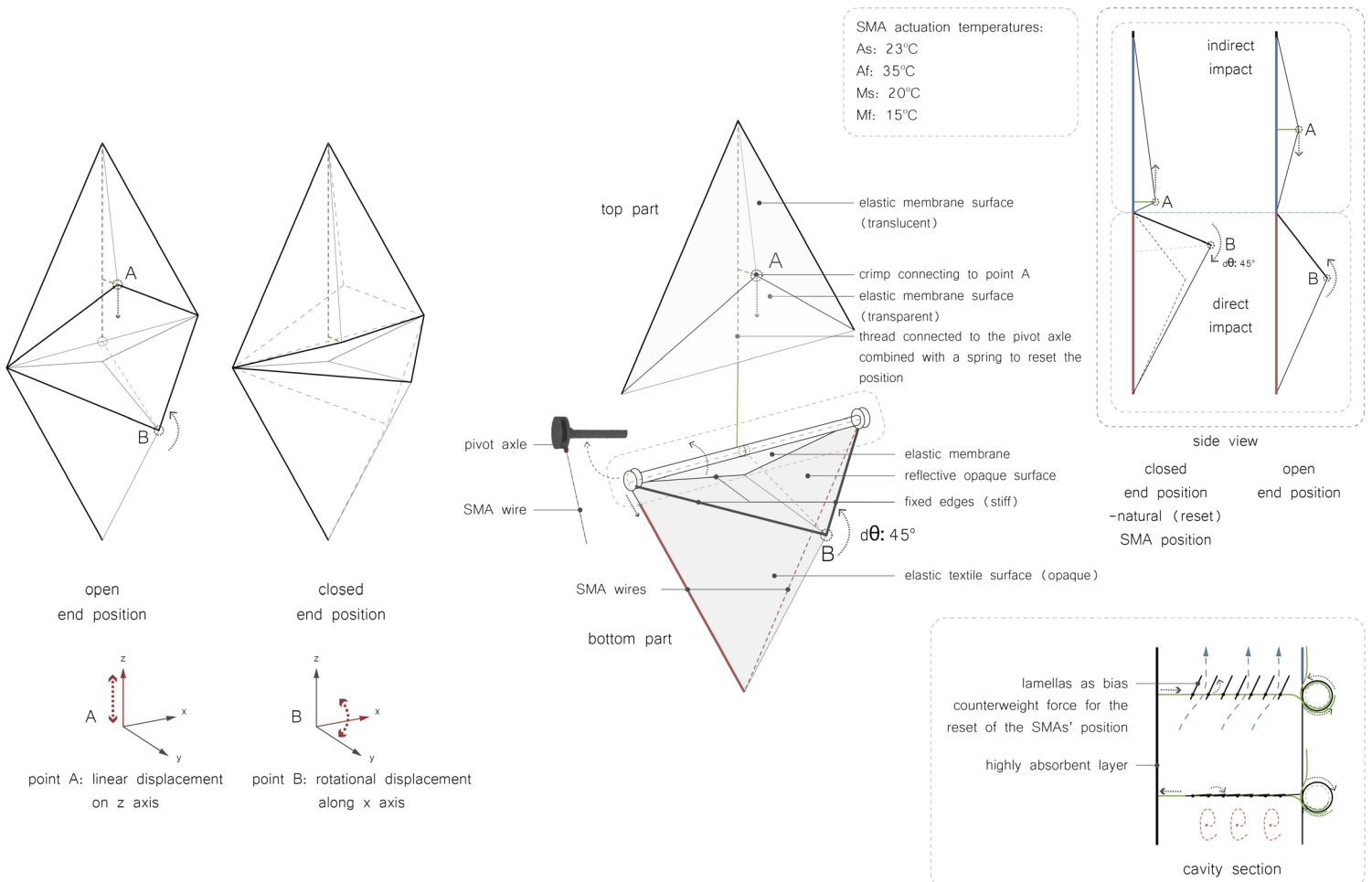
Figure 103: Conceptual sketches illustrating the SMA operating mechanism and components. [own work]

7.1. DESIGN PARAMETERS

7.1.1. FORCE BALANCE EQUATION

The operating mechanism is dependent on the properties and activity of a set of acting forces, which are constantly present during the dynamic operation and counteract each other to bring the entire system in balance throughout the different stages. An overview of the main forces in play is schematically illustrated in Figure 104. More specifically, these can be analyzed as the force caused by the SMA wire, the pivot axle, the threads and the self-weight of the top textile, which altogether act against the forces originating from the spring, the self-weight of the bottom textile and the lamellas in the cavity, as well as the friction.
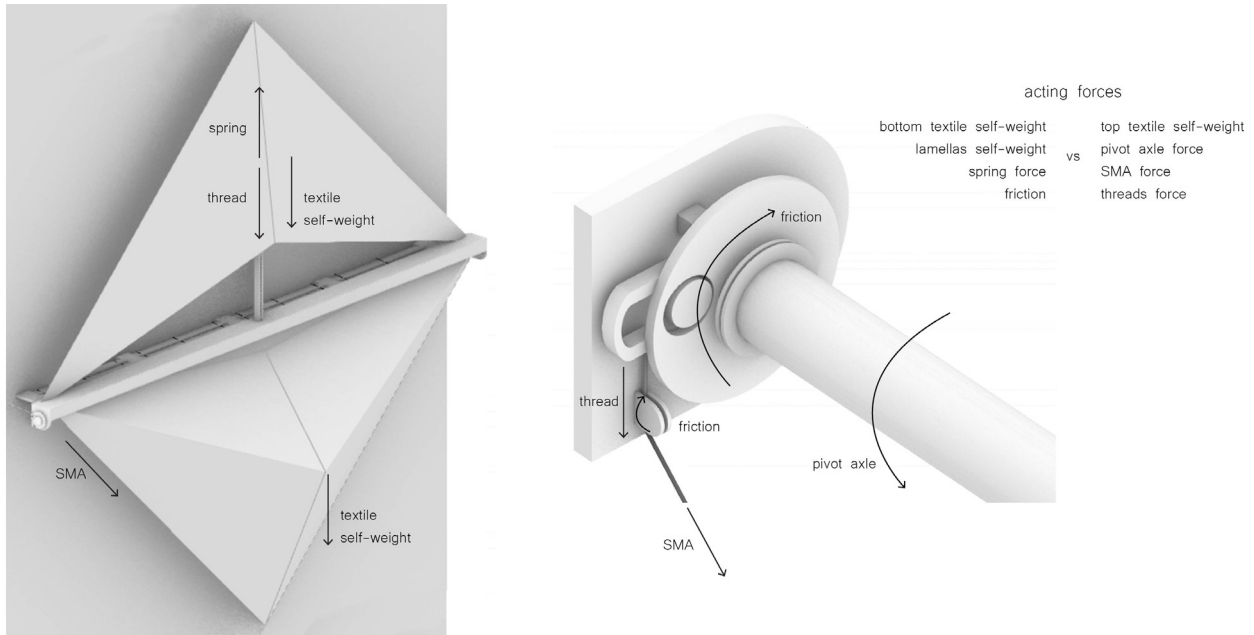
Figure 104: Schematic representation of the system's acting forces. [own work]

Three stages can be identified: the movement towards the summer situation, when the SMA wire's length is reduced, the stabilization at the end position and the stabilization during the winter situation, when the SMA has recovered its original length.

When the system is in equilibrium, the force balance equation can be described as follows:

spring self-weight + lamellas self-weight + textiles self-weight + threads self-weight = SMA pivot axle

Once the SMA is activated and starts deforming, the above equation is transformed accordingly:

SMA force + pivot axle + top textile self-weight + threads force > bottom textile self-weight + lamellas self-weight + spring force + friction

Finally, when the SMA's length is reduced, the equation takes the following form:

SMA force + pivot axle + top textile self-weight + threads force = bottom textile self-weight + lamellas self-weight + spring force + friction

The above variables involved in the force equilibrium are highly dependent on the actual material properties of each working component of the system. To proceed with this process and to accurately replace them with the actual values, the development of prototypes and testing is required. This is important to be able to calculate the required SMA wire needed, based on tensile stress and trial-and-error tests that would provide information about the strain and the strength of both the SMA and the counteracting bias springs, as well as the properties of the rest of the components. For the scope of the thesis and the available time and methods, the force balance equation remains, therefore, conceptual at this early design stage and can be subject for further research and development in the future.

7.1.2. SMA OPERATING MECHANISM

The SMA operating system consists of a pivot axle mechanism that is positioned around the common edge of the top and bottom facade components and works in combination with a Scotch Yoke mechanism on the side. In its principle, the latter is a mechanism for converting the linear motion of a slider into rotational motion or vice-versa. The piston or other reciprocating part is directly coupled to a sliding yoke with a slot that engages a pin on the rotating part. In this way, the SMA's linear deformation can be translated to the rotational movement of the pivot axle, while the SMA remains linear during the whole dynamic process, without compromising its durability through a bending movement. The axle is then connected to a series of threads, which depending on their attachment position to it, follow the same or opposite rotational movement, and thus resulting to a linear stretching or shrinking accordingly. Some of these threads are connected

horizontally to the lamellas of the cavity, which are the counterweight forces and are responsible for the opening or closure of the cavity zones. Apart from these, in the middle of the axle, a thread is connected vertically to enable the vertical linear movement of the top textile and is connected to a bias spring that helps recover the original position.

The whole operating system works, therefore, in an internal group of cause-effect forces that are interdependent and related to each to other, where the SMA is the principal source of force that initiates the series of movements and deformations in a completely mechanical and passive manner. This process is realized without any additional external force to cause its activation and by minimizing non-essential mechanical or structural parts. The main components of this system and their function are shown in Figure 105.

Scotch Yoke pivot mechanism
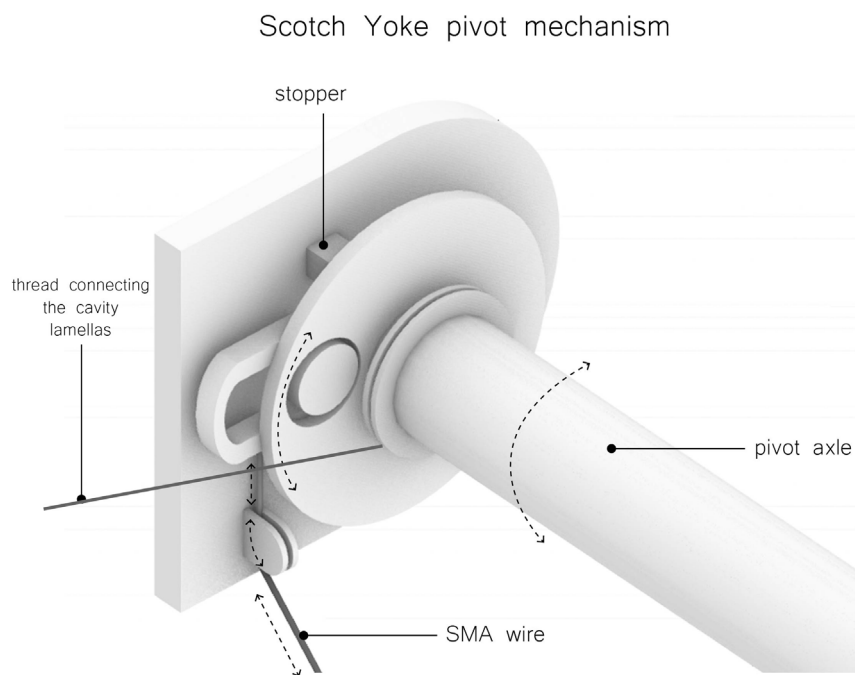
Figure 105: Pivot mechanism components. [own work]

Equally important was the placement of the SMA wire in relation to the rotating mechanism, because the angular stroke is highly dependent on the distance between the SMA attachment and pivot point. The diagrams below [Figure 106] show a couple of alternative explorations on this regard. From the sun ray trace analysis studies, it was estimated that at least a 45° stroke should be achieved to ensure that the top pyramid will have a top surface perpendicular in relation to the seasonal sun's horizontal position, but a slightly larger one with a tolerance of 5°–10° may also have the same effect and allow for some discrepancies in the movement. However, this should not exceed the limit, because a smaller distance between attachment and pivot would mean that more force is needed to apply the same moment to the rotation, so in the end, there is a trade-off between force needed and angular stroke. For these reasons, Option 2 was chosen for the positioning of the SMA wire that would achieve about 50°–55° angular stroke with a 3% strain.

In practice, however, these explorations would need the help of a prototype to examine the different positions and validate the results, in relation to the SMA's behaviour and rotational movement. In this respect, it would have been important to control whether during the SMA wire's austenite transition, when the length becomes smaller, the movement results to the assumed rotation or causes a deformation of the threads involved instead. Because of this possibility, it is important to consider that there is enough stiffness in the different components to keep them in the desired positions at all intermediate and end stages.

Shorter SMA length in austenite form: 484mm
Longer SMA length in martensite form: 500mm
Strain: 3.2%
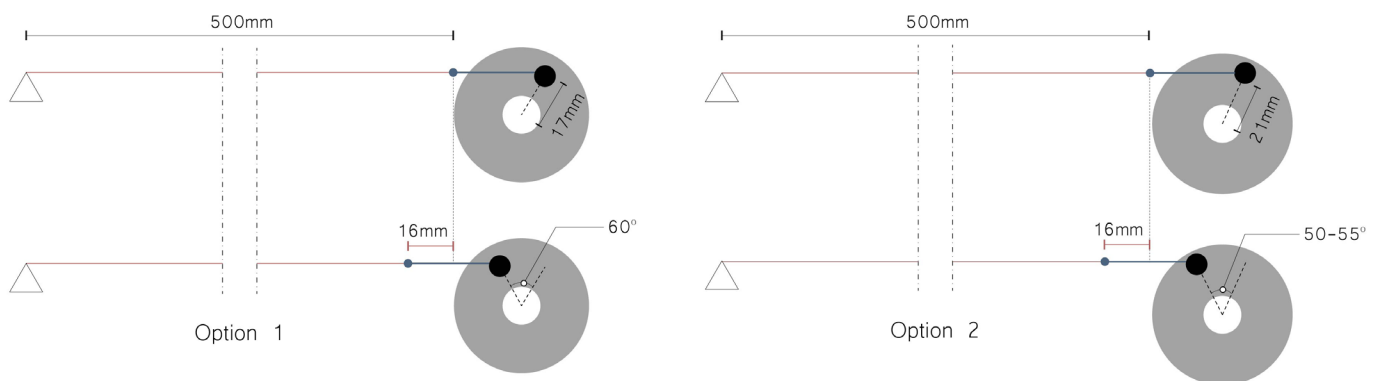
Figure 106: Diagram showing the relation between the angular stroke and the distance between the SMA attachment and pivot point. [own work]

7.1.3. MATERIALS & PROPERTIES

The materials that have the main impact on the performance of the facade component are namely the SMA wires and the membranes used, the properties of the first one affecting significantly the dynamic and seasonal movement of the system, while the latter ones are related mostly to the energy and environmental performance of the facade skin. There is also here an interdependency between the materials, since the deformations caused by the SMA force would rely on a certain degree of flexibility and elasticity of the membranes and other smaller components (e.g. threads) to accommodate the constant tensile stresses and operation cycles.

SMA wire

Apart from the general guideline of allowable strain within 3-5% of the original length, the rest of the properties highly rely on the manufacturer and the actuation process to set the required force that will cause the stress and strain at the desired martensite and austenite temperatures. These properties can be defined through prototyping and tensile stress tests, that will also determine the required force of the bias spring, the self-weight of the lamellas and the rest of the counterweight forces.

In the current thesis, this aspect could not be explored due to time and accessibility constraints and thus the only variable that could be estimated at this early design stage was the required wire strain to achieve the desired angular stroke within the strain limits as a rule-of-thumb. Based on the explorations on the placement of the wire on the pivot mechanism, the original length of the wire was then set to be 500mm and to undergo approximately 3% strain. It was preferred to keep the strain at its low limit, to avoid a larger wire diameter and to ensure a longer durability.

Membrane materiality

The decision for the material to be used as the membrane of the top and bottom parts was mainly guided by the need for elasticity and tensile strength, due to the continuous deformations and dynamic changes, but also the need for a lightweight structure to reduce the force needed by the SMA wire for its actuation. Apart from that, the rest of the required properties were related to the energy and environmental performance regarding both the direct and indirect UHI impact, which concerned

a high solar reflectivity and a low Solar Heat Gain Coefficient (SHGC). Additionally, the top part had also the requirement for a certain degree of solar control, since it was conceived to be translucent to evenly disperse the sunlight to the interior working spaces, with a combination of a transparent membrane surface to allow some clear views when no sun-shading is required.

Because of these requirements, the material choice was directed towards ETFE foils and PTFE/PVC opaque membranes and a study was realized on different material types, coatings, possibilities for fritted patterns and perforated meshes [Mainini et al., 2014, Cremers et al., 2019]. An overview of the Ethylen-Tetrafluorethylene (ETFE) visual and thermal properties can be seen in Table 35. In relation to the allowed air through the facade skin, an alternation between open and closed vents at the top and bottom membranes was explored, which was informed by the stretching and relaxing of the meshes that would have a positive effect on the interior during the summer and winter situation. The top part features an additional transparent ETFE layer that remains folded during the summer scenario and is stretched during the winter to allow for direct sunlight, but at the same time not allow air inflow through the cavity. A conceptual intention was also to have a double-sided textile on the top surface of the bottom pyramid, which would be facing a reflective light-coloured side during the summer and when stretched during the winter, it would switch to an absorbent dark-coloured one.

Lastly, a highly absorbent coating would be placed on the outermost surface of the insulation on the opaque areas of the existing building's inner facade, which would intensify the heating effect during the winter.
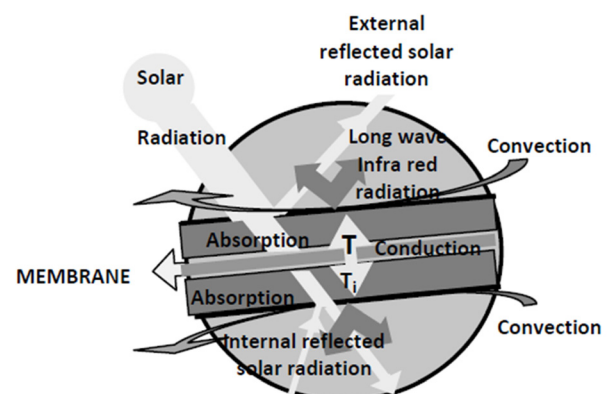
Figure 107: Diagram showing the heat transfer model of the thermal behaviour of membranes. [Harvie, 1995]

To elaborate further on the membrane properties, a study and distinction was further realized on different types and material options, regarding the opaque, translucent and transparent parts of the design, with a focus on the optical and thermal properties. This study is analyzed below.

Optical properties

The thermal optical properties of the material describe its radiant behaviour within the thermal spectrum. Compared to other commonly used structural materials in the building industry, membranes can exhibit a wide range of transparency levels. The transmittance of coated woven fabric membranes typically ranges between 0-25%, although the exact values depend on the specific material used, the angle of incidence and the radiation wavelength. In this way, the penetration of solar radiation is allowed to a certain extent, with the rest of the amount being absorbed or reflected back [Wu, 1984].

Even though fabric membranes can be translucent, their optical properties are quite different from the ones of glass, with the effect of solar reflectance being higher in fabric membranes, allowing daytime lighting to be reduced. More specifically, some membrane materials, such as Teflon coated fiberglass, can reach a reflectivity of around 70%. This is helpful especially in warm climates, since it can help reduce the heat within the enclosure due to insolation and at the same time discharge the heat at night and by doing so, reduce the air conditioning load.

The graph in Figure 108 shows the solar optical properties of some membrane materials, also in comparison to typical glass products, based on sample measurements by Harvie [Harvie, 1995].

Thermal properties

Due to the large surface area of the membranes compared to their thickness, they are characterized by a relatively low thermal mass. They have, therefore, a high U-value, while their thermal behaviour is mostly derived from the convection heat transfer on their surface and their optical absorptance. Because of that, they are applied mostly as exterior shading screens,

direct wind and rain protection and visual barrier. At the same time, the amount of the heat conduction through the fabric is highly dependent on the air temperatures, the wind speed, U-value, the thickness and layers of the membrane. The heat transfer is then influenced by the solar transmission and absorption, emissivity in relation to long wave radiation and the light transmission [Wu, 1984]. Figure 107 shows diagrammatically the heat transfer model of the thermal behaviour of membranes.

Opaque textile membranes

There have been developed different materials and combinations for the available textile membrane composites. Architectural fabrics are often woven from Polyester (PES) coated with Polyvinylchloride (PVC) or from glass fiber coated with either Polytetrafluorethylene (PTFE) or silicone. The coating allows the protection of the fibers from environmental influences, but also a better seamed welding between the individual membranes. Those membrane types can either have a full-face coating, with transucency factors between 0-40% depending on the material composition, or the textile membrane can be woven with gaps between the yarns forming an open mesh membrane with a local coating only of the yarns. Table 35 gives an overview of available textile membranes used in architectural applications [Paech, 2016].

Translucent and transparent foils

Regarding the foils, the ETFE are the ones more broadly used in architectural applications. They are thin films with transparency up to 96%, with, however, a reduced strength compared to the textile membranes. They can also have printing or tinting in different patterns and coatings to either improve the durability of the material or filter out certain wavelengths of the sun to avoid overheating of the interior conditions. As for the other optical properties, a single layer of medium weight ETFE has an approximate 85% light transmission and can also absorb a large proportion of infrared light transmitted, which can be exploited to improve the building's energy consumption [Paech, 2016]. An overview of the optical properties of different ETFE options is shown in Table 36.
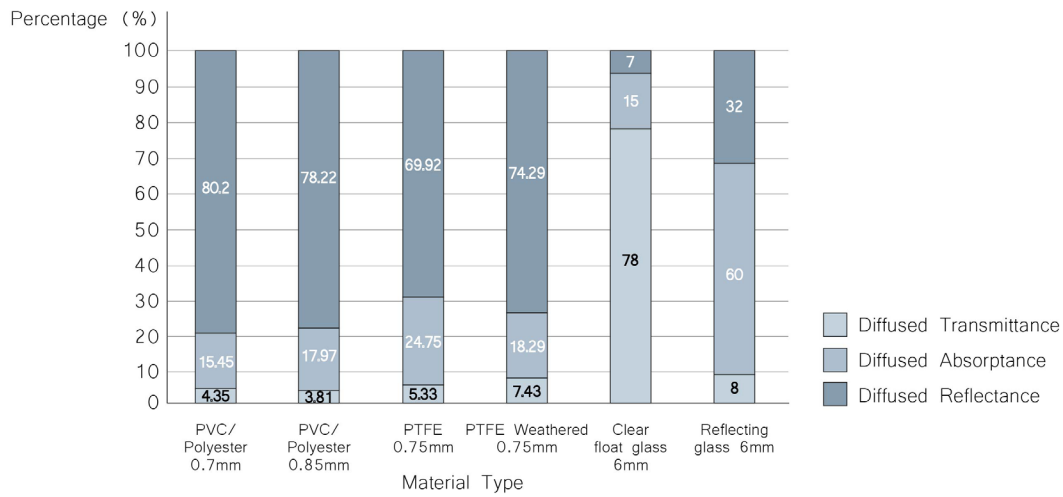
Figure 108: Graph showing the comparison of solar optical properties of membrane samples and typical glass products. [adapted from Harvie, 1995]

Table 35: Characteristics of common textile membranes. [Paech, 2016]

Category	Composition	Characteristics	UV Resistance	Expected Lifetime	Translucency [%]
Closed mesh with full-faced coating	PES cloth with PVC coating	Versatile applicable standard material	+	~20 years	0-25
Closed mesh with full-faced coating	Glass cloth with PTFE coating	High quality standard material	++	>25 years	4-25
Closed mesh with full-faced coating	Glass cloth with silicon coating	Soiling behaviour in exterior application could be improved	+	>20 years	10-20
Closed mesh with full-faced coating	PTFE cloth with PTFE coating	Very high quality material with excellent foldability characteristics, durability and soiling behaviour	++	>30 years	20-40
Open mesh, coated yarns	PES mesh cloth with PVC coating	Different mesh sizes available, standard material	+	~20 years	Up to 90%
Open mesh, coated yarns	Glass mesh cloth with PTFE coating	Different mesh sizes available, high quality standard material	++	>20 years	Up to 90%
Laminated open mesh	Glass mesh PTFE coated laminated with Fluopolymer-film	Few mesh sizes available, custom-made material	++	~20 years	Up to 70%
Closed mesh without coating	PTFE cloth uncoated	Very good durability and foldability for retractable structures, custom-made	++	>30 years	Up to 40%

Table 36: Overview of the ETFE foil types with their visual and thermal properties. [own work]

Textile type	Solar transmittance	Solar reflectance	Visual transmittance	Visual reflectance	UV-transmittance	UV-reflectance	Thermal emissivity	Solar Heat Gain coefficient	Thermal transmittance coefficient [W/m^{2}K]
Clear single-layer ETFE	0.93	0.06	0.92	0.07	0.85	0.12	0.83	0.93	6.9
ETFE silver printing 65%	0.57	0.30	0.57	0.30	0.52	0.34	0.61	n/a	n/a
Nowoflon Z-IR	0.50	0.05	0.60	0.05	0.39	0.08	0.88	n/a	n/a
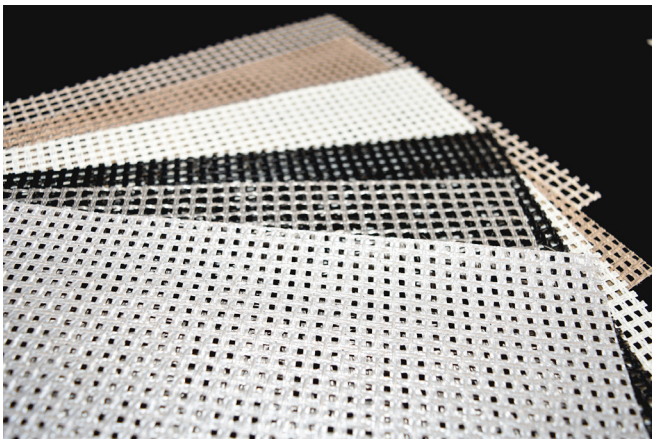
Figure 109: PTFE coated fiberglass ventilated open mesh sample. [source: PTFE Fiberglass. (2021, April 02). Retrieved from https://www.structurflex.com/materials/ptfe-fiberglass/]

Figure 110: PTFE shading panels at the Hazza Bin Zayed Stadium. [source: Hazza Bin Zayed Stadium: MakMax Group (Taiyo Kogyo): Tensile Membrane Structures. (2020, September 06). Retrieved from https://www.makmax.com/de/applications/sports-de/hazza-bin-zayed-stadium-de/]

Figure 111: ETFE Facade at the Unilever Building in Hamburg. [source: ETFE facade Unilever building, Hamburg. (n.d.). Retrieved from https://www.tensinet.com/index.php/about/members-of-tensinet?view=project&id=4456]
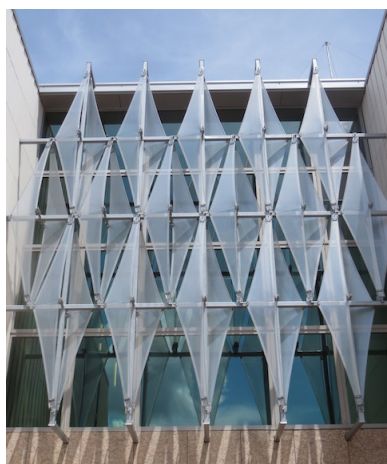
Figure 112: ETFE Entrance canopies at the US Embassy in Laos office building. [source: US EMBASSY IN LAOS OFFICE BUILDING AND ENTRANCE CANOPIES. (2018, May 18). Retrieved from https://www.structurflex.com/projects/us-embassy-laos/]

Figures 113 and 114: Fritted ETFE examples. [source: What is ETFE? - Fabritecture, Experts in ETFE Projects. (2019, October 29). Retrieved from https://fabritecture.com/knowledge/etfe/]

Based on the above material exploration, for the needs, optical and thermal requirements of the current facade design, each material type was chosen to address the specific performance requirements for the purpose of its design and function of the shading system. Therefore, each decision in the material selection was informed also in this case by the material research and is performance-driven, in parallel to the geometry design goals and requirements.

More specificaly, a PTFE coated fiberglass ventilated open mesh was chosen for the bottom part of the facade component, which would display <10% transmittance, about 70-75% reflectivity and would enable certain ventilation through the open mesh during the summer. The top concave surfaces of the bottom pyramid would be composed of a light-coloured PTFE single-layer opaque membrane, to reflect the incident solar radiation, complimenting, in this way, the geometry concept of sun rays' reflection.

As for the top parts, a combination of translucent and transparent ETFE foils would be more suitable, the first one acting as a sun-shading layer, evenly dispersing the sunlight to the interior, while the second one enabling more clear views and a higher solar admittance during winter, trapping at the same time the heat inside the cavity. A fritted pattern was not chosen as an option, because, even though it would reduce heat gains, it would also result to a certain deformation of the pattern when the foil would be stretched, causing visual disturbances. Additionally, in relation to its function, the bottom pyramid is the main shading component, which, thanks to its depth, obstructs the direct sunlight from the sides and the top. Nevertheless, these types of foil cannot eliminate glare. This aspect would then have to be addressed with additional internal shading units, if required, to reduce the impact from possible low-angle sun rays that would inevitably enter the interior.

ETFE single-layer translucent membrane: sun-shading, evenly dispersing sunlight

ETFE single-layer transparent membrane: clear view, solar admittance during winter

light-colored PTFE single-layer opaque membrane: reflection of incident solar radiation

PTFE coated fiberglass ventilated open mesh: open vents during summer when stretched - closed vents during winter

Figure 115: Diagram illustrating the performance-driven material selection, where each decision is informed by the purpose of the membrane material based on the specific performance requirements. [own work]

7.2. FACADE COMPONENT & STRUCTURE

Figures 116, 117 and 118 illustrate the main components of the facade system, its main structure and the differences in the function between summer and winter. The facade skin component is part of an exterior diagrid structure consisted of steel cables that are connected to the diagrid nodes, on which the pivot axles are fixed on two sides as well. The steel cables also consist the substructure of the membranes, accommodating the clipping profiles on each edge. At the bottom face of the diagrid node, the bias spring is fixed, which is then connected to the steel thread and a bullet terminal connector that is attached to the textile's end node. Along the pivot axle is a series of additional rings which are attached to steel threads. These are connected to the lamellas and are deforming linearly according to the rotational movement of the axle. As also explained in the previous section, to enable solar admittance, but avoid incoming air during the winter situation, the top membrane is a combination of a tranluscent and a deployable transparent part, which is in its folded position during summer.

diagrid substructure node

steel cable

ETFE single-layer translucent membrane

Keder rail

ETFE single-layer transparent membrane

PTFE coated fiberglass ventilated open mesh

bias spring

bulllet terminal connector attached to textile

steel thread

thread fixed on the cavity lamellas
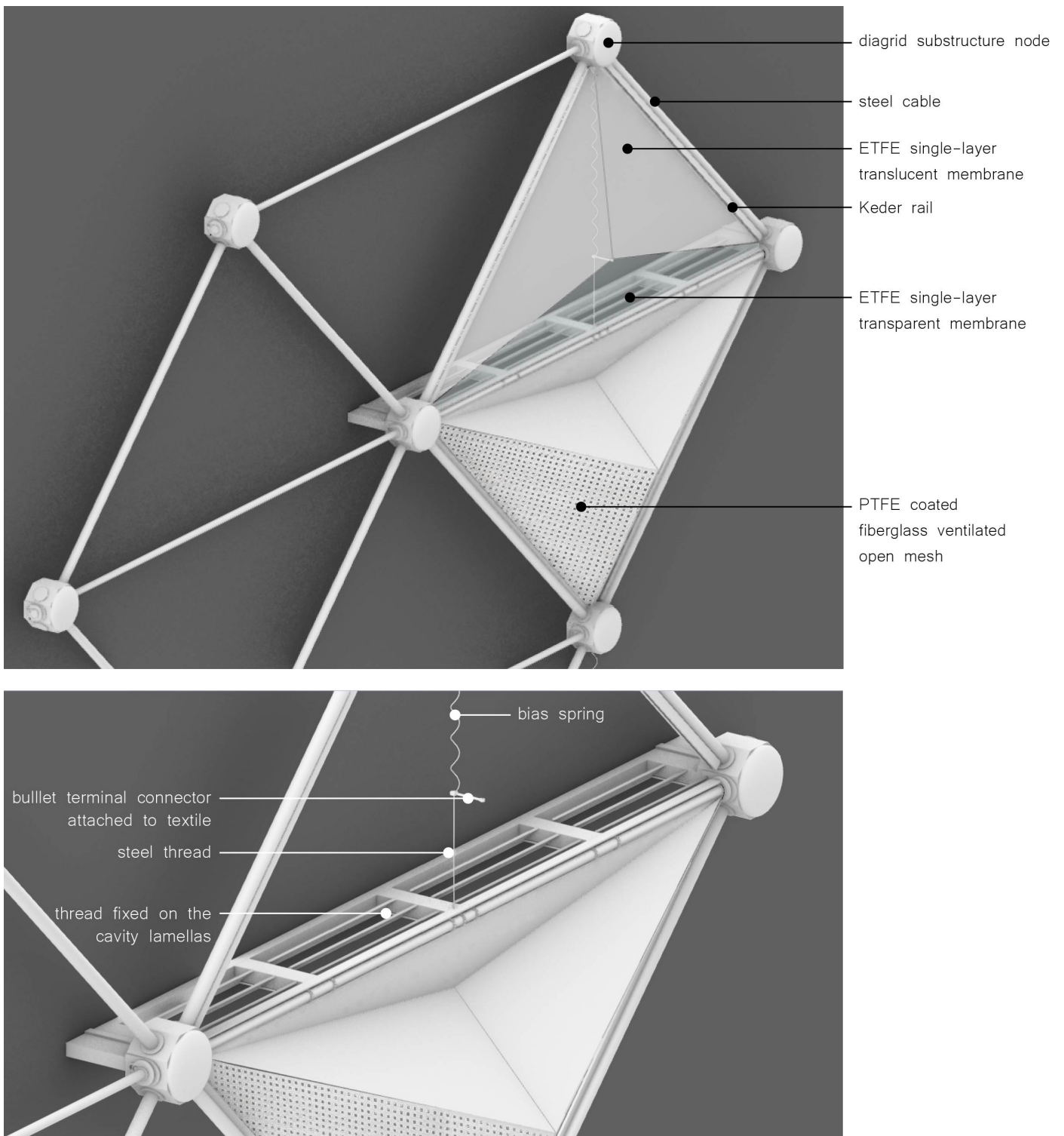
Figure 116: Close-up views of the facade component and its structure. [own work]

summer situation

ETFE single-layer
translucent membrane

PTFE coated fiberglass
ventilated open mesh
（stretched）

winter situation

deployable ETFE
single-layer
transparent
membrane

PTFE coated fiberglass
ventilated open mesh
（closed vents）

top mechanism zoom-in

lamellas in
open position

top mechanism zoom-in

bias spring

bullet terminal
connector attached
to textile

steel
thread
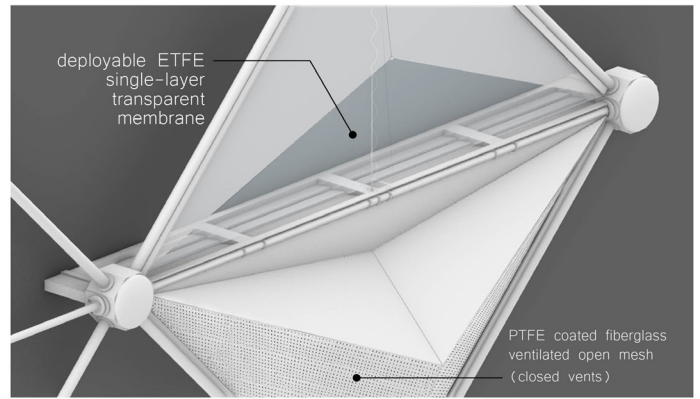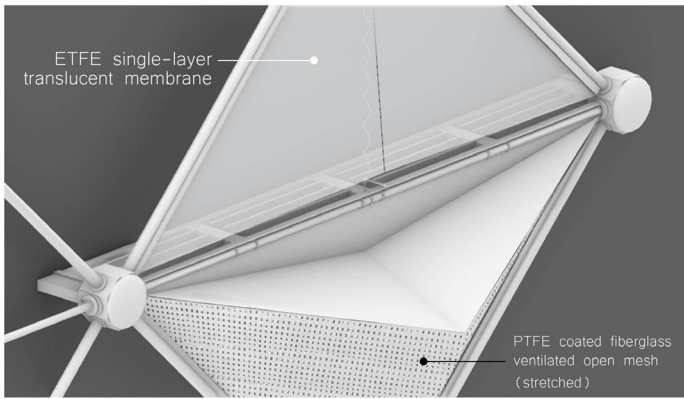
lamellas
in closed
position
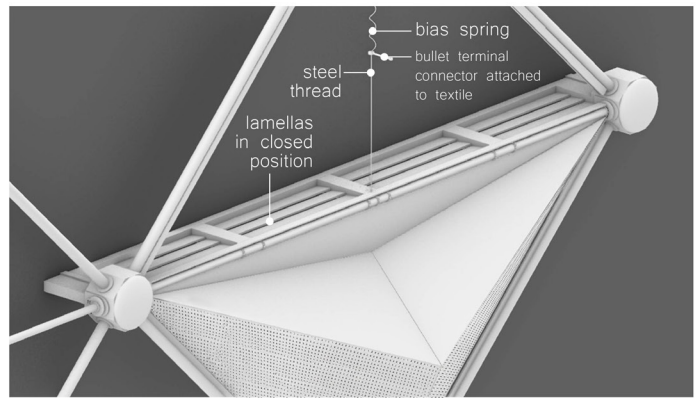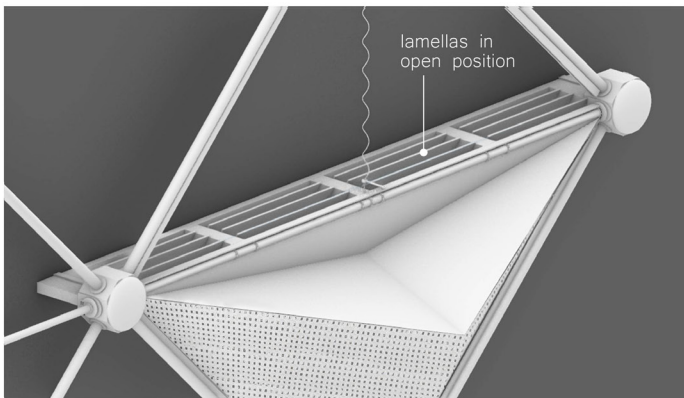
Figure 117: Close-up views of the facade component and mechanism towards the summer and the winter situation. [own work]

steel cable

Keder rail
ETFE clipping profile

pivot axle

diagrid node

SMA wire

Scotch Yoke rotating
mechanism

SMA wire

bias spring
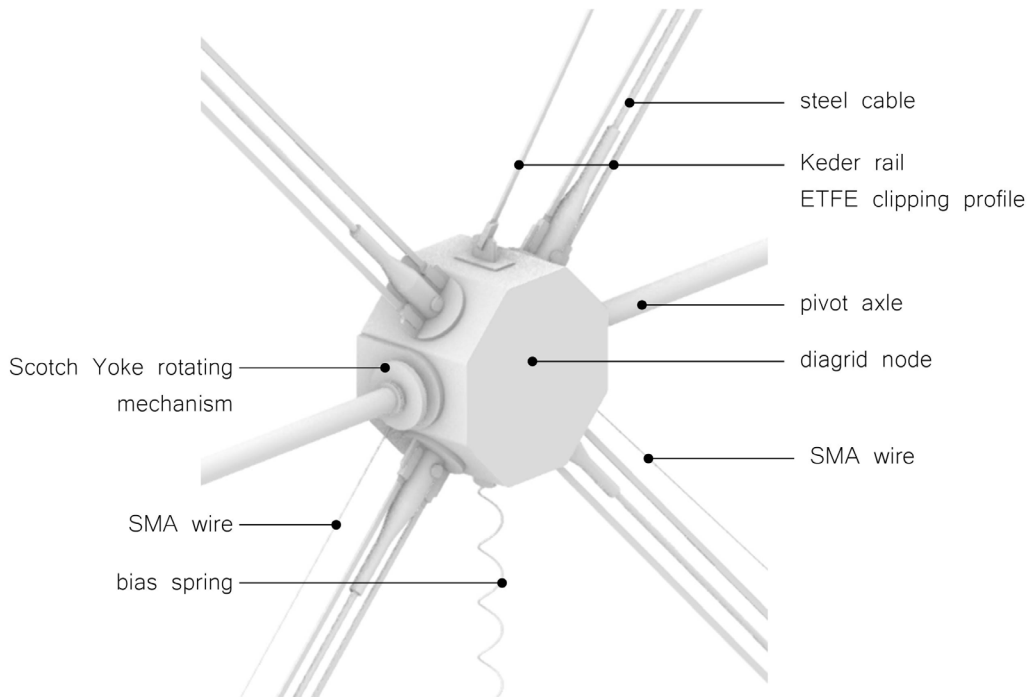
Figure 118: Close-up axonometric view of the facade component's diagrid node and connecting components. [own work]

vertical substructure
horizontal anchoring

cavity steel frame &
rotating lamellas

diagrid structure &
connecting components

ETFE single-layer
membranes

PTFE single-layer
opaque membrane

PTFE coated
fiberglass ventilated
open mesh
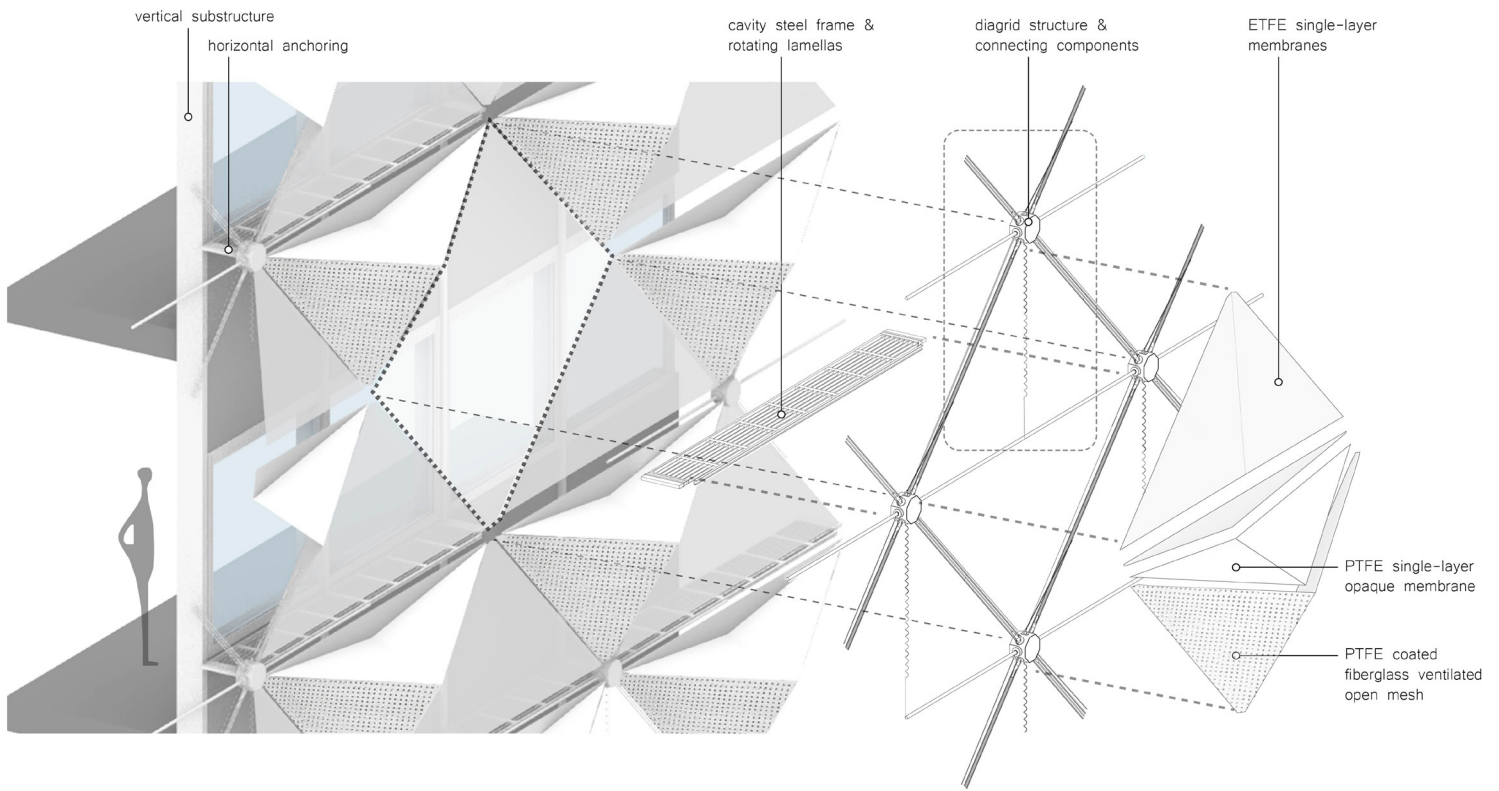
Figure 119: Exploded axonometric view of the main structure and components of the facade system. [own work]

Keder rail   clipping profile   steel cable

PTFE coated
fiberglass ventilated
open mesh

ETFE single-layer
translucent
membrane

ETFE single-layer
transparent
membrane

pivot axle
attachment rings

pivot disk & yoke
mechanism

diagrid node

SMA wire

fixing profiles

bias spring

bullet terminal
connectors

steel thread
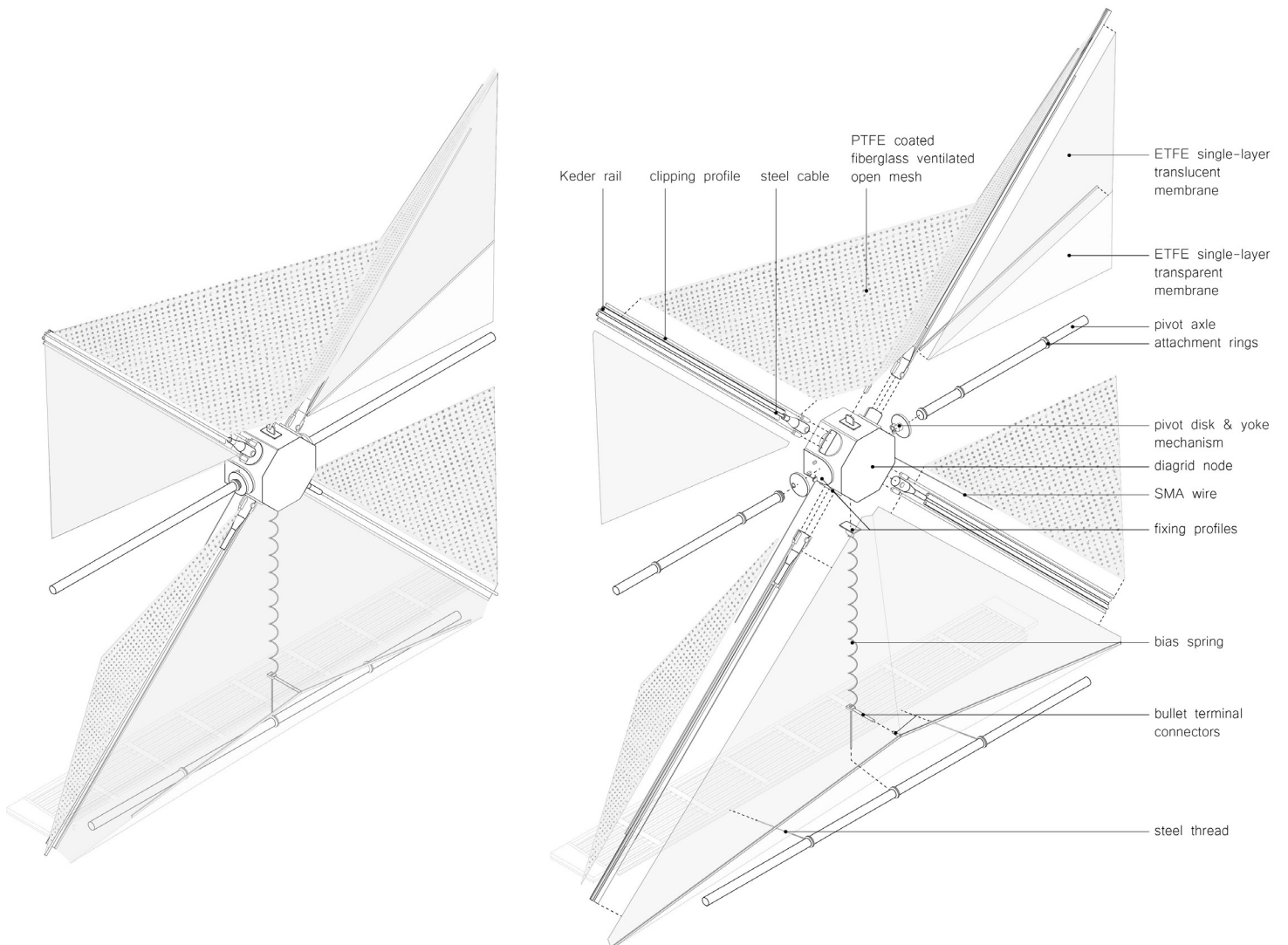
Figure 120: Exploded axonometric view, showing the assembly between the components of the facade system at the area of the connecting node [zoom-in area from Figure 119]. [own work]

7.3. DETAILS

Some additional details and drawings can be found in this section.

100mm 100mm 400mm

fixing steel plate

channel steel frame

horizontal steel support T profile

end side profile

pivot axle

Keder rail

steel lamellas profiles

steel thread

rotation axis

vertical steel supporting substructure

clipping profile

PTFE coated fiberglass ventilated open mesh

closed cavity

open cavity
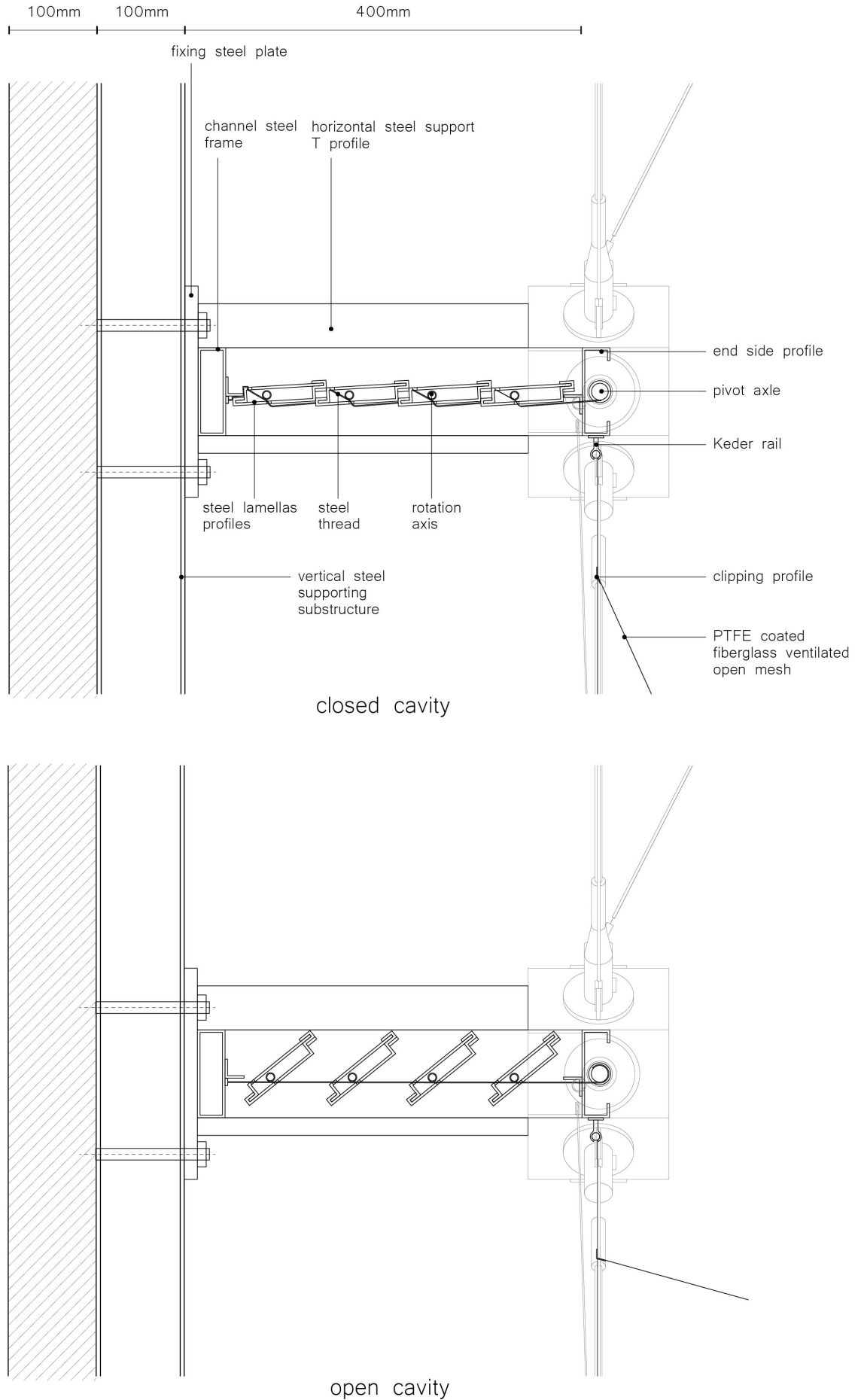
Figure 121: Vertical section details of the cavity area during the winter [top] and summer situation [bottom]. [own work]

side profile

stopper

pivot base

pivot disk

pivot axle

rotating
pin

sliding yoke
with slot

steel thread

SMA wire

steel thread connecting the
cavity lamellas

start position （summer situation）

end position （winter situation）
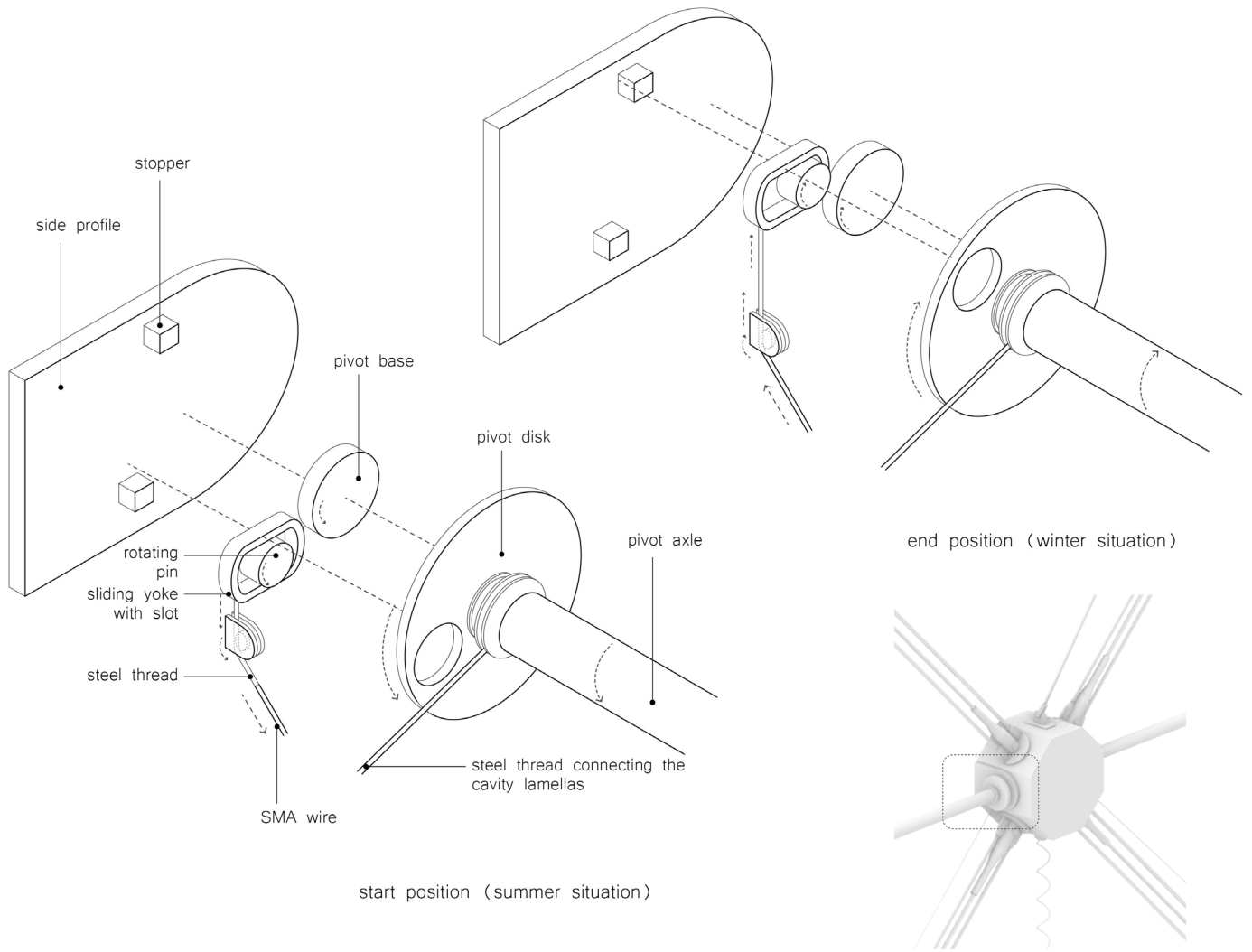
Figure 122: Exploded drawings of the pivot mechanism at the end positions. [own work]
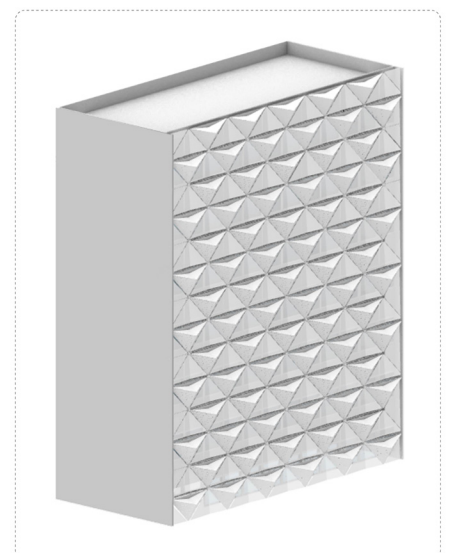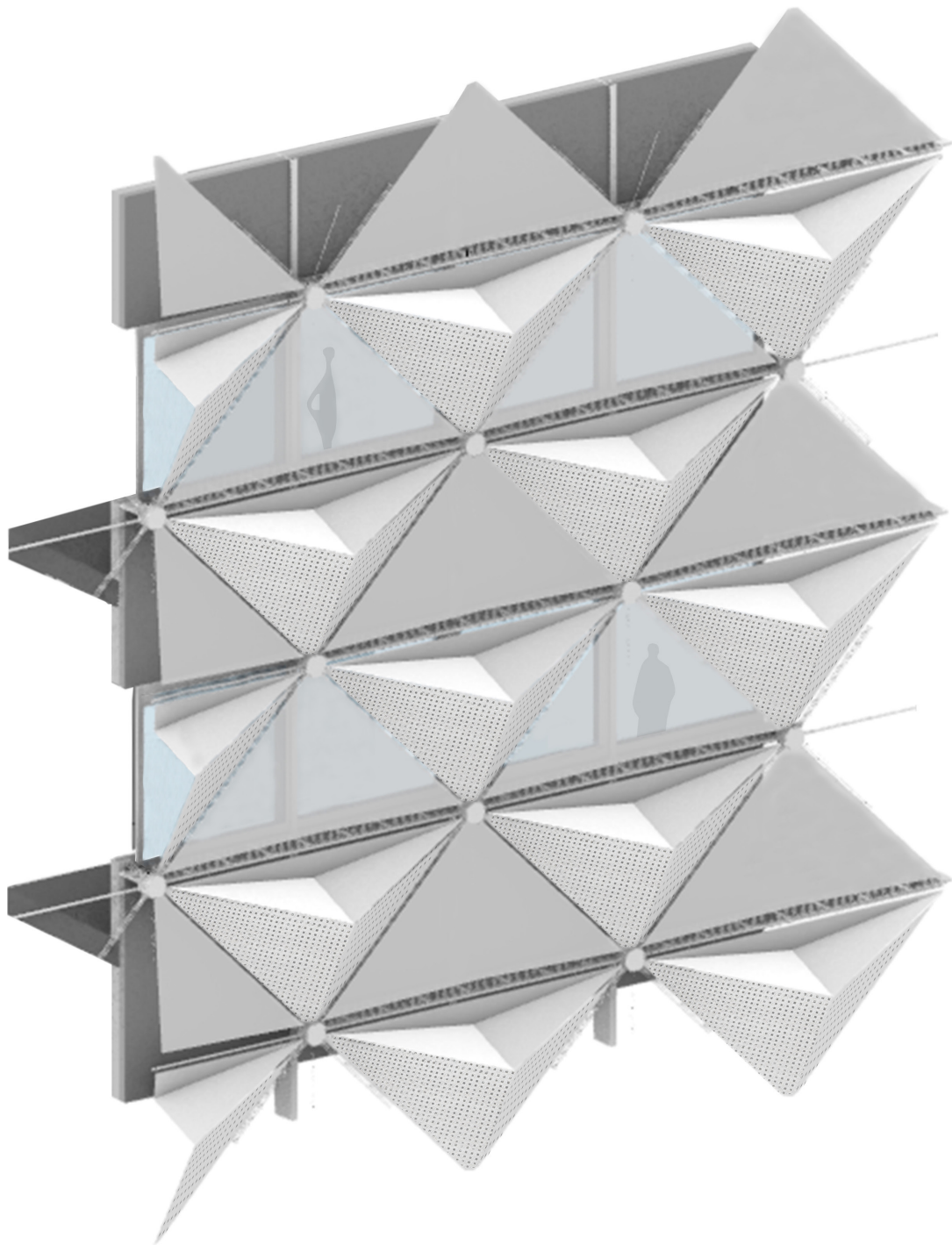
Figure 123: Axonometric view of a facade segment during the summer situation. [own work]
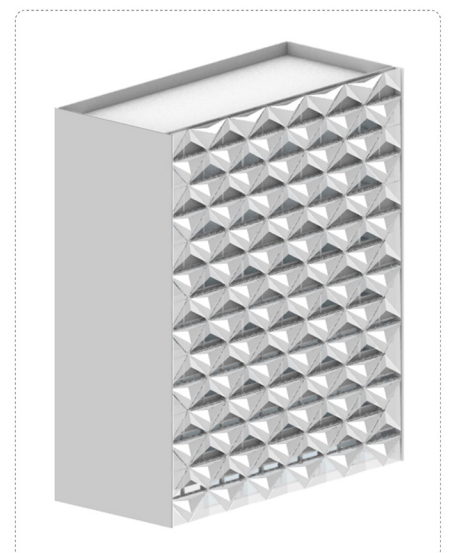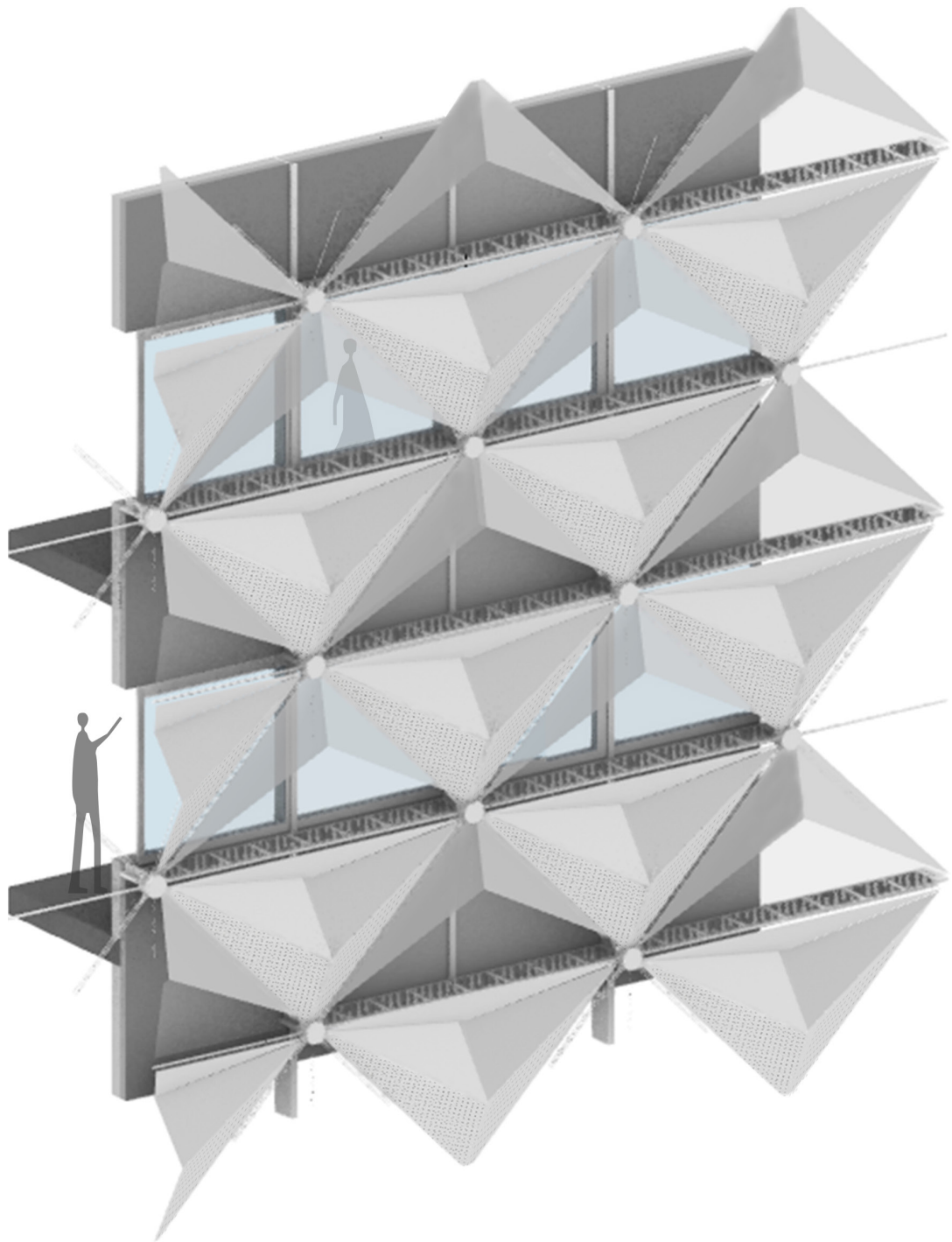
Figure 124: Axonometric view of a facade segment during the winter situation. [own work]
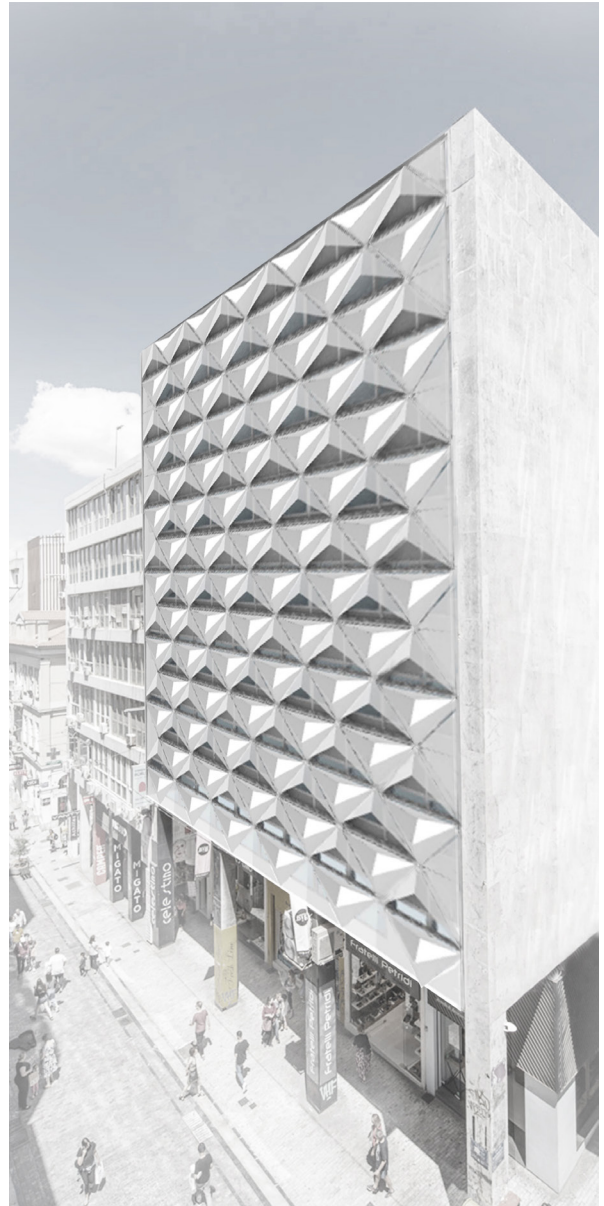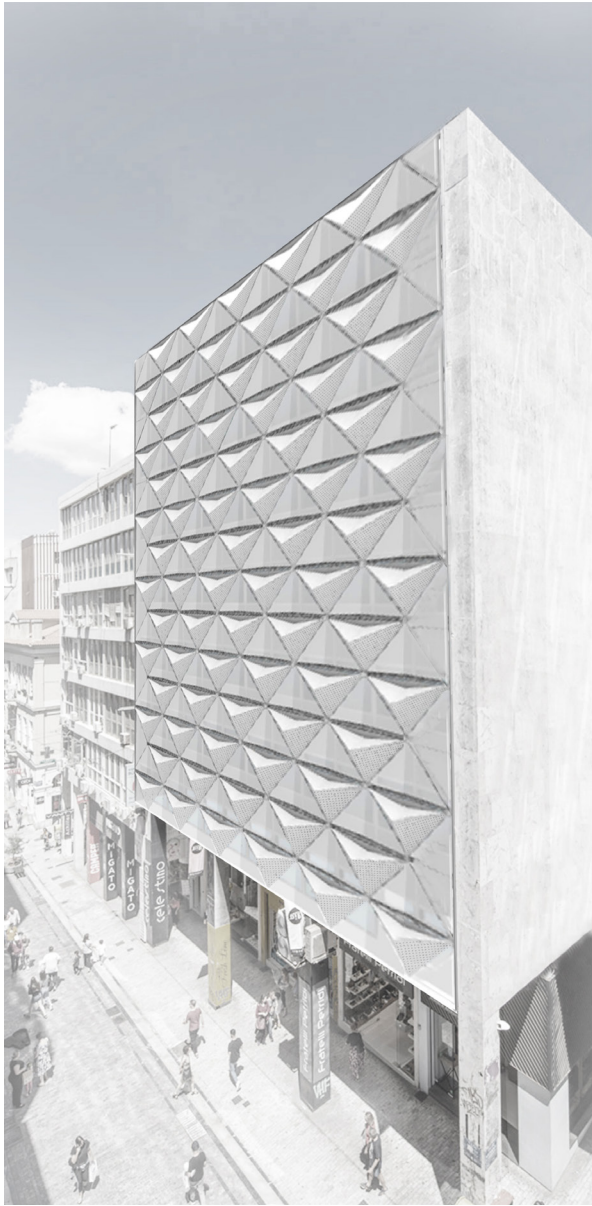
Figure 125: Visualizations of the facade retrofit in the Athens urban context during the summer (left) and winter (right) situation. [own work]
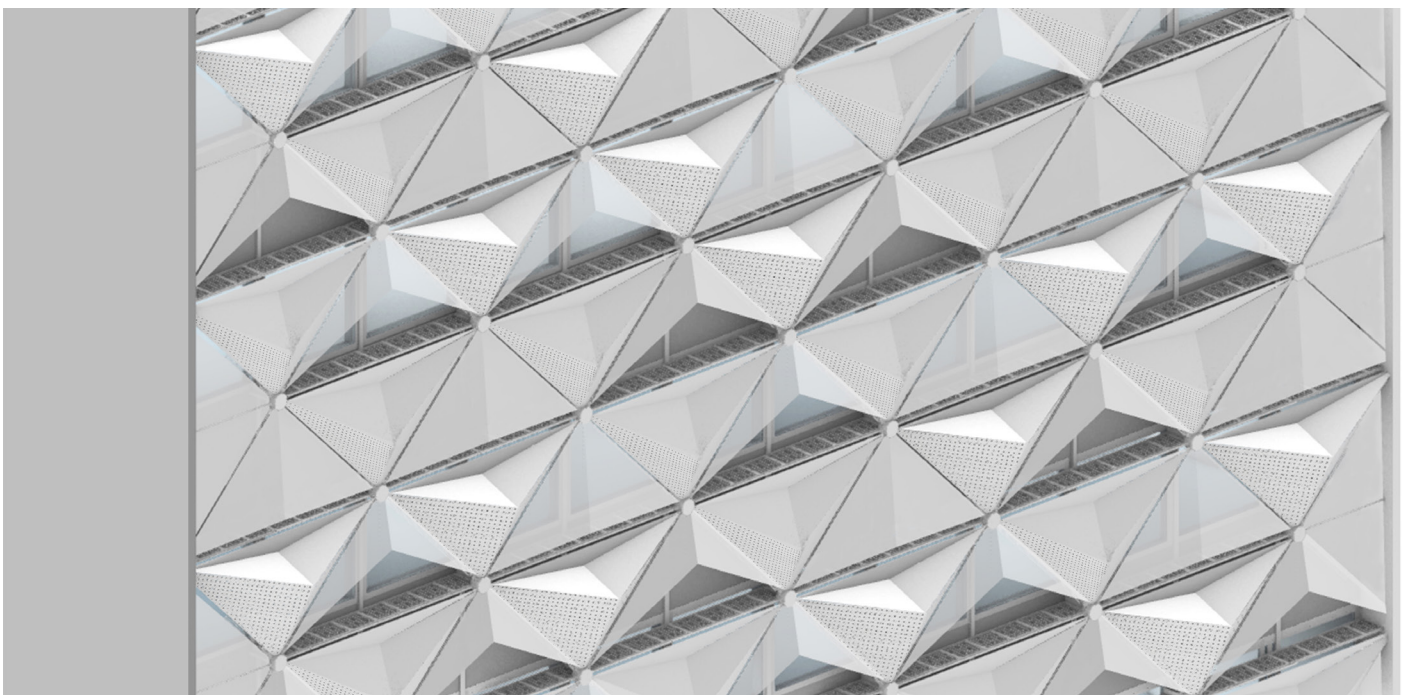
Figure 126: Close-up visualization of the facade skin with some closed and open shading components in a system's override scenario. [own work]
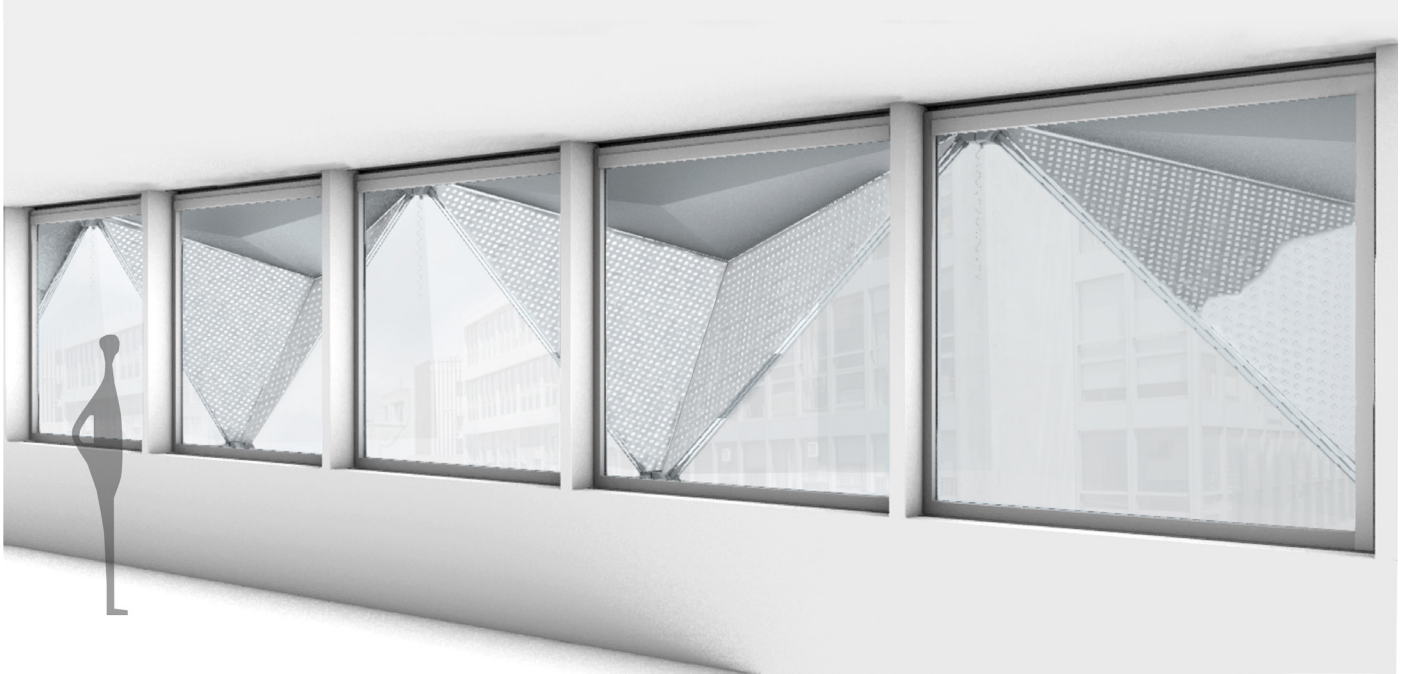
Figure 127: Visualization showing the facade skin as seen from the interior of the building. [own work]

08   EVALUATION & DISCUSSION:
POTENTIAL FOR FACADE INTEGRATION

As a conclusion from the research process and assessment methodology, it can be argued that the evaluation of the proposed facade system in the end depends to an extent on the comparison benchmarks and the perspective of evaluation. As seen during the initial stages of the research layout, since UHI concerns a multi-layered environmental issue, the evaluation also lies on multiple levels. Some of these observations can be summarized below and illustrated in the diagrams in Figure 128:

– If the system is evaluated as a stand-alone solution and only compared to the existing building situation before the retrofit, then the impact on the UHI effect is significant, more visible on the indirect one, but also contributing positively to the direct one.

– If the comparison lies only on the direct impact, it has a better effect compared to both the existing facade and other shading devices, since the judgement lies on the materiality and reflectivity degree of the building's geometry. In this case, however, it is also noted that the building's direct impact is not high compared to potentially other more commonly applied mitigation strategies and interventions, such as vegetation or urban shading to be able to provide a noticeable improvement on the UHI reduction in the urban microclimate.

– If only the indirect effect is evaluated, then it has an impact on the reduction of the building's cooling demands of the existing building situation, working as an external sun-shading skin and reducing the solar heat gains during summer. However, when compared to other shading devices on the same criterion, then the effect is similar, if not slightly less.

– If the evaluation lies only on the impact on the UHI effect as an isolated scenario, as it is the main objective of the thesis, then the facade design performs overall better than the other shading devices, because of the additional contribution in the direct impact on the urban microclimate.

– When the design is additionally being assessed as an overall dynamic facade system, including both energy and environmental performance, it brings added benefits to the building's annual operation. This is achieved by functioning as a closed-cavity double facade during the winter and, thus, reducing heat losses. In addition to that, even though the cooling demands are reduced almost equally compared to the other shading devices, the last ones operate only during warm and sunny periods.

– On this aspect, when compared also to other double skin and similar state-of-the-art facade systems, the question lies mostly on feasibility variables, such as cost-effectiveness, operation complexity and maintenance. This qualitative assessment is showcased in the following section with a set of suchlike criteria and radar charts. However, merely on the energy aspect, a typical double skin facade would only have positive effects during the winter, especially in a warm climate like the Mediterranean one, and would possibly require additional sun-shading within the cavity, since it would cause overheating during the summer. On the other hand, the proposed facade design has an annual dynamic operation, shifting from sun-shading function during the cooling-dominated periods to double facade during the heating-dominated ones.

The assessment is, therefore, in general greatly dependent on the reference points and what the objective focus in each situation is.

Environmental performance
Building's UHI impact

Qualitative comparative ranking
+ positive contribution
– negative contribution

direct   +   indirect   ⟶   UHI overall impact

stand-alone
solution

in comparison
to similar
interventions
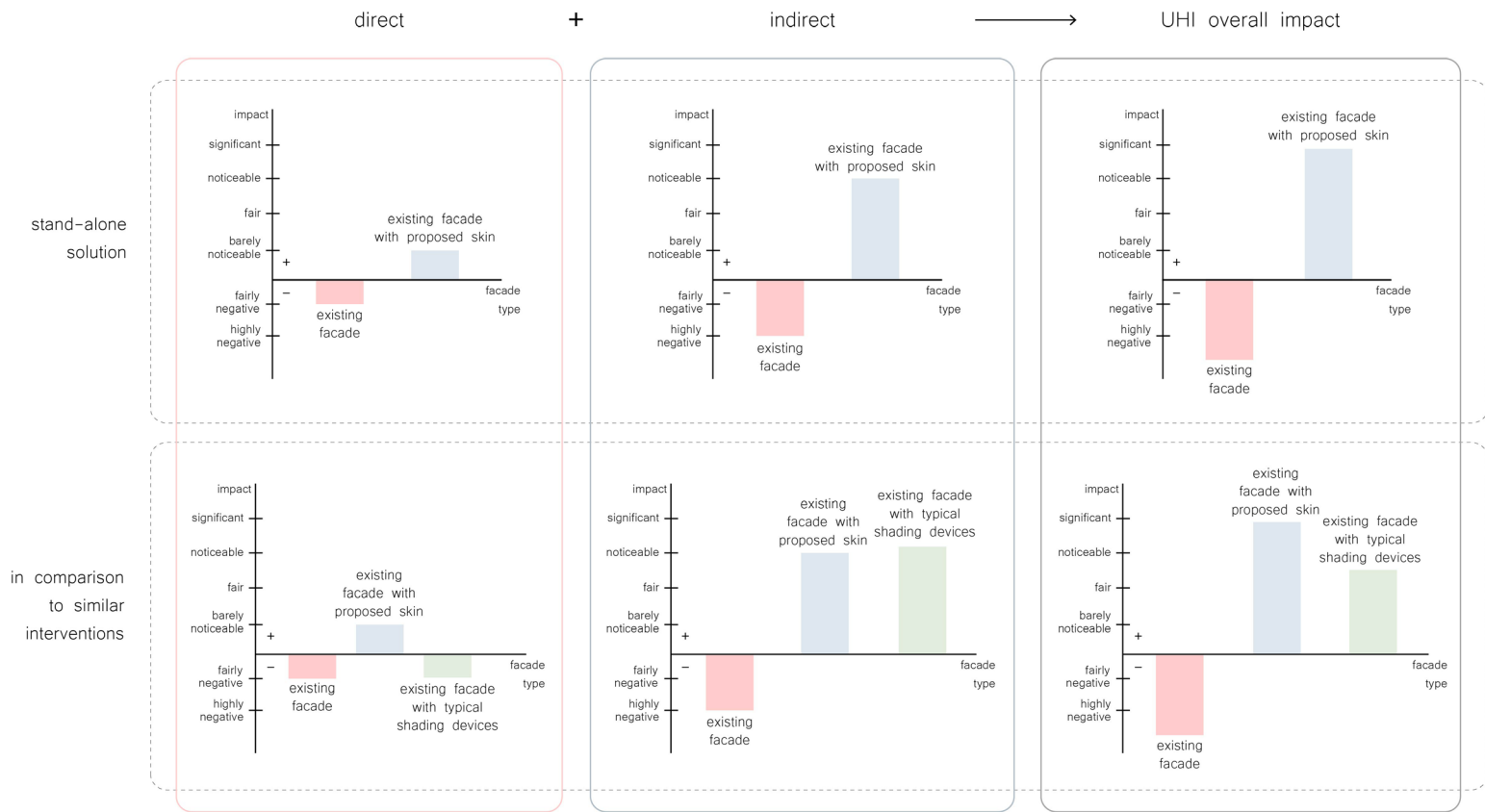
Energy performance
Intervention's contribution to building's
annual performance improvement

proposed facade design   typical shading devices   typical double skin
                                                                    glazed facade
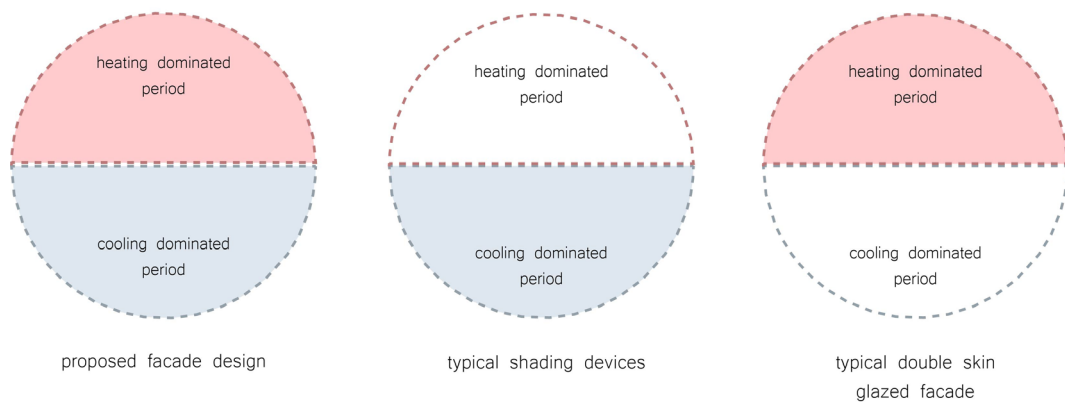
Figure 128: Building's energy and environmental performance comparative evaluation charts. [own work]

8.1. FEASIBILITY ASSESSMENT MAPS

The feasibility assessment aimed to discuss the potential of the proposed facade design to be integrated in building envelopes and in comparison to similar state-of-the-art double facade skins. The evaluation was conducted in respect to the following benchmark criteria, [adapted from the research paper of Prieto et al., 2019]: Overall performance, Technical & financial feasibility, Durability & Maintenance, Physical Integration and Availability, which are summarized in Table 37, together with the corresponding score values. The objective was to provide a referential qualitative assessment and to reflect on how the facade design fares regarding different relevant aspects for facade integration.

Table 37: Main identified barriers for facade integration and score system for the evaluation. [own work]

Barriers	Description	Score values		
		+	++	+++
Overall performance	Impact on the energy and environmental performance in relation to both the building's performance and the impact to the urban microclimate.	The facade system leads to a low energy and/or environmental performance, increasing both the energy demands and having a negative effect to the urban microclimate.	The facade system improves the building's energy and/or environmental performance, but the positive impact is either negligible or is limited to a certain period of operation.	The facade system improves the building's energy and environmental performance. The positive impact covers a larger operational schedule when the system is active.
Technical & Financial feasibility	Overall feasibility to integrate systems into façade components, considering functional and physical constraints for integration. Evaluation based on: - Ease of fabrication and manufacturing / Assembly / Costs (Real-scale building applicability factors) - Maturity of technology and material integration - Complexity level (in processing, manufacturing, assembly)	Too complex to be realized in a real-scale building application or too expensive for its erection. The technology required is not mature enough to allow an easy processing and fabrication.	The complexity of the components is reduced and they can be easier combined for a better integration. The materials and technology are already applied in practice, but there are still some limitations in terms of know-how or costs.	The fabrication and assembly process is better facilitated, the technology is mature enough and there is already knowledge for large scale applications. The investment required is also within reasonable limits.
Durability & Maintenance	Durability of components over time, maintenance requirements and ease to perform repairs or replace components and parts.	Fragile components with costly and frequent maintenance. Many customized parts that are not easily replaced, difficult accessibility, low operation cycles.	Robust components, but still with complicated or costly maintenance.	Robust systems and components virtually maintenance free, easy accessibility and disassembly/ replacement of facade components.
Physical Integration	Externalities derived from the physical integration of components and parts, considering compatibility of sub-systems, modularity, working materials and connections.	Components and working materials incompatible with facade functions.	Connections between operating sub-systems of mild complexity/ compatible components.	Modular components with simple plug&play connections. High level of compatibility of the separate sub-systems and working materials.
Availability	Potential to allow for design flexibility and variability, which may grant freedom for architectural expression and facade composition.	Operating principles and potential sizes greatly restrict design choices.	Some restrictions and isolated options for façade design, but there are various options for components.	High design flexibility and variety of options for materials and components.

For the comparison, two examples of realized double facade projects in office buildings located in Athens and the surrounding area were selected. The first one [Figure 129] is of a seven-storey office building, consisting of three blocks, with the middle one being a double facade with tempered laminated glass panes (2600x4000mm) fixed with a spider point system. This system expands to a glass rooftop skylight and is utilizing glass motorized rotating louvers to enable natural ventilation. Additionally, shading blinds and coatings are placed both within the cavity and in the interior of the building.

The second building [Figure 130] features a double facade skin with glass panels. These are suspended by a tension rod system consisting of stainless steel tension rods and pre-stressed cables and also in this case, the double skin is combined with motorized glass shades.

The above buildings were considered as the reference projects for the feasibility assessment evaluation, as they feature double facade skins in the same context and building type as the one studied during the thesis.
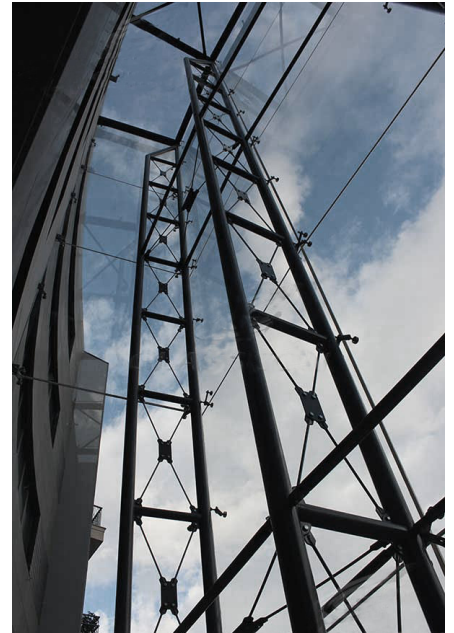
Figure 129: Images of the office building in Leoforos Alexandras avenue in Athens. [source: Office Building Skin. (2019, November 15). Retrieved from https://www.glasscon.com/projects/office-building-skin]
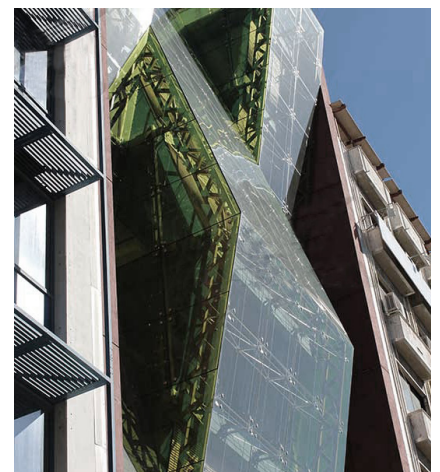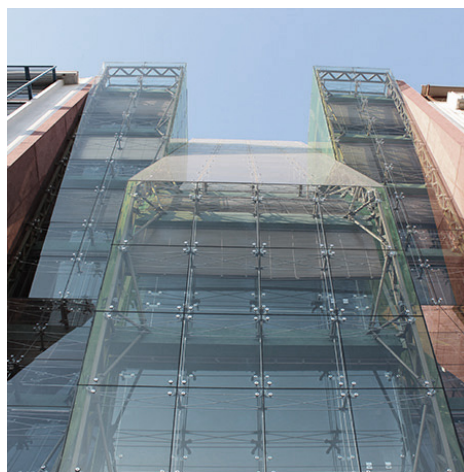
Figure 130: Images of the office building in the center of Piraeus. [source: 3D Building Envelope & Motorized Illuminated Glass Shades. (2019, November 15). Retrieved from https://www.glasscon.com/projects/3d-building-envelope-motorized-illuminated-glass-shades]

The resulting radar charts are shown in Figure 131 and the above scoring is briefly explained below:

Overall performance

This aspect refers to the overall energy and environmental performance and is informed by the summarized qualitative assessment of the previous section. It was concluded that the proposed facade design scores higher on the overall performance, due to both the annual operation reducing the energy loads by adapting its function throughout the year and the additional environmental impact resulting from the direct UHI reduction.

In that respect, the double facade systems have one degree less efficient performance, since during the summer they would mostly operate to avoid overheating, because of the accumulated heat trapped within the cavity and this is also why double skin facades are not recommended as a practice in warm climates.

Technical & financial feasibility

Here, the overall practicability of integrating all required components in a facade system is addressed, as well as the complexity of its erection, assembly and maturity of technology used, while the initial and long-term investment are also included. On that matter, the proposed design offers a lower complexity and reduction of the mechanical parts needed for its assembly, however, the technology based on smart materials is not so broadly used in integrated facade systems in Greece and might lead to complications or difficulties in its manufacturing and operation.

On the other hand, even though double facade systems are more commonly used, they can have a high level of complexity, especially if they also integrate responsive shading systems, whereas they still require a relatively high financial investment for their erection and maintenance. As seen in the photos of the two examples, the structure and substructure are quite demanding and extensive, even though they use modern technologies to minimize the fixings and try to reduce steel elements. Additionally, to avoid the negative overheating effect during the summer, they need to be combined with both mechanical ventilation louvres and shading blinds, which add even more to the complexity and costs. Lastly, a further remark that advocates their cost-intensivesess can be the fact that they are already described as luxirious offfice buildings in the project overview.

Durability & Maintenance

This refers to the durability of the required components over time, as well as maintenance requirements that have an impact on operational costs associated to each facade system technology. Regarding the proposed system, in its design principles, it aimed to achieve a certain level of simplicity associated with the smart materials technology and its passive operation, to avoid operational complications and malfunctions, while SMAs feature a high durability during their working cycles and the membranes used have a good resistance against UV exposure and can be self-cleaned. However, certain maintenance checks would be required, especially due to its direct exposure to weather conditions, the risk of parts malfunctioning or the SMAs being deactivated throughout their operation due to weather extremities. Another aspect that can be a matter of question is the extent at which the system would eventually operate on a seasonal basis, which would also determine the frequency of maintenance and its overall durability in the end.

In comparison, the double skin facades typically require frequent, intensive and costly maintenance, both in the exterior and the inner layer and in both cases, the maintenance might also require demanding accessibility solutions.

Physical Integration

Physical integration refers to the connection of the required facade components and the compatibility of sub-systems and working materials. In this case, the proposed facade system aimed to associate most of the components with their functional placement, and to integrate them with the overall geometrical design, to make more efficient use of the materials required for its operability. This was intended both for the SMAs integrated in the system, as well as the rest of the components, which most of them were directed to operate either as counterweight elements or to be associated with the energy and environmental performance, such as the use of textiles.

Regarding the double skin facades, the components comprising the systems are most of the times compatible to each other, wtih modular and scalable dimensions and advanced knowledge in the connections, thanks to the maturity of the technology and the broad applications. However, one downside that can potentially hinder the overall physical integration of the separate parts is the complexity that is associated with the double facade systems. This aspect is more apparent, when the geometry adopts non-regular forms that would require a more complex substructure, as it can be seen in the second example, where the structure is very noticeable and expressive with increased complexity. The integration would also be more challenging when additional components and structures are implemented, for example, ventilation and shading systems.

Availability

This relates to both the material and the technology availability to produce the facade components, as well as the potential to allow for design flexibility and variability, which may grant freedom for architectural expression and facade composition. Here, the downside of the proposed design lies on the lack of broad applications and knowledge of smart material facade technologies, which might create difficulties adopting similar systems and to hinder their broader applicability. However, the lack of complexity and the modularity of the sizes and scales of the separate and overall component could compensate and facilitate the material assembly and their integration, as well as to increase the design flexibility.

On the other hand, as explained before, standard double skin facades typically rely on commonly used facade materials and structural components with great variety and applications, which are often based on standardized, modular and prefabricated components, facilitating the process.
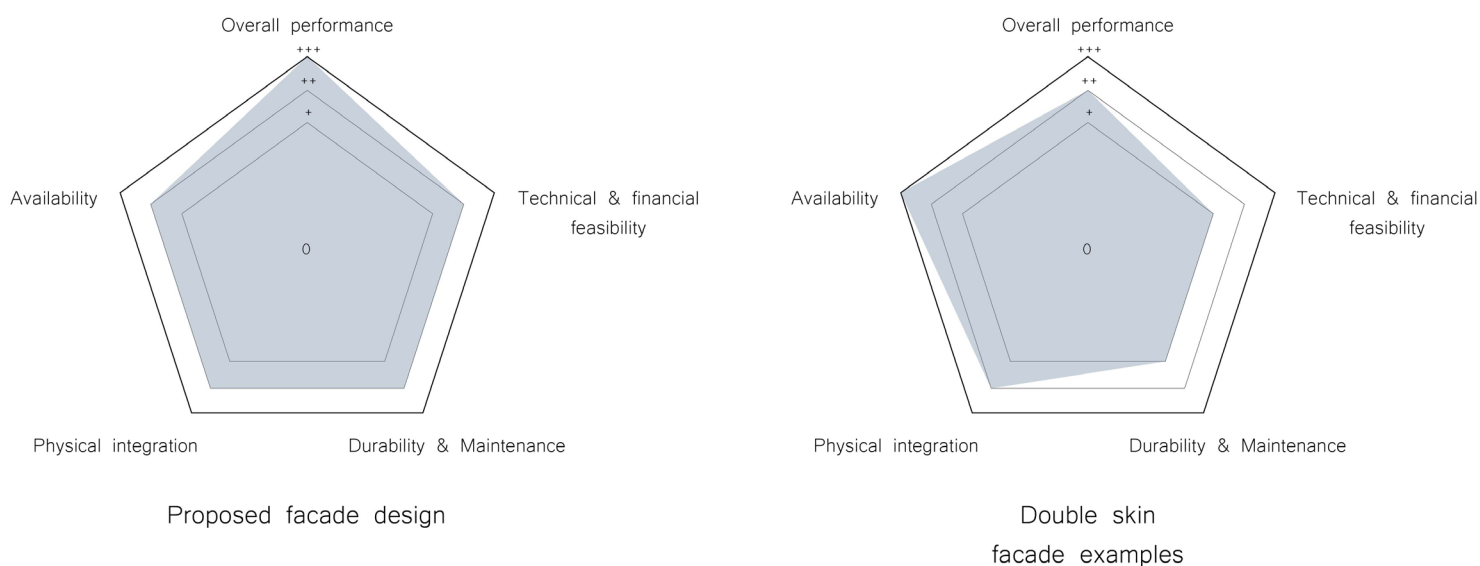
Figure 131: Feasibility assessment radar charts of the proposed facade design and the double skin facade examples. [own work]

8.2. LIMITATIONS – FUTURE IMPROVEMENTS

During the research process, certain limitations were encountered, regarding the methodology followed, the available time and means, as well as related to the complexity and nature of the UHI environmental issue in question and the facade design integration. In relation to the methodology, even though the interoperability chain between the different digital tools enabled a good enough compatibility and data transfer between the various analyses, certain modelling simplifications were required to be able to translate the geometries properly and to assign the right properties and boundary conditions. It can be assumed that small tolerances were expected during the simulations, which, however, were negligible in such an early design phase and did not necessarily lead to significant discrepancies that could affect the validity of the results. The same applies to certain performance assumptions, where certain boundary conditions and material properties were not possible to be defined precisely to reflect the real conditions.

This relates to the next limitation and future improvement, concerning the insightful feedback that a real prototyping and material testing would provide. This process was not possible to be realized during the current research project due to time and accessibility constraints. However, for a more holistic understanding of the facade design's overall performance, trial-and-error material tests on different SMA wires and other materials, such as the textiles, would help to define and evaluate the dynamic, thermal and visual properties and to better understand the dynamic behaviour in different temperature changes more accurately. Especially the SMA's properties and dynamic behaviour were in this thesis based on guidelines and expert recommendations and, by nature, require prototyping to be able to precisely define the required wire, strain and bias forces. This would be useful as inherent part of the feedback-loop methodology workflow and might lead to an additional set of optimization and refinement stages, since the system's effectiveness and feasibility depends highly on the actual material properties and their interdependencies. A suggestion for the workflow of this iterative process is presented in Figure 132, where some of the stages are realized in parallel and inform each other.
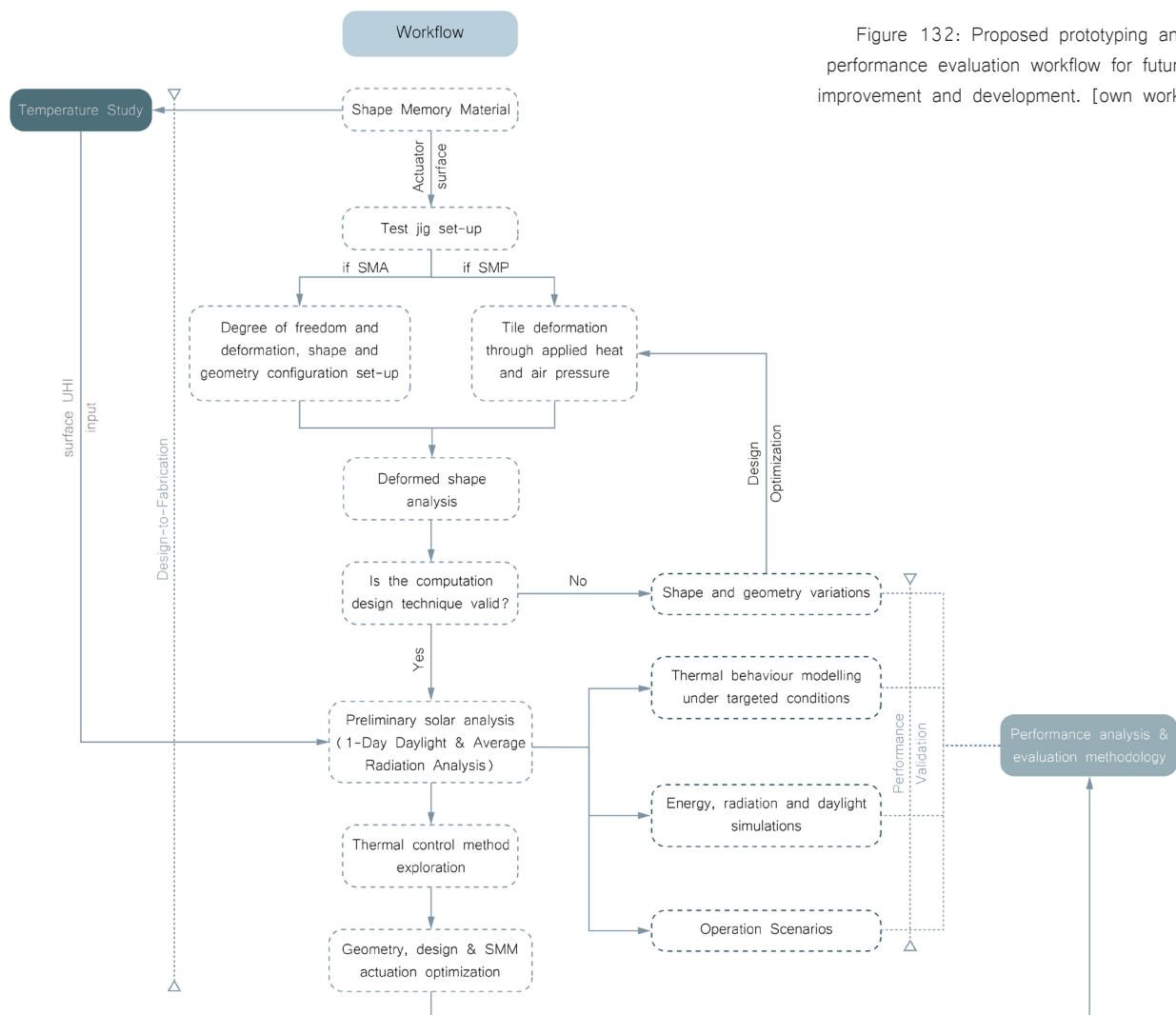
Figure 132: Proposed prototyping and performance evaluation workflow for future improvement and development. [own work]

Regarding the design applicability and facade integration limitations, even though the system relies on a passive responsive operating mechanism, which does not require any user's interference and works independently, this aspect might lead to certain comfort conflicts once the user's interaction becomes higher. For example, as it was showcased during the inner-to-outer facade relation tables, the facade system can work as a fully passive one with an opaque inner facade. However, once the window-to-wall ratio increases, the needs for more interaction with the outer facade and visual comfort are also increased. This could potentially lead to a more hybrid system, with a combination of passive and active operation, where the user's manual control is also enabled to override the passive automated function.

Throughout the research and design process, certain scenarios were considered as default decisions to evaluate a specific case study and facade application, as for example the choice of Athens as location, a south facade orientation and a retrofit application with a certain window-to-wall ratio. The end result, with its expressive design, can then have a specific application based on the chosen scenario. An interesting exploration would be to examine the design adaptations and performance implications, if the current proposal was to be applied in a different location and climate, orientation and facade application, which would also concern the feasibility of its application as a new building design from the beginning and not a retrofit intervention. A different scenario would then also have implications not only on the general geometry orientation as a shading unit, if, for example, applied on a west facade, but also on the required actuation movement to be able to better track the sun's movement at this position. Different starting points would lead to a different series of feedback loops that would then inform and optimize the design in another way to achieve in the end the desired energy and environmental performance goals of the specific set of variables in each case.

8.2.1. COMPUTATIONAL TOOL DEVELOPMENT

Moreover, throughout the research process, the analysis studies were realized in different facade test scales, ranging from component to facade segment to the urban level, as well as the building's interior, whereas it was observed that the simulation studies could also be grouped based on the objective and focus of interest. This clustering could offer an interesting potential and a recommendation for future development, to create a digital tool as a result of this methodology toolchain. This would be divided in the above categories of analysis level and base of test study, while including the sets of the relevant simulation studies in each group case. Even though such customized scripts exist and can be searched by theme in open-source online platforms, the idea for the proposed digital tool development would be to specialize the analyses under the facade performance evaluation theme as a useful toolset for possible facade-related simulation studies in an organized and easy-to-navigate flow.

Additionally, a common hindrance in some of the existing digital tools is that in most of the cases they require some level of parametric understanding and navigation in the Grasshopper environment, which might occasionally become time- and energy-consuming for new users and often leads to a series of questions in allocated forums. To simplify this process, the idea would then be to create the design tool in a user-friendly interface, where the user would not need to interfere with the script and the only inputs required would be the climate data and other similar boundary conditions, mostly related to other than parametric design information, for example, material properties or air flows. The only input geometry expected would then be described by the focus of each study cluster, whether it is the facade surface, street surface or building's interior, respectively. In the end, this would help to make the energy and environmental facade analysis studies and simulations more accessible to users who are not necessarily familiar with computational tools, but wish to exploit their potentials. Figures 133 and 134 diagrammatically illustrate the conceptual clustering of the proposed design tool.

More significantly, the thesis project relied highly on the parallel development and aid of computational tools for the energy and environmental simulation and performance evaluation of the design. This workflow promotes the importance of these digital tools in the service of the architect, designer or building physicist, among other relevant disciplines. To elaborate further, the current project followed a systematic step-by-step workflow and explored the potentials of this method with the objective to evaluate the design and building's performance. In this sense, the design itself can be perceived as just a demonstration case study and outcome of this iterative computational workflow that is applied in practice, out of many other possible alternatives. In this sense, a different scenario with a different initial geometry input and another set of parameters and requirements would lead to a different design result. At the same time, the study objectives and the computational workflow remain intact as the core of the feedback-optimization process and as the available toolset at disposal to aid the performance assessment and design development, as shown in Figure 135.

In the end, an important contribution and one of the main deliverables of the thesis project is, therefore, the computational logic behind the design process rather than the final design result and it can be relevant to develop further as a useful tool for a broad range of professions in the field. This is because it offers a universal computational background methodology and a series of systematic and comprehensive stages for the facade study and evaluation. Most significantly, at its core, this iterative process is not bound to the specific design each time, but rather offers a workflow platform as an independent step-by-step guideline, with the design's performance assessment as clear objective.
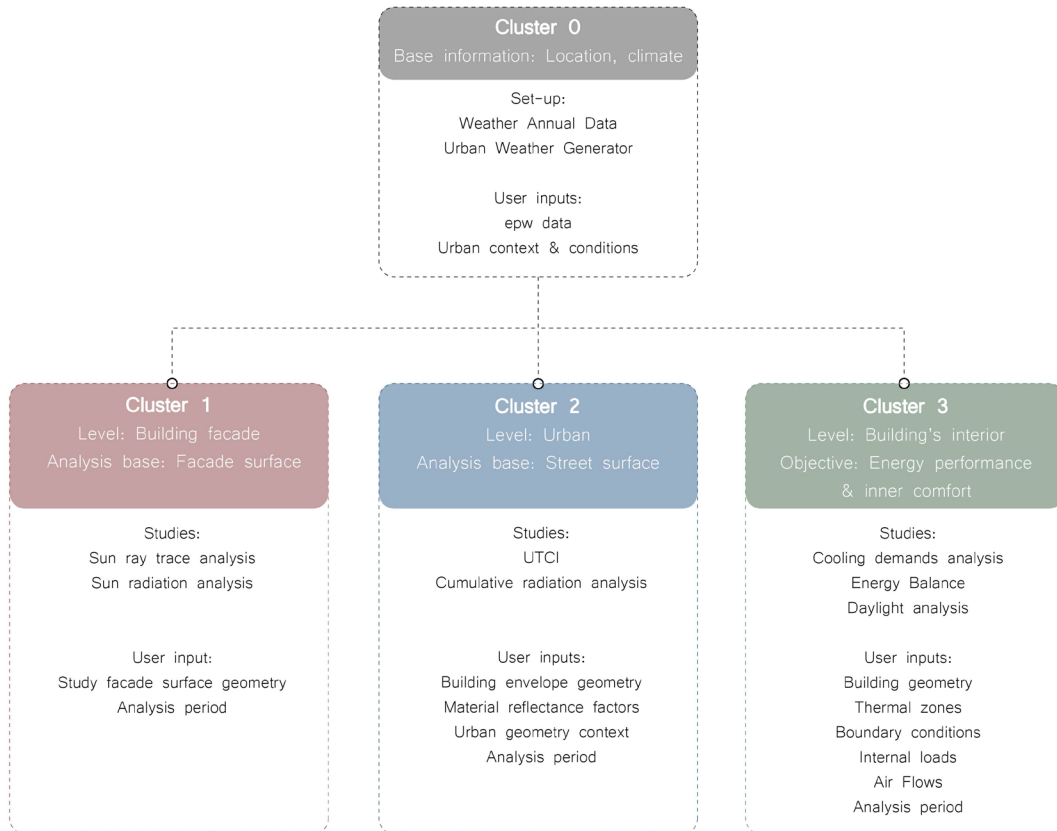
Figure 133: Clustering concept for the division of the analysis studies. [own work]
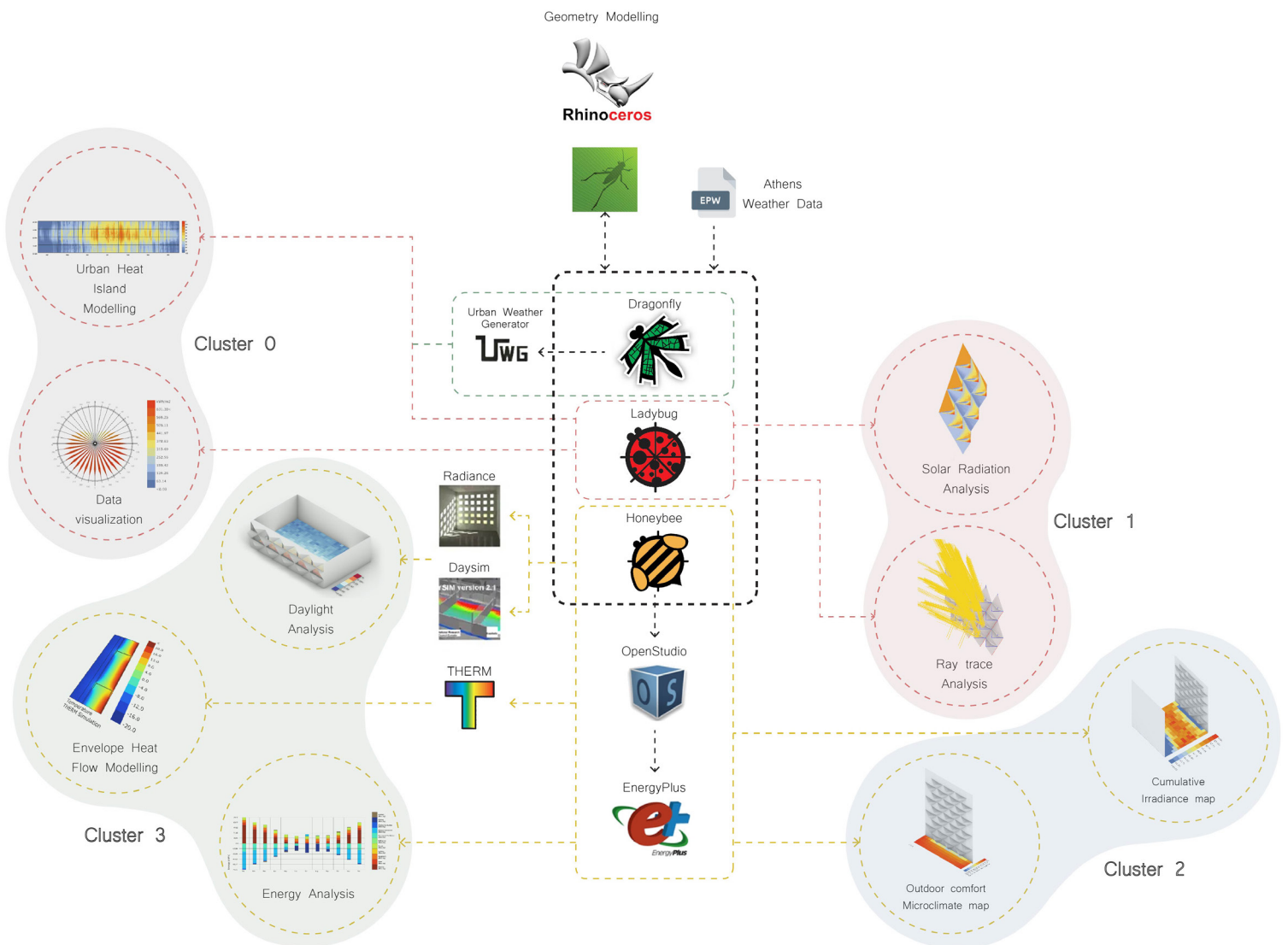
Figure 134: Subdivision of the followed computational workflow and clustering overview for the development of the digital tool. [own work]

Example x

Geometry Input

Feedback

Optimization

Performance
evaluation workflow

Computational
toolset

Cluster 0

Cluster 1

Cluster 2

Cluster 3

Final Design Output
&
Performance improvement
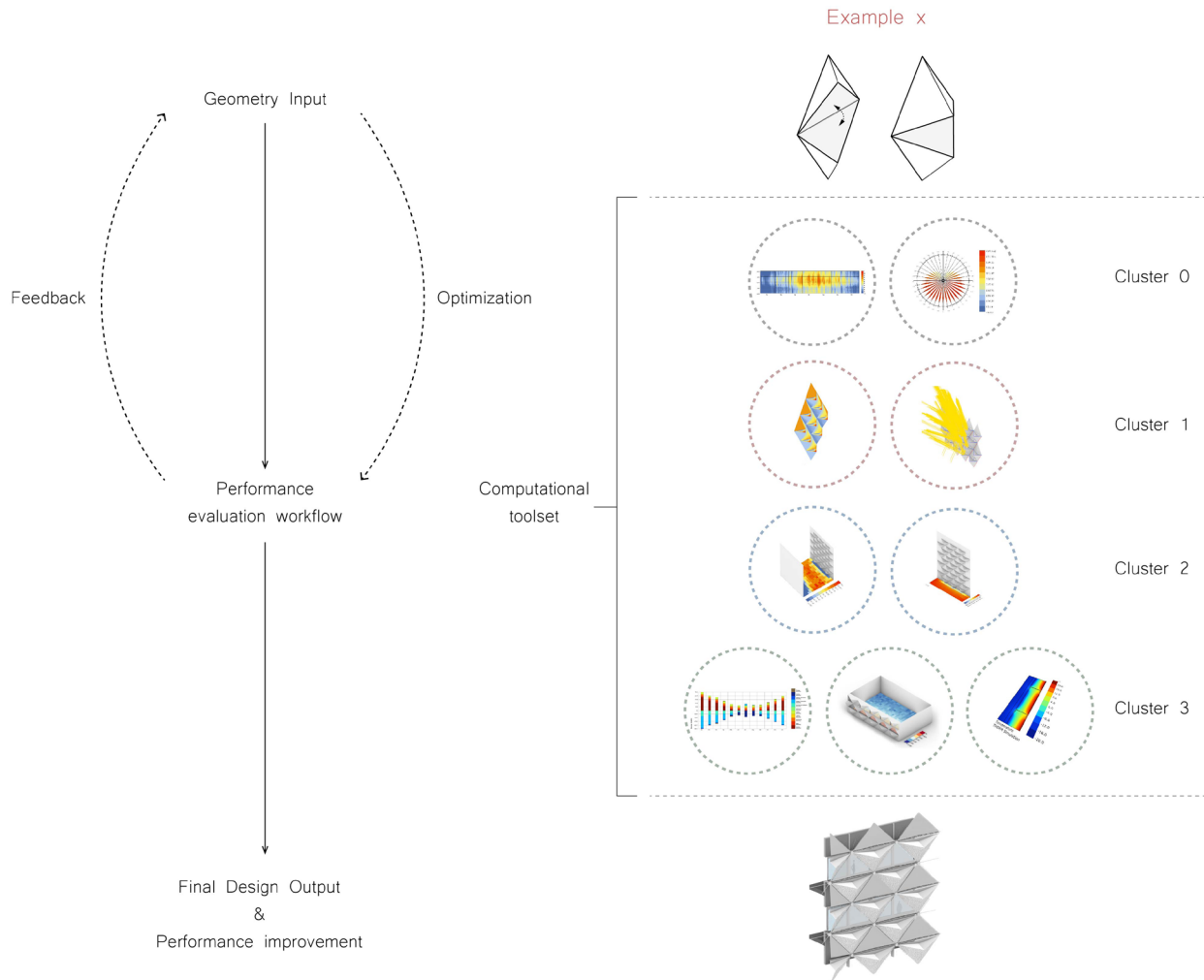
Figure 135: The feedback-optimization logic of the performance evaluation as part of the computational tool workflow and the current design as an example of its application in practice. [own work]

8.3. REFLECTION

As seen throughout the graduation project, an interesting part of the design and performance evaluation process was to reflect on the potentials, challenges and restrictions of the implementation of smart materials in facade applications. More specifically, further research could provide with additional insights on this subject, to explore under which conditions and to what extent such technologies have benefits and perform equally well or better than other standardized and mechanically controlled systems to justify their use over them. The current explorations give way to further open research questions on the dynamic effect of these passive responsive systems in relation to their operation, user's interference, durabilty cycles and feasibility. The same applies to the spectrum of the applied context, in which they can be compatible to have high dynamic performance. For example, a consideration would be to reflect on the effect of a different climatic context or the results of the exposure of the autoreactive mechanism to a short period of extreme weather conditions and to what extent the operation would be affected in that case.

Apart from that, the operation basis is also a parameter that can be further studied to assess in real conditions whether a seasonal operation can be achieved in practice, if a daily one would be more feasible or if the movements in the end are so negligible and not so frequent that a simple control and automated switch between the two seasonal modes would be sufficient. It would be, therefore, interesting to explore further the arguments that favour the passive operation and application of SMAs, and smart materials in general, when placed in a larger context and with more parameters involved. At the bottom line, the picture is larger than merely the UHI impact and, in the end, the discussion lies mostly on the extent and the conditions that promote the development of autoreactive systems in future facade applications.
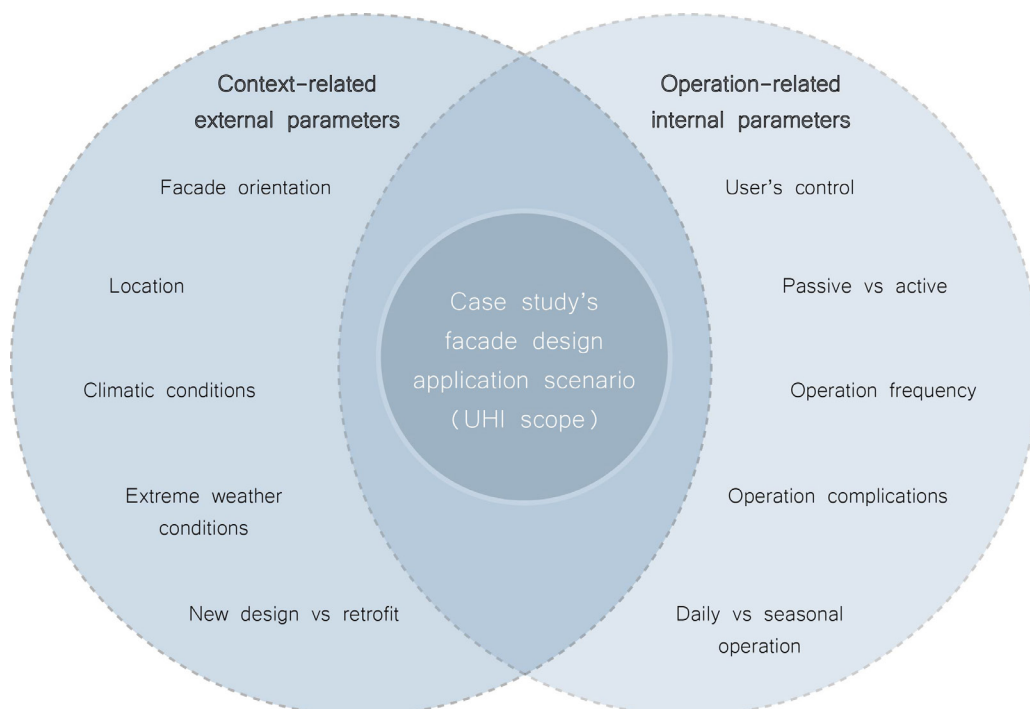
Figure 136: Diagram showing the current research project's specific scope and the broader context with the parameters involved. [own work]

Finally, as a short example of this exploration and to spark further discussion, a comparison on the visual and mostly the reflective values of the current design's shading membranes with other applied UHI mitigation strategies aimed to evaluate the impact of the materiality of the proposed design to other common practices and to reflect on the possible benefits of each case. The examples chosen for this comparison were a standard white paint, an ultra-white one, cool-colored paints and retro-reflective materials. These examples were chosen for being relevant with the thesis' objectives, because they are based on the principle of radiative cooling, which is a passive cooling technology that offers potentials to reduce space cooling cost and tackle the UHI effect.

Standard white paint

Starting with the most basic application, white paint has been traditionally used in sunbaked countries, where buildings are regularly painted white to reflect as much sunlight as possible. However, white paints typically reflect about 86% of visible light [Yuan et al., 2015], they still absorb ultraviolet (UV) and near-infrared (near-IR) rays, which warm buildings, while they also reflect the solar radiation towards the urban environment.

To counteract these issues, new materials have been developed, which incorporate substances or structures that reflect nearly all the sun's incoming rays, including near-IR heat and, in some cases, UV as well:

Ultra-white paint

A recent development on the radiative cooling strategies is showcased in the work of Li et al. [Li et al., 2021], where $BaSO_4$-based nanoparticle films and nanocomposite paints were developed, which can reach an ultrahigh solar reflectance of 97.6% and a high sky window emissivity of 0.96. Even though these radiative cooling solutions are still undergoing experimental tests, they can potentially provide a competitive and convenient paint form, ease of use, and compatibility with the commercial paint fabrication process.

Cool-colored paints

The use of highly reflective "cool" coatings, which contain infrared reflective pigments, can also help maintain lower exterior surface temperatures of roofs and building facades and consequently contribute to increased indoor thermal comfort during hot periods. It was found during studies that the cool paints showed similar absorption in the visible range compared to unpainted surfaces and to conventional paint of the same color. In addition, however, they significantly improved reflectance in the near-IR range and, therefore, can absorb less solar energy, which keeps the surface at a lower temperature and decreases the energy transfer by radiation [Uemoto et al., 2010] [Table 38].

Retro-reflective materials

Lastly, compared to other highly reflective coatings, which yield diffuse reflection, retro-reflective materials can reflect light back along the incident direction [Figures 137, 138]. For this reason, it has been studied that replacing typical highly reflective materials on building outer surfaces with retro-reflective materials can partially solve the problem of reflected sunlight towards neighboring buildings and roads and consequently reduce the UHI phenomenon. [Yuan et al., 2015]. The reflective characteristics of these materials are summarized in Table 39.
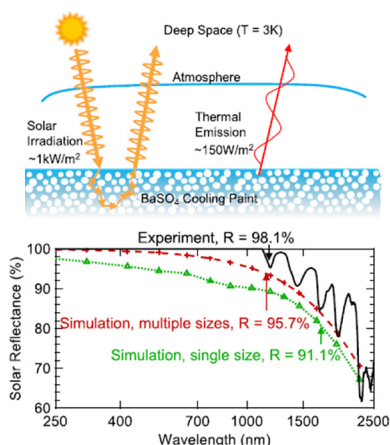
Figure 137: Radiative energy transfer for ultra-white cooling paint [top] and simulation on the solar reflectance [bottom]. [Li et al., 2021]

Table 38: Measured reflectance of unpainted specimens and those painted with conventional and cool paint. [adapted from Uemoto et al., 2010]

Types	Reflectance [%]			
	UV	VIS	NIR	Total
Unpainted	32.0	48.5	50.4	47.3
Cool white	6.5	84.9	80.1	77.9
Conventional white	7.3	86.0	63.8	65.5
Cool brown	8.0	26.4	72.9	61.9
Conventional brown	5.7	24.4	32.8	30.2
Cool yellow	5.8	46.3	76.2	67.9
Conventional yellow	5.8	44.4	44.4	42.8
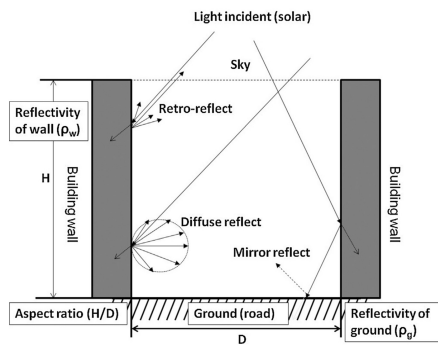
Figure 138: Schematic diagram of two-dimensional urban canyon space and the effect of retro-reflective materials. [Yuan et al., 2015]

Table 39: Reflective conditions of different building surface types. [adapted from Yuan et al., 2015]

Building surface type	Retro-reflectivity	Diffuse reflectivity	Total reflectivity
Diffuse	–	0.81	0.81
Retro	0.44	0.37	0.81
Mirror	–	–	0.81
Ground surface reflectivity: 0.2			

From the above applications, the ultra-white paint and the cool-colored materials can offer higher reflective percentages and to a broader wavelength range compared to a standard white paint, and, by doing so, already provide some additional benefits. However, retro-reflective materials can have a more targeted contribution to the UHI effect by avoiding the reflection towards the urban environment and, therefore, are a more competitive solution against the design of the current project. The question that follows is then to which extent of building applications and context this solution would be equally beneficial without increasing the complexity of the intervention.

It can be assumed, for example, that in a fully opaque facade, the application of retro-reflective materials could be a more efficient solution, since it is simpler to apply, more time and cost-efficient, it can achieve same or even better results, since a PTFE membane can achieve about 70% of solar reflection, whereas it can be easily replicated in many similar situations. In contrast, as mentioned during the design process, once the window-to-wall ratio starts increasing, then more parameters are intertwined, with the user's inner comfort having a more central role. In this case, retro-reflective materials alone will not be sufficient to lower the building's cooling demands and additional measures

will be required, such as solar and ventilation control. In this sense, the proposed design can probably gain advantage, because of the added benefits it provides through an integrated solution with more variables taken into account and incorporated in its dynamic and seasonal function.

Under this application scenario, the question and boundary conditions lie mostly on the level of complexity up to which simpler solutions are no longer self-sufficient as a stand-alone solution to provide high enough energy and environmental performance, and consequently to have a significant impact on the UHI effect and urban microclimate. This threshold is where, due to the complexity of the context, the choice for the current design can be justified, however seen as one building application and not a repeated strategy. Once the complexity and requirements increase even more, on the other hand, then a passive mechanism is also potentially not enough as an argument by itself and should be combined or overriden by a more reliable mechanical control and programmed automation. In the end, each case is better suitable for a certain application range, but the design goal and decisions remain, nevertheless, intact, aiming to provide a solution which is able to develop a facade system with both high overall performance and little internal complexity.
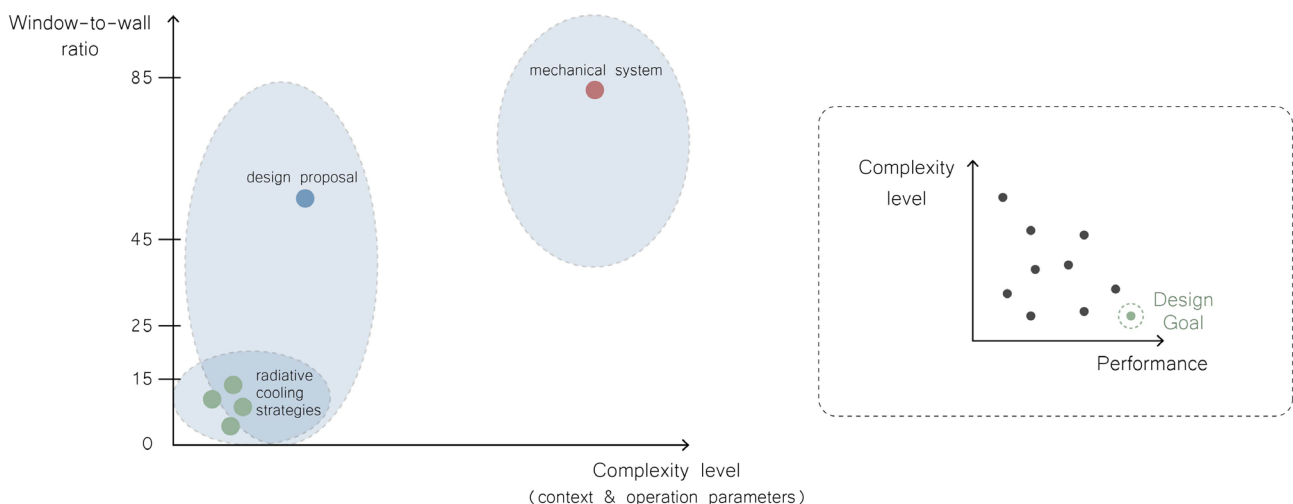
Figure 139: Qualitative estimation chart of the optimal range of building application for each option over other alternatives in relation to performance and complexity as external parameters and conditions (left) to achieve the desired design goal as an internal system (right). [own work]

GRADUATION PROCESS

The graduation project explored the potentials of the application of an SMA-based passive adaptive facade system to be integrated as an exterior dynamic shading skin on an office building in Athens, Greece. The main research objective was focused on the impact of such a technology system on the reduction of the building's impact on the UHI effect and followed an iterative evaluation methodology that informed the design and guided the performance assessment through a feedback-loop computational workflow. The focus was based on a combination of Facade Design and Design Informatics, which are two of the basic directions of the Building Technology graduation studio. It is also related to the specific graduation topic, which lies under the "Urban Facades" theme, directing the scope of the research and design explorations. The graduation project dealt with research on the behaviour and properties of SMMs, with a focus on the SMAs, and used a broad range of digital tools in an interoperable computational workflow that was developed to analyze and simulate the energy and environmental performance of the proposed facade system.

The process involved a large part of literature review on the various aspects that are important and relevant to address the research objectives and answer the main question and sub-questions. The research was divided into the contextual part, understanding the environmental issue in question associated with the specific location on one hand, and the material and technology research on the other one. During the design phase, both aspects were associated with certain difficulties. Because of the complexity of the UHI problem and the multitude of variables involved, it was not always clear to evaluate and quantify the building's impact and certain assumptions or isolated scenarios needed to be assumed. Similarly, regarding the behaviour of the SMAs, the lack of prototyping and material testing did not allow for a holistic understanding of the dynamic behaviour and to assess the extent at which the design would have the desired dynamic performance in practice. For these reasons, parts of the process were based on general guidelines from experts and literature review of precedent projects. Nevertheless, the adopted toolchain methodology helped to establish a comprehensive evaluation between the various analysis studies and focus areas and to create a compatible and comparison between the different options and stages with a clear transfer of information between the different data and computational flows.

RELATIONSHIP BETWEEN RESEARCH AND DESIGN

Both research and design are connected to the main research question: *"How can thermo-responsive Shape Memory Materials be integrated in a passive adaptive facade system to reduce the building's impact on the Urban Heat Island effect in the Mediterranean climate, with a focus on the case study of Athens, Greece?"*. Large part of the research deals with evaluating the design decisions in relation to the building's impact on the UHI effect and to propose ways for its reduction. Furthermore, the research provides a basis of technological knowledge and computational tool workflow, regarding the energy and environmental performance of the facade proposal, which feed the design process for optimization during the different stages of analysis and provide insights for further research and improvements. At the same time, during the various design and evaluation stages, the decision-making process is performance-driven and each decision is specifically targeted to address the performance requirements and meet the energy and environmental goals.

RELATIONSHIP TO MASTER TRACK

The graduation studio combines the Facade Design and Design Informatics fields, which are inherent part of the Building Technology Track. The focus of the project lies on the implementation of smart material technologies in the architectural facades and the evaluation of the design's performance through the development of a computational workflow and toolset. There is, therefore, a strong relation between the graduation topic, the Master Track and Study Programme in general. The building envelope is the threshold between the built environment and the urban conditions and, as such, the current research aims to reduce the impact of the building on the Urban Heat Island effect and to exploit innovative technologies and materials. The goal is to mitigate the environmental issue by means of passive thermal self-regulation mechanisms of a kinetic shape-changing facade. There is, therefore, a connection between building technology practices that are applied to enhance the building's energy performance and, consequently, improve the conditions of the built environment.

SCIENTIFIC RELEVANCE

The objective of the thesis is to additionally contribute with some knowledge as part of the framework commissioned to the Adaptive Facade Network set by the EU COST (European Cooperation in Science and Technology) in 2014. The main aim of this COST Action is to harmonize, share and disseminate technological knowledge on adaptive facades at a European level. By harnessing this knowledge, it will contribute to the generation of new ideas and concepts at a fundamental and product/system development level. Especially in the case of smart and autoreactive materials and mechanisms, the current lack of knowledge in the implementation of such technologies in building envelopes opens the way to investigate such potentials and propose innovative solutions and ideas. By exploring their applicability in the field of architecture, these could potentially offer some possibilities to be broader used in the built environment and to assess the challenges and restrictions they could entail.

RELATIONSHIP TO SOCIAL, PROFESSIONAL AND SCIENTIFIC FRAMEWORK

From a social and environmental perspective, there is a need to achieve a high level of user well-being and indoor environmental quality, to reduce building energy consumption and neutralize building-related environmental impacts. The integration of passive and active design technologies in the building envelope, as studied here, can have high potentials to improve indoor comfort conditions and reduce the environmental impact during the life cycles of buildings. In this respect, the dynamic adaptive facades have a significant effect on achieving the performance requirements, by adapting to changing boundary conditions in the form of short-term weather fluctuations, diurnal cycles, or seasonal patterns. Another important aspect concerns the potential reduction of energy demand in buildings, heat regulation and CO_2 emissions with the conversion of building envelopes from passive to active regulators of energy balance, which is promoted as part of the Climate and Energy Action Plans (Directive 2010/31/EU). In order to work effectively as a surface-regulator, the building skin must adopt different physical features at different times of the day, requiring different levels of environmental intelligence.

With the UHI phenomenon at its rise and its foreseen increasing intensity in the Mediterranean region over the next years, the current thesis aims to address a challenge with scientific and societal relevance and, by so doing, to achieve sustainability targets in the built environment.

ETHICAL ISSUES AND DILEMMAS

During the research process, no particular ethical issues or dilemmas were encountered or became a conflict of different interests.

8.4. CONCLUSION

The thesis aimed to investigate the feasibility and process of implementing Shape Memory Alloys in a passive adaptive kinetic facade system with the objective to assess its performance on the building's direct and indirect impact on the UHI effect in the Mediterranean context and, more specifically, in Athens. The idea was to propose a system that exploits the autoreactive properties of the SMAs to adapt to the building's seasonal needs, to reduce its energy demands, with a focus on the cooling demands during the summer, to increase the reflectivity of the incoming solar radiation to the atmosphere and minimize the overheating of the urban microclimate. From the literature study it was found that the building's impact on the UHI amplification results mostly from the increasing cooling loads from the air conditioning systems. The main question was, therefore: "How can thermo-responsive Shape Memory Materials be integrated in an autoreactive facade system to reduce the building's impact on the Urban Heat Island effect in the Mediterranean climate, with a focus on the case study of Athens, Greece?"

The design proposed a facade shading system, which featured a double function during the summer and winter, that was enabled through a dynamic movement triggered by the SMAs combined with a pivot mechanism. In the first case, it worked only as a (self-)shading system with increased reflective surfaces and geometries to dissipate the solar radiation, whereas during winter, the dynamic movement resulted in more solar radiation to be admitted to the interior and the function shifted to a double facade system with multiple closed-cavities for heat amplification and reduction of the heat losses.

The research followed a systematic methodology in a feedback-loop approach, adopting computational tools in an integrated workflow logic for the energy and environmental studies, which were mostly integrated in the Grasshopper environment. The goal was to create an interoperable toolchain between the different study analyses to enable a compatible data flow and interchange. The design process also followed a series of iterative evaluation and optimization steps, starting from feasibility control checks in terms of the SMA's workability restraints, followed by the evaluation on the direct impact and then the indirect one. The direct impact aimed to increase the reflectivity of the sun rays towards the atmosphere, while the indirect one assessed different alternatives based on the reduction of each option on the cooling loads. In parallel, the effect of the heat buffer zones

during the winter situation was also explored and visualized through CFD convective heat transfer simulations. Finally, a few daylight studies were conducted for validation of the operation and the interference to the user's inner comfort.

At the same time, the operating mechanism was developed to a certain allowable extent, since it was not possible to realize prototypes and material tests. The system consisted of a pivot mechanism, which was connected to two SMAs and a Scotch Yoke mechanism, combined with other components working in an internal cause-effect logic. The movement was initiated by the SMAs, which would be actuated by the change in ambient temperature that would cause their linear deformation within an allowable stress limit of about 3%. The rest of the surfaces were covered in membranes of different types, SHGC and transparency levels, depending on their function, in a performance-driven material selection logic.

In the end, the conclusions from each evaluation study led to the observation that the proposed facade design can potentially reduce the building's direct impact on the urban microclimate. However, compared to other possible mitigation strategies, the impact was negligible (only 6% of the total cumulative radiation on the street level resulted from the reflected radiation from the facade surface). On the contrary, the reduction of the cooling demands and, consequently the indirect UHI impact was more noticeable, with the proposed facade design able to reduce the cooling loads by about 21%. At the same time, during winter, the heat buffer zone could increase the temperature inside the cavity that could reach up to around 25°C.

Moving forward, based on the reflection and feasibility assessment studies realized in the end, it can be summarized that there are potentials to explore and enhance the use of SMAs in facade applications. The challenges lie mostly on the feasibility, the user's control and operation cycles of such autoreactive systems and their implications when placed in a broader context. To this regard, it is important to critically evaluate to what extent their implementation can lead to added benefits, taking more parameters into account in practice during the entire life cycle operation. The question is, therefore, how to optimally integrate passive strategies to promote sustainability through adaptiveness and smart-material-based solutions and under which conditions, to be able to adapt the indoors to the outdoor environmental changes and maximize both the energy and environmental performance.

COMPLIANCE TO THE DESIGN GOALS

Part of the reflection of the final design is also the compliance to the facade design goals and guidelines set in the beginning. This is evaluated based on a ranking gradient similar to the previous ones, according to the score values described in the table below [Table 40]. The assessment of the proposed design on these barriers is then shown in the radar chart in Figure 141. Overall, the facade proposal met the desired environmental performance to the extent of its potential and achieved a satisfactory level of simplicity in the mechanical and structural parts that enable its operating mechanism. In principle, it can also function in a fully passive operation, with the exception of the various scenarios for user's manual control.

However, what is more open for debate is the feasibility level, which is closely associated to the complexity one. This is because these two aspects relate mostly to the performance of the facade system throughtout its annual operation in a real-case building application scenario and use. Even though the intentions are the facade system to feature a simple operation with no intensive maintenance or function implications, there are still some parameters that cannot be predicted in advance at this early design stage, but might affect the operation of the system in practice. For instance, it could potentially lead to partial operation during the seasonal and temperature changes or to malfunctions due to the exposure to weather conditions, where local extremities might cause defects on the facade system and its responsive mechanism. Another aspect could be that the system in the end is active only a few times a year and in this case a smart responsive mechanism would not contribute significantly and could have been replaced with a simple switch from the summer to the winter operational mode. These are some of the examples that can spark further explorations and research, related to the building's operation on a broader context and not isolated scenarios, as well as the technical feasibility of such smart systems, their challenges and potentials that advocate for their implementation in facade applications.
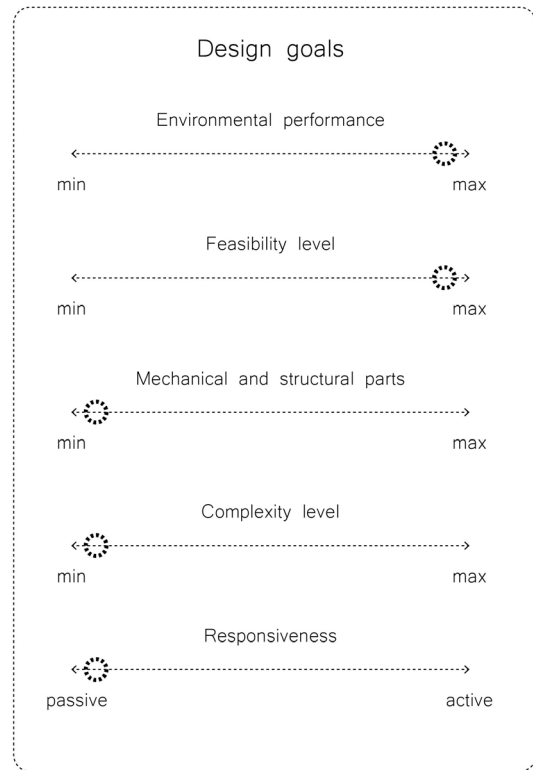
Figure 140: Overview of the main design goals. [own work]

Table 40: Main identified barriers for facade integration and score system for the evaluation. [own work]

Barriers	Description	Score values		
		+	++	+++
Environmental performance	Impact on the environmental performance in relation to the building's direct and indirect impact on the UHI effect in the urban microclimate.	The facade system leads to a low environmental performance, having a negative or barely noticeable positive effect to the urban microclimate.	The facade system improves the building's environmental performance, but the positive impact is either negligible or is limited to a certain period of operation.	The facade system improves the building's environmental performance, meeting to a satifactory degree its potentials. The positive impact covers a larger operational schedule when the system is active.
Feasibility level	Overall feasibility to integrate systems into façade components, considering functional and physical constraints for integration. Evaluation based on: – Ease of fabrication and manufacturing / Assembly / Costs (Real-scale building applicability factors) – Maturity of technology and material integration – Complexity level (in processing, manufacturing, assembly)	Too complex to be realized in a real-scale building application or too expensive for its erection. The technology required is not mature enough to allow an easy processing and fabrication.	The complexity of the components is reduced and they can be easier combined for a better integration. The materials and technology are already applied in practice, but there are still some limitations in terms of know-how or costs.	The fabrication and assembly process is better facilitated, the technology is mature enough and there is already knowledge for large scale applications. The investment required is also within reasonable limits.
Mechanical & structural parts reduction	Optimization and reduction of unnecessary mechanical and structural parts, minimizing the components to the merely functional ones.	The facade system requires too many mechanical and structural parts for its assembly.	The components are slightly reduced, but there is still some level of complexity in the working mechanisms.	The working components are simplified with clear connections and are optimized to the minimum required for its functional operation.
Complexity level	The level at which the facade system can be perceived as complex or simple for its manufacturing, assembly, operation and maintenance. It is related to the physical integration of components and parts, considering compatibility of sub-systems, modularity, working materials and connections.	Components and working materials incompatible with facade functions and too complicated, compromising the system's physical integration.	Connections between operating sub-systems of mild complexity/ compatible components.	Modular components with simple plug&play connections. High level of compatibility of the separate sub-systems and working materials.
Passive responsiveness	The level at which the facade system relies on a passive or active operation.	The system relies highly on an active operation and/or system override.	There is a combination of active and passive operation in a hybrid system where user's control is enabled when necessary.	The system operates on a fully passive and responsive manner with no external energy or control required.

Compliance to the design goals
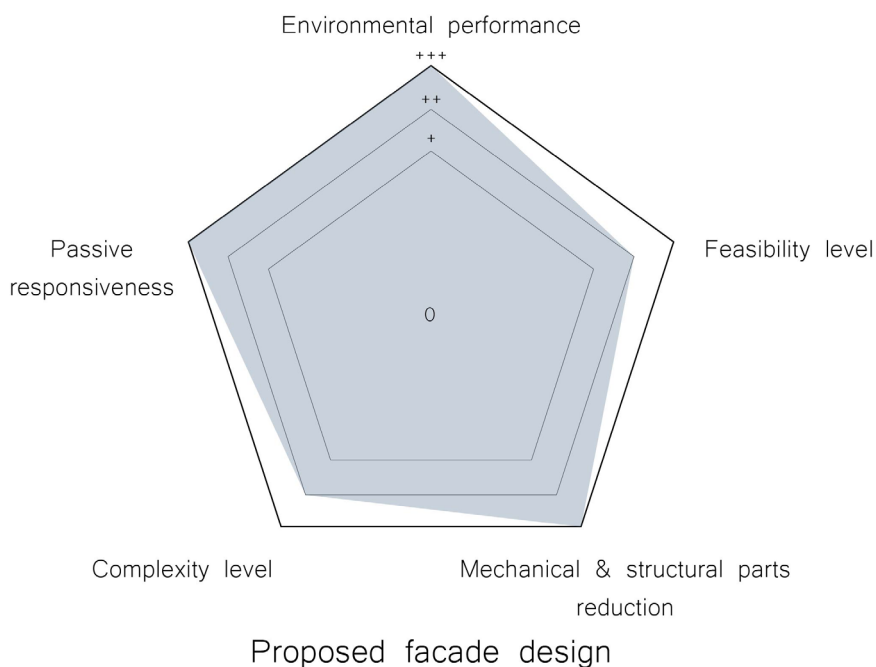
Figure 141: Radar chart evaluating the compliance of the proposed facade design to the design goals. [own work]

EVALUATION OF RESEARCH QUESTIONS

Main Research Question:

"How can thermo-responsive Shape Memory Materials be integrated in an autoreactive facade system to reduce the building's impact on the Urban Heat Island effect in the Mediterranean climate, with a focus on the case study of Athens, Greece?"

In the recent years, Shape Memory Materials have gained more attention and projects are being developed that integrate them in facade systems, with a more mature knowledge and technology for the implementation of the SMAs, whereas SMPs and SMHs are still undergoing research to be applied in real-scale building components. These systems utilize the Shape Memory Effect of the material which can be predefined to passively activate the mechanism and create a dynamic movement, either placing the actuator on a node, edge or as a programmed 3D printed surface. In the design concept for this thesis, which assumes a case study office building in Athens, the two SMAs are integrated on the edges of an external shading component, which utilizes the two different strained lengths in its hot and cold state to create a dynamic seasonal movement in response to the external air temperature and to adapt to the different energy and environmental demands in each situation. In the hot phase, the wire has a reduced length, whilst in the cold state, the wire is weaker and the bias elements can stretch it to the original position. This adaptive movement aims on one hand to reduce the building's cooling demands by reducing the incoming solar heat gains and by means of self-shading and on the other hand to increase the reflective effect towards the atmosphere. In this way, the building's direct and indirect UHI impact are addressed and controlled by the passive autoreactive behaviour of the SMAs.

Sub-questions:

"What is the effect of responsive dynamic facade systems in respect to climate adaptiveness and UHI?"

In the current project, a passive responsive facade system was explored that is actuated and adapts according to the outdoor temperature changes throughout a seasonal operating schedule. The system exploits the autoreactive dynamic deformation of an SMA-based mechanism, which helps adjust the building's energy demands to the high temperatures during the hot periods, which are amplified by the UHI effect. This is achieved by creating shading and reflective geometries to both protect the building from overheating and to dissipate the solar radiation to the atmosphere and not have a negative impact on the urban microclimate.

"How can thermo-responsive SMM-integrated technologies have potentially an impact on the building's energy performance and contribute to UHI reduction in the Mediterranean climatic context?"

Thermo-responsive SMMs have the ability to initiate dynamic movements using high ambient temperatures as a trigger with no external energy required. This ability can be exploited especially in the Mediterranean basin, where the high temperatures are the cause of the increase of both the UHI and the building's cooling demands, which are interrelated. In this way, these technologies have the potential to exploit the extreme environmental conditions on their advantage to create dynamic movements that can be integrated as a passive adaptive mechanism. By implementing, for example, kinetic shading devices on the building envelope, they can help regulate the building's performance, being the threshold between urban environment and building's interior.

"How can the dynamic responsiveness parameters of the SMM be controlled and pre-determined to achieve the desired material dynamic effect in an adaptive facade system?"

For the scope of the thesis, the potentials of the SMAs were further explored, whereas the exploration of rest of the SMMs remained in the initial literature review stage. Regarding the SMAs, for the actuation of the element, for example wire or spring, there is already an advanced knowledge and technology behind its mechanism. This enables to achieve the desired actuation temperatures with a high accuracy, by inducing the required force through tensile stress tests. This in practice is realized with prototypes and material tests and because of the broad knowledge and maturity of the technology, it can be already defined by the manufacturers and SMA suppliers, when the desired properties and deformation are known. Due to time and other external constraints, this part of research was not able to be realized in the given timeframe of the thesis.

"Which are the main principles and strategies of natural systems and how can they be relevant to the SMM behavioural ones and to responsive mechanisms in controlling the building's thermal behaviour in a climatic context?"

The principles of nature for self-regulation that are relevant to the dynamic behaviour and response mechanism of the SMAs are related to an extent to the self-organization strategies found in nature, that can rapidly fabricate lightweight structures using self-folding strings or sheets with the following features:
- Reduced material consumption
- Creation of structures with improved strength-to-weight ratios
- Structural rigidity across the planar faces
- Hinged flexibility along the fold lines

Regarding the four main principles of nature, Heterogeneity, Anisotropy, Hierarchy and Multifunctionality, the ones followed mostly in the end were Anisotropy is terms of material and Multifunctionality in terms of mechanism, whereas the two other features were not present in the system. More specifically, processed SMAs show a behaviour, in which, like other metals, the texture of the material and the presence of internal stresses are found to be responsible for such anisotropy, whereas

multifunctionality resulted from the operating mechanism and the coordination of materials and acting forces. At the same time, another set of principles relates to the geometrical features and control mechanisms, which aim to protect the natural organisms from the environmental extremities. These concern the undulated geometries of the succulent plants and the layered surfaces of the butterflies that offer high level of self-shading for heat dissipation and solar reflection, as well as the stomata of the leaves, which help control and regulate the intake or air. These strategies were then translated in the project design, with the aim to adapt to the building's needs for solar reflection and shading protection, as well as to adjust the incoming air flows. However, this was followed to a certain degree, being mostly adapted as an initial inspiration spark during the geometrical explorations and design guidelines.

"How can thermo-responsive SMMs be integrated in a passive adaptive solar morphing envelope combining autoreactive and bio-inspired responsive mechanisms?"

The final design aimed to integrate SMA wires in a passive adaptive kinetic shading component, which combines a pivot mechanism to rotate the shading surfaces in coordination to the SMA's autoreactive deformations. This enables a reversible seasonal movement that follows the gradual temperature changes with the objective to increase the (self-)shading effect of the facade during the hot periods, whereas an unhindered ventilation is enabled to avoid overheating, similarly to the heat and ventilation regulation strategies found in nature. In the contrary, during the winter, the undulation is decreased to increase the solar heat gains of the building and at the same time to trap warm air between closed cavity zones.

"How can motion be achieved in an integrated facade system by using latent energy in an energy-effective and autoreactive way, with optimal use of sensors and actuators, where material, form, function, structure and motion are interdependent in a fit combination?"

One of the core objectives of the project was to minimize the use of actuators and mechanical parts and integrate merely the functional elements of the mechanism, with no additional parts. This was achieved by introducing simple mechanisms, such as the Scotch Yoke mechanism that works in combination with a

pivot axle, a series of steel threads and a bias spring, translating the SMA's linear deformations to a sequence of linear and rotational movements. The movements are realized in a chain reaction of forces that do not require any other external force apart from the SMA's triggering actuation. In this way, material, form, function structure and motion are interdependent and integrated in the facade component itself as a modular unit in an energy-efficient and autoreactive manner.

"To what extent are SMM-based facade technologies feasible solutions and what are the challenges, restrictions and potentials for future facade applications?"

The SMMs have potentials to be implemented in the building industry, either as new designs or interventions, to enhance the building's performance due to their intrinsic properties and passive autoreaction that facilitate the integration of adaptive technologies in facade systems. From the available materials, the SMAs have a more mature and advanced knowledge in this respect, with the SMPs and SMHs still having limited real-scale applications and currently undergoing research and development stages to be broadly used. As for the SMAs, their implementation is mostly related to adaptive shading components, because they can enable dynamic movements with little force and material required. Nevertheless, there are still some challenges in practice, which partly lie on the building's performance and demands. One aspect that usually needs consideration throughout the operation of the technology is the possibility for user's manual control and system override. As explored during the thesis, the desire for active over passive control becomes increased, the more the interaction between user and outdoor environment becomes present, because daylight and view control also need to be satisfied. On the contrary, when being implemented as an opaque facade skin, this challenge is out of the scope and the system can potentially function in a fully passive way.

Additionally, in some of the cases of SMM-based technologies, another challenge is to be able to simplify as much as possible the mechanism used, so as to justify the use of such an autoreactive technology and not result to an overly complicated mechanism with too many mechanical parts that in the end would cause operating implications and be out-of-use or manually controlled most of the time.

Lastly, a further challenge is related to the proper programming of the autoreactive material, the properties and boundary conditions, intrinsic and external, to achieve the desired dynamic performance, since all parts are interconnected in an internal system that is activated by the SMM. As for example in this project, the actuation temperatures were estimated based on the annual air temperature values. However, in practice, the production of a prototype is necassary to test the mechanism in real environmental conditions, to assess whether certain adjustments and optimizations need to be considered and which conditions in the broader context favour its operation and application. It is, therefore, based on a trial-and-error iterative process, where the feedback of the prototype is critical and insightful to produce a facade system with the desired performance.

09   LITERATURE

1. 3D Building Envelope & Motorized Illuminated Glass Shades. (2019, November 15). Retrieved from https://www.glasscon.com/projects/3d-building-envelope-motorized-illuminated-glass-shades.

2. Addington, M. (2012). Smart Materials and Technologies in Architecture. doi:10.4324/9780080480954.

3. Aelenei, L.; Aelenei, D.; Romano, R.; Mazzucchelli, E.S.; Brzezicki, M.; Rico-Martinez, M.J. Case Studies—Adaptive Facade Network; Aelenei, L., Aelenei, D., Romano, R., Mazzucchelli, E.S., Brzezicki, M., Rico-Martinez, M.J., Eds. (2018). TU Delft Open: Delft, The Netherlands. ISBN 9789463661102.

4. Attia, S., Lioure, R., Declaude, Q. (2020). Future trends and main concepts of adaptive facade systems. Energy Science & Engineering, 8(9), 3255-3272. doi:10.1002/ese3.725.

5. Behl, M., Kratz, K., Noechel, U., Sauter, T., Lendlein, A. (2013). Temperature-memory polymer actuators. Proceedings of the National Academy of Sciences, vol. 110, no. 31, pp. 12555–12559.

6. Behl, M., Lendlein, A. (2011). Shape-Memory Polymers. Kirk-Othmer Encyclopedia of Chemical Technology. doi:10.1002/0471238961.1908011612051404.a01.pub2.

7. Böke, J., Knaack, U., Hemmerling, M. (2018). State-of-the-art of intelligent building envelopes in the context of intelligent technical systems. Intelligent Buildings International, 11(1), 27-45. doi:10.1080/17508975.2018.1447437.

8. Bothe, M., Pretsch, T. (2012). Two-way shape changes of a shape memory poly(ester urethane). Macromolecular Chemistry and Physics, vol. 213, no. 22, pp. 2378–2385.

9. Boyvat, M., Koh, J., Wood, R. J. (2017). Addressable wireless actuation for multijoint folding robots and devices. Science Robotics, 2(8). doi:10.1126/scirobotics.aan1544.

10. Bradley, A., Thornes, J., Chapman, L., Unwin, D., Roy, M. (2002). Modelling spatial and temporal road thermal climatology in rural and urban areas using a GIS. Climate Research, 22, 41-55. doi:10.3354/cr022041.

11. Bröde P. et al. (2012). Deriving the operational procedure for the Universal Thermal Climate Index (UTCI). International journal of biometeorology 56:3, 481-494.

12. Capeluto, G., Ochoa, C. E. (2016). Design Considerations. Intelligent Envelopes for High-Performance Buildings Green Energy and Technology, 51-79. doi:10.1007/978-3-319-39255-4_3.

13. Carlucci, S., Causone, F., Biandrate, S., Ferrando, M., Moazami, A., Erba, S. (2021). On the impact of stochastic modeling of occupant behavior on the energy use of office buildings. Energy and Buildings, 111049. doi:10.1016/j.enbuild.2021.111049.

14. Cartalis, C., Synodinou, A., Proedrou, M., Tsangrassoulis, A., Santamouris, M. Energy Conversion and Management. (2001). Modifications in energy demand in urban areas as a result of climate change: an assessment for the southeast Mediterranean region.

15. Chen, S., Hu, J., Zhuo, H., Zhu, Y. (2008). Two-way shape memory effect in polymer laminates. Materials Letters, vol. 62, no. 25, pp. 4088–4090.

16. Chen, S., Mahadevan, L. (2019). Rigidity percolation and geometric information in floppy origami. Proceedings of the National Academy of Sciences, 116(17), 8119-8124. doi:10.1073/pnas.1820505116.

17. Chen, S., Choi, G. P., Mahadevan, L. (2020). Deterministic and stochastic control of kirigami topology. Proceedings of the National Academy of Sciences, 117(9), 4511-4517. doi:10.1073/pnas.1909164117.

18. Chung, T., Romo-Uribe, A., Mather, P. T. (2008). Two-way reversible shape memory in a semicrystalline network. Macromolecules, vol. 41, no. 1, pp. 184–192.

19. Clifford, D. T., Zupan, R. J., Brigham, J. C., Beblow, R. V., Whittock, M., Davis, N. (2017). Application of the dynamic characteristics of shape-memory polymers to climate adaptive building facades. Proceedings of 12th Conference of Advanced Building Skins, pp. 171–178, Bern, Switzerland.

20. Cremers, J., Mirbach, D., Liebhar, H., Marx, H., Hajek, O. (2019). The ideal ETFE fenestration: The influence of material properties on the thermalperformance, in: E.O.C. Lázaro, K.-U. Bletzinger (Eds.), Proc. IASS Annu.Symp.— Struct. Membr. 2019 Form Force, International Centre for Numerical Methods in Engineering (CIMNE), Barcelona, Spain.

21. Dakheel, J. A., Aoul, K. T. (2017). Building Applications, Opportunities and Challenges of Active Shading Systems: A State-of-the-Art Review. Energies, 10(10), 1672. doi:10.3390/en10101672.

22. Daylight calculations and measurements – Daylight, Energy and Indoor Climate Book. (n.d.). Retrieved from https://www.velux.com/what-we-do/research-and-knowledge/deic-basic-book/daylight/daylight-calculations-and-measurements.

23. Daylight Factor. (n.d.). Retrieved from http://patternguide.advancedbuildings.net/using-this-guide/analysis-methods/daylight-factor.

24. Daylight Factor. (n.d.). Retrieved from http://patternguide.advancedbuildings.net/using-this-guide/analysis-methods/daylight-factor.

25. Daylight requirements in building codes – Daylight, Energy and Indoor Climate Book. (n.d.). Retrieved from https://www.velux.com/what-we-do/research-and-knowledge/deic-basic-book/daylight/daylight-requirements-in-building-codes.

26. Decker, M., Yeadon, P. (2010). Projects Smart Screen: Versions I, II and III.

27. Doumpioti, C., Greenberg, E.L., Karatzas, K. (2010). Embedded intelligence: Material responsiveness in façade systems. New York. p. 258-62.

28. Drossel, W., Kunze, H., Bucht, A., Weisheit, L., Pagel, K. (2015). Smart3 − Smart Materials for Smart Applications. Procedia CIRP, 36, 211-216. doi:10.1016/j.procir.2015.01.055.

29. EnergyPlus. (n.d.). Retrieved from https://www.energyplus.net/.

30. ETFE Properties - Fluorotherm™. (2017, February 13). Retrieved from https://www.fluorotherm.com/technical-information/materials-overview/etfe-properties/.

31. Fan, K., Huang, W. M., Wang, C. C., Ding, Z., Zhao, Y., Purnawali, H., . . . Zheng, L. X. (2011). Water-responsive shape memory hybrid: Design concept and demonstration. Express Polymer Letters, 5(5), 409-416. doi:10.3144/expresspolymlett.2011.40.

32. Felton, S. M., Tolley, M. T., Shin, B., Onal, C. D., Demaine, E. D., Rus, D., Wood, R. J. (2013). Self-folding with shape memory composites. Soft Matter, 9(32), 7688. doi:10.1039/c3sm51003d.

33. Fiorito, F., Sauchelli, M., Arroyo, D., Pesenti, M., Imperadori, M., Masera, G., Ranzi, G. (2016). Shape morphing solar shadings: A review. Renewable and Sustainable Energy Reviews, 55, 863-884. doi:10.1016/j.rser.2015.10.086.

34. Founda, D., Santamouris, M. (2017). Synergies between Urban Heat Island and Heat Waves in Athens (Greece), during an extremely hot summer (2012). Scientific Reports, 7(1). doi:10.1038/s41598-017-11407-6.

35. Fuliotto R, Cambuli F, Mandas N, Bacchin N, Manara G, Chen Q. (2010). Experimental and numerical analysis of heat transfer and airflow on an interactive building facade. Energy and Buildings, 42: 23-28.

36. Geometry-Material Coordination for Passive Adaptive Solar Morphing Envelopes. (2017). Proceedings of the 2017 Symposium on Simulation for Architecture and Urban Design (SimAUD 2017). doi:10.22360/simaud.2017.simaud.023.

37. Giannopoulou, K., Santamouris, M., Livada, I., Georgakis, C., Caouris, Y. (2010). The impact of canyon geometry on intra Urban and Urban: Suburban night temperature differences under warm weather conditions, Pure Appl. Geophys. 167 1433−1449. doi:10.1007/s00024-010-0099-8.

38. Golden, J. S. (2004). The Built Environment Induced Urban Heat Island Effect in Rapidly Urbanizing Arid Regions − A Sustainable Urban Engineering Complexity, Environmental Sciences, 1:4, 321-349, doi: 10.1080/15693430412331291698.

39. Gong, T., Zhao, K., Wang, W., Chen, H., Wang, L., Zhou, S. (2014). Thermally activated reversible shape switch of polymer particles. Journal of Materials Chemistry B, vol. 2, no. 39, pp. 6855−6866.

40. Greevenbroek, S.L. (2018). Folding Structures: Developing a new method using the principles of origami and CNC Milling.

41. Guattari, C., Evangelisti, L., Balaras, C. A. (2018). On the assessment of urban heat island phenomenon and its effects on building energy performance: A case study of Rome (Italy). Energy and Buildings, 158, 605-615. doi:10.1016/j.enbuild.2017.10.050.

42. Harvie, GN. (1995). An investigation into the thermal behaviour of spaces enclosed by fabric membranes. [Phd Thesis]. Cardiff: University of Cardiff.

43. Hawkes, E., An, B., Benbernou, N. M., Tanaka, H., Kim, S., Demaine, E. D., Rus, D., and Wood, R. J. (2010), Programmable Matter by Folding, PNAS, 107(28), pp. 12441−12445.

44. He, G., Shu, L., Zhang, S. (2011). Double skin facades in the hot summer and cold winter zone in China: Cavity open or closed? Building Simulation, 4(4), 283-291. doi:10.1007/s12273-011-0050-7.

45. Hea 01 Visual comfort. (n.d.). Retrieved from https://www.breeam.com/BREEAM2011SchemeDocument/Content/05_health/hea01.htm.

46. Huang W.M., Ding, Z., Wang, C.C., Wei, J., Zhao, Y., Purnawali, H. (2010). Shape memory materials, Materials Today, Volume 13, Issues 7−8, Pages 54-61, ISSN 1369-7021, https://doi.org/10.1016/S1369-7021(10)70128-0.

47. Ingpuls - Smart Materials made in Bochum. (n.d.). Retrieved from https://ingpuls.de/en/.

48. Jeronimidis G, Atkins AG. (1995). Mechanics of biological materials and structures: nature's lessons for the engineer. Proceedings of the Institution of Mechanical Engineers, Part C: Journal of Mechanical Engineering Science. doi:209:221-35.

49. Juaristi, M., Konstantinou, T., Gómez-Acebo, T., & Monge-Barrio, A. (2020). Development and Validation of a Roadmap to Assist the Performance-Based Early-Stage Design Process of Adaptive Opaque Facades. Sustainability, 12(23), 10118. doi:10.3390/su122310118.

50. Kadri, L. B. (2012). Towards the LIVING envelope: Biomimetics for Building Envelope Adaptation, Technical University Delft. doi:10.4233/uuid:4128b611-9b48-4c8d-b52f-38a59ad5de65.

51. Karlessi, T., Santamouris, M., Synnefa, A., Assimakopoulos, D., Didaskalopoulos, P., Apostolakis, K. (2011). Development and testing of PCM doped cool colored coatings to mitigate urban heat island and cool buildings. Building and Environment, 46(3), 570-576. doi:10.1016/j.buildenv.2010.09.003.

52. Khoo, C.K,. Salim, F., Burry, J. (2011). Designing architectural morphing skins with elastic modular systems. International Journal of Architectural Computing. doi: 9:397-419.

53. Knippers, J., Speck, T. (2012). Bioinspir. Biomim. 7 015002.

54. Lebée, A. (2015). From Folds to Structures, a Review. International Journal of Space Structures, 30, pp. 55-74. https://doi.org/10.1260/0266-3511.30.2.55.

55. Leng, J., Lan, X., Liu, Y., Du, S. (2011). Shape-memory polymers and their composites: Stimulus methods and applications. Progress in Materials Science, 56(7), 1077-1135. doi:10.1016/j.pmatsci.2011.03.001.

56. Leonidaki, K., Kyriaki, E., Konstantinidou, C., Giama, E., Papadopoulos, A. M. (2014). Thermal performance of office building envelopes: the role of window-to-wall ratio and thermal mass in Mediterranean and Oceanic climates. Journal of Pow-er Technologies, 94(2), 128-134. http://papers.itc.pw.edu.pl/index.php/JPT/article/view/550.

57. Li, J., Duan, Q., Zhang, E., Wang, J. (2018). Applications of Shape Memory Polymers in Kinetic Buildings. Advances in Materials Science and Engineering. vol. 2018. Article ID 7453698. https://doi.org/10.1155/2018/7453698.

58. Li, X., Peoples, J., Yao, P., Ruan, X. (2021). Ultrawhite BaSO4 Paints and Films for Remarkable Daytime Subambient Radiative Cooling. ACS Applied Materials & Interfaces, 13(18), 21733-21739. doi:10.1021/acsami.1c02368.

59. Lienhard, J., Schleicher, S., Poppinga, S., Masselter, T., Milwich, M., Speck, T., et al. (2011). Flectofin: A hingeless flapping mechanism inspired by nature. Bioinspiration and Biomimetics.

60. Lignarolo, L., Lelieveld, C., Teuffel, P. (2011). Shape morphing wind-responsive facade systems realized with smart materials. Adaptive Architecture: An International Conference. London (U.K.).

61. Liu, B., Silverberg, J. L., Evans, A. A., Santangelo, C. D., Lang, R. J., Hull, T. C., Cohen, I. (2018). Topological kinematics of origami metamaterials. Nature Physics, 14(8), 811-815. doi:10.1038/s41567-018-0150-8.

62. Liu, K., Paulino, G. H. (2017). Nonlinear mechanics of non-rigid origami: An efficient computational approach. Proceedings of the Royal Society A: Mathematical, Physical and Engineering Sciences, 473(2206), 20170348. doi:10.1098/rspa.2017.0348.

63. Liu, Y., Zhang, W., Zhang, F., Lan, X., Leng, J., Liu, S., . . . Chou, T. (2018). Shape memory behavior and recovery force of 4D printed laminated Miura-origami structures subjected to compressive loading. Composites Part B: Engineering, 153, 233–242. doi:10.1016/j.compositesb.2018.07.053.

64. Lobo, P. S., Almeida, J., Guerreiro, L. (2015). Shape Memory Alloys Behaviour: A Review. Procedia Engineering, 114, 776–783. doi:10.1016/j.proeng.2015.08.025.

65. Lomholt, I., Welch, A. (2020, October 21). Athens Office Building: Greece Offices – e-architect. Retrieved from https://www.e-architect.com/athens/athens-office-building.

66. Loonen, R. C. G. M., Favoino, F., Hensen, J. L., Overend, M. (2016). Review of current status, requirements and opportunities for building performance simulation of adaptive facades. Journal of Building Performance Simulation, 10(2), 205–223. doi:10.1080/19401493.2016.1152303.

67. Loonen, R.C.G.M., Rico-Martinez, J.M., Favoino, F., Brzezicki, M., Menezo, C., La Ferla, G., Aelenei, L. (2015). Design for facade adaptability – Towards a unified and systematic characterization. In Proceedings of the 10th Energy Forum – Advanced Building Skins. Bern, Switzerland. pp: 1274–1284.

68. Luible, A. (2015). COST Action 1403, in: Proc. Energy Forum 2015, Bern, Switzerland.

69. Macias-Escriva, Frank D., Haber, R., del Toro, R., Hernandez, V. (2013). Self-adaptive Systems: A Survey of Current Approaches, Research Challenges and Applications. Expert Systems with Applications 40: 7267–7279. doi:10.1016/j.eswa.2013.07.033.

70. Mainini, A. G., Poli, T., Paolini, R., Zinzi, M., Vercesi, L. (2014). Transparent Multilayer ETFE Panels for Building Envelope: Thermal Transmittance Evaluation and Assessment of Optical and Solar Performance Decay due to Soiling. Energy Procedia, 48, 1302–1310. doi:10.1016/j.egypro.2014.02.147.

71. Mardaljevic, J., Heschong, L., Lee, E. (2009). Daylight metrics and energy savings. Lighting Research & Technology, 41(3), 261–283. doi:10.1177/1477153509339703.

72. Matzarakis, A., Balafoutis, C. (2004). Heating degree-days over Greece as an index of energy consumption. International Journal of Climatology, 24(14), 1817–1828. doi:10.1002/joc.1107.

73. Modern architecture in Athens. (n.d.). Retrieved from https://www.wikiwand.com/en/Modern_architecture_in_Athens#/The_modernism_of_the_1960s.

74. Mokhtar, S. Leung, C., Chronis, A., Kingdom, U. (2017). Geometry–Material coordination for passive adaptive solar morphing envelopes. In 2017 Proceedings of the Symposium on Simulation for Architecture and Urban Design. The Society for Modeling and Simulation International: Toronto, ON, Canada. Volume 49. pp. 211–218. doi:10.22360/simaud.2017.simaud.023.

75. Nabil, A., Mardaljevic, J. (2005). Useful daylight illuminance: A new paradigm for assessing daylight in buildings. Lighting Research & Technology, 37(1), 41–57. doi:10.1191/1365782805li128oa.

76. Nakano, A. (n.d.). Urban Microclimate: Uwg: Download. Retrieved from https://urbanmicroclimate.scripts.mit.edu/uwg.php.

77. Oke, T.R. (1979). Review of urban climatology, 1973–1976. WMO Technical Note no. 169. WMO No. 539. Geneva: World Meteorological Organization.

78. Otsuka K, Wayman, CM. (1998). Shape Memory Materials. Cambridge (UK). Cambridge University Press.

79. Paech, C. (2016). Structural Membranes Used in Modern Building Facades. Procedia Engineering, 155, 61–70. doi:10.1016/j.proeng.2016.08.007.

80. Papamanolis, N., Dimelli, D., Ragia, L. (2015). "The urban heat island intensities in Greek cities as a function of the characteristics of the built environment," presented at 9th International Conference on Urban Climate jointly with 12th Symposium on the Urban Environment, Toulouse, France.

81. Pappas A, Zhai Z. (2008). Numerical investigation on thermal performance and correlations of double skin facade with buoyancy-driven airflow. Energy and Buildings, 40: 466–475.

82. Parlac, V. (2014). Surface Dynamics: From dynamic surface to agile spaces.

83. Payne, A.O., Johnson, J.K. (2013). Firefly: Interactive prototypes for architectural design. Architectural Design. doi: 83:144–7.

84. Peraza-Hernandez, E., Hartl, D., Malak Jr, R., Lagoudas, (2014). Origami-inspired active structures: a synthesis and review. Smart Mater. Struct., 23(9):094001. ISSN 0964-1726. doi: 10.1088/0964-1726/23/9/094001. URL http://stacks. iop.org/0964-1726/23/i=9/a=094001?key=crossref.6226c53c3ab2492e5686c0d4be08ea2e.

85. Persiani, S. G. (2020). Energy of Autoreaction. Design Science and Innovation Design of Autoreaction, 89–114. doi:10.1007/978-981-15-6178-8_4.

86. Persiani, S.; Battisti, A.; Persiani, S.G.L.; Wolf, T. (2016) Autoreactive architectural facades-discussing unpoweredkinetic building skins and the method of evolutionary optimization. In Proceedings of the 11th Conferenceon Adaptive Building Skins, Bern, Switzerland.

87. Persiani, S.G.L.; Molter, P.L.; Aresta, C.; Klein, T. (2016). Mapping of Environmental Interaction and AdaptiveMaterials for the Autoreactive Potential of Building Skins. In Proceedings of the 41st IAHS World CongressSustainability and Innovation for the Future, Algarve, Portugal.

88. Pesenti, M., Masera, G., Fiorito, F., Sauchelli, M. (2015). Kinetic Solar Skin: A Responsive Folding Technique. Energy Procedia. doi:70:661–72.

89. Phelan, P. E., Kaloush, K., Miner, M., Golden, J., Phelan, B., Silva, H., Taylor, R. A. (2015). Urban Heat Island: Mechanisms, Implications, and Possible Remedies. Annual Review of Environment and Resources, 40(1), 285–307. doi:10.1146/annurev-environ-102014-021155.

90. Prieto, A., Knaack, U., Auer, T., Klein, T. (2019). COOLFACADE: State-of-the-art review and evaluation of solar cooling technologies on their potential for façade integration. Renewable and Sustainable Energy Reviews, 101, 395–414. doi:10.1016/j.rser.2018.11.015

91. Rawn, E. (2014, September 10). IaaC Students Develop Material System with Responsive Structural Joints. Retrieved from https://www.archdaily.com/546834/iaac-students-develop-material-system-with-responsive-structural-joints.

92. Rogers, C. A., Giurgiutiu, V. (1999). Concepts of Adaptronic Structures. Adaptronics and Smart Structures, 13–34. doi:10.1007/978-3-662-03819-2_3.

93. Saatchi, M., Behl, M., Nochel, U., Lendlein, A. (2015). Copolymer networks from oligo (ε-caprolactone) and n-butyl acrylate enable a reversible bidirectional shape-memory effect at human body temperature. Macromolecular Rapid Communications, vol. 36, no. 10, pp. 880–884.

94. Saito, K., Tsukahara, A., Okabe, Y. (2015). New Deployable Structures Based on an Elastic Origami Model. Journal of Mechanical Design, 137(2). doi:10.1115/1.4029228.

95. Salvati, A., Roura, H. C., Cecere, C. (2017). Assessing the urban heat island and its energy impact on residential buildings in Mediterranean climate: Barcelona case study. Energy and Buildings, 146, 38-54. doi:10.1016/j.enbuild.2017.04.025.

96. Santamouris M. (2007). Heat Island Research in Europe: The State of the Art, Adv. Build. Energy Res. 1 123–150. doi:10.1080/17512549.2007.9687272.

97. Santamouris, M. (2020). Recent progress on urban overheating and heat island research. Integrated assessment of the energy, environmental, vulnerability and health impact. Synergies with the global climate change. Energy and Buildings, 207, 109482. doi:10.1016/j.enbuild.2019.109482.

98. Santamouris, M., Haddad, S., Saliari, M., Vasilakopoulou, K., Synnefa, A., Paolini, R., . . . Fiorito, F. (2018). On the energy impact of urban heat island in Sydney: Climate and energy potential of mitigation technologies. Energy and Buildings, 166, 154-164. doi:10.1016/j.enbuild.2018.02.007.

99. Santamouris, M., Papanikolaou, N., Livada, I., Koronakis, I., Georgakis, C., Argiriou, A., Assimakopoulos, D.N. (2001). On the impact of urban climate on the energy consuption of building, Solar Energy 70 (3) 201–216.

100. Schleicher, S., Lienhard, J., Poppinga, S., Speck, T., Knippers, J. (2015). A methodology for transferring principles of plant movements to elastic systems in architecture. Computer-Aided Design, 60, 105-117. doi:10.1016/j.cad.2014.01.005.

101. Schmitt O.H. (1969). Some interesting and useful biomimetic transforms. Proceeding, Third International Biophysics Congress, Boston, Mass.

102. Silverberg, J. L., Na, J., Evans, A. A., Liu, B., Hull, T. C., Santangelo, C., . . . Cohen, I. (2015). Origami structures with a critical transition to bistability arising from hidden degrees of freedom. Nature Materials, 14(4), 389-393. doi:10.1038/nmat4232.

103. Simulation Software: Engineering in the Cloud. (2021, May 03). Retrieved from https://www.simscale.com/.

104. Speck, T., Speck, O. (2008). Process sequences in biomimetic research. Design and Nature IV. doi:10.2495/dn080011.

105. Stroganov, V., Al-Hussein, M., Sommer, J. U., Janke, A., Zakharchenko, S., Ionov, L. (2015). Reversible thermosensitive biodegradable polymeric actuators based on confined crystallization. Nano Letters, vol. 15, no. 3, pp. 1786–1790.

106. Sun, L., Huang, W., Ding, Z., Zhao, Y., Wang, C., Purnawali, H., Tang, C. (2012). Stimulus-responsive shape memory materials: A review. Materials & Design, 33, 577-640. doi:10.1016/j.matdes.2011.04.065.

107. Suralkar, R. (2011). Solar Responsive Kinetic Facade Shading Systems inspired by plant movements in nature. People and Buildings. London (UK).

108. Tachi T. Geometric considerations for the design of rigid origami structures. (2010). In: Proceedings of the International Association for Shell and Spatial Structures(IASS) Symposium, 2010 Aug 3–7, Shanghai, China.

109. Tolley, M. T., Felton, S. M., Miyashita, S., Aukes, D., Rus, D., Wood, R. J. (2014). Self-folding origami: Shape memory composites activated by uniform heating. Smart Materials and Structures, 23(9), 094006. doi:10.1088/0964-1726/23/9/094006.

110. Uemoto, K. L., Sato, N. M., John, V. M. (2010). Estimating thermal performance of cool colored paints. Energy and Buildings, 42(1), 17-22. doi:10.1016/j.enbuild.2009.07.026.

111. Wang, J., Beltrán, L. O., Kim, J. (2012). From static to kinetic: A review of acclimated kinetic building envelopes. In World Renewable Energy Forum, WREF 2012, Including World Renewable Energy Congress XII and Colorado Renewable Energy Society (CRES) Annual Conference (pp. 4022-4029). (World Renewable Energy Forum, WREF 2012, Including World Renewable Energy Congress XII and Colorado Renewable Energy Society (CRES) Annual Conferen; Vol. 5).

112. Wei, Z.G., Sandstrоröm, R. Miyazaki, S. (1998). Shape-memory materials and hybrid composites for smart systems: Part I Shape-memory materials. Journal of Materials Science 33, 3743–3762. https://doi.org/10.1023/A:1004692329247.

113. Wu HF. (1984). The stratification in fabric roof structures: A strategy of energy conservation and system design. Proceedings of the International Symposium on Architectural Fabric Structures: The design process.; The Architectural Fabric Structures Institute. Orlando, Florida, USA. pp. 192-6.

114. Yoon, J., Bae, S. (2020). Performance Evaluation and Design of Thermo-Responsive SMP Shading Prototypes. Sustainability, 12(11), 4391. doi:10.3390/su12114391.

115. Yuan, J., Farnham, C., Emura, K. (2015). Development of a retro-reflective material as building coating and evaluation on albedo of urban canyons and building heat loads. Energy and Buildings, 103, 107-117. doi:10.1016/j.enbuild.2015.06.055.

116. Zhou, J., Chen, Y. (2010). A review on applying ventilated double-skin facade to buildings in hot-summer and cold-winter zone in China. Renewable and Sustainable Energy Reviews, 14(4), 1321-1328. doi:10.1016/j.rser.2009.11.017.

117. Zhou, J., Turner, S. A., Brosnan S. M., et al. (2014). Reversible shape memory in semicrystalline elastomers.Macromolecules, vol. 47, no. 5, pp. 1768–1776.

APPENDIX

SMA			Alloy-based classification		
+	–	Mechanism	NiTi based	Cu-based	Fe-based
As an actuation material, SMAs are more powerful than SMPs. The actuation stress in SMAs is 10s MPa and above, while that in SMPs is a few MPa at the most	The difficulties in working with SMAs are related to their different behaviour and characteristics due to many different possible martensitic configurations	Thermo-responsive SMAs are featured by the four characteristic temperatures, namely austenite start temperature (A_s), austenite finish temperature (A_f), martensite start temperature (M_s) and martensite finish temperature (M_f). Upon cooling from high temperature austenite phase, the martensitic transformation starts at M_s and finishes at M_f. Upon heating from low temperature martensite phase, the reverse martensitic transformation starts at A_s and finishes at A_f. While at low temperatures, SMAs have the SME, at high temperatures, recovery can be achieved instantly and simultaneously upon releasing the applied load. This is called the super-elasticity (SE). According to the definition above, the SME is the characteristic of the SMM, while the SE is that of the SCM.	+ Higher recoverable strain (around 7%), generated force and corrosion resistance		
Biocompatibility, high corrosion resistance and high electrical resistance	Possible change in the mechanism properties after programming		+ High actuation stress (up to 500 MPa)		
			+ High biocompatibility		
Super-elastic behaviour			– Higher costs		

SMA features [information retrieved from Fiorito et al., 2016]

SMP features. [information retrieved from Sun et al. (2012), Leng et al. (2011)]

SMP

Mechanism

The SME in SMPs is based on a totally different mechanism. Regardless of the types of the stimuli, there are two basic segments/domains in a SMP, one is elastic segment, and the other is transition segment While the elastic segment always maintains high elasticity within the whole SME cycle, the transition segment does change its stiffness significantly at the presence of the right stimulus. Carefully examining the mechanism behind the SME reveals that opposite to that in SMAs, SMPs normally are hard at low temperatures and become soft at high temperatures. Therefore, SMPs alone are normally not applicable in cyclic actuation, unless there is a V-shape in the stiffness vs. temperature curve upon heating, which has been found in a couple of SMPs

Advantages and disadvantages

−	+
More difficult to predict the behaviour of the polymers precisely due to significant relaxation, degradation, etc	Lower density PU SMP: 1.25 g/cm3 NiTi SMA: 6.4 g/cm3
The SME in SMPs may be affected by the programming conditions	Lower cost in fabrication and processing
Possible change in the mechanism properties after programming	Easily produced with high quality into almost any specified shapes at different scales using various traditional and advanced polymer processing technologies
The successful synthesis of a particular SMP for a special application normally requires strong chemical/polymer background, years of experience and great efforts in trial and error	Recoverable strain is normally an order higher than that in SMAs
Current understanding of the thermomechanical behaviour of SMPs is limited to one-dimensional deformation	It is easy to tailor the thermo-mechanical properties of SMPs by means of, for instance blending with different types of fillers or varying the compositions
	It is possible to be always transparent
	Shape recovery temperature range can be easily altered within a wide range and even gradient
	Damping ratio in particular within the transition range is higher
	The potential for recycle and reuse at low cost is higher
	Many SMPs have excellent chemical stability, biocompatibility and even biodegradability
	SMPs are more flexible in surface patterning for different patterns at different scales, and the resulted surface patterns are more permanent
	SMPs can be integrated into mechanical/ structural design as one part or parts of a structure for load carrying under normal working situation

Chemical architecture classification

chemically cross-linked glassy thermosets	chemically cross-linked semicrystalline rubbers	physically cross-linked amorphous thermoplastics	physically cross-linked semicrystalline block copolymers

Market diffused SMPs

Base Material SMP	Ttrans [°C]	Company / Producer
Styrene butadiene	60-70	Asahi company
Styrene-based (Veriflex®)	60-70	Cornerstone research group
One part epoxy	90	Cornerstone research group
Two parts epoxy	104	Cornerstone research group
Cyanate ester	135-230	Cornerstone research group
Thermosetting epoxy	113	Composite technology development
Thermoplastic polyurethane	40-55	Mitsubishi heavy industry

Main characteristics of SMPs					
Category	Material	Ttrans [°C]	Rr [%]	Mechanical properties	Comments
Melting transition based	EOC	60-100	>95	–	Opportunity of tailoring Ttrans by a variation of chemical composition
	Natural Rubber	0-45	–	E(20℃) = 6-16 MPa	Stress-induced shape memory effect
	Natural Rubber	75	88-95	–	Commercial rubber band swollen in molten stearic acid
	EOET	45-55	84-85	–	–
	PEG-SMPU	40-50	82-98	–	–
	PU	60	80-100	E' (-75℃) = 2000-2800 Mpa E' (45℃) = 50-385 MPa E' (75℃) = 15-165 MPa	–
	PMMA-SPEG	46-52	>98	E' (0℃) = 682-2740 MPa	–
	PMMA-LPEG	50-53	75-93	E' (0℃) = 958-1465 MPa	–
	PCLU	45-60	94-100	–	Properties could be adjusted
	Radiation cross-linked PCL	54-56	99-100	–	–
	PCL methacrylate	30-50	92-97	E (25℃) = 2.4-72 MPa E (70℃) = 0.7-6 MPa	–
Glass transition based	ZDA Epoxidized natural rubber	20-46	>90	E (25℃) = 1.5-21.1 MPa	–
	Epoxy	31-93	~100	E' (T=Ts) = 1751-3017 MPa E' (T=Td) = 4.5-18.9 MPa	–
	CPU networks	48-66	>99	E (25℃) = 330-600 MPa E (70℃) = 0.77-5.85 MPa	Biodegradable
	PPS	15-45	~100	E (20℃) = 1.8-130 MPa	–
	Hybrid hydrogels	45	~100	E (23℃) = 0.06-0.2 MPa	–
	MMA-co-PEGDMA	56-92	–	E (T=Tg) = 9.3-23 MPa	Biocompatible materials

Continuation of the overview table of the SMP characteristics. [information retrieved from Sun et al. (2012), Leng et al. (2011)]

SMH features. [information retrieved from Sun et al., 2012]

SMH		Mechanism	Matrix/inclusion structure
+	−		
Based on simple concepts and ordinary materials with well-understood properties	Not enough research carried out to beeter understand their thermo-mechanical properties	The mechanism behind the shape memory phenomenon in SMPs is the elastic-transition segment/domain system. For example, if silicone and wax are selected, both are biocompatible, as the elastic matrix and the transition inclusion, respectively. While silicone normally keeps its high elasticity characteristic within a wide range of temperatures, wax melts upon heating to its melting temperature, and becomes very soft. As such, the sample can be easily compressed. The silicone matrix is elastically deformed, so that an elastic energy is stored in it. When the sample is cooled back to room temperature, wax becomes solid again, which can effectively prevent the release of the elastic energy in the silicone matrix. Consequently, after the constraint is fully removed, the sample largely maintains its deformed shape until it is heated again to above the melting temperature of wax.	Silicone/wax
The accessibility, flexibility in design and fabrication of SMH provides an easy access to ordinary people, even without much chemical/ polymer background	Due to the different composition of SMHs, their modelling requires a specific applied study, even if SMHs can be modelled in similar ways to SMPs		Silicone/water
Can be biocompatible			
Both the matrix and inclusions are not limited to polymers only, but can be selected from any materials			
There is not any chemical interaction between the matrix and the inclusion, so that the properties of individual materials are largely maintained			
The properties can be well predicted from the very beginning by means of materials selections and simple estimation			
Aging, relaxation, and fatigue etc. can be well controlled			
They are convenient to be tailored to meet the exact requirement(s)			
Proven ability of silicon-wax SMH for cyclic actuation			
Similar shape memory effect to the SMPs' one			

	SMAs	SMPs	SMHs
Description / Composition	Most diffused are NiTi-based alloys. Classified in Ni-Ti based, Cu-based and Fe-based	More than 20 different types of SMPs. Most common are thermoplastic polyurethanes and epoxy SMPs	Composed of materials with no shape memory effect on their own. They are "custom made". The most studied are Silicon-Wax Hybrids
Movement / Morphing effect	Stress recover and original shape recover. Small contraction (up to 10%) and deformation. A force is required to re-establish the original shape	Stress recover and original shape recover. High deformation (up to 800%). A force is required to reestablish the original shape	Stress recovery and original shape recovery. Small reversible strain (up to 6-8%). A force is required to reestablish the original shape
Durability issues	More than 200,000 cycles for NiTi alloys. In NiTi alloys high resistance against corrosion and external weather	Up to 200 cycles for SMPU tested. Can be affected by external weather conditions	Currently no experimental data. External weather condition resistance related to composition
Recovery temperature	−10 ℃ to +200 ℃ NiTiCu alloys can be tailored for shading devices, As ~ 45-60 ℃	+25 ℃ to +200 ℃ Can be tailored at lower temperatures Tg ~ 60-90 ℃	Vary with the components: silicon-wax hybrids have an activating temperature of ~ 45 ℃
Density	6000−8000 kg/m3	900−1100 kg/m3	Variable
Elastic Modulus E above Ts	70−100 Gpa	0.5−4.5 GPa 1.24 GPa (Polystyrene SMP)	Variable
Elastic Modulus E below Ts	28−41 GPa (NiTi SMAs)	2−10 GPa (Polystyrene SMP)	Variable
Transformation strain	6−8%	250−800% 50−100 % (Polystyrene SMP)	~6% (Silicone-Wax)
Actuation stress	150−300 MPa ~100 MPa (NiTi SMAs)	2−10 MPa	Variable
Market availability and shape	Wires (different diameters, already educated in range from few μm to 1 mm) Springs Plates/Sheets	Easily customized shape	Mainly derived from DIY approach User's desired shape
Sustainability	Biocompatible	The potential for recycle and reuse at low cost is higher Many SMPs are biocompatible and even biodegradable	Can be biocompatible Organic materials can be used

SMM families comparison. [information retrieved from Sun et al., 2012]